Identification and characterisation of tracheal cartilage derived stem cells for airway tissue engineering

Navid Moshkbouymatin

Submitted to Swansea University in fulfillment of the requirements for the degree of
Doctor of Philosophy

Swansea University
Medical School

2019

DECLARATION

This work has not previously been accepted in substance for any degree and is not being concurrently submitted in candidature for any degree.

Signed:

Date .....

STATEMENT 1

This thesis is the result of my own investigations, except where otherwise stated. Where correction services have been used, the extent and nature of the correction is clearly marked in a footnote(s).

Other sources are acknowledged by footnotes giving explicit references. A bibliography is appended.

Signed:

Date .....

STATEMENT 2

I hereby give consent for my thesis, if accepted, to be available for photocopying and for inter-library loan, and for the title and summary to be made available to outside organisations.

Signed:

Date .....

Abstract

The trachea is a complex organ composed of multiple cell types and is just one integral part of the respiratory system and as a result of injury or insult there is an immediate need to engineer a neo-trachea as there currently no long-term treatments for tracheal defects. This thesis has for the first time successfully identified a mesenchymal derived stem/progenitor cell component that reside within the tracheal C-ring cartilage by means of selective adhesion protocol of fibronectin for airway tissue engineering applications. These cells were found to be, plastic adherent, colony forming, expressed the minimal cell surface markers and were capable of undergoing tri-lineage. Further analysis revealed mechanical property changes in that the tracheal colony forming cells became stiffer with each passage and the gene expression of collagen I, II and X were reduced. To investigate the chondrogenic potential of tracheal stem/progenitor cells traditional pellet culture over a 21-day time course resulted in matrix formation consisting of collagen type II, aggrecan, collagen type I and possible calcification. To rule out the influence of plastic culture 3D gelatin- derived microcarrier culture techniques in both static and wave culture technology were employed for large expansion of tracheal chondroprogenitors. Post expansion analysis revealed that lubricin (PRG4) transcription was observed in all wave expanded cells which is indicative of superficial zone of articular cartilage and not tracheal cartilage. Post differentiation analysis of the microcarrier constructs revealed similar gene profiles to that observed in traditional pellet culture, although with a slight reduction in gene expression. However, microcarrier based differentiation reduced collagen type X gene expression when compared to traditional pellet culture in all the microcarrier groups. These findings taken together show great potential in the wider cartilage research community in that microcarrier and bioreactor expansion can induce the transcription of PRG4 which is specific to the superficial zone of articular cartilage. Furthermore, as a proof concept C-ring like structures were fabricated using tracheal cartilage derived stem/progenitor cells and microcarriers in 3D printed moulds for use as a customisable new method for airway tissue engineering.

Acknowledgments

I would like to express my gratitude to my academic supervisors Dr. Ilyas Khan and Dr. Lewis Francis for their continuous guidance, support and encouragement during my PhD studies. Special thanks to Dr. Lewis Francis for going above and beyond in this project and to set the wheels in motion with Dr. Mark Whittaker for our trip to Instron, UK.

Big appreciations also go to Dr. Richard Webb, Dr. Yadan Zhang, Dr. Rachel Smith, Dr. Oliver Gardner, Zara Ahmed and Guillermo Bauza for their countless efforts and support as friends and colleagues. Their advice and areas of expertise has led to my professional development as a better scientist. I would also like to sincerely thank the Reproductive Biology and Gynaecological Cancer group members, both past and present especially Dr. Andrea Gazze and Dr. Seydou Yao who helped, motivated and encouraged me throughout my time in this research project as well as educating me with valuable scientific skills.

I would also like to mention Professor Owen Guy for his kindness for allowing me to use the 3D printer, which made this research even more interesting. Thanks to Chris Mortimer for his help to design the 3D mould and additional thanks to Jacob Mitchel for refining this design. Cheers to Ryan Bigham for his support throughout these past few years.

I would like to massively thank my Italian friends Simo, Marti, Manu, Francie, Carla and Robbie situated both in Institute of Life Science 1&2 and some who have left the nest. Cheers to you guys for being there during the good and the bad times and providing essential inspirations. Grazie a tutti voi!

Last but by no means least, I am eternally grateful to my parents whom without a doubt my greatest appreciations go to for their unconditional love, inspiration and financial support throughout my studies in the UK without which I could not achieve my goals. I would also like to thank my friends and family both back home and Cardiff for their heart-warming encouragement, motivation and support during the past few years.

I dedicate this thesis to my parents, Shahnaz and Masoud .

Contents

List of figures

List of tables

Abbreviations

AA	Antibiotic-antimycotic
AC	Articular cartilage
ACI	Autologous cartilage implantation
ACP	Articular cartilage derived chondroprogenitors
ADV	Adventitia
AFM	Atomic force microscopy
ALP	Alkaline phosphatase
AM	Additive manufacturing
BMP	Bone morphogenetic protein
CaCl2	Calcium chloride
CAD	Computer-aided-design
CD	Cluster of differentitaion
CD 105	Endoglin
CD 105	Endoglin
CD 106	Vascular cell adhesion protein 1 (VCAM1)
CD 13	Aminopeptidase N
CD 166	Activated cell adhesion molecule
CD 29	Beta 1 integrin
CD 34	CD 34
CD 44	Hyaluronan receptor
CD 45	Protein tyrosine phosphatase, receptor type C
CD 45	Protein tyrosine phosphatase, receptor type, C
CD 73	Ecto-5'-nucleotidase
CD 90	Thymocyte differentiation antigen-1 (Thy-1)
cDNA	Complementary deoxyribonucleic acid
CO2	Carbon dioxide
COMP	Cartilage oligomeric protein
CT	Connective tissue
DAPI	4',6-diamidino-2-phenylind
Dex	Dexamethasone
DI	Deionised water
DMEM	Dulbecco's modified Eagle's medium
DMMB	Dimethylmethylene blue
DTT	DL-Dithiothreitol
ECM	Extracellular matrix
EDTA	Ethylenediaminetetraacetic acid
ESC	Embryonic stem cells
FACS	Fluorescence-activated cell sorting
FBS	Foetal bovine serum
FGF	Fibroblast growth factor
FN	Fibronectin

GAG	Glycosaminoglycan
GAPDH	Glyceraldehyde 3-phosphate dehydrogenase
H2O2	Hydrogen peroxide
HA	Hyaluronic acid
HCL	Hydrochloric acid
HPRT1	Hypoxanthine phosphoribosyltransferase 1
IBMX	Isobutylmethylxanthine
IGF	Insulin-like growth factor
iPS	Induced pluripotent stem cell
ISSCR	Interntaional socienty for stem cell research
ITS	Insulin-transferrin-selenium
Krt14	Cytokeratin14
Krt5	Cytokeratin 5
MgCl2	Magnesium chloride
MMPs	Matrix metalloproteinases
MSC	Mesenchymal stem cell
MTT	3-(4, 5-dimethylthiazol-2-yl)-2, 5-diphenyltetrazolium bromide
NaAc	Sodium acetate
NaCl	Sodium chloride
NBFS	Neutral buffered formalin solution
NEAA	Non-essential amino acid
NKX2.1	NK2 Homeobox1
O2	Oxygen
PBS	Phosphate buffered saline
PBST	PBS containing tween-20 (polyethylenesorbitan monolaurate)
PG	Proteoglycan
PTFE	Polytetrafluoroethylene
PVA	Polyvinyl alcohol
qPCR	Quantitative polymerase chain reaction
RNA	Ribonucleic acid
RT-PCR	Reverse transcripatse polymerase chain reaction
SHH	Sonic hedgehog
SMAD	Small mothers against decapentaplegic
SOX	Sex determining region Y-box
STRO-1	Mesenchyme-1 epitope
TBX	T-box
TC	Tracheal cartilage
TGFβ	Transforming growth factor beta
Wls	Wntless

Chapter 1: General Introduction

1.1 Airways

The human respiratory system functions to enable the intake of oxygen and the expulsion of carbon dioxide. A complex system, it can be divided to multiple tissues and organs. As shown in **Figure 1.1**, the respiratory system is divided essentially to upper and lower airways. The upper airway consists of the conducting or cartilaginous zone; composed of the nose, sinuses, oral cavity, pharynx, larynx and trachea. The conducting zone is not directly involved in the gaseous exchange and the main purpose is to provide a course for inhaled and exhaled air, removal of foreign materials and to regulate the humidity of the incoming air [1]. The lower airway, the respiratory zone, is responsible for gas diffusion in and out of capillaries and is composed of bronchi, bronchioles, alveolar ducts, and alveolar sacs. The lower airway can further be subcategorised into the cartilaginous zones known as conducting zones and non-cartilaginous zones known as the respiratory zone [2]. Several organs of the respiratory system have functions other than non-vital purposes such as; speech production, sensing smell and straining during coughing. Coughing is a prime example to depict the role of the trachea in the airway system. During coughing, the trachea undergoes drastic deformations due to the high intrathoracic pressures and high expiratory flow rates [3]. From a mechanical point of view, trachea is a reinforced tube that has the ability to change its cross sectional area [4]. When coughing happens the cross sectional area changes in a contractile manner which leads to an increase in the velocity in the constriction area thus enhancing the cough efficiency [5].

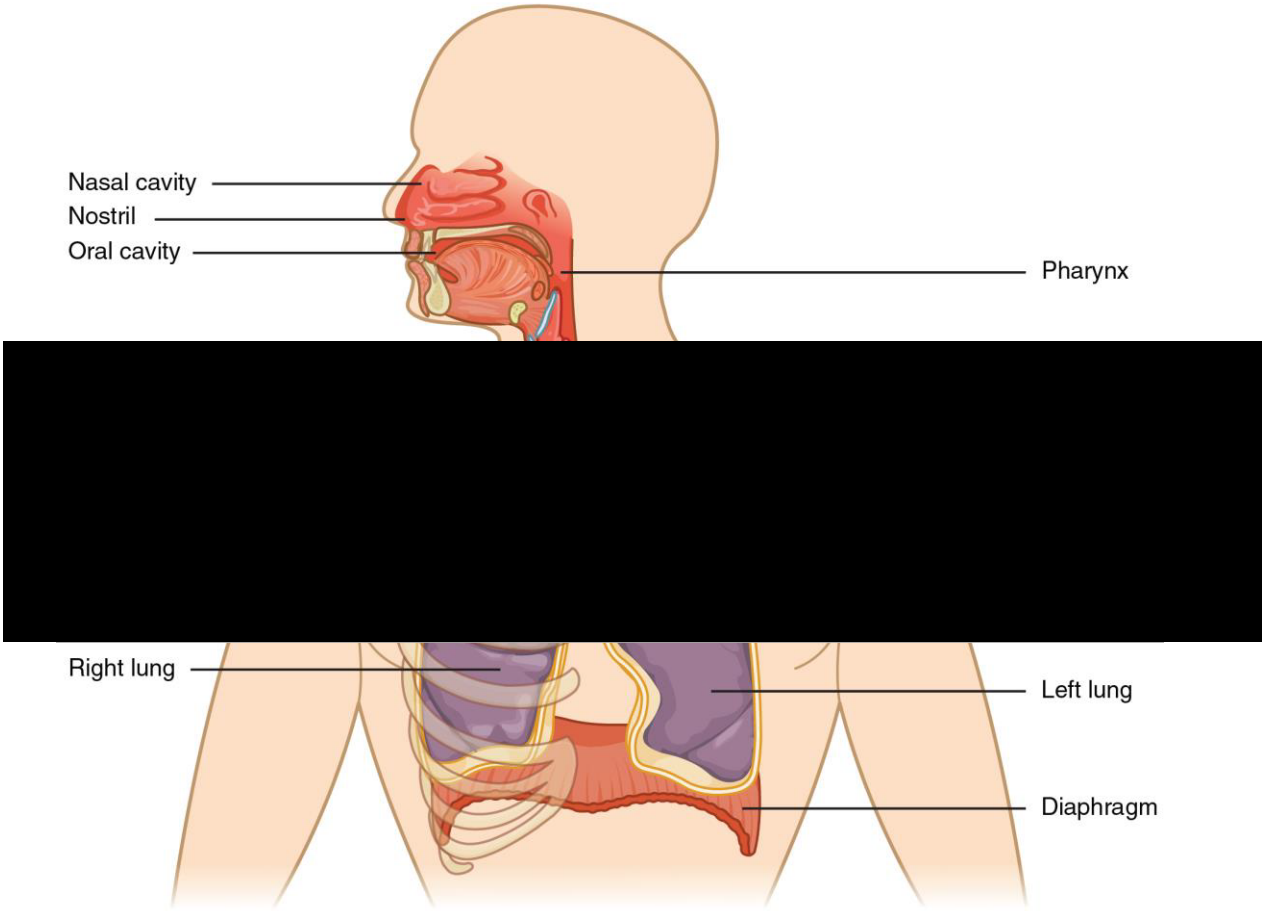

Figure 1.1. Anatomy of the respiration system. Air is breathed in through the nose or the mouth. Air then moves into the pharynx, a passage that contains the intersection between the oesophagus and the larynx. From the larynx, air moves into the trachea and down to the right and left primary bronchi. Each of these bronchi branch into smaller airways called bronchioles that eventually connect with tiny specialized structures called alveoli that function in gas exchange [2].

1.1.1 Embryonic development of airways

Development of the airways initiates by the process of differentiation, where specific stem and progenitor cells generate cells that form tissues specialised in structure and function in order to perform certain tasks in the body. By understanding the stages of tissue formation during embryogenesis it may be possible to replicate such processes to tissue engineer replacement tissues and organs.

First stage of mammalian development begins by fertilization when a sperm and an egg combine, and their nuclei fuse together. This diploid single cell, called a zygote contains all of the genetic information required for foetal development. After fertilization the zygote gives rise to the first embryonic totipotent cells that have the ability to differentiate into all the cells required to support foetal development including the placental tissue, such as the trophectoderm [6]. As cell proliferation progresses a blastocyst with restricted differentiation capacity emerges, consequently the three major cell lineages are established within the embryo during gastrulation. Each of these lineages of embryonic cells forms the distinct germ layers from which all the tissues and organs of the mammalian body eventually form. Each germ layer is identified by its relative position: ectoderm (outer), mesoderm (middle), and endoderm (inner) **(Figure 1.2)** [7].

One of the major milestones in embryonic development is the initiation and generation of the asymmetrical architecture, which underpins the orientation, and polarity of the three-axes, rostral (head) – caudal (tail), dorsal (back) – ventral (front), and left–right which will become the basic body plan along which embryonic development will follow [8].

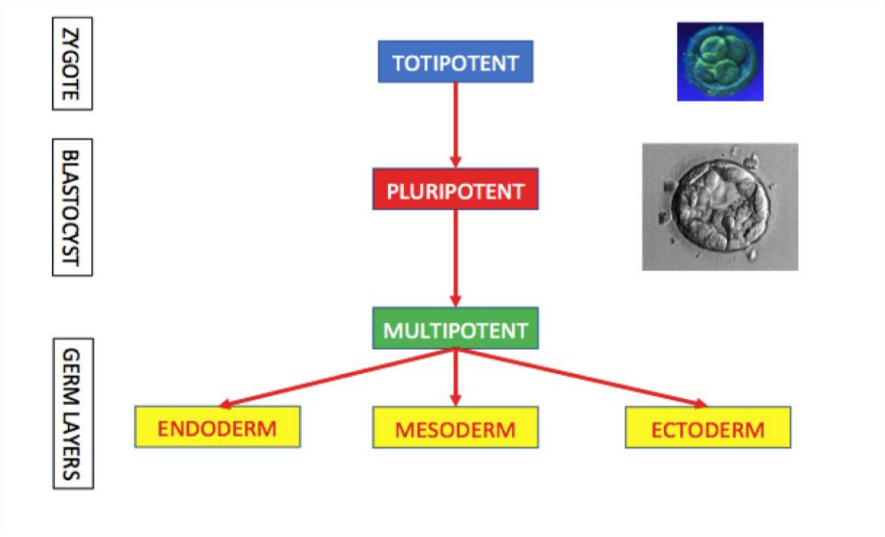

Figure 1.2. Summary of germ layer formation. Totipotent stem cells can be found in the early stages of embryo development. These cells have the capability to differentiate into all types of embryo tissues. Blastocyst contains a cluster of cells, which the embryo

develops and embryonic stem cells (ESCs) are isolated; ESCs are defined as pluripotent because they can differentiate into cells of the three germinal layers (ectoderm, mesoderm, endoderm).

Understanding the developmental biology of the respiratory system is extremely complex due to the cross talk between the endoderm and mesoderm-derived cells that are involved in orchestrating the generation of the airway system [9]. Studies examining the early development of the airway system have mainly used mouse models [10]. It has been shown that the dorsal–ventral patterning is mediated by signalling molecules such as bone morphogenetic proteins (BMPs), sonic hedgehog (SHH) and transcription factors such as sex determining region y-box 2 (SOX2) and NK2 homeobox1 (NKX2.1) in the early foregut prior to the separation is crucial for the generation of oesophagus and trachea [11].

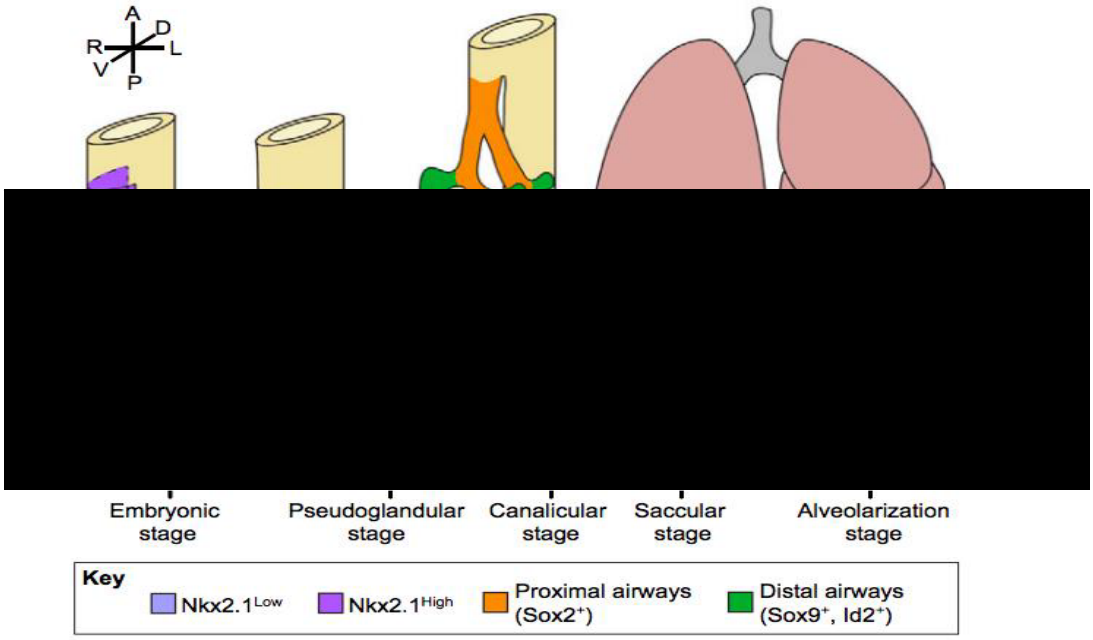

Figure 1.3. Stages of lung formation. lung endoderm specification commences at E9.0 in the foregut with initiation of NKX2.1 expression begins. By E10.0 the formation of trachea starts and the embryonic stage of lung development begins at E12.5[12].

During development, the anterior portion of the endodermal foregut begins as a single lumen that separates into two tubes, the trachea on the ventral side and the oesophagus on the dorsal side **(Figure 1.4A)**. Lung formation begins at mouse embryonic development stage 9 (E9.0), from endodermal cells of the anterior foregut that are marked by homeodomain protein gene NKX2.1 **(Figure 1.3)**. By E9.5 trachea and lung bud modelling begins by evagination of the epithelial cells [13]. The interaction between the endoderm and surrounding mesenchyme results in separation of the airway from the oesophagus during embryonic stages E12.5-16.5 [14]. SOX2 is highly expressed dorsally in tissue that eventually develop into the oesophagus while NKX2.1 is expressed ventrally in the future trachea. The latter pattern of expression is highly dependent on signals from the surrounding mesenchyme including BMPs, noggin, fibroblast growth factors (FGFs) and wingless proteins (WNTs) **(Figure 1.4B)**. It has been shown that depletion of some of these genes does not result in the separation of the foregut. The Wnt signaling plays a particularly important role at this stage [15]. Loss of WNT2 and WNT2B, results in the loss of NKX2.1 expression, expansion of SOX2 expression, and failure in foregut separation [15].

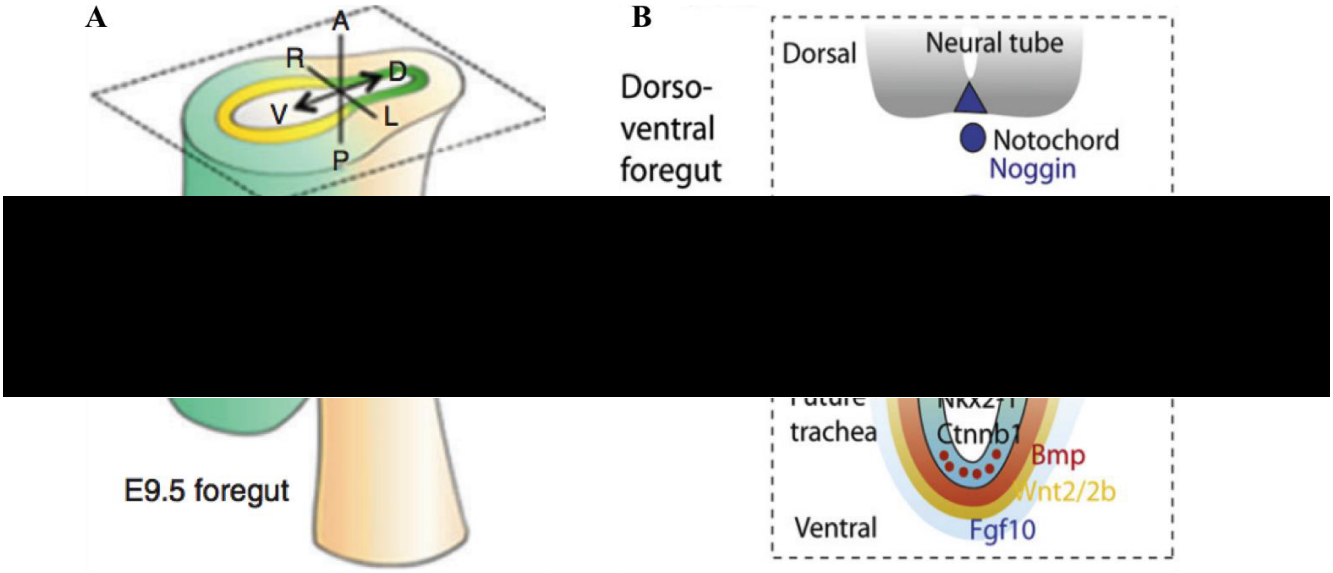

Figure 1.4. Trachea formation and separation from the foregut. Schematics summarising the molecular mechanism involved in endoderm-mesoderm for early patterning and development of tracheal tube [16].

Only in recent years, the importance of endoderm-mesoderm cross-talk in airway developmental biology has become apparent due to its role in the trachea formation. However, the precise function of each gene is unknown fully understood as researchers are at the early stages in identifying representative models on how the separation of the oesophagus and trachea take place [17]. Identifying specific genes involved in tracheal development is crucial and may lead to new insights for use in regenerative medicine.

Cartilage tissue of the upper respiratory tract is formed by commitment of mesenchymal stem cells (MSC) towards a chondrogenic lineage, resulting in the production of specific cartilage matrices [18]. Mesoderm-derived cells are positioned ventral to the developing tube express SOX9 around E9 of embryonic development [19][20]. Expression of collagen type II in cartilaginous tissues, one of the earliest cartilage biomarkers, is observed at E11.5. This expression later becomes more sporadic, indicative of expanding tissue structures with tracheal C-ring cartilage development occurring at E13.5 [21]. Recent discoveries have identified genes with specific roles in lung branching morphogenesis and cartilage formation and involving multiple signaling pathways, including WNT2, FGF10, BMP4, transforming growth factor beta-2 (TGFβ2) and sonic hedgehog (SHH) [22]. SOX9 is the master chondrogenic transcriptional factor during precartilagenous formation and it is strongly expressed in trachea-bronchial mesenchyme. Ablation of SOX9 disrupts cartilage growth [23] but does not affect lung morphogenesis [24]. Molecules that influence SOX9 expression include TBX4 and TBX5, a subset of the T-box (TBX) transcription factor family that are vital during embryonic development for specifying limb identity. TBX4/5 are expressed by trachea-bronchial mesenchyme, and regulate SOX9 expression [25]. Tracheal epithelium directly influences SOX9 expression in the ventral tracheal mesenchyme region through a BMP4 directed signalling mechanism [26][27]. Additionally FGF10 from mesenchymal regulates the periodic expression of SHH through epithelial receptor FGFR2 that is crucial for cartilage ring formations [28]. It has been demonstrated that deletion of Wntless (Wls), a putative G-protein coupled receptor that transports WNTs intracellularly for secretion from tracheal epithelium disrupts cartilage formation causing thickening and expansion of the muscle layer into a region of the lumen where tracheal

cartilage is normally laid down. Studies have concluded that Wnt signalling is significant in influencing differentiation and proliferation of cartilage and smooth muscle during tracheal development [29]. Therefore, SOX9 and wnt signalling play central roles in the process of chondrogenesis during early airway development and their deletion hinders cartilage ring formation [19][27].

1.2 Structure and function of the trachea

The Trachea is a hollow tube that is situated midline in the neck and extends from the cartilaginous cricoid to the carina where it bifurcates into the left and right main bronchi. The trachea extends from the larynx and is a flexible, vascularised and cylindrical tissue that directs the airflow to the lungs [30] **(Figure 1.5)**. The inhaled air is then directed to the respiratory bronchioles, alveolar ducts and alveoli where gaseous exchange takes place [31]. An adult trachea is structurally composed of 16 -20 C-shaped hyaline cartilage rings with the first ring being generally broader than the rest. On average, in an adult, the tracheas' length ranges from 10cm to 13cm with a transversal diameter of 2.3cm and a sagittal diameter of 1.8cm in the adult male (2.0cm and 1.4cm in female) and a 3mm wall thickness [30]. The length of the trachea is proportional to the size of the individual and varies with the persons' height.

C-shaped cartilaginous rings, annular ligament, trachealis muscle, and epithelium are the primary structural components of the trachea [32]. The rings are connected together with annular ligaments and this facilitates longitudinal extensibility. A highly elastic connective tissue, the adventitia, wraps around the rings tightly keeping the structure intact. The cartilage rings are lined internally with a pseudostratified mucosa layer and the posterior regions are fused to a fibromuscular membrane, providing extra flexibility [33]. The trachea is exposed to constant airflow during inspiration with velocities varying from 1mm/sec through quiet breathing mechanism to 250 km/hr during coughing in an adult. Throughout the coughing process narrowing of the trachea occurs

resulting in high velocities of air [30]. To comply with high pressures the trachea requires a highly elastic structure. The cartilage portion of the trachea embodies almost two thirds of the entire luminal structure that has to withstand the extreme force dynamic during expiration. An inner epithelial lining functions as a barrier to environmental exposure to foreign particles and also acts as clearing mechanism for airway secretion. This epithelium has extraordinary regenerative self-repairing properties for injured epithelium [34][35]. Submucosal glands are present in between cartilage rings and epithelium and are responsible for serous secretion and mucous production.

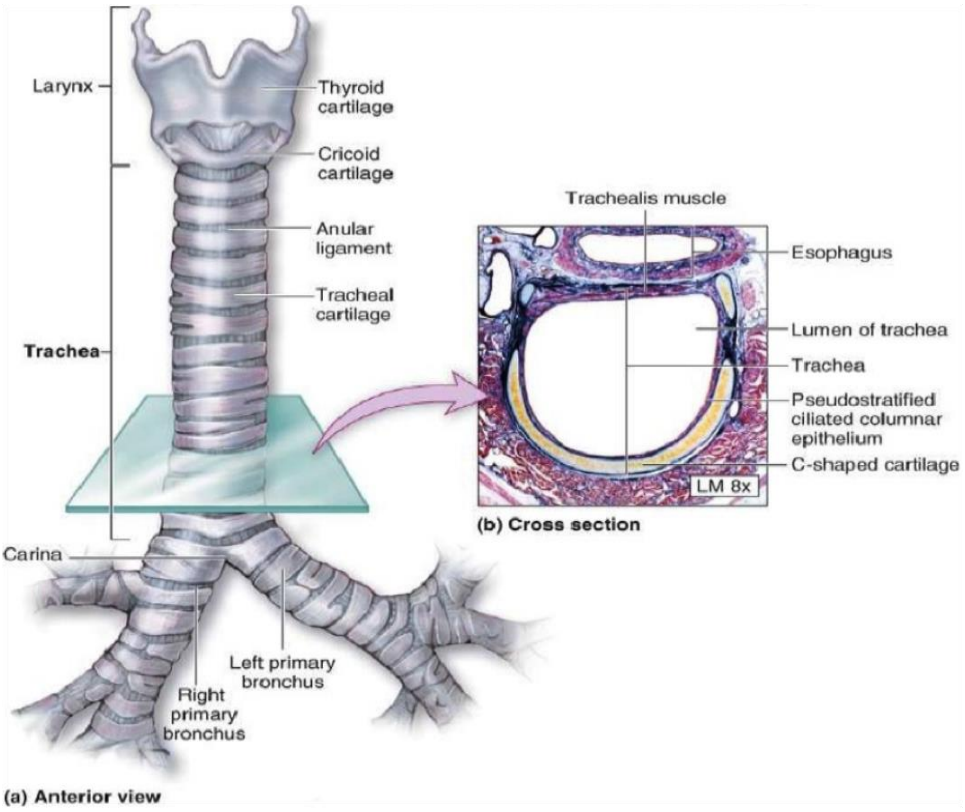

Figure 1.5. Gross anatomy of trachea tissue. Trachea lumen is consisted of annular ligaments between cartilage rings, cartilage rings, muscles on the dorsal to close up the lumen and pseudostratified epithelium layer [36].

1.3 Tracheal disease

The British Lung Foundation has reported respiratory diseases as the second largest cause of death globally after cardiovascular diseases [37]. There are more than 40 conditions that affect the airway which in turn indirectly or directly perturb cartilage structure and organisation of the tissue [38][39]. The airway can be damaged due to cancer [40], infection [41], congenital abnormalities [42], trauma [43], stenosis [44] and calcification in the cartilageous part of the trachea due to aging, and causing limited breathing movement due to increased stiffness [45]. The clinical solutions to overcome these clinical problems range from minor surgical interventions to total organ replacement depending on the severity of the condition.

Stenosis **(Figure 1.6)** is one of the conditions shown to affect tracheal cartilage directly, where a narrowing of the trachea is observed, as a result of a loss of mechanical stability. Stenosis affects 4-13% of adults in the USA alone and 1-8% of newborns [44], [46]. The aetiology of this condition is not well understood but it has been assumed that congenital stenosis starts during the fourth week of gestation and affects development of the remaining respiratory system [39]. Acquired tracheal stenosis develops from a number of origins; tracheotomy where an incision in the windpipe is made to relieve difficulties for breathing, surgical reconstruction, endotracheal intubation, cancer, autoimmune conditions such as; polychondritis (a rare disorder of painful and destructive inflammation of the cartilage and other connective tissues in many organs), sarcoidosis (where abnormal collections of inflammatory cells arrange into lumps) and fungal, viral and bacterial infections [44][47]. The gold standard to treat stenosis is an end-to-end anastomosis where the defect area is removed, and the other two ends are connected back together. This approach becomes problematic where the defect length exceeds 6cm and therefore other strategies are required [48].

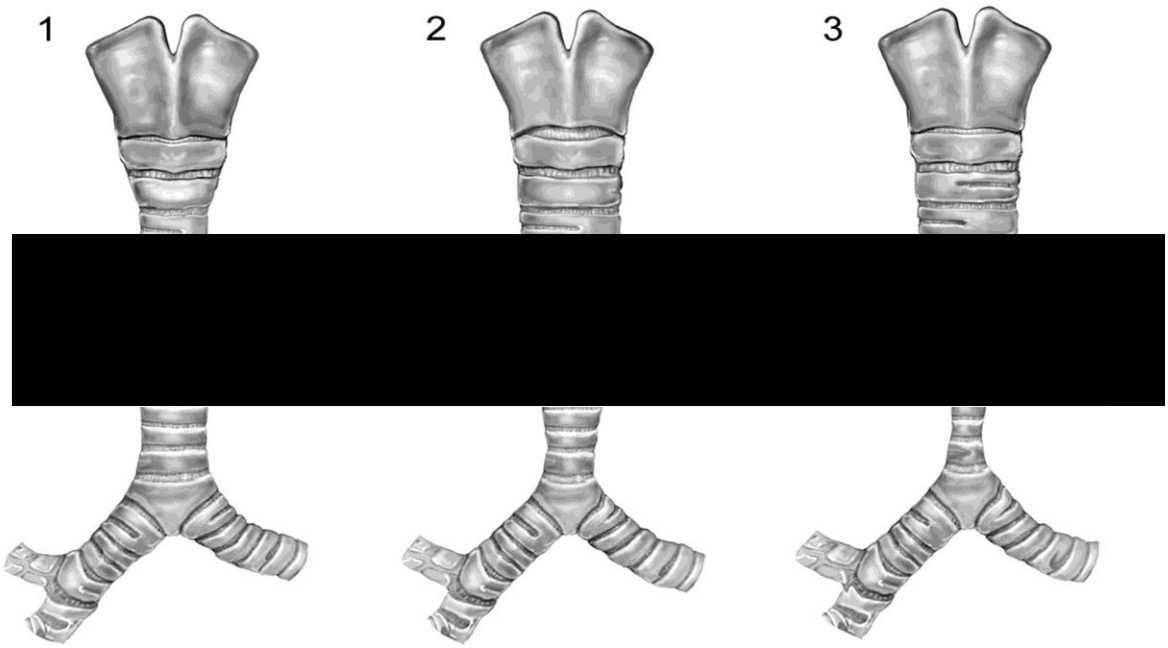

Figure 1.6. Anatomic classification of tracheal stenosis. (1) Shows a generalized congenital under-developed trachea also known as hypoplasia, (2) is a funnel type stenosis and (3) is an example of short segment stenosis [44].

The majority of airway diseases will lead to narrowing of the airway structure and eventually stenosis [49]. Standardised measurements have been proposed for laryngotracheal stenosis depending on the staging severity to reduce the influence of individual assessors on the analysis of outcome and are as follows:

1) The McCafeery system [49][50] catalogs laryngotracheal stenosis based on the extent of the lesion:
    a. Stage I lesions are restricted to the subglottis or trachea and are less than 1cm long.
    b. Stage II lesions are isolated from the subglottis and are greater than 1 cm long within the cricoid ring.
    c. Stage III is subglottic/tracheal lesion void of glottis.
    d. Stage IV lesions involve the glottis directly with fixation or paralysis of one of both vocal cords.

2) The Myer-Cotton staging system [51][52] is used for subglottis stenosis and it classifies the severity based on luminal obstruction. It is simple to use and easy to remember but has some limitations as an indicator of decannulation. These are divided into four grades of luminal narrowing which are as follow:
    a. Grade I lesions < 50% obstruction.
    b. Grade II lesions 51%-70% obstruction.
    c. Grade III lesions 71%-99% obstruction.
    d. Grade IV lesions complete stenosis.

1.4 Tracheal repair

The trachea is a multi-complex structure and to restore and recapitulate this composite biomaterial's function is very challenging. Its exceptional cartilaginous rings maintain lumen integrity during respiration and provide effortlessness movement of the neck. Blood vessels penetrate the ligaments between each ring to perfuse the epithelium where effective mucosa clearance takes place. Removal of a tracheal segment due to non-malignant and malignant obstruction requires airtight restoration of the missing fragment. When few methods such as an end-to-end anastomosis **(Figure 1.7)**, permanent tracheostomy and palliative stenting are no longer an option, full tracheal reconstruction is required to restore full function. The missing tissue must be replaced with a vascularised, epithelium and elastic cartilaginous composite, which is non-immunogenic, non-tumorigenic, functional and compatible and integrated with the surrounding tissues.

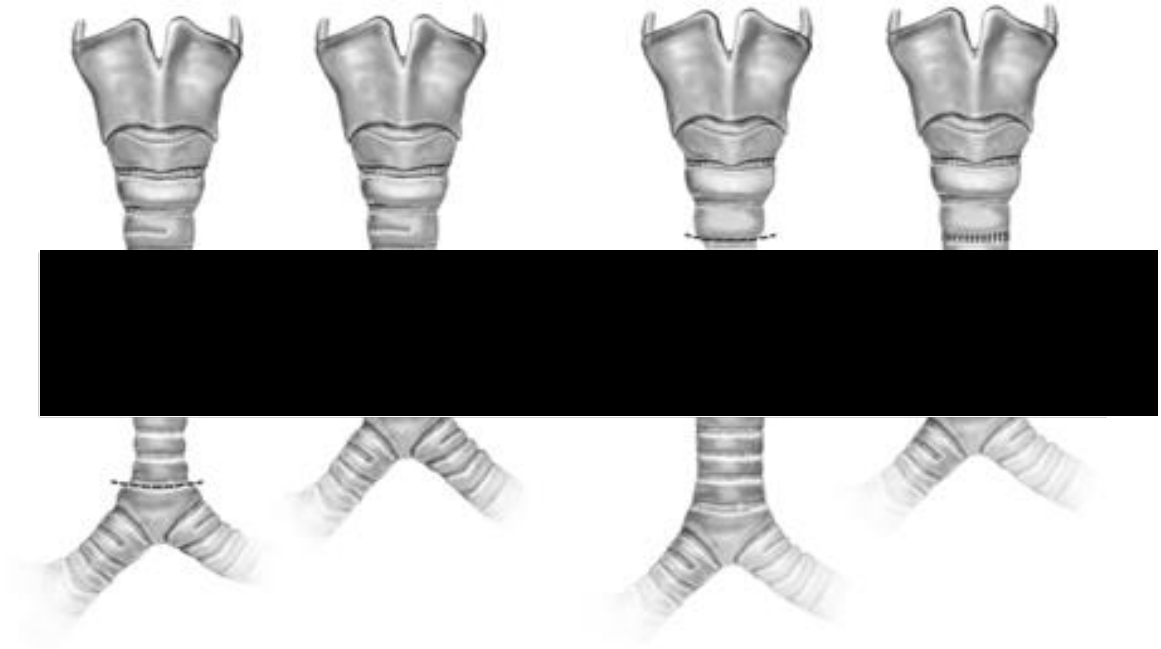

Figure 1.7. Typical example of short end-to-end anastomosis. (A) displays a distal trachea and (B) displays a proximal trachea of congenital tracheal stenosis treated by using the resection and suturing the two ends. Many approaches have been proposed for trachea replacement including autologous and allogeneic long-segment tracheal reconstruction, stents, synthetic prostheses and scaffolds, transplantation of vascularised and non-vascularised grafts, some techniques based upon regenerative medicine and tissue engineering approaches. Each technique will be further discussed with their advantages and shortcomings [44].

1.4.1 Autologous long-segment construction

Autologous donor tissue that is available can be used in a technique called slide tracheoplasty to treat tracheal stenosis with whole tracheal ring with normal epithelium attached. The procedure begins with dividing the middle point **(Figure 1.8A)** of the stricture horizontally and the upper and the lower segments vertically. The trimmed ends are slid onto one another and sutured together **(Figure 1.8B & 1.8C)** [53]. In this technique the circumference of the trachea is doubled and the cross-sectional area is almost quadrupled **(Figure 1.8D,E)** [53][54]. Although this is a preferred technique in many surgical centers the potential for recurrence of stenosis is high because of tissue granulation development [55]. Furthermore, It would be most troublesome in such patients with agenesis of the right lung or extensively long-segment stenosis as

shown in our series. In unilateral lung agenesis, mortality and risk of vascular compression are known to be higher with right lung agenesis [55].

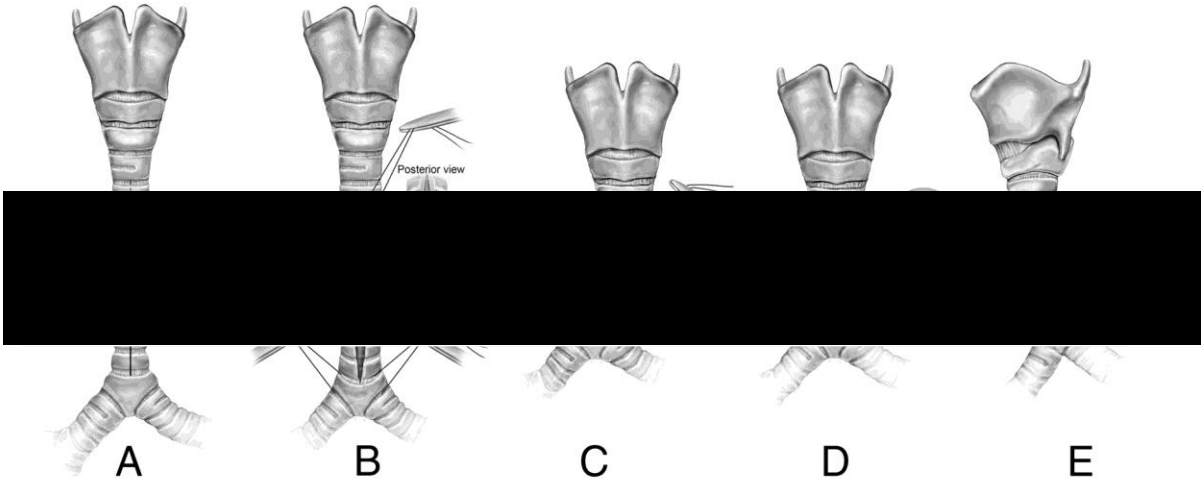

Figure 1.8. Slide tracheoplasty procedure. (A) Stenotic segment is divided transversely in its midpoint. The upper stenotic segment is incised vertically posteriorly, and the lower segment is incised anteriorly for the full length of stenosis. (B) Right-angled corners produced by these divisions are trimmed above and below. (C) The 2 ends are slid together after placement of running sutures around the entire oblique circumference of the tracheoplasty. (D) and (E), the tracheal circumference is doubled, resulting in quadrupled cross-sectional area [44].In the situation where there are no other readily available autologous donor tissues to repair the defect in the tracheal composite, the alternative is to use autologous free flaps as vascular carriers for cartilaginous strips to assemble a neo-trachea. It must be mentioned that the following interventions, although have been reported to be successful, are extremely invasive and patient morbidity is high.

A new method was developed to use rib cartilage and a free radial forearm fasciocutaneous flap to create a tube-like structure. Cartilage strips were integrated between skin and fascia to reinforce the tube and ensuring transverse rigidity. Out of 12

patients; 4 needed additional resections of which 2 died due to pulmonary infection and 8 patients were reported a successful treatment after 36 months [56].

Another surgical technique uses a corticoperiosteal-cutaneous free flap from the medial femoral condyle with local random-pattern skin flaps and has reported no change in shape, diameter or function of the fabricated neo-trachea 14 months following treatment [57]. Other innovative surgical solutions include the use of a tongue-shaped autologous pulmonary tissue flaps with alloy stents [58], an osteocutaneous radial forearm flap [59] and auricular cartilage prelaminated in radial forearm fascia [60].

Regardless of the important progress made with autologous approaches there are some drawbacks. For example cartilages from non-tracheal sources sources have a high chance of undergoing distortion, leading to mechanical failure and stenosis [61]. Another problem is using radial forearm skin or fascia that may not be rigid enough or too thick for small trachea lumen [60]. Finally, if the ciliated epithelial layer is not replaced or even partially replaced the patient has to cough excessively to overcome the deficient mucociliary transport, which ultimately exerts more force onto the reconstructed neotrachea.

1.4.2 Allogeneic long-segment tracheal reconstruction

Similar principles as for autologous tracheal reconstruction, are used for allogeneic transplantation. Donor tracheas from the same species are used in this method, and, the implanted tissue has to be vascularised, possess a rigid cartilaginous framework, be capable of mucocillary transport and have the ability to clear foreign materials upon inhalation. Allogeneic transplantation approach requires administrating patients with immuno-suppressive drugs to prevent immune-rejection [62].

To vascularise an allografted trachea, a heterotopic prelamination-step can be incorporated. Once the trachea is perfused by a transplantable vascular pedicle of the recipient, a transfer of the organ and its pedicle to the orthotic position can be performed [63]. Various strategies have been proposed to restore the function of trachea

allogencially. Rose *et al.* [64] implanted a donor trachea heterotopically, in the sternocleidomastoid muscle of the male recipient and then transferred to the orthotopic position three weeks later without any immunosuppressive therapy. No long-term effect of the latter procedure has been documented. Wurtz *et al.* [65][66] took a new approach by using an allogeneic aorta enclosed with pectoralis muscle to repair long segment tracheal defects.. Wurtz *et al.* also reported significant shrinkage and partial focal epithelium formation.

1.4.3 Stents

Silicone [67] and expandable metallic [68] stents have been widely used as a choice of treatment for long segment treatments, which are sutured, to the upper and lower margins of the defect. They provide good mechanical stability but tissue remodelling and functioning is poor, and generally, this type of reconstruction must be considered temporary due to inevitable stent-related complications such as lack of neck movement, poor re-epithelisation, migration of stent and high chances of infection and reoccurrence of stenosis [69].

1.4.4 Prostheses and scaffolds

Vast majority of synthetic materials have been used in pre-clinical testing in large animal such as glass [70], polyethylene [71], silicone [72], stainless steel [73] and Teflon™ [74]. Clinical trials have also been carried out with stainless steel [75], steel coil [76], silicone [77], polythene [78] and Teflon™ [79]. The purpose for examining such vast choice of materials selection are due to obstructive tissue granulation and scar tissue formation, lack of cellular migration and lack of vascularity caused by implantation of foreign substances which ultimately results in further resection of the native undamaged/undiseased trachea.

The next generation of devices to counter the failure of solid biosynthetic tubular structures was the development of porous structures for better tissue integration [80]. To maintain biomechanical stability steels wire [81], polytetrafluoroethylene (PTFE) [82], titanium [83], Marlex™ [84] and polyurethane [85] have been used. In order to enhance the integration of prostheses with surrounding tissues porous structures have been wrapped with tissues such as omentum [86], fascia [87] or natural biopolymeric materials such as fibrin or collagen [88][89]. An improvement was observed but nevertheless, the lack of vascularisation, overgrowth of scar tissue and stenosis was persistent features of these latter biosynthetic approaches.

1.5 Regenerative medicine and tissue engineering

Regenerative medicine is a multidisciplinary field that relies on a triangular approach in which living cells (fully committed or precursor cells), a supportive 3D or matrix environment and biomolecules are used in order to repair, provide homeostasis, replace or enhance tissue function as well as developing new tissues/organs in cases of total organ replacement **(Figure 1.9)**. Therefore, in recent years more attention has been given to tissue engineering applications in the hope of recreating *in vitro* replacement biological tissues and organs. However, to date very few engineered tissues or organs have been successfully implanted and our original narrow concepts of the components required to successfully engineer a tissue have expanded.

While the field of regenerative medicine, with its multidciplinary approach aims to replace damaged tissues with mimicry in mind; i.e. total replacement or tissue with a like for like replacement, the current clinical gold standard is replacement transplantation from unrelated donors [90]. Allogeneic transplantation is the standard procedure for severe cases of tracheal tissue damage but there are significant problems in terms of immune reaction, donor rejection, the need for repeated follow-up procedures and lack of donors for transplantation [91]. While regenerative medicine aims to recapitulate tissue, structure using autologous or allogeneic cell sources in the

presence and absence of a matrix support, similar issues regarding immunogenicity and rejection exist, alongside implant necrosis.

Toovercome the issues associated with recapitulating complex tissue structures, regenerative medicine has evolved a three-pronged strategy **(Figure 1.9)**. Underpinning these three components, which are often researched individually and occasionally collectively requires an in-depth understanding of fundamental components, both at molecular (signalling and structure) and cellular levels in which are the significant steps required for engineering a complex tissue .

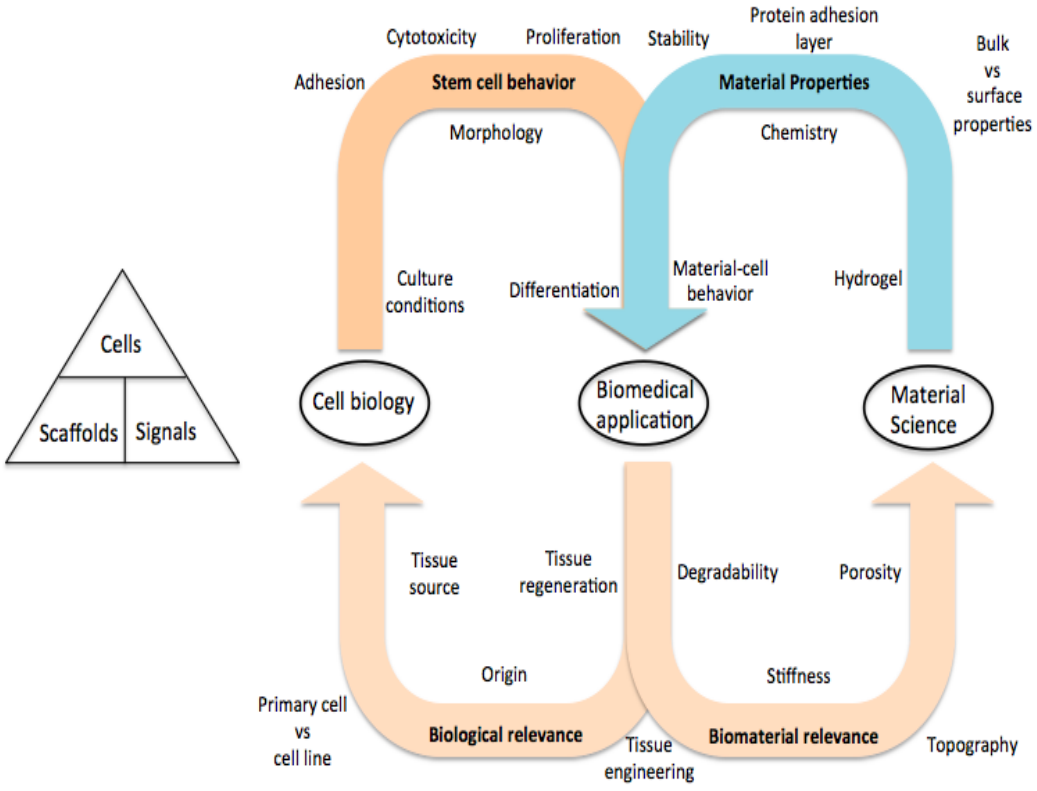

Figure 1.9. Typical triangular approach aiming recreating any tissues is depicted on the left. Individual factors to consider for successful experiment strategies on a wider scope are shown on the right.

The triangular approach, considering the biomaterial (scaffold) signalling and cellular properties required for tissue engineering branches off into more sub-segments, which in turn influence other parameters in developing optimised environments to enhance the growth and differentiation of the intended tissue. From the cellular point of view, the ease of harvest, proliferative capacities, differentiation potency and immuno-privileged nature of donor cells are the most significant factors **(Figure 1.9)**.

From the biomaterials point of view; material porosity, degradation and mechanical properties, the ability of a biomaterial to promote cellular attachment, cell survival, proliferation and differentiation, are all major contributors to consider for tissue engineering **(Figure 1.9)**. An ideal 3D matrix should be biocompatible, bioactive, porous, biodegradable, non-immunogenic, cytocompatible for cell growth and differentiation, have an appropriate microarchitecture and functional properties, possess biomechanical strength, promote long term remodelling at a similar rate to degradation and be relatively inexpensive so as to be used as a clinical tool. Investigated materials can be categorised as natural and/or decellularised versus synthetic variants, and, further subdivided on the basis of biodegradability. Natural scaffolds can be further classified by the donor tissue source of origin (i.e. autologous/syngeneic/allogeneic/xenogeneic) each with their advantages and disadvantages [90][92][93]. Collectively synthetic materials provide more suitable mechanical stability but lack bio-inductive properties; therefore, attention has remained with biological materials. Most biomaterials do not meet the mechanical requirements to be considered as an implantable material. Next generation biomaterials have exploited co-polymer strategies to generate stiffer structures [94] where a composite 3-layer scaffold consisting of a collagen sheet, a polyglycolic acid mesh, and a copolymer (l-lactide/ε-caprolactone) coarse mesh for the development of a tracheal lumen has been used [95]. Epithelisation, of the lumen in the latter biomaterial, occurred at day 14 *in vitro* but analysis had shown new cartilage formation did not match the native trachea composition. Regardless of the efforts being made no single pre-clinically validated strategy has been selected for clinical applications so far. In summary it is important to take into account many elements and understand the addition or removal of factors, but one clear strategy is to include and

consider the effects and traits that are seen in the *in vivo* environments and implement these to *in vitro* scenarios.

1.5.1 A brief history of tracheal tissue engineering

The three key components of airway tissue engineering are formation of the cartilaginous tube, its epithelisation and vascularisation, similar to the aforementioned criteria for long segment transplantations.

For constructing a stable tissue engineered trachea, ideally a small biopsy tissue source must be used in which cells should ideally have high growth kinetics allowing them to be isolated and expanded to the necessary numbers for tracheal tissue generation *in vitro*. However as mentioned previously, to date no stem cell population from the postnatal upper airway has been identified that gives rise to all tissue components.

The current standard tissue engineering procedure in airway tissue engineering relies on organ decellularisation. Decellularisation is believed to be a rich source of scaffold material where ECM content is well preserved. It has been shown that decellularised tissue can be bio-inductive and promote cell adhesion, viability, proliferation, tissue-specific differentiation, and functionality [96][97]. Although it is the best current choice of present tissue engineering-based treatments, it has it's disadvantages, namely; the need for administration of immunosuppressive drugs, lack of available donors, inefficient decellularisation protocols for cartilage tissue (where the matrix to cell volume ratio is high), and mechanical stability deficits are documented shortcomings of this approach [98]. It has been suggested that re-epithelisation of decellularised matrices has a high rate of success whereas chondrocyte repopulation does not effectively take place [91]. Furthermore, current decellularisation protocols are lengthy, post analysis to confirm total removal of nuclear contents are also time-consuming. Decellularised tissue could be a useful baseline model for scaffold fabrication for tissue engineering strategies for future studies.

1.6 Cartilage

Tracheal cartilage is classified as a hyaline type cartilage. However, in the adult human body, there are three types of cartilage present that are classified based on their gross morphology and ECM components: hyaline, elastic and fibrocartilage. Fibrocartilage is a very stiff cartilage that is predominantly made form collagen type I [99] and is found in intervertebral discs and at the enthesis attachment sites of ligaments and tendon. Elastic cartilage can be found in the external ear and epiglottis and is characterised by the ECM being enriched in elastin fibers [100]. Hyaline cartilage is shiny, glass-like in appearance, avascular and aneural in nature and is the most frequent cartilage found in the body, covering synovial joints in tissues such as, hips, ribs and is also located in tracheal rings and larynx [101]. The cartilaginous ECM of hyaline cartilage is highly organised from the superficial surface to the deeper zones where there are topographical differences in the cartilage thickness, matrix composition and cellular alignment that are directly linked with the level of forces experienced and distributed throughout the tissue [102][103].

Chondrocytes are the sole differentiated cellular component of hyaline cartilage and produce a proteoglycan (PG) and collagen-rich ECM. Chondrocyte alignment and matrix composition varies significantly from the superficial surface through to the deep zone of the tissue. The cells are flattened and discoid-like at the surface, in the mid zone chondrocytes are rounder and more randomly organised, and in the deeper zones, chondrocytes are aligned in columnar fashion **(Figure 1.10)**. In articular cartilage, the calcified zone connects the overlying cartilage with underlying subchondral bone plate, and chondrocytes in this zone express collagen type X and is more hypertrophic.

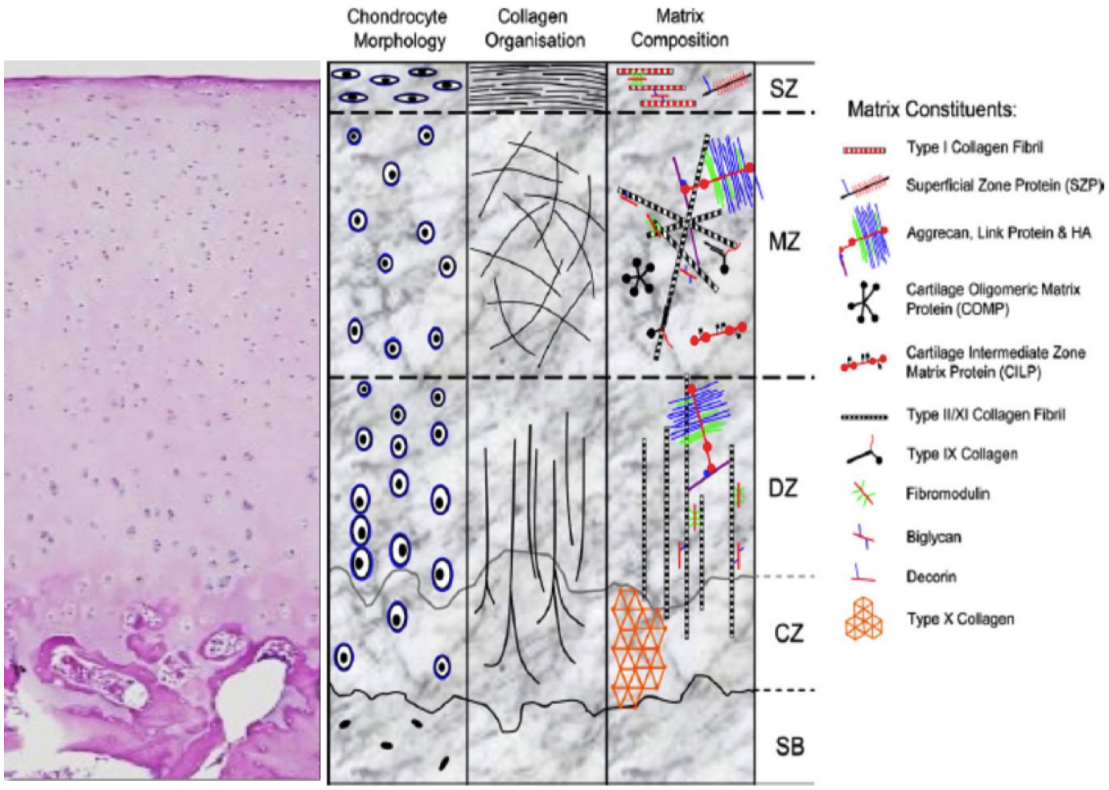

Figure 1.10. Hematoxylin and eosin stain and schematic representation of hyaline cartilage morphology and structure for articular cartilage. SZ, superficial zone; MZ, middle zone; DZ, deep zone; CZ, calcified zone; SB, subchondral bone [104]

The collagen fibril and proteoglycan organisation is zone specific. The collagen orientation in the superficial zone is densely packed and runs parallel to the apical surface of the cartilage and the content is high which allows cartilage to tolerate sheer and tensile forces [105]. The proteoglycan content is relatively low in the superficial zone [106]. The middle zone is characterized by randomly oriented collagen fibrils [106] and the highest proteoglycan content [107] that contributes to withstand high compression forces. The deep zone has the lowest concentration of collagen and the fibers are radially oriented and are arranged perpendicular to the surface [108]. The proteoglycan content is the highest in this zone and has the lowest concentration of water [109].

1.6.1 Composition of hyaline cartilage ECM

Hyaline cartilage is the major cartilage tissue in the body and comprises chondrocytes and ECM, which together convey the tissue mechanical properties which are required to produce a structurally functional tissue. Hyaline cartilage has a large matrix to cell volume ratio and the basic structure is composed principally by dry weight of a collagenous scaffold, proteoglycans and chondrocytes [110]. The main collagen in hyaline cartilage is collagen type II but other collagen types (IX and XI) are present that are responsible for interfibrillar cross-linking and interactions with surrounding proteoglycans [111]. Aggregating proteoglycans such as aggrecan are the second most abundant matrix component by dry weight in hyaline cartilage.

1.6.1.1 Collagens

There are 29 distinct collagens present in animal tissues; they are the main ECM structural proteins. Collagens are triple-helix proteins that assemble into multimeric fibrils through end-to-end and lateral interactions. Collagen can be found in a number of different isoforms, of which the composition vary significantly across different tissues [112]. The fibril forming isoforms, such as collagen types I, II, III, V and XI provides mechanical strength and stability [113]–[115] . They are laid down as individual fibrils that later are able to form thick collagen fibres by linking together to form bundles. Collagen network gives cartilage its structural integrity and tensile strength, and accounts for the majority of the dry weight of mature tissue. The collagens composition of articular cartilage include types I, II, III, V, VI, IX, X, XI, XII and XIV [108].

Type II collagen is the most abundant collagen [116] and is synthesised from precursors to form type IIA and type IIB procollagen that are abundantly found within extracellular space. Due to the high content of hydroxylysine, glucosyl and galactosyl residues; proteoglycans such as aggrecan, decorin and fibromodulin are incorporated into the

collagen type II meshwork. Collagen type II is able to promote chondrocyte attachment to the ECM through adhesion to its helical domain [111].

1.6.1.2 Proteoglycans

In addition to collagen, other macromolecules that form the backbone of cartilage ECM include proteoglycans, elastin and glycoproteins. Proteoglycans are present in the ECM of all connective tissues. Proteoglycans such as aggrecan contain sulfated glycosaminoglycan (GAG) chains, which are assembled from repeating disaccharide units that are then covalently attached to a protein core [117]. Hyaline cartilage contains predominantly aggregating proteoglycans, which are composed of many aggrecan molecules that interact with a long polysaccharide, hyaluronic acid (HA) through a link protein. The aggrecan molecule itself has an extended core protein with many chondroitin sulphate and keratin sulphate chains that lie perpendicularly to the core protein. The resultant sugar chains negative charge attracts and entrap water molecules within cartilage matrix to augment compressive resistance under loading. The proteoglycan aggregate provides the tissue with its resistance nature that withstands compression [117].

1.6.2 Comparison of trachea cartilage with other hyaline cartilages

Despite being relatively less studied, tracheal cartilage, comprising the C-ring structure, is analogous, in terms of structure and function to articular cartilage. Tracheal cartilage biopsy harvest for repair is extremely difficult because of its non-redundant structure and function, and therefore more attention has been given to other cartilage sources as alternatives for reconstructing airways. Although tracheal cartilage has been labelled as a hyaline type cartilage no definitive studies have been made to confirm this assumption and further examination is required. Some evidence regarding the nature of tracheal cartilage by comparison with other tissues have been presented and these are described below.

Thyberg *et al.* analysed proteoglycan monomers from guinea-pig costal cartilage, bovine nasal and bovine tracheal cartilages and observed similarities in the cartilage sources using electron microscopy. This study showed similarities in filament core length, number and length of side chain per core filament across all cartilage sources [118].

Onnertjord *et al.* compared the proteome from eight different cartilage sources from articulating joints, trachea, rib and intervertebral disc in humans [119]. There were significant variations in the protein composition of the ECM of cartilage from different anatomical sources, such as the amounts of collagen types I and III between the tracheal and articular cartilage. Other proteins with substantial differences between these latter two cartilages include fibronectin, cartilage oligomeric protein (COMP), and lysozyme C. Comparison of rib and tracheal cartilage, although much more similar to each other, still had significant differences in COMP and lysozyme C. Thus, hyaline cartilages from different anatomical location have differences in their proteomic composition, possibly because of differences in the various mechanical, biological stresses experienced by each cartilage. Wachsmuth *et al.* compared various types of human cartilage tissues and reported that tracheal cartilage has high cellularity and collagen types II, III, V, VI, and X were present in tracheal cartilage, with some variation between the ring margins and centre [120]. However, no microscopic images of immunohistochemical analaysis of collagen types I, II and X were reported in the latter study. Furthermore, this paper also lacked western blotting analysis and gene expression analysis. Nevertheless, another study reported ossification of tracheal cartilage at the lateral peripheral region in humans with an age range of 40-70 years old [45] similar to the range targeted as Wachsmuth *et al*. study.

1.7 Cell sources for tracheal tissue engineering

As traditional approaches for tracheal repair have proven to be either limited or unsuccessful, tissue engineering is a promising strategy to deliver clinical therapies. The sources of the cells are particularly important as they constitute the primary resource for tissue engineering. Appropriate cells can possibly accelerate regeneration of damaged tissue even without scaffolds. Apart from autologous mature cells, various other stem

cells, including bone marrow-derived mesenchymal stem cells, adipose tissue-derived stem cells, umbilical cord blood-derived mesenchymal stem cells, embryonic stem cells (ESCs) and induced pluripotent stem cells, have received extensive attention in the field of trachea tissue engineering.

1.7.1 Hierarchy of stem cells

The shared ability of stem cells is their ability for unlimited self-renewal capacity and multi-lineage differentiation potential, which make them fundamental during embryonic development and throughout the adult life. The hierarchy of stem cells can be categorised based on their differentiation abilities: totipotent, pluripotent, multipotent, progenitors and finally committed cells **(Figure 1.11)**. Totipotent stem cells are found in the early stages of embryonic development and they are capable to give rise to the placenta and blastocyst. The blastocyst contains a cluster of cells of which embryonic stem cells (ESC) are isolated. These cells are pluripotent and have the ability to give rise to the germ layers. Lower down the hierarchical tree multipotent or oligopotent progenitors that give rise to complete tissues. Unipotent progenitors generally are committed to undergo division to generate a terminally differentiated cell and a self-renewing progenitor.

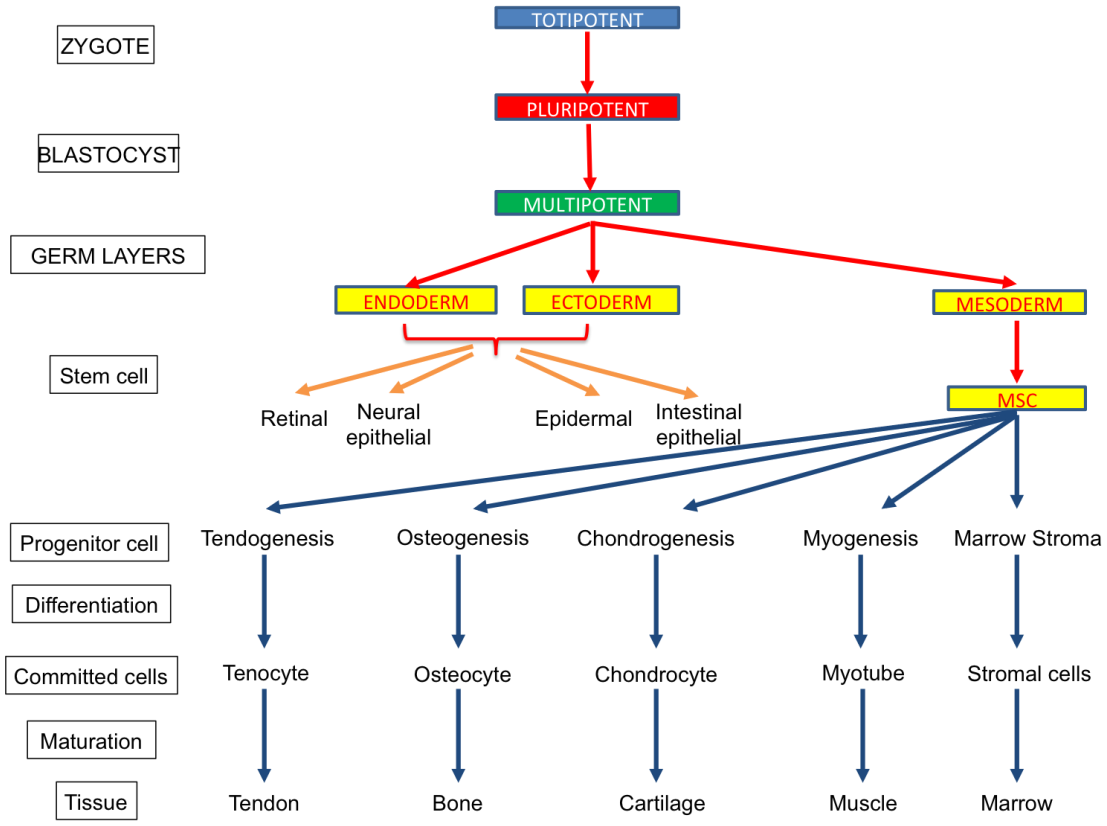

Figure 1.11. Stem cell hierarchy. Schematic representation summarizing the specification of stem cells during development from totipotency to terminal differentiation with intermediate stem cell types highlighting the divergence of cell lineages.

Stem cells exist in specific niches within many organs and can generate many differentiated cell types. Progenitor cells with more restricted differentiation potential, which are defined as tissue specific or adult stem cells and in general, are committed to producing cells from the tissue of origin [121].

1.7.1.1 Tracheal derived epithelial cells

The trachea is lined with a pseudostratified epithelium, which is derived from the endodermal germ layer during embryonic development post-cavitation. The epithelium consists of basal, ciliated, goblet, Clara and less well categorised cells known as indeterminate or intermediate cells [122]. Each cell type has a very unique

morphological feature. Basal cells are recognised by their rounded shape with pyramidal nuclei; ciliated cells and goblet cells are identified by their columnar shape. The goblet cells are distributed within the epithelium and they contribute to a small proportion of the mucous produced compared to mucous glands [123]. The ciliated cells are exposed to the inhaled air and protect the airway by propelling secretions and inhaled particles.

The epithelium lining is continuously exposed to the outer environment, including airborne bacterium and viruses [124]. It must maintain a constant and extensive turnover to balance proliferation and differentiation of cells in order to compensate for the cell loss that occur during normal tissue' function [125]. This has prompted many recent studies to isolate stem/progenitor cells that are responsible for such delicate and precise tissue stability.

Studies have shown the majority of tracheal basal cells have the ability of self-renewal and differentiation capacity to generate the surface epithelium [126][127]. It has been reported that Clara cells in a postnatal mouse bronchiole give rise to ciliated cells and a similar trait was observed in the trachea where the derived ciliated cells did not possess extensive self-renewal capacity but retained a repair mechanism [128]. There is also evidence that the residing basal cells from the submucosal gland possess regenerative capacity [129].

Thus far no single stem/progenitor cell source from the airway has been identified that can give rise to both endoderm and mesoderm compartments of the conducting pathway. The regeneration of epithelium is very complex due to variety of different types of epithelial cells such as ciliated, goblet and basal cells. Epithelial cells for airway tissue engineering are either isolated from nasal, bronchial mucosa or tracheal mucosa [130] or are derived from multipotent cells that can be directed towards specific lineages to synthesis an epithelial layer [131]. However, the degree of differentiation towards cellular and tissue specificity for the native tracheal function of epithelial layer varies greatly. Research has also focused on using endogenous stem/progenitor cells present in the respiratory tract such as ductal cells, basal cells and Clara cells; and exogenous stem/progenitor cells isolated from other sources such as MSC, ES and induced pluripotent stem cells (iPS) cells [131].

1.7.1.2 Mesoderm-derived tracheal progenitor populations

Thus far no studies have identified a mesoderm-derived stem/progenitor cell that give rise to solely to tracheal chondrocytes. Peripheral mesenchyme cells that express FGF10 have been identified and these cells serve as a progenitors for smooth muscle and vascular tissues [132] [133]. Derks *et al.* isolated a potential perichondrial progenitor cell-type from the tracheal compartment. However the isolation and purification techniques to classify these cells was ambiguous and it was not possible to state whether cells were isolated from adventitia or tracheal cartilage [134]. In a following section (Section 1.10) the range of cell types as cell sources for tissue-engineered tracheal cartilage will be addressed, including chondrocytes, adult stem cells, ES cells, iPS cells and other cells obtained from many different donor tissues.

1.7.1.2.1 Stem cell/progenitor isolation criteria

Presently there are two main methods available for isolation of MSC/progenitor cells. Fluorescence-activated cell sorting (FACS) is a widely used technique to isolate specific cell populations from tissues and relies on a series of positive and negative markers known as cluster of differentiation (CD) cell surface markers . The positive panel for mesenchymal stromal cells includes CD29, CD44, CD73, CD90, CD105, CD166 and STRO-1 and negative surface markers include hematopoietic markers CD13, CD34 and CD45 [135]. The appropriate isolation panel in terms of specificity is debatable as certain surface markers are also expressed by fully differentiated cells which could potentially result in lack of purity and chondrogenic potential [136].

A more convenient technique relies on differential adhesion to fibronectin where it has been demonstrated that stem or progenitor cells originating from a region of tissue expressing higher levels of integrins α5 and β1 fibronectin receptors can be isolated on fibronectin coated culture dishes [137]. Differential adhesion to fibronectin is relatively inexpensive, easy to set up and it allows for enrichment and isolation of monoclonal cell-lines, resulting in less experimental variability following culture expansion. As stated previously chondroprogenitors have similar biological properties as MSCs, they

are oligopotent, capable of differentiating into only a few cell types, but they preferentially differentiate towards the permanent (hyaline) chondrogenic lineage and therefore are advantageous for cartilage tissue engineering. Although differential adhesion to fibronectin has not been used to isolate chondroprogenitors from tracheal cartilage, cells with progenitor-like properties have been successfully isolated from articular and auricular cartilage [137][138].

1.8 Smooth muscle tissue engineering

One of the areas of the greatest improvement has been dedicated to the smooth muscle development. Fabricating smooth muscle would be invaluable to patients who suffer from the loss of motor function in the airway. This is vital for swallowing, phonation and coughing. An accessible source of smooth muscle is important as satellite cells are not capable to regenerate the damaged muscle tissue when the loss is greater than 20% of the total length [139]. Tissue-engineered muscle cells should meet the following criteria: be from a non-invasive source with high yield, be able to grow homogenously for a long time without losing phenotype and be able to reach sites of muscle regeneration through a systemic delivery route [140]. Regarding the first criterion, the urinary bladder [141] and small intestine submucosa in pigs [142] have aided in the de novo formation of large amounts of skeletal muscle. How applicable this technique would be in humans has yet to be determined. Stem cells have also been investigated as inducers of smooth muscle. Mesangioblasts have been tested *in vitro* and *in vivo* in mouse [143] and dog [144] muscular dystrophy. One study induced skeletal muscle lineage cells from human, rat and canine BM-MSCs with 89% efficiency and transplanted the cells into injured posterior cricoarytenoid muscles. The muscle choice is significant as the posterior cricoarytenoid is the only abductor muscle in the human larynx. The authors found that autologous induced muscle cells effectively restored vocal fold moment, whereas control and allograft transplants did not [145]. The use of stem cells has been furthered by the first reported transplantation of iPSCs into a mouse muscular dystrophy model [146]. Not only did the iPSCs resolve the dystrophic phenotype, but they also replenished the depleted progenitor supply.

1.9 Vascularisation

Vascularization is crucial to extend the survival of a transplanted graft and avoid necrosis, especially in a large and thick graft as diffusion is inadequate to meet metabolic demands and remove metabolic waste [147]. In a rabbit model, Luo *et al.* implanted tracheal scaffolds intramuscularly in the sternohyoid muscle for 4 weeks to pre-vascularise the graft [148]. Compared to an unvascularised scaffold pre-implanted subcutaneously, pre-vascularised graft wrapped with a muscle flap demonstrated better epithelialization with the presence of epithelial formation. Furthermore, they also found that pre-vascularisation helped to maintain the cartilage structure of the graft. For short tracheal grafts, endothelial cells can grow inward from the native trachea to form blood vessels in time in order to maintain the survival of the epithelium. In contrast, neovascularization cannot reach the midpoint of a long tracheal graft in time, thus resulting in ischemic changes. Poor cell survival after *in vivo* implantation due to delayed neovascularization not only happens to tissue- engineered trachea, but it is a common problem faced by all engineered tissues that are large and thick, with a high cell number and considerable metabolic demands. Several approaches can be applied to accelerate new vessel formation. Walles *et al*. generated a vascularized tissue-engineered trachea by seeding autologous endothelial cells into the vascular network of decellularized porcine jejunum segments [149]. However, the functionality of the vascular network in terms of withstanding the system's arterial pressure and cell shedding upon reperfusion were not tested. Multiple factors, such as human recombinant erythropoietin (hrEPO) and vascular endothelial growth factor (VEGF) have been tested to expedite the neovascularization of tracheal grafts [150]. Furthermore, decellularized scaffolds were found to contain basic fibroblast growth factor (bFGF), which pro- mote angiogenesis [151].

1.10 Chondrogenesis

Chondrogenesis is the initiation process of cartilage development and also occurs during repair and regeneration of damaged tissues. In early development chondroblasts (mesenchymal progenitor cells) proliferate and form condensates that undergo differentiation under the control of signalling pathways that regulate SOX9 expression [152], which cooperatively functions with L-SOX5 and SOX6 [153] to induce the expression of COL2B encoding collagen type II, and, other components of the ECM (e.g., aggrecan).

The first step in guiding multipotent cells to become fully differentiated chondrocytes is to provide the right biochemical cues to direct their differentiation and this is promoted by growth factors. Pre-chondrocytes undergo condensation, forming cell aggregates as a prerequisite step to chondrogenesis [154]. The process is regulated by multiple cell-cell and cell-matrix interactions [155]. Cells in the condensate then differentiate into chondrocytes, which secrete the ECM proteins such as collagen types I, II, IX and XI as well as proteoglycans that ultimately form the cartilage template that pre-figures the skeletal system in animals [156].

Many factors have been identified which stimulate chondrogenesis [157] such as TGFβs, BMPs, insulin-like growth factors (IGFs), FGFs, hedgehog proteins (Hh) and the Wnt growth factor family. Of these latter factors, TGFβs and BMPs are the two most potent growth factors families used in research to induce chondrogenesis [158].

1.10.1 Methods to optimise chondrogenesis

As outlined, studies in developmental biology have shown that a number of factors are important in the process of chondrogenesis. In order to engineer a hyaline cartilage *in vitro* it would be useful to design approaches that are analogous to those occurring during normal development of cartilage.

Many studies have shown that use of non-native MSCs sources for chondrogenesis results in an inferior type of cartilage, both biochemically and biomechanically [159], [160]. Recently other parameters such as co-culture strategies coupling fully

differentiated chondrocytes with MSCs have been identified to positively affect the degree of chondrogenesis. Such methods have improved the proliferative capacity of MSCs and enhanced *in vitro* chondrogenesis [148][149]. Some groups have shown that the biomolecules released by chondrocytes provide chondroinductive signals, which ultimately result in improved chondrogenesis and inhibition of MSC hypertrophic maturity [163][164].

1.10.1.1 Mechanical loading

Hyaline cartilage experiences a variety of complex combinations of tensile, shear, and compressive stresses and strains during development, maturation and throughout daily life. The influence of mechanical loading has therefore been reported to improve MSC metabolic activity and chondrogenic differentiation capacity [165]. Mechanical loading has a direct effect on the matrix synthesis and acts as a signalling factor; providing a crucial influence in musculoskeletal development [166].

1.10.1.2 Bioreactors

Another important aspect for successful tissue formation in vitro is bioreactors. Bioreactors are pivotal in the field of tissue engineering because they enhance the interaction between cells and biomaterials that are important in regulating cell function and tissue remodelling, to produce an engineered tissue that closely resembles the dynamic native tissue. Bioreactors allow for successful large tissue-engineered constructs to be formed where using conventional static culture systems have reached their potentials. Bioreactors can be classified into static and dynamic systems and when compared to the static one, the dynamic culture system has the advantages of a more homogenous cell distribution, allowing for fluid flow that aids in nutrient supply and waste removal, and providing mechanical stimuli (such as hydrodynamic shear stress, compression, pressure and stretch) that guide cell differentiation, matrix secretion and tissue formation [167].

For a tissue-engineered trachea, the bioreactor should be constituted of double chamber for the seeding and culturing of different cell types on the inner and outer surfaces of the tubular construct. It should also rotate to homogeneously distribute the cells to the matrix and to enhance oxygenation, nutrient supply and waste removal, and provide a hydrodynamic stimulus to promote proper cell growth and differentiation [168].

The first tissue-engineered trachea transplanted clinically was cultured inside a bioreactor that aided in cell seeding, nutrient distribution and waste removal while providing the necessary shear stress through constant rotation to stimulate cell growth [168]. The bioreactor permitted the seeding of chondrogenic-induced mesenchymal stem cells and epithelial cells on the outer and inner surfaces of the tracheal graft, respectively. Chondrocytes are quite responsive to mechanical signals, remodelling the matrix according to the loads, and thus the choice of loading regime is important for regulating development of a structure like native cartilage [169], [170]. Lin *et al.* demonstrated chondrocytes seeded on a poly(ε-caprolactone)-type II collagen scaffold and grown in a rotational bioreactor had a higher proliferation rate, increased matrix deposition, aligned along the direction of flow and achieved a morphology similar to that of native tracheal tissue, confirming that shear stress plays an important role in regulating cell function [171]. Kajbafzadeh *et al.* implanted a decellularized tracheal graft in a mouse to use the body as an *in vivo* bioreactor to recellularize the construct [172]. The graft was harvested 12 months after implantation and showed well-organized cartilage and connective tissue formation with the presence of blood vessels. Nevertheless, the epithelial layer was not regenerated and the feasibility of this graft for tracheal replacement was not tested.

1.10.1.3 Oxygen tension

Since cartilage is an avascular tissue and lacks blood supply a hypoxic environment is generated [166]. Propagating adipose MSCs in low-tension oxygen environment improved proliferation and differentiation and induced a better chondrogenic growth and

remarkably prevented calcification by suppression of collagen type X expression and synthesis [96], [173].

1.10.1.4 Growth factors

Chondrogenesis *in vitro* is initiated by several growth factors such as TGFβ, BMP, IGF, FGF, and regulated by other soluble factors such as hedgehog proteins and the Wnt [158]. These biomolecules play an essential role in modulating cell-to-cell signalling and cellular activities within developing and maturing hyaline cartilage. To obtain hyaline-like cartilage *in vitro* is extremely challenging and no consistent protocols have been founded to date.

The TGFβ family have been shown to be potent inducers of chondrogenesis, widely used in cartilage tissue engineering studies, due to their critical roles in all stages of chondrogenesis including mesenchymal differentiation, chondrocyte proliferation, ECM production and terminal differentiation [174]. As well as their role in development, TGFβ are extensively expressed in mature chondrocytes that play a pivotal role in the maintenance of cartilage homeostasis. TGFβ sequentially binds to type II receptors which then phosphorylate type I receptors that then activate signaling proteins small mothers against decapentaplegic (SMAD) 2 and 3 [175]. Research has also shown that SMAD3 is required primarily during chondrogenesis and chondrocytes maturation [176]. Activated SMAD2/3 complexes have been shown to switch on SOX9 gene expression, a key transcriptional factor in regulating chondrocyte differentiation and cartilage formation which in turn regulates the expression of chondrogenic genes such as collagen type II [177]. Lack of SOX9 expression has been studied in MSC-derived chondrocytes where its inactivation caused inhibition of chondrocyte proliferation, prompting defects in joint formation [178]. Moreover conditional loss of SOX9 causes an acceleration of chondrocyte maturation and cellular hypertrophy, due to the fact that under normal conditions SOX9 suppresses the activity of RUNX2 and thus inhibits up-regulation of genes such as collagen type X and osetocalcin [179][180]. TGFβ is comprised of different isoforms including TGFβ1, 2 and 3 [158]. Each subtype has a

different impact on chondrogenesis. It has been shown that treatment with 10 ng/ml of TGFβ1 gives the most favourable results in terms of abundant production of proteoglycan and collagen II and least amount of collagen X and calcification [181]. Additionally it has been reported that both TGFβ1 and TGFβ3 induce hypertrophy [182] during MSC chondrogenesis but generate distinct differences in the cartilage made. TGFβ3 promotes better cellular proliferation while TGFβ1 induces an enhanced chondrogenesis [183].

BMPs are TGFβ superfamily ligands that are involved in chondrogenesis and osteogenesis *in vivo* play a pivotal role in the induction of mesenchymal cells along chondrogenic pathway influencing cellular proliferation, differentiation and maturation during the, formation of joints and bones [184]. Although BMPs are part of the TGFβ family the signalling cascade to induce chondrogenesis are facilitated by distinct pathways; TGFβ signalling is regulated by SMAD2/3 whereas BMP signalling is mediated by SMAD1/5/8 [175]. The SOX family are similarly involved in chondrogenesis via the BMP pathway. Zehentner *et al.* showed that BMP treatment upregulates the expression of SOX9 which in turn encourages increased cartilage marker expression [185]. Liao *et al.* reported an overexpression of SOX9 by BMP2, which resulted in chondrocyte proliferation and condensation in an *ex-vivo* limb culture system [186]. The role of SOX6 has also been highlighted in relation to BMP2, where collagen type II expression was upregulated demonstrating an important role of SOX6 in regulating BMP signalling during chondrogenesis [187]. The correlation between BMP signalling and SOX expression is essential in the initial stages of chondrogenesis while the role of BMP has also been highlighted in later stages of growth and maturation via chondrocyte proliferation and hypertrophy [184]. In addition to BMP2, other BMPs are involved in the process of chondrogenesis including BMPs 4, 6, 7, 9, 12 and 14 [158]. BMP2 is the most studied isoform of the BMP family. BMPs 4, 7 and 14 exhibit the ability to stimulate chondrogenesis to some degree, each having differential outcomes. BMP4 expression correlates with an increased collagen type II and aggrecan and suppression of collagen type X regulation [188]. In the presence of BMP7 it has been reported that there is an enhancement in cartilage matrix production but a reduction in MSCs proliferation [189]. BMP14 has been identified to have a role in the survival of

MSCs and chondrocyte maturation [190]. BMP9 is the least investigated amongst all the other isoforms. Compared to BMP2 and BMP6 a study revealed the potency of BMP9 to be the most promising in chondrogenic differentiation [189]. It was also demonstrated that BMP9 induces the phosphorylation of SMAD1/5 in a dose and time dependent manner [191].

1.10.1.5 Soluble metabolites

Supplementing chondrogenic media with ascorbic acid [192] and dexamethasone (Dex) [193] in conjunction with the use of growth factor causes up-regulation of chondrogenic gene expression. Ascorbic acid (vitamin C) is required for efficient collagen synthesis [175][176] specifically it is required for enzyme activity in the synthesis of hydroxyproline and hydroxylysine [177][178]. The presence of the modified amino acids is crucial as hydroxyproline stabilises the collagen helix and hydroxylysine is involved in collagen crosslinking, further enhancing the mechanical stability of the collagen mesh [197]. This supplementation effect was also shown by Temu *et al.* who observed an increase in collagen type II produced by chondrogenically induced ATDC5 cells in the presence of ascorbic acid [192]. Dexamethasone, a steroid molecule, is another widely used culture supplement used as an inducer of cartilage matrix formation. When bovine MSCs were treated with Dex and TGFβ1 upregulation of chondorgenic genes was observed, however no significant changes occurred when Dex used in conjunction with BMP2 [192].

1.11 Cell types used for cartilage tissue engineering

Cartilage should, in theory, be one of the simplest tissues to reverse engineer as it only contains one cell type, the chondrocyte. One currently employed therapy in clinical practice is autologous cartilage implantation (ACI). Where a biopsy of the articular cartilage is taken and from it cells are isolated and expanded *ex vivo*. Once an adequate number of cells have been sub-cultured from the original biopsy the cellular component

is then used to repair the defect site [198]. Thus far research has shown that using expanded chondrocytes for surgical procedures provides temporary relief from the symptoms of pain and swelling for articular cartilage repair [199]. Post-analysis of biopsied tissue revealed that cartilage produced by chondrocyte implants is inferior to that of native tissue, both in terms of mechanical properties and biochemical composition, in essence it is analogous to fibrocartilage rather than true hyaline cartilage [200] [201]. The same complications arise during tissue engineering of tracheal cartilage where lack of biophysical functionality and biochemical composition is observed even when using fully differentiated cells [183][184]. Auricular chondrocytes are usually preferred in airway reconstruction approaches because of their ready availability and minimally invasive procedure to obtain tissue and cells [94][184]. Another study has targeted bovine chondrocytes from four different cartilage sources and found that each tissue type derived chondrocyte had different biophysical and biochemical characteristics, indicating that cellular selection is an important consideration when used for non-orthotopic transplantation [204].

In order to regenerate any damaged cartilage an ideal cell source should have an ability to be non-immunogenic, be harvestable using minimally invasive surgical procedures and be expandable *in vitro* without losing any chondrogenic potency. Presently the ideal cell source for cartilage tissue engineering remains elusive and the current stem cell research has identified ESCs [205], iPSCs [206], and, MSCs from various tissues such as bone marrow [207], adipose tissue [208] and umbilical cord [209] as ideal candidates for cartilage regeneration. Although early results seem very promising the ethical issues arising from the use of ESCs may provide intractable obstacles and therefore more attention should be given to adult progenitors.

To obtain a sufficient number of cells for defect treatment, a long term culture system is needed which does not result in the loss of cell potency, i.e. the ability to re-differentiate into the chondrogenic lineage, a common problem when culturing full-depth articular chondrocytes [210][211]. Fully differentiated chondrocytes have the ability to reproduce cartilage [180][181] but culture expansion of these cells beyond 5-6 population doublings causes cellular de-differentiation. Redifferentiation of culture-expanded

chondrocytes is inefficient, and the resultant ECM is therefore not equivalent to native tissue and therefore deficient in integrity and biomechanical function[212]. Alternatives to chondrocytes are MSCs that have the potency to undergo multilineage differentiation including chondrogenesis, osteogenesis and adipogenesis [213] as well as having high proliferation capacity in culture [121] making them ideal candidates to re-surface larger lesions. Johnstone *et al.* for the first time formulated an efficient *in vitro* model of chondrogenesis by using pellet culture in the presence of TGFβ1 and dexamethasone [214]. This method of culture, is commonly used to examine the potency of chondrogenic factors [215]. Pellet culture provides a three-dimensional culture environment, with cells in close contact with each other, similar to that is observed during pre-cartilage condensation during embryonic development. *In vitro* differentiation using MSCs does not necessarily reproduce hyaline cartilage as the cells transition through to an endochondral developmental programme resulting in an up-regulation of collagen type X [214] and alkaline phosphatase (ALP) both of which are indicative of hypertrophic epiphyseal chondrocyte markers [216]. Furthermore, due to lack of specific surface markers isolating pure MSC population is difficult as there are non-MSCs cellular contaminants, which interfere and minimise the chondrogenic potential of MSCs.

In recent years it is becoming clearer that tissue-specific stem and progenitor cells exist [217] and it is more logical to target and study the progenitor populations from relevant tissues. In the past decade chondroprogenitors a cell source native to adult cartilage have been identified [218][219]. It is a rational strategy to use progenitors that originate from the native tissue for repair as they require less manipulations to direct their differentiation and produce the required ECM. Chondroprogenitors have the same characteristics as MSCs, possessing the same minimal surface biomarker profile, which can be used to isolate progenitors from a mixed cellular population, and they also have the potential for multi-lineage differentiation [220][221]. Chondroprogenitors display higher expression of integrins α5/β1 and therefore have a high affinity for fibronectin which can be exploited for the purpose of enrichment, they have high colony forming efficiency that is indicative of self-renewal ability, they maintain telomerase activity and SOX9 expression during extended monolayer culture and thus retain their chondrogenic

potential upon serial expansion [222][136]. It has also been shown, that upon chondrogenic induction, chondroprogenitors do not express any epiphyseal chondrocyte markers and are negative for markers such as RUNX2 and ALP and the synthesized matrix resembles hyaline cartilage [220][223].

1.11.1 3D culture (environment)

Cells naturally interact with other cells, grow and differentiate within their ECM. These interactions regulate complex biological functions like cellular migration, apoptosis, or receptor expression. Most of these interactions are significantly dampened, in traditional 2D cell cultures. 3D culture systems allow scientists to provide a biomimicry environment and bridge the gap between classical 2D cell culture and *in vivo* animal models **(Figure 1.12)**. Recently, the use of advanced 3D cell culture methods such as pellet culture, tumour spheroids, stem cell organoids and tissue engineering via 3D bioprinting has produced environments closer to that of native tissue. Improving 3D cell culture models to accurately replicate the natural environment will provide more meaningful scientific data and ultimately enhanced health care. To recapitulate the 3D environment, it is crucial to understand the role of ECM in a given native environment.

The ECM is characterised as a three-dimensional network of extracellular macromolecules, such as; collagens, proteoglycans, glycoproteins and enzymes that provide structural and biochemical support for tissues, and, is important for maintaining tissue function. All cells are in contact with the ECM, which is a dynamic environment of macromolecules with different physical and biochemical properties providing structural integrity, promoting cellular adhesion and supporting signal transduction. Surrounding cells constantly maintain and remodel the ECM's components to maintain homeostasis. Matrix metalloproteinases (MMPs) and proteolytic enzymes play a critical role in tissue homeostasis and ECM-cell signaling [205][206] by creating a balance between ECM degradation and remodelling which ensures that mechanical stiffness is not compromised and that adequate diffusion through the scaffold is maintained. From a biophysical point of view the ECM is the non-cellular component of tissues and organs

and owing to its properties such as topography, porosity and stiffness it can directly influence cellular behaviour such as cell migration and division [226]. In terms of biochemistry, the ECM has direct and indirect signalling properties by anchoring to integrins, which are transmembrane cellular receptors, that integrate cells with their surrounding protein microenvironment to mediate cell attachment, shape, and motility. These microenvironments/niches can greatly influence biological responses such as proliferation and differentiation events.

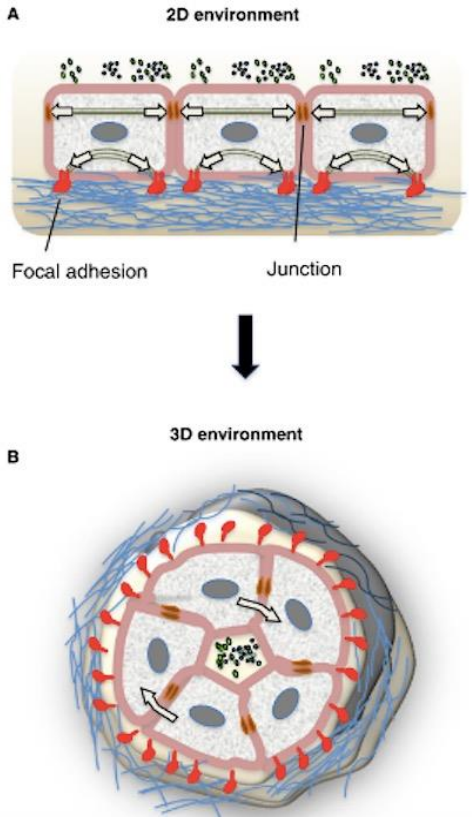

Figure 1.12. 3D environment recapitulates *in vivo* niches. (A) Cells on a rigid 2D surface organise focal adhesions and actin stress fibers at the basal surface of the cell and transfer forces to their surface and to other cells. With their apical side, cells interface with secreted factors present in the medium, whereas with their basal side they interact with the ECM, which confers mechanical properties. (B) Inside a 3D microenvironment, the curvature and the softness of matrix materials limit the formation of actin stress fibers. Cells inside a 3D environment experience stress around the whole structure, both in planar and perpendicular directions to the cell basal surface. Secreted factors can be highly concentrated in the inner compartment [227].

Stem cells are usually in a quiescent state in the adult tissue and in order for them to undergo self-renewal they have to divide and give rise to a pool of progenitors of undifferentiated cells [209][210]. Through this mechanism stem cells maintain tissue homeostasis. Stem cells reside in very highly interactive and specialised local microenvironments called the stem cell niche in which communications between stem cells and ECM are reciprocal. These interactions regulate stem cell behaviour regulating the balance between quiescence, self-renewal and differentiation states [211][212]. Niches are highly specific depending on the anatomical localisation; the diverse dynamic composition of ECM provides precise biochemical, physical, structural, and mechanical signatures to stem cells regulating their behaviour. Moreover, factors such as signalling molecules, shear stress, oxygen tension and temperature also contribute to control stem cell function [213][214].

The ECM varies in composition and concentration, both within and between tissues, leading to different ECM properties and therefore the complexity of different niches adopts based on their function and forms the necessity protection uniquely for tissue specific stem cells. However, identifying and characterising stem cell niches have been challenging mostly due to lack of specific markers for their precise *in vivo* localisation. This has led to a shift in designing smart materials to replicate the native environment to some degree to better monitor the cell-matrix interaction. This will be discussed further how mechanotransduction takes a critical role in stem cells fate. Nevertheless, much effort has been made in identifying stem cell niches in several tissues, including the hematopoietic, epidermal, intestinal, muscular and neural stem cell compartments [234]. Replicating niches in tissue engineering, particularly in developing materials that exploit the ability of cells to remain quiescent and promote long term renewal of tissues is still a largely an unexplored aspect of tissue engineering.

1.11.1.1 Biomaterials

Culturing cells in 2D does not recapitulate the *in vivo* situation and as previously stated differentiated chondrocytes tend to become de-differentiated and MSCs express more

collagen type I than collagen II and GAG. One of the first strategies to mimic the condensation procedure during developmental biology is pellet culture where cells are aggregated to form a cell pellet and treated with chondrogenic media to study the cell signalling and molecular pathways leading to cartilage formation [235]. Although this model has provided initial information about molecular mechanisms of chondrogenesis, cell necrosis in the centre of the pellet and lack of suitability as a model for transplantation are the major drawbacks [217][218]. Because of the many critical functions that are ascribed to the ECM it is logical to employ a biomimicry environment to replicate both the organisation and function of ECM proteins in new scaffold materials. In doing so, biomimetic ECM materials are able to engage integrins, create cell adhesions, and initiate signaling cascades that are typically seen *in vivo.* Biomaterials have been used as a 3D scaffold to provide a temporary biophysical support for adhered cells to maintain their phenotypes and stimulate the synthesis of cartilage specific ECM. However, the choice of materials, fabrication techniques and design parameters directly affect the rate and quality of matrix synthesis. When designing biomaterials for tissue engineering applications two factors need to be considered. From a biochemical point of view the material backbone and biological properties that influences cellular behaviour and secondly the physical design which entails the interior and exterior structure, degradation properties and overall mechanical stability. The starting material is one of the main design considerations to take into account. The scaffold material must maintain its structural integrity during fabrication, clinical handling and fixation at the implant site [238]. It should also provide a stable structural support to protect embedded cells from harmful mechanical stresses and allow them to withstand the *in vivo* loading environment until the neo-tissue is formed. In the following section we focus more on the physical architecture and fabrication techniques that directly influence the formation of tissues.

The most common 3D designs are porous 3D sponges, nonwoven fibrous structures [239], gradient fibrous [240] and woven architectures [241]. What differs between these designs are the pore distribution, pore sizes and geometry and tortuosity which are all-important in the maintaining morphology, composition, mechanical properties and formation of the new tissue. The presence of both macropores and micorpores are

proven to be important in the design criteria. Macropores are important as they assist in cell migration [242] and micropores enhance cell-cell interaction and mass transport, which directly improves the formation of tissue especially *in vivo* [243]. The general belief is that small pore sizes help to maintain cellular phenotypes and ECM contents [225][226] whereas bigger pore sizes enhance the ECM formation [246]. Subsequently 3D scaffolds must be designed as interconnected network with sufficient porosity while maintaining mechanical integrity. The choice of fabrication techniques to create 3D constructs can influence different parameters of the scaffold, including structural architecture, mechanical properties, biocompatibility, and biochemical properties (cell/bioactive agent incorporation) [247].

The conventional fabrication techniques include solvent casting, particulate leaching, melt moulding, phase separation, freeze-drying, and gas foaming. Using such methods involve highly toxic solvents and processing conditions such as high temperatures or pressure to enable to create porous structures, [248] and scaffold properties can only be controlled by equipment parameters rather than design parameters [249]. Such techniques although suitable to study the structure aspect of 3D designs, are not very suitable for clinical settings. They are disadvantages for advanced designs and strategies, such as integration of biological agents such as viable cells and bioactive molecules during biofabrication [247].

Alternative methods such as electrospinning offer the opportunity of building scaffolds from fibres that are similar in size of collagens found in the ECM of cartilage [250]. Electrospinning allows for creation of oriented meshes with similar anisotropic structure of cartilage tissue [232][233]. However fabricating nanofibres and building scaffolds with greater structural complexity such as gradient structure and spatially controlled properties are difficult technically to achieve.

Rapid prototyping is a computer-assisted fabrication method that enables construction of scaffolds with precise internal and external architectures. Briefly additive manufacturing (AM) uses data computer-aided-design (CAD) software or 3D object scanners to direct hardware to deposit material, layer upon layer, in precise geometric shapes. The main

benefits of this technique are to achieve designs with a range of mechanical properties, copolymer composition, and porosity and pore geometry [230][234]. Some modern AM techniques such as 3D bioprinting have made it possible to closely monitor the cellular response to scaffold architectural design [235][236]. The ability to reproduce 3D constructs by bioprinting with similar architectures as found *in vivo* greatly increases the scope for generating larger, organized and vascularised structures. Critical factors for the success of bioprinting include; maintenance of cell viability and function during bioprinting and post-printing and shape fidelity [256].

1.11.1.2 Microcarriers

Tissue engineering relies on a large number of cells that are phenotypically stable for a successful implantation. To obtain a sufficient number of cells extensive cell expansion is needed. There is certain complication involved with conventional 2D cell culture of chondrocytes, namely cellular dedifferentiation and inefficient redifferentiation, therefore research has focused on 3D culture to maintain chondrogenic potency, in particular using microcarrier culture. Another disadvantage of 2D culture is the need for extensive materials for large-scale culture expansion of cells; using microcarriers which amplify the surface area for cell growth can circumvent this limitation on space and resources. Anchorage-dependent cells are able grow on suspended microcarriers either cultured on low adhesive dishes or stirred bioreactor vessels. Propagated cells then can be retrieved in large numbers for further analysis or implantation. One gram of microcarriers is equivalent to a surface area of fifteen T75 culture flasks [257]. This culture method is therefore more cost effective in terms of the culture medium usage and other biological additives such as serum and growth factors. It also provides a more effective gas-liquid oxygen transfer and creates a better culture environment for the cultured cells, and therefore may encourage retention of critical phenotypic determinants for stability and potency.

The successful attachment of cells to microcarriers depends on some crucial factors such as their chemical composition, degree of porosity and surface topography, in particular, cells adhesion to microcarrier surfaces is highly dependent on the pore diameter. Also, the chemical composition of microcarriers influences the ease of retrieving viable cells by enzymatic digest. Trypsin and collagenase are the most common enzymes used to recover cells from the microcarriers, but the efficiency of viable cells retrieved directly correlates with the chemical composition and degree of porosity. Lastly, the microcarriers must be able to withstand sterilization conditions that involve high temperature and pressure without losing their structural integrity.

Various cell types have been coupled with microcarrier culture systems to induce proliferation and differentiation. Freed *et al.* for the first time reported culturing of chondrocytes on collagen-coated dextran beads that remained viable for more than four months though the doubling time was much lower than in static culture [258]. Human articular chondrocytes expanded in bovine type I collagen microcarriers showed similar characteristics to hyaline cartilage even after long period of culture in monolayer, which demonstrates that 3D microcarriers have the capability of retaining the native tissue phenotype [259]. Moreover, improved phenotypic stability by microcarriers has been reported in chondrocytes from other tissue sites. Human nasal chondrocytes were propagated on collagen microcarrier beads derived from bovine corium showed enhanced proliferation and maintained features of hyaline cartilage [260]. Malda *et al.* also showed bovine articular chondrocytes grown on Cytodex-1 microcarriers improved chondrogenic properties as opposed to 2D culture [261].

As previously described MSCs are mechanosensitive cells, which are responsive to their microenvironment such as applied forces and substrate stiffness. Furthermore, these cells are responsive to the biochemistry of the substrates for cell adhesion and proliferation. In an effort to recapitulate these properties various natural and synthetic materials have been widely used as the backbone of commercially available microcarriers for stem cell proliferation and differentiation. The list of materials available materials can be found in Table 1.1.

Type	Manufacturer	composition	Diameter (µm)	Surface area (cm^2/g)	Pore size	coating
Biosilon	Nunc	Polystyrene	160-300	255	Solid	None
Collagen	SoloHill	Polystyrene	90-150	480	Solid	Type I porcine collagen
Cultisphere-S	Percell-Biolytica	Gelatin	130-380	7500	20µm	None
Cytopore 2	GE Healthcare	Cellulose linked with DEAE	200-280	11000	30µm	None
Cytodex 1	GE Healthcare	Dextran linked with DEAE	190±58	4400	Solid	none
Cytodex 3	GE Healthcare	Dextran	141-211	2700	Solid	Cross-linked with gelatin
RapidCell	MP Biomedical	Glass	150-210	325	Solid	None

Table 1.1. Properties of commercially available microcarriers used for the large-scale manufacturing of various types of stem cells [262].

Though a brief summary of microcarriers is provided in Table 1.1 extensive structural characterisation of these biomaterials have not been performed. For example, Cultispher-S and Cytodex-3 have distinct differences in their surface composition and gelatin composition. Cultispher-S exhibits a homogeneous gelatin composition whereas Cytodex-3 is found to be more heterogeneous and consisted of gelatin and polysaccharides [244][245]. These differences could be the reasons why MSCs behave differently on these two types of microcarriers. The stiffness of microcarriers also play a critical role for better cellular responses but biomechanical characterisation using conventional instrumentation of microcarriers is challenging due to their small sizes. Nevertheless, using reconstructed relative elasticity images it's been demonstrated that CultiSpher-S is stiffer compared with the gel of the same material [249]. Most of the microcarriers are usually derived from cross-linking or polymerisation of raw materials

in which the preparation methods can affect the stiffness and in turn have differential outcomes when combined with cells such as; chondrocytes, MSCs and iPS cells [246] [247]. One study compared different microcarriers to screen the proliferative capacity of human placental-derived MSCs. Seeding efficiency was reported to be over 70% for Cytodex-1, -3 and Cultispher-S. However, Cultispher-S had the highest cell retrieval and a 15-fold cell expansion rate [267]. Yang *et al.* reported that Cultispher-S gave the best outcome for cell expansion and proliferation in comparison to Cytodex-1 and Cytopore-2 when coupled with rat bone marrow MSCs [268]. Therefore, based on this evidence seen bulk 3D culture differences in biomechanical properties of microcarriers have the potential to regulate stem cell proliferation.

ECM proteins, growth factors and other biological compounds can be functionalised to microcarriers, or, they can adhere to microcarriers dependent on microcarrier biochemical and geometrical properties [269]. For example the topography and architecture of microcarriers has an effect on fibronectin and laminin adsorption that in turn can regulate stem cell focal adhesion [251][252]. Cytodex-1 microcarriers, a cationic-based microbead display better binding to bovine serum albumin and fibronectin than neutral charged microcarriers [272]. Fibronectin binds specifically to Cultispher-S microcarriers due to their gelatin composition [273]. Chen *et al.* showed that coating different microcarriers with ECM proteins and synthetic peptides increased cellular adhesion and proliferation of pluripotent cells [264].

Compared to cellular proliferation studies, less attention has been paid towards the potential of MSC differentiation on microcarriers. The norm is to propagate cells on microcarriers and, after dissociating them, re-plate onto 2D culture dishes, seed biomaterial constructs or make pellet cultures. Recently the ability of MSCs to differentiate towards chondrogenic lineage on microcarriers showed that there is a relationship between actin organisation and differentiation capacity of cells. It was shown that microcarriers that induced a spherical morphology and disorganised actin filament organisation in adhered cells enhanced chondrogenesis while the opposite was observed on beads favouring cell spreading and formation of stress fibres [263]. Cultispher-S and Cytodex-3 and collagen microcarriers were found as ideal choices for

MSC osteogenesis independent of tissue origin and species [249][255][256]. These findings show the benefits of 3D culture, although the underlying mechanisms accounting for such improvements are still unclear. They might be due to the biomechanical factors that regulate cell-cell interactions and activating the relevant signalling pathways and in turn upregulating their downstream genes. There is also a clear indication that the composition of the scaffolding material and the biomechanically active environment provide molecular cues that activate both proliferation and phenotype expression, which subsequently induces differentiation.

Cell Source	Microcarrier type	Morphology	Differentiation
Bone marrow, ESC-derived MSC	Collagen	Aggregates with increased cellular tension	Enhanced Osteogenesis compared with 2D
Human bone marrow	Cultispher S	Spreading cells	Osteogenic differentiation after plating
Rat Cartilage	Cultispher S	Round shape	Increased adipogenesis and osteogenesis
Rat Cartilage	Cytopore 2 vs Cultispher S	Round shape	Enhanced chondrogenesis compared with 2D
Human fetal bone marrow	Cytodex 3	Spreading cells	Increased Osteogenesis compared with 2D
Human amniotic membrane	Cultispher S	Polygonal shape and aggregates	Osteogenic differentiation
Rat bone marrow	Cultispher S	Spreading cells	Increased Osteogenesis compared with 2D

Table 1.2. MSC differentiation on various types of microcarriers [160].

1.11.2 Mechanotransduction and substrate stiffness

All living entities are exposed to mechanical forces ranging from the forces around a bacterium to more extreme cases such as in a human knee during climbing or sprinting. The process of converting mechanical forces into biochemical signals to influence cellular response is known as mechanotransduction. Mechanotransduction occurs as a multi-stage process where initially conversion of mechanical forces into biochemical signals are sensed by cells, secondly the signal will be received by cells through

integrins and finally the cell can be responsive to signal through gene activation. Integrins are transmembrane receptors for intercommunication between cells and ECM proteins. They are responsible for creating cytoskeleton-matrix adhesions and signal transduction [276]. Integrins are heterodimers that are composed of both α and β subunits, each with multiple types. The binding affinity and specificity of these subunits for various ECM ligands are different, and some integrin receptors have an especially strong affinity for a specific ECM ligand. As an example β3 integrin modulates MSC myogenic differentiation with medium substrate stiffness whereas α2 integrin regulates osteogenic differentiation of MSCs in stiffer matrix [277]. Cells are not only sensitive to extrinsic dynamic mechanical loading in ECM but are also sensitive to the mechanical properties of the ECM such as the stiffness. Understanding the underlying mechanism of mechanical stimulation and stiffness during differentiation of MSCs is of great interest for tissue engineering applications. Research has shown even without any exogenous growth factor stimulation, introducing mechanical loading enhances collagen type II and aggrecan gene expression, and sGAG production of MSCs. The degree of chondrogensis has been shown to be synergistic when growth factor treatment such as TGFβ1 is coupled with mechanical loading [278].

Cells reside and function within various biomechanical environments from soft brain tissue to stiff cortical bone. *In vitro*, matrix or substrate stiffness have been shown to play a role in regulating the differentiation of MSCs towards specific lineages [279], [280]. It has been shown that culturing MSCs on 2D substrates with different stiffnesses has profoundly different outcomes for cellular differentiation as shown by cellular morphology, transcriptional markers and protein expression [279]. Parker *et al.* showed MSCs grown on softer substrates had greater adipogenic and chondrogenic potential whereas on stiffer substrates stronger myogenic and osteogenic differentiation was observed [280].

Cell morphology also has been identified as a key property for differentiation studies. McBeath *et al.* showed that cell shape is a key regulator of MSC differentiation [281]. Cell shape is regulated by both interactions with ECM and adjacent cells and the internal configurations of cytoskeleton. Many studies have shown that matrix stiffness influence

cellular morphology and this in fact could be due to changes in integrin binding, cellular stiffness and adhesion strength [282]–[284].

1.11.3 Atomic force microscopy

To further understand the biomechanical attributes of single cells, atomic force microscopy (AFM), a high-resolution scanning probe microscopy, has been used to monitor single cell biomechanical properties. When using AFM, a tip is attached to a microcantilever, which scans over a sample immobilized onto a flat substrate. A laser beam then is reflected on the back of the cantilever and the upward and downward deviations of the cantilever are detected on a photosensor. As stated in 1.10.2 living cells are responsive to forces exerted from their surrounding environments. Cellular responses [285] to external forces have drawn the attention of the fields of nanomedicine, cell biology, cancer studies and tissue engineering [267][268]. During tissue development and remodeling cells are exposed to mechanical stimuli with biological changes such as alterations to nuclei [288], cell spreading [289], and cytoplasmic changes such as actin and microtubules reorganisation. These changes may in fact modify cellular functions and in turn alter the mechanical properties of cells. For example, it has been shown that tumor cells inherit different elastic moduli compared to normal cells [290]. AFM enables performing mechanical analysis on single cells at the nanometer scale, which would be a beneficial step for characterisation and control of the mechanical properties of reconstituted tissues particularly in tissue engineering [291].

AFM is used to measure the local elastic responses of cell content and it has been reported that mammalian cells have stiffness typically ranging from 1-100 kPa [292], [293]. Recently, single-cell mechanical properties were found to be akin to gene and protein expressions, capable of distinguishing differences in cellular subpopulations, disease state, and tissue source [275] [277]. It has been shown that that the difference between a malignant and benign cell type could be utilised as a biomarker. Softness associated with cancerous cells has been linked to the deformability of the cytoskeleton, which has long been known to play a role in metastasis [297]. Darling *et al.* reported viscoelastic properties of zonal articular chondrocytes by AFM using colloidal tips and

found that the chondrocytes residing on the superficial zone are stiffer than the chondrocytes residing in the middle/deep zone [298]. Guilak *et al.* found that there are distinct differences across primary human chondrocytes, adipocytes, osteocytes and bone marrow MSCs, where, the osteocytes were reported to be stiffest followed by MSCs, adipocytes and chondrocytes [294]. Early results suggest mechanical profiling of cells may be utilized as suitable biomarkers.

Although AFM is capable of reporting differences across different cell types there are some drawbacks involved with this microscopic technique. As of now, we are still at early stages in embracing the ability of AFM for nanomechanical characterisation of cells, and many more refinements in hardware and software are needed. For example, many research groups use different methods and varied elasticity reports can be reported for the same cell type [299]. This is due to differences in animal models used, mathematical modelling, tip geometry and localisation and preparation of cells [300], [301]. For example, the biggest hurdle with measurements above the cytoplasm arise where the mechanical data is obtained blindly, and the localisation is not accurate and therefore it is not clear what part of the structural component of the cytoplasm is being deformed: F-actin, microtubules or intermediate filaments. Thus it is more logical to target the nucleus as it may be involved in mechanotransduction through changes in gene expression and nuclear transport [302].

1.12 Mechanical properties of trachea tissue

The trachea is constantly exposed to a variety of forces during quiet breathing or in a forced expiration or a cough. Despite being the stiffest structure of the bronchial tree, the trachea undergoes significant deformation. Accurate characterisation of the tracheal deformation has significant clinic relevance in order to estimate baseline values for biomaterial integrity evaluation. It is well documented that prosthetic materials have reached their potentials, as dislodgement, migration and occlusion are frequent occurrences when they are used. In terms of biomaterials; collapsing, lack of longitudinal extensibility, radial rigidity are still problematic concerns, however, even in

cases where mechanical stability is sufficient, stenosis is still a serious clinical problem [284][285].

The trachea lumen consists of cartilaginous rings, annular ligament, trachealis muscle, and epithelium. Although the epithelium layer is a very crucial part of this composite material from a biological point of view, it does not contribute structurally to maintaining a patent airway. Other components in trachea are highly anisotropic materials where each component tissue's properties are different for the same sample measured in different orientations. These data correlate with the previous findings which discovered that tracheal cartilage, smooth muscle and annular ligaments demonstrate longitudinal extensibility and lateral rigidity of the native trachea [305]. The general belief is that the cartilage rings are responsible for holding the trachea lumen open despite changes in interthoracic pressure which occur during respiration, yet are capable of significant deformations to allow for changes in the cross-sectional area [306]. The ligaments and muscle provide flexibility by allowing changes in diameter and length.

It has been reported that tracheal cartilage is exposed to both transient and sustained loads. For example during coughing, maximum expiratory flow results in higher magnitude of transient loads whereas contraction of the tracheal muscle can apply sustained loads [307]. There is a large variation in reporting Young's modulus of the human trachea and this is due to both variation in measurements methods and mathematical modelling; this discrepancy ranges from 1 to 20 MPa [307]–[309]. Table 3 summarizes the mechanical properties of trachea across various types of species. Both tensile and compressive values have been reported and these values are relevant to the performance of tracheal cartilage as rings are loaded in such a way that bending generates tensile loads on the outer half of the rings and compressive loads on the inner half [307]. Whilst efforts have been done to provide insights into biomechanical properties of tracheal cartilage it is very challenging to establish longitudinal mechanical properties of ligaments due to short inter-ring length. Safshekan *et al.* through mathematical modelling evaluated the properties of annular ligaments from whole strips of tracheal cartilage and assuming that the hard cartilage segment accounts as ligaments [310].

Species	Test type	Model type	Values reported
Human	Uniaxial tensile with preconditioning	Linear elastic	Average Young's modulus= 16.92±8.76 MPa
Pig	Compression, tensile	Linear aggregate and elastic	Compressive modulus= 1.36±0.49 MPa; Tensile elastic modulus=5.62±2.01 MPa
Lamb	Radial tensile and compression with preconditioning	Analytical using curved beam theory	Tensile 33.50±30.94 MPa; Compression 17.4±12.24 MPa
Pig	Bending with preconditioning	Fung-type strain energy strain function	41.9 MPa main stiffness parameter for linear tensile test
Lamb	Uniaxial tensile test	Linear elastic	Young's modulus= 10.6±1.8 MPa
Human	Uniaxial tensile test	Linear elastic	Equilibrium modulus= 13.6±1.5 MPa
Human	Uniaxial tensile test	Linear elastic	Equilibrium modulus= 1-15 MPa
Human	Bending with preconditioning	Analytical using curved beam theory	Young's modulus 2.5-7.7 MPa

Table 1.3. Mechanical characterisation of tracheal cartilage across different species using various methods and mathematical modeling.

1.13 Summary

The surgical interventions for long-segment circumferential tracheal segments have shortcomings and the postoperative care is intense as opposed to treating the short segments. It is becoming more apparent that fabrication of a functional prosthetic trachea for grafting is very challenging, and, following failures in their implantation and engraftment the main lesson learnt has been that the trachea must not be viewed as a 'simple cylindrical tube'. Therefore, it is crucial to understand the anatomy, developmental biology, molecular pathways and cellular components needed to generate a trachea that resembles the native tissue not only in anatomical features but also in

tissue architecture and function. This project aims to describe the complexity of trachea and uniqueness of tracheal cartilage.

The cellular and extracellular matrix components required for its precise function at cellular, molecular, nano and macro level are examined to provide a wide spectrum platform for future studies. This thesis aims to identify a novel autologous mesoderm-derived stem/progenitor cell type from relatively small initial trachea tissue sources, from which cells can be significantly expanded for reconstruction of the tracheal cartilage as an ideal cell source to consider for chondrogenesis in the hope of providing a functional cell source and the potential to scale up airway tissue engineering approaches.

Hypothesis:

Tracheal C-ring cartilage contains a progenitor population, which is capable of *in vitro* chondrogenesis and that will provide an expandable cell source for tissue engineering C-ring cartilage for repair and replacement of damaged tissues.

Aims and objectives:

This study aims to isolate tracheal cartilage specific stem/progenitor and characterise these cells for autologous repair strategies. However, other relevant tracheal components will also be identified and characterised. Stem cell international society minimum criteria was used as an initial guideline to characterize these cells to identify their differentiation potency in particular chondrogenesis. Once characterised and chondrogenically induced we then attempt as a proof of concept to recreate the tracheal cartilage C-ring for airway tissue engineering applications.

To achieve this:

- Characterisation of native tracheal cartilage at mRNA level, protein level using immunohistochemistry and biomechanical analyses
- Determine mesoderm-origin of isolated stem/progenitor cells using minimal stem cell surface markers at gene level and tri-lineage potency assays.
- Examine cellular biophysical characteristics such as morphology and nano-mechanics to further assess our cellular isolation technique
- Assess chondrogenesis in 3D pellet culture to further assess chondrogenic ability of tracheal cartilage tissue specific stem/progenitor cells with biochemical assays, gene expression and immunohistological studies
- Using materials-based moulding techniques, biofabricate a C-ring like tissue model for assessment of functional tracheal characteristics.

Chapter 2: Materials and methods

2.1 Sources of cartilages and ethical permissions

Suitable animal models mimic physiological processes, which occur in disease states and are used for cell and molecular research investigation prior to translational strategies toward human clinical applications. Choosing an animal model in accordance to the designated application is critical and is dependent on ethical approval, availability, required housing, experience and expertise. For airway tissue engineering and tracheal tissue, large animals are recognized as the most suitable models with respect to gross morphological and physical appearances [292][293]. Six-month-old male welsh large white porcines were chosen for this study due to their abundance, ease of access to tissue and number of relevant literature publications. All animal work conducted in this study conformed to the guidance issued by Swansea University regarding ethical permissions, working standards and disposal. The European Council's directive for all Establishments to be registered for the use of Animal By-products (No. 1069/2009) was followed (ABP Registration: U1268379/ABP/OTHER).

2.2 Tissue isolation

2.2.1 Tracheal tissue

Fresh-6-months-old, juvenile porcine lung tissue with attached trachea lumen was obtained on the day of slaughter, from Maddock Kembrey Meats abattoir (Bridgend Rd, Swansea). Following transport at ambient temperature to the lab, the tracheal lumen was detached from the lungs and rinsed in deionized (DI) water three times to eliminate any debris or clotted blood. The lumen was then incubated at 37 °C and 5% carbon dioxide (CO_2) in phosphate buffered saline (PBS; Gibco, UK) supplemented with a mixture of 10 μg/mL gentamicin (Gibco, UK) and 100 μg/mL antibiotic-antimycotic (Gibco, UK) prior to tissue harvest. This process was repeated three times for a period of 30 minutes per cycle. The inner luminal epithelial tissues were then removed as well as the outer connective layer using a scalpel blade and scissors, to obtain pure hyaline tracheal cartilage. Using disposable scalpels (Swann-Morton), cartilage tissues, epithelial membrane and adventitia were cut into 1-2 mm^2 pieces ready for enzymatic digestion **(Figure 2.1)**.

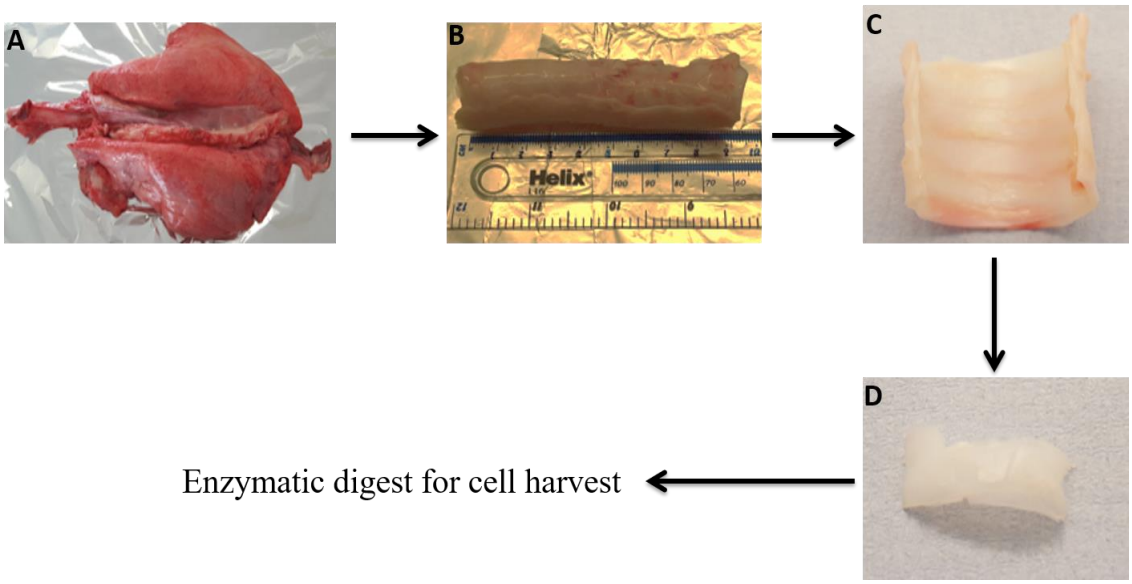

Figure 2.1. Image showing porcine tracheal cartilage extraction. (A) Anterior view of semi-mature 6 months old trachea. (B) Dissected trachea free from associated tissue. (C) Shows the structure of C-shaped cartilage and removal of the mucosa and submucosa membrane. (D) White pearlescent cartilage component void of connective and adventitia which was used for sequential digest to obtain chondrocytes and chondroprogenitors.

2.2.2 Articular cartilage

Porcine articular cartilage (AC) from the metacarpal phalangeal joint was used to provide baseline data for chondrogenesis and primer validation. Articular cartilage from 6-month-old juvenile porcine trotters was harvested as follows. Following transport at ambient temperature, pig trotters were thoroughly washed with soap and water and sprayed with 70% ethanol before removal of skin to reduce the risk of contamination. Articular cartilage explants were harvested by opening up the joint using a sterile scalpel (Swann-Morton, Sheffield) enabling tissue collection from the lateral ridges, lateral condyles and femoral condyles **(Figure 2.2)**. Similarly, to tracheal cartilage, articular cartilage tissues were then diced into 1-2 mm^2 sections prior to sequential enzymatic digestion using pronase and collagenase.

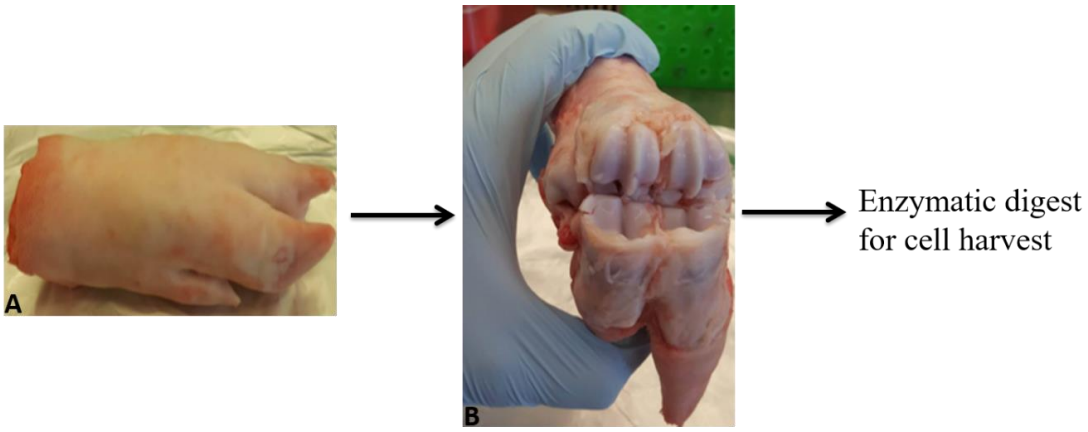

Figure 2.2. Porcine articular cartilage extraction. (A) Shows the juvenile 6-month-old porcine trotters after washing and sterilisation with 70% ethanol. (B) A dissected and opened joint displaying the cartilage surfaces that were harvested for explant tissue.

2.3 Cell isolation and *in vitro* culture

2.3.1 Enzymatic digestion and cellular isolation

Primary cartilage, adventitia and connective tissue derived cell populations were isolated from each tissue compartment and were subjected to sequential digestion in a sterile 50 mL Falcon tube with pronase (70U/mL; Sigma, UK) for 2 hours and following removal of the latter solution, with collagenase (300 U/mL; Sigma, UK) overnight at 37 °C and 5% CO_2 on a roller platform (Miltenyi Biotec, UK). The digested tissue solution was then sieved through a 40 μm cell strainer (BD Biosciences, UK) into a 50 mL Falcon tube and diluted with serum-free Dulbecco's modified Eagle's medium (DMEM, Thermofisher, UK). Isolated cells were mixed with Trypan Blue (Gibco, UK) at a volume ratio of 1:1 and counted using a TC20^{TM} automated cell counter (Bio-Rad, UK) to obtain the total number of cells as well as a live cell count. Counted cells were then plated either as full depth population or subjected to differential fibronectin adhesion for active selection of stem/progenitor cells from each tissue compartment [200][202].

2.3.2 Stem/progenitor selection using differential adhesion to fibronectin

Tissue specific stem/progenitors have been shown to have higher affinity for fibronectin-coated culture plates when compared to full depth chondrocytes, due to relatively higher protein expression of integrin $\alpha5\beta1$. To isolate progenitor cells from each tissue layer, six-well culture plates were coated with 10 μg/mL fibronectin (FN; Sigma, UK) in 0.1 M PBS (pH 7.4) containing 1 mM magnesium chloride ($MgCl_2$) (Gibco, UK) and 1 mM calcium chloride ($CaCl_2$) (Gibco, UK) and incubated overnight at 4°C. One thousand cells isolated from full depth tissue were then seeded onto the FN coated plates for a period of 20 minutes at 37 °C and 5% CO_2 in serum-free DMEM. After incubation the cell culture media containing non-adherent cells was aspirated and replaced with fresh media supplemented with 10% FBS (DMEM+; see **2.3.4**). Adherent cells were kept in culture prior to clonal isolation.

2.3.3 Colony isolation

Following 2-3 weeks of culture with media changes taking place every 3 days, single colonies had formed. Colonies of 32 cells or more derived from a single cell were isolated using 8mm diameter sterile cloning rings (Sigma, UK). At this point, all culture media was aspirated, and cells were rinsed in PBS prior to sterile cloning rings coated in Vaseline being immobilised over the colonies in order to isolate them for clonal expansion. One hundred microlitres of trypsin was added to each colony and incubated at 37 °C and 5% CO_2 for 5 minutes before the trypsinised cells were lifted by pipetting inside the ring and transferred to T25 flasks (Corning, UK) containing DMEM+.

2.3.4 Cell culture

DMEM+ culture medium used in this study contained low glucose DMEM (1g/L D-glucose, Gibco) supplemented with; 1 mM sodium pyruvate, 25 mM HEPES pH 7.5, 4 mM L-glutamine, 10% foetal bovine serum (FBS), 100 μg/mL antibiotic-antimycotic containing 10,000 U/mL penicillin and 10,000 μg/mL streptomycin, 25 μg/mL of

amphotericin B and 100 μg/mL non-essential amino acids (NEAA).

2.3.4.1 Monolayer expansion

Cells were propagated in DMEM+ with fresh media changes every 72 hours. For routine sub-culture when the cells were 80% confluent, cells were rinsed in PBS pre-warmed to room temperature (RT) prior to incubation with 0.05% trypsin-EDTA, at 37 °C and 5% CO_2 for 5-10 minutes. Following gentle agitation, free-floating cells were transferred to a 50 mL Falcon tube and diluted with an equal volume DMEM+. The cells were centrifuged at 200g for 5 minutes at room temperature using an S-4-104 rotor (5810R, Eppendorf, UK). The supernatant was aspirated, and the pelleted cells were re-suspended in 5 mL of fresh DMEM+ and seeded into a sterile culture flask with the appropriate volume of fresh media.

2.3.4.2 Chondrocyte medium

Full depth tracheal or articular chondrocytes were plated as single cell isolates from tissue without selective fibronectin adhesion assay capture and expanded in culture with DMEM/F12 (Gibco, UK), supplemented with 0.2 mM ascorbic acid-2-phosphate, 1% v/v insulin transferrin selenium (ITS, Invitrogen), 10 mM HEPES (pH 7.5), 10% FBS and 100 μg/mLantibiotic-antimycotic (AA). For routine sub culture when the cells were 80% confluent, cell preparations were rinsed in pre-warmed PBS prior to incubation with 0.05% trypsin-EDTA, at 37 °C and 5% CO_2 for 5-10 minutes. Following gentle agitation, free-floating cells were transferred to a 50 mL tube and diluted with an equal volume DMEM/F12 with supplements. The cells were centrifuged at 200g for 5 minutes at room temperature using an S-4-104 rotor. The supernatant was aspirated, and the pelleted cells were re-suspended in 5 mL of fresh DMEM/F12 with supplements and seeded at a 1:3 or 1:4 dilution into fresh sterile culture flasks with the appropriate volume of fresh media.

2.3.5 3D culture

2.3.5.1 Pellet

A pellet culture system was used initially to assess the chondrogenic ability of stem/progenitor cells with various growth factors. Prior to 80% confluency, cells were trypsinised as described in section **2.3.4.1**, and total viable cell number was counted. 500,000 cells were placed in 1.5 mL low retention tubes with chondrogenic media (see **2.4.1**) and then centrifuged at 200g for 10 minutes and incubated 37 °C and 5% CO_2. Pellets remained in culture for a period of 21 days and media was changed every 3 days.

2.3.5.2 Cultispher® microcarrier cell expansion

The media used for the expansion of cells on the Cultisphers® G contained low glucose DMEM (1g/L D-glucose, Gibco) supplemented with; 1mM sodium pyruvate, 25 mM HEPES pH 7.5, 4mM L-glutamine, 10% (FBS), 100 µg/mL AA containing 10,000 U/mL penicillin, 10,000 µg/mL streptomycin, 25 µg/mL of amphotericin B, 100 µg/mL NEAA supplemented with 1 ng/mL TGFβ1 (Peprotech, UK) and 10ng/mL FGF-2 (Peprotech, UK).

2.4 Tests of progenitor phenotypic plasticity

To examine the stem-like potential of the stem/progenitor cell populations differentiation studies were undertaken.

2.4.1 Chondrogenic differentiation (Monolayer and 3D)

To induce stem/progenitor cells to undergo chondrogenesis, DMEM/F12 plus 10% heat-inactivated FBS (FBS was inactivated in 60 °C water bath for 45 minutes) was supplemented with; 0.1µM dexamethasone (dex) and either 10 ng/mL of TGFβ1 or 100 ng/mL of BMP9 (Peprotech, UK). Media was changed twice weekly.

2.4.2 Osteogenic differentiation

To induce stem/progenitor cells towards the osteogenic lineage α-minimal essential media (α-mem) (Gibco, UK) contained 2mM glutamine and was supplemented with 10% heat inactivated FBS, 100 μg/mL AA, 0.1 μM dexamethasone, 0.2 mM ascorbic acid-2-phosphate and 10 mM β-glycerophosphate. Media was changed twice weekly.

2.4.3 Adipogenic differentiation

To induce stem/progenitor cells towards adipogenesis α-mem (Gibco, UK) contained 2 mM glutamine and was supplemented with10% heat inactivated FBS100 μg/mL AA, 1 μM dexamethasone, 1.72 μM of bovine insulin, 0.2 mM indomethacin and 0.5 mM of isobutylmethylxanthine (IBMX). Media was changed twice weekly.

2.5 Cultispher® preparation for cell seeding

2.5.1 Sterilisation

Porous gelatin derived micro-carriers with diameter ranging between 130-380 μm (Cultispher® G standard porosity, Sigma, UK) were weighed and added to 50 mL of PBS and let stand for 1 hour. Cultisphers® were then placed in an autoclave at 15 PSI at 121°C for one 20 minutes cycle and allowed to cool down. After PBS/Cultispher® microcarriers had reached room temperature they were spun down at 230g for 10 minutes and the PBS aspirated off. The Cultisphers® microcarriers were then washed 3 times with sterile PBS containing 100 μg/mL AA. After each wash the suspension was centrifuged at 230g for 10 minutes to allow complete settlement of the Cultispher® microcarriers. After the washing cycles the excess PBS was removed and the Cultispher® microcarriers were placed in appropriate coating solution.

2.5.2 Coating of microcarriers

Sterilised Cultisphers® microcarriers were coated with either 50 mL of 10% FBS or 3% gelatin from bovine skin (w/v) (Sigma) to enhance cellular attachment. FBS/Cultispher® or Gelatin/Cultispher® microcarriers were mixed with cells on a platform roller at 37 °C and 5% CO_2 for 30 minutes and allowed to stand for 1 hour. This cycle was repeated 4 times for even coating of the microcarriers surface.

2.5.3 Seeding and expansion of progenitor cells on Cultispher® microcarriers

Passage 4 monoclonal progenitor cells were trypsinised as described in section **2.3.4.1** and re-suspended in a fresh media (refer to **2.3.4**). Twenty cells per Cultispher® microcarrier were seeded for each experimental group ($8x10^6$ cells in 0.4 g as there are $1x10^6$ microcarriers per gram as stipulated by the manufacturer) in a 50 mL tube and further suspended to 20 mL per experimental group. Seeded Cultispher® microcarriers were placed on a platform roller at 37 °C and 5% CO_2 for 30 minutes and allowed to stand for 1 hour. This cycle was repeated 4 times for better cellular distribution throughout the microcarriers. Cells and Cultispher® microcarriers were then transferred to 25 cm^2 polystyrene ultra-low attachment surface flasks (Corning, UK) and cellular propagation on 3D culture occurred either in static mode or wave mode on a PMR-30 compact-fixed angle platform rocker at a speed of 15 rocks per minutes (Grant-Bio) at 37 °C and 5% CO_2. Media changes took place every 3 days, at which point cell counts were taken.

2.5.4 Assessment of cellular attachment and cell number

2.5.4.1 Cell number

To monitor the seeded Cultisphers® microcarriers growth cell number measurements were made by assaying the metabolic activity of chondroprogenitors by PrestoBlue™ cell viability reagent (Life Technologies, UK). Serial dilution of a known number of cells was used to derive a standard curve. In brief, every 3 days Cultisphers® microcarriers were spun down and the media was aspirated off and 25 μL (n=3) of each experimental group was taken out and incubated with 10μl of PrestoBlue™ at 37 °C and 5% CO_2 for an hour. The absorbance was measured by a plate reader (FLOUstar Omega, BMG labtech) at an excitation and emission wavelengths of 544 nm and 590 nm respectively. The cell number was then calculated against the standard curve of known cell number. The total cell number was attained by multiplying the total remainder volume of cells/Cultisphers® by the number of cells calculated from the standard curve.

2.5.4.2 Cellular attachment

3-(4, 5-dimethylthiazol-2-yl)-2, 5-diphenyltetrazolium bromide (MTT) staining was used to visualise cell growth on microcarrier beads. Samples, which were used for PrestoBlue™, were utilised for MTT staining. Briefly, PrestoBlue™ was aspirated off and 100 μL of 5mg/mL MTT solution (Sigma, UK) was added to each sample and incubated for 1 hour at 37 °C and 5% CO_2. After one hour had elapsed samples were fixed and then imaged under light microscopy (Primo Vert, Zeiss) [313].

2.5.5 Transwells culture for chondrogenic differentiation

300 μL aliquots of each cell/Cultisphers® experimental group were pipetted onto dry 12 mm diameter hydrophilic polytetrafluoroethylene (PTFE), 0.4 μm pore size inserts (Millipore Ltd, UK) in a 24-well plate. One mL of chondrogenic media (2.4.1) was added to the inserts making sure that media covered the top of the inserts.

2.5.6 Mould fabrication

3D scaffold fabrication was done with polylactic acid (PLA) filament (Flashforge, China). Briefly PLA was melted at 110°C in a heating cylinder using CreatorPro 3D printer (Flashforge, China). PLA was ejected through a heated nozzle and deposited layer-by-layer. The C-ring shape was deposited at (55 mm x 56 mm x 110 mm) **(Figure 3)**. Following printing, the moulds were sterilised by incubation in alcohol and placed under UV light. Filter papers was sterilized in the same fashion and used as a membrane between cells/Cultisphers® for improved media exchange with the construct.

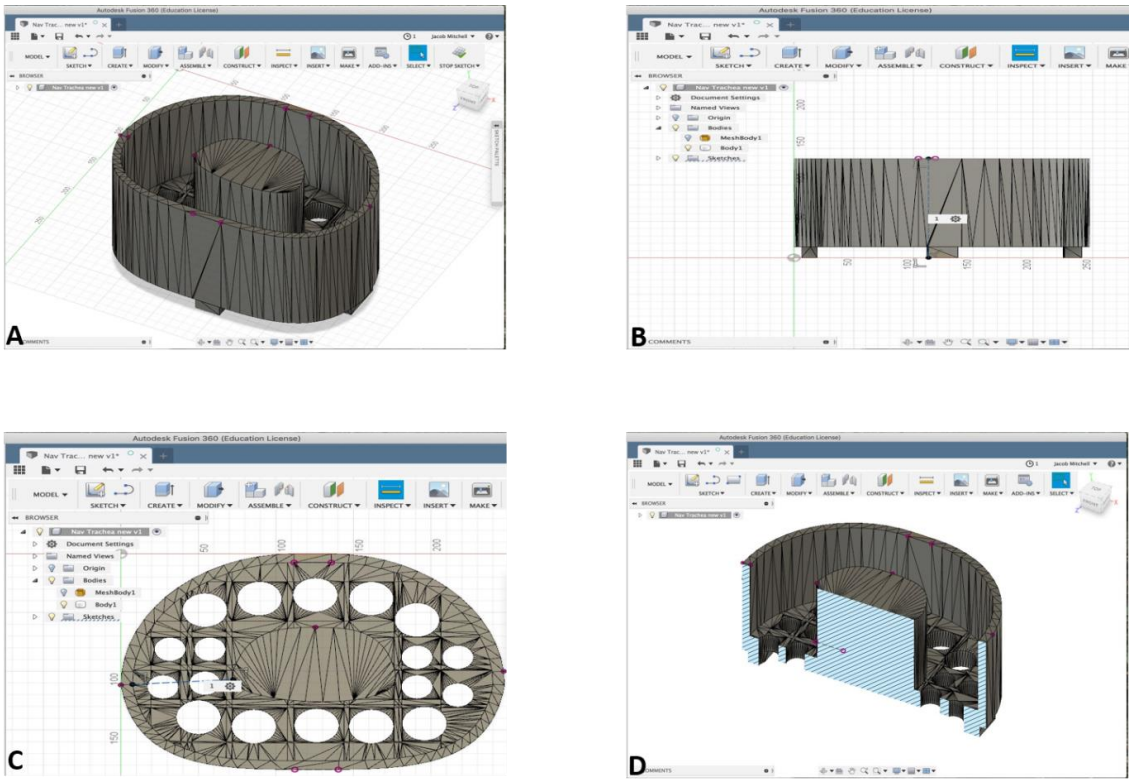

Figure 2.3. Preparation of 3D-printed PLA scaffolds for seeding of cells/Cultispher® microcarriers. Same principle as transwells were adopted in the C-ring scaffold. The 3D printed tracheal C-ring mould was designed to be placed in a 6-well plate with porous structure for improved nutrient diffusion.

2.6 Ribonucleic acid (RNA) extraction and complementary deoxyribonucleic acid (cDNA) synthesis

2.6.1 RNA protocol

Total RNA was extracted from cells and tissue (native or tissue engineered) using RNeasy kit and a DNase1 on-column digest; manufacturer's instruction was followed accordingly (Qiagen, UK).

2.6.2 RNA from cells

2.6.2.1 Cells after digest

Immediately after sequential pronase/collagenase **(2.2.1; 2.2.2)** 1 million cells were aliquoted and pelleted down in an Eppendorf tube in a microcentrifuge (Centrifuge 5424, VWR). Media was removed, and the pellet was disrupted and washed with PBS and centrifuged. This process was repeated twice. 350 µL of RLT lysis buffer (RNAEasy kit: Qiagen) was added to the pelleted cells which were gently disrupted using a pipette and stored at -80°C until further use. On the day of RNA extraction, cells were thawed on ice and the manufacturer's protocol for downstream processing for RNA extraction was followed with no deviation.

2.6.2.2 Primary cultured cells

RNA from monoclonal cultured cells were lysed by a cell scraper (Greiner Bio-one) at various passages by primarily washing the cells by PBS and adding 350 µL of RLT buffer. Samples were then stored at -80 °C until further use. On the day of RNA extraction, cells were thawed on ice and the manufacturer's protocol was followed to process to total RNA isolation using mini-columns.

2.6.3 RNA from pellets

After 21 days of chondrogenesis treatment was over pellets were snap frozen in a hexane ethanol dry ice bath and samples were stored at -80 °C. On the day of RNA lysing,

samples were thawed on ice and 350 μL of RLT buffer was added to each sample. Pellets were lysed and homogenized for 20-30 seconds using a probe and TissueRuptor (Qiagen, UK) at full speed. The lysis process took place on ice to reduce the heat produced by vigorous grinding. Lysed pellets were then stored at -80 °C for further use. On the day of RNA extraction, lysed pellets were thawed on ice and the manufacturer's protocol was followed.

2.6.4 RNA extraction from native tissue and Cultispher® microcarrier-based constructs

2.6.4.1 Native tissue

3mm^2 native tissue was prepared as outlined in **(2.2.1, 2.2.2)** and snapped frozen in a hexane ethanol dry ice bath and stored at -80 °C for further use. RNA processing took place in a clean fume hood. The frozen samples were placed in metal chamber lids containing grinding ball and 250 μL TRI reagent that was previously immersed in liquid nitrogen and further snapped frozen in liquid nitrogen. Tissue was then immediately lysed and homogenised using a micro-dismembranator (B. Braun Biotech) for 2 minutes at 230g. The powdered tissue/TRI was then transfer to a new Eppendorf tube with a spatula and transferred to -80 °C for further use. On the day of RNA extraction, lysed tissues were thawed on ice and 150 μL of chloroform was added to each sample and left at room temperature for 5 minutes. The next stage is as outlined in section **2.6.1**.

The chambers and grinding balls were cleaned between each cycle of dismembration by placing in soapy water, rinsing with tap, ddH_2O and placing in 5 M NaOH for 5 minutes and rinsing three times with ddH_2O.

2.6.4.2 Constructs

Same principle as outlined in section **2.6.4.1** was applied to Cultispher® microcarrier discs and constructs after the chondrogenic incubation period was completed. The discs were cut into quarter sized pieces and a single quarter was harvested and homogenised

for RNA isolation.

2.6.5 RNA quantification and purity

Purity of RNA was measured by absorbance at 260 nm and 280 nm using a NanoDrop NDI100 spectrophotometer (NanoDrop Technologies, UK). Nuclease-free water was used as a blank and samples were measured against it. The A_{260}/A_{280} ratio was used to assess RNA purity. An A_{260}/A_{280} ratio of ~2.0 is indicative of highly purified RNA.

2.6.6 Complementary DNA (cDNA) conversion

cDNA was synthesized from the purified RNA. 1 μg of RNA was used per reaction. The master mix contained 400 μM dNTPs (Promega, UK), 0.4μg of random primers (Promega), 0.2U/μL reverse transcriptase (RT) enzyme (Promega), 0.5U/μL RNasin (Promega) in a 50 μL volume. Samples were placed in a T100 thermocycler (Bio-Rad, UK) at 25°C for 10 minutes, 48°C for one hour and then 95°C for 5 minutes. Samples were immediately transferred to -20°C and kept for further use.

*For pellets 50-100 ng of purified RNA was used per reaction. Shredders (QIAshredder; Qiagen) were used to increase the amount of RNA recovered from pellets.

2.7 End-point polymerase chain reaction

To analyse the genes of interest cDNAs were amplified. The reaction mixtures were carried out in 100 μL volume consisting of 1.5 mM $MgCl_2$, 200 nM of each forward and reverse primer, GoTaq Flexi buffer and 1 unit of GoTaq Hot start DNA polymerase with the addition of 200 μM dNTPs and 0.2 ng/μL of template DNA. Amplification of cDNA occurred at the following protocol; denaturation at 95 °C for 3 minutes, amplification for 40 cycles at 95 °C for 30 seconds, allowed annealing at a specific temperature (T_m) for 30 seconds and the extension stage was held for 30 seconds at 72 °C. A final extension was held at 72 °C for 10 minutes. Samples were immediately transferred to -20 °C and kept for further use.

2.7.1 Primer design and sequences

The primers for this study were designed using porcine gene sequences from NCBI Map Viewer or Ensemble Genome Browser. Designed primers were evaluated in NCBI Primer-BLAST to check for binding specificity. Primer sets were purchased from (Sigma, UK). Primers are shown below. RT-PCR and quantitative polymerase chain reaction (qPCR) were performed using the listed primers.

Gene name	Forward primer sequence	Reverse primer sequence	Tm (°C)	Product size
CD73	TGGGGATGGATTCCGGATGA	TGGATCCGACCTTCAACTGC	60	129
CD90	ATTGGCATCGCTCTCTTGCT	GAATGGGCAGGTTGGTGGTA	60	133
CD105	AGGACTTGGTCCCTGGATGT	GTGTGCGAGTGGATGTACCA	60	170
CD166	GACAACGTGTTTGAGGCACC	ACCACGTGATGTTGCCATCT	60	157
Nestin (Nest)	GGAGAAACAGGGCCTACAGAG	CAGCTCCAACTTAGGGTCCA	60	193
CD13	ATCGACAGGACTGAGCTGGT	ACGTTGCCCTCCATGTACTC	60	161
CD 34	TACAACAGTACCAGCCCTGC	CTCATTTCGCTCCAGGCAGA	60	144
CD 45	ATGTTGTCAAGCTGAGGCGA	GAGAAGGTTCACTGGGTGGG	60	177
COL2A1	GAACAAGGACCCAGAGGTGA	CCTTCTCATCGAATCCTCCA	58	184
COL1A1	GTGCTGTTGGTGCTAAGGGT	CAGGAGCACCAGCAATACCA	60	189
COL10A1	CATCCCCTACGCCATAAA	TCTCTCCCCTGGTTTTCCTT	60	232
SOX9	GAAGCTGGCGGATCAGTACC	GTTCTTCACCGACTTCCTCCG	58	190
Aggrecan (ACAN)	CGCAGACTACAGAAGCGGAG	TGGGTGGGTGCATACACAAT	58	222
PRG4	TTGCAAGAGGAAGGGAGTGT	TGATTTGGGTGAACGTTTGA	60	185
Elastin (ELN)	CTGGTCTTGGACTGTCTCCT	ACCAACGTTGATGAGGTCGT	60	196
HPRT1	GGGAGGCCATCACATCGTAG	CGCCCGTTGACTGGTCATTA	60	167
GAPDH	CAAGGAGTAAGAGCCCCTGG	AGTCAGGAGATGCTCGGTGT	58	123

Table 2.1. Porcine gene primer sequence.

2.7.2 Agarose gel electrophoresis and imaging

The agarose gel was prepared one hour prior to the electrophoresis run by adding 2% agarose (w/v; Promega, USA) to 1 x TAE (20 mL of 50x TAE buffer was added to 980 mL of ddH_2O to obtain a working concentration of 1x TAE buffer). The agarose in TAE buffer was heated using a laboratory microwave set to full power (800W) until the agarose was fully dissolved and the solution was completely clear. Once the agarose was

dissolved 10 μL of SYBR™ safe DNA gel stain (Invitrogen, UK) solution was added, and the solution poured into the gel mould and allowed to set with a gel comb in place for 45 minutes to allow the gel to set. The gel was removed from the mould and placed in the electrophoresis tank containing 1x TAE buffer. The comb was removed from the gel and the ladder (Thermofisher, UK) and samples were then mixed with 5x loading dye (Sigma, UK) and loaded into the wells. The gel was visualised using a ChemiDoc MP system (Bio-Rad, UK).

2.8 qPCR

qPCR was undertaken using CFX96 Real Time PCR Detection system (Bio-Rad, UK). Primers were designed to amplify a single PCR product of approximately 100-200bp in length. An internal reference glyceraldehyde 3-phosphate dehydrogenase (GAPDH) was used for normalisation as well as non-reverse transcribed RNA as a negative control. Each reaction was prepared to a total volume of 10 μL; 2.5 μL 4μM primer mix (forward and reverse), 2 μL sample cDNA and 5 μL SYBR Green. All PCR reactions were conducted in triplicate to reduce pipetting error. All PCR reactions were performed in a clear unskirted 96 well plate (cat: MLL-9601, Bio-Rad) sealed with a microseal (cat: MSB-1001, Bio-Rad). Plates were heated for 30 seconds at 95 °C then real time data was collected during 40 cycles containing a 2 second step at 95 °C and 5 seconds at the optimal annealing temperature for specific primers outlined in Table 2.1.

2.9 Biochemical analysis

To measure the main extracellular matrix content biochemical assays were used to compare the levels present in tissue-engineered constructs against the native tissue.

2.9.1 Sample digestion (native tissue, pellets, constructs)

Snap frozen samples were digested with papain (Sigma, UK). The digestion buffer consisted of 20 mM sodium acetate (NaAc) pH 6.8, 1 mM ethylenediaminetetraacetic

acid (EDTA), 2mM DL-dithiothreitol (DTT), 300 μg/mL papain. One millilitre of papain digestion buffer was added to the samples and incubated at 60 °C in water bath for 60 minutes or longer if any tissue had remained after this time. Digested samples were stored at -20 °C prior to biochemical analysis.

2.9.2 DNA quantification

Assessment of cell numbers in samples were performed by quantitating the total DNA content in the samples using Quant-iT^{TM} (Invitrogen) PicoGreen dsDNA according to the manufacture's protocol. Samples were quantified against a series of λ DNA standard diluted in 1x TE buffer provided in the kit (0-10 μg/mL). Fluorescent absorbance was measured using FLUOstar Omega plate reader.

2.9.3 Dimethyl methylene blue (DMMB) assay

For each reaction, 25 μL of papain-digested samples were added to 200 μL of DMMB reagent (16 mg/L DMMB, 3 g Polyvinyl alcohol (PVA), 3.04 g glycine, 2.37 g sodium chloride (NaCl), 95 mL 0.1M HCl at final pH 3) in a 96 well. Concentrations of glycosaminoglycan were determined against standards of chondroitin-4-sulphate (0-40 μg/mL-diluted in ddH_2O) by spectrophotometric measurement of absorbance at 525 nm using a FLUOstar Omega plate reader.

2.9.4 Hydroxyproline assay

Hydroxyproline content was determined as a measure of total collagen present in each construct by assaying acid hydrolysates of papain digested samples. Briefly, standard concentrations of trans-4-hydroxy-L-proline (Sigma) were produced (0-100 μg/mL-diluted in ddH_2O) to determine the quantity of the total collagen. Papain digested samples were firstly hydrolysed in 6N HCl for 24 hours at 110°C using a heating block. Hydrolysed samples were then vacuum dried overnight and subsequently reconstituted in ddH_2O. After centrifugation to remove impurities, 30 μL of each sample was added to

a 96 well plate and 120 µL (70 µL of diluent plus 50 µL oxidant) was added to each sample prior to shaking for 5 minutes at room temperature. 125 µL of colour reagent was then added and samples shaken prior to incubating at 70 °C for 15 minutes. Hydroxyproline content was then quantified against a standard curve and a plate reader to measure absorbance at 540nm.

- Stock buffer: 28.5 g sodium acetate trihydrate, 18.75 g tri sodium citrate dehydrate, 2.75 g citric acid, 200 mL Propan-2-ol
- Diluent: 100 mL propan-2-ol, 50 mL H_2O
- Oxidant: 0.7 g Chloramine T, 10 mL H_2O, 50 mL stock buffer
- Colour reagent: 7.5 g dimethylamino benzaldehyde, 11.25 mL perchloric acid (60%), and 62.5 mL propan-2-ol

2.10 Histological analysis

2.10.1 Sample embedding (native tissue, pellets, constructs)

Samples were washed with PBS then fixed in 10% neutral buffered formalin solution (NBFS; Sigma, UK) overnight at 4 °C. After fixation, samples were washed twice with PBS and stored in 4°C fresh PBS. Samples were then handed over to the Pathology Unit at Singleton Hospital (ABMU, NHS) for wax embedding and stored at 4 °C prior to sectioning.

2.10.2 Paraffin wax sectioning

Samples in wax blocks were placed on ice for an hour before sectioning. A microtome was used to section the samples at 8µm thickness. Samples were then placed into a water bath at 45 °C to flatten. Flattened samples were removed from the water bath and immobilised to poly-l-lysine coated Poly-Prep slides (Sigma, UK) and dried at 45 °C for 48h. Samples were then stored at room temperature, in darkness until histological staining was performed.

2.10.3 Sample processing

On the day of staining samples were deparaffinised in xylene (2x10 minutes) and rehydrated in graded alcohol for 2 minutes at each concentration; concentrations of ethanol were 100% (x2), 95% and 70% followed by 2 minutes in tap water. Following each staining protocol samples were dehydrated in graded alcohols (70%, 95% and 100% x 2) with changes of 2 minutes each before being cleared in xylene (one change of 10 minutes). Stained sections were and mounted using DPX and then dried at 45°C overnight (Raymond A Lamb Medical, UK).

2.10.4 Haematoxylin and eosin

Nucleus and tissue morphology were detected by haematoxylin (TCS Biosciences, UK) and eosin (TCS Biosciences, UK) staining. Rehydrated slides were stained in 1% (w/v aqueous) haematoxylin for one minute and then washed in running water until excess stain had removed. The stain was differentiated in 1% acid-alcohol for 2 seconds and washed with running water before proceeding to staining with 1% (w/v aqueous) eosin for two minutes and then washed in running water until excess stain had been removed. Samples were dehydrated in graded alcohols and cleared in 2 changes of xylene before mounting under DPX on a cover slip.

2.10.5 Alcian blue

Sulphated GAGs were detected by alcian blue (Sigma, USA) staining. 1% alcian blue staining solution was made by dissolving 1g in 100 mL of 0.1N hydrochloric acid (HCL; Sigma, UK). On the day of use the pH was adjusted to 2.5. Cells stained in alcian blue solution for 30 minutes and rinsed three times with 0.1N HCL.

2.10.6 Toluidine blue staining

Sulphated GAGs were detected by toluidine blue (BDH chemicals, England) staining.

Rehydrated slides were stained in 0.5% aqueous toluidine blue for 30 seconds. Following staining, sections were washed in running water for 2 minutes. Toluidine blue stained sections were air-dried overnight and mounted on coverslips using DPX the following day.

2.10.7 Oil red-O staining

To confirm lipid deposition oil red-O (Sigma, UK) staining was carried out. Cells were fixed in 10% neutral buffered formalin with saline (NBFS) for 10 minutes and washed in PBS. Fresh Oil red-O was prepared from a stock solution of 3% (w/v) Oil red-O in 100% isopropanol by diluting 30mL stock solution in 20ml distilled water. Cells were rinsed in 60% isopropanol and stained with Oil red-O working concentration for 30 minutes at room temperature.

2.10.8 Alizarin red staining

To detect calcium deposition alizarin red (Sigma, UK) staining was carried out. Slides were rehydrated, and cells were fixed in 10% NBFS for 10 minutes then washed in PBS. Samples were stained in 2% aqueous alizarin red with adjusted pH 4.22 solution for 30 minutes. Samples were dehydrated in acetone for 20 seconds, then acetone: xylene (1:1) for 20 seconds before clearing in xylene. Samples were mounted using DPX under a cover slip prior to light microscopic analysis.

2.10.9 Crystal violet staining

To visualise colonies derived from single progenitor/stem cells crystal violet (Sigma, UK) staining was used. Cells were fixed in 10% NBFS for 10 minutes and washed in PBS. Samples were stained in 0.05% aqueous crystal violet solution in dH_2O for 30 minutes and washed multiple times in tap water until excess stain was removed. Cells were then imaged using light microscopy.

2.10.10 Verhoeff's

To detect elastin fibers Verhoeff's staining was carried out. Slides were deparaffinised and rehydrated. Samples were then placed in Verhoeff's solution for 15 minutes and were washed with running water until cleared. Samples were then differentiated until the elastic fibres were visible based on the appearance of fibres in area of interest. Samples were then washed with running tap water and placed into 95% ethanol for 5 minutes to remove iodine discolouration. Samples were washed in running water and dehydrated in graded alcohols and cleared in 2 changes of xylene before mounting under DPX on a cover slip.

- Stock Verhoeff A: Hematoxylin 1 g, absolute ethanol 20 mL
- Stock Verhoeff B: Ferric chloride 10 g (Sigma, UK), ddH_2O 100 mL
- Stock Verhoeff C: Potassium iodide 4 g (Sigma, UK), iodine 2 g (Sigma, UK), ddH_2O 100 mL
- Working Verhoeff's solution: Stock solution A: 20 mL, stock solution B: 8 mL, stock solution C: 8mL
- Differentiator solution: Stock solution B: 10 mL, ddH_2O 40 mL

2.11 InCell analysis

An InCell Analyser 2000 (GE Healthcare) was used to examine the physical characteristics of different stem/progenitor cells from tracheal cartilage, adventitia and connective tissue by staining F-actin and nucleus of cells using phalloidin and 4′,6-diamidino-2-phenylindole (Dapi) respectively. All cells were expanded as described in Section **2.3**. The earliest passage cells that were utilized for physical property analysis were P2 cells as monoclonal cells were propagated and analysed. In brief 20,000 cells were seeded in a 12-well plate and left at 37 °C and 5% CO_2 overnight. After 24 hours had elapsed cells were fixed with 10% NBFS for 10 minutes and washed with PBS twice. Following fixation, cells were permeabilised with 0.01% Triton X-100 (Sigma, UK) in PBS for 10 minutes at room temperature. Cells were then stained with phalloidin-Atto 594 (Sigma, UK), Stock solution was prepared at 10 nM in methanol

and working concentration was prepared by adding 15 μL of stock to 985 μL of PBS with the working concentration of 66 pM. Fixed cells were incubated with phalloidin at 37°C and 5% CO_2 for 3 hours, then washed twice with PBS and countered stained with Dapi (1:500, Sigma, UK) for 5 minutes at room temperature and washed twice with PBS and re-suspended in PBS prior to imaging. Image data was obtained using two emission spectra channels; Dapi nuclear staining (Channel 1: λ 470 nm for 0.1 seconds) and phalloidin-Atto F-actin staining (Channel 2: λ 594 nm for 3 seconds). The exposure time kept consistent throughout all samples. For each well, 6 random fields were chosen and once analysis was completed, a data file (XDCE) was produced containing all accumulated images from the channels and fields of view selected. Segmentation settings were applied the same way in all samples and it was made sure no overlapping had occurred. Morphological parameters were selected on the software for analysis of the shape and gross morphology of different stem/progenitor cells.

2.12 Mechanical properties

Mechanical integrity of the native tissue and constructs were analysed both at nano-indentation level and macro tensile level. Atomic force microscopy was further used to assess the mechanical properties of different stem/progenitor cells.

2.12.1 Nanoscale (AFM)

2.12.1.1 Single cells

The biomechanical properties of the progenitor cells at various passages were examined by nano-indentation. Cells were prepared as previously described in 2.3. one thousand cells were seeded onto a polystyrene petri dish (Corning, UK) and incubated at 37 °C and 5% CO_2 overnight. After 24 hours had elapsed cells were fixed with 10% NBFS for 10 minutes and washed with PBS twice.

Cells were analysed in fluid using a BioScope Catalyst atomic force microscope (Bruker Instruments, Santa Barbara, California, USA). Bruker MLCT-D pyramidal silicon nitride cantilevers were used as probes, with spring constant of (k ~ 0.03-0.04 N/m),

225μm length, and 20μm width and deflection sensitivity experimentally determined prior to each measurement. For each cell type, a minimum of 20 cells from a 5μm^2 area, consisting of nucleus and cytoskeleton, were analysed, by mapping 25 force curves within each area. 1nN was applied to all the cell types and the contact regime of the approach curve was fitted with the equation of a spherical indenter (Hertz model), using the fitting module of Nanoscope Analysis software, v1.50, and only curves with a goodness of fit between 0.90 and 1 were considered for statistical analysis.

2.12.1.2 Native tissue, pellets and constructs

Snap frozen tracheal tissues were brought to room temperature and localized nano-indentation took place in fluid at 37 °C with MLCT-E pyramidal silicon nitride cantilevers as probes, with spring constant of (k ~ 0.1-0.2 N/m), 140 μm length, and 18μm width and deflection sensitivity experimentally determined prior to each measurement. Three individual biological samples were analysed with contact mode for each tissue compartment and 5nN was applied to all the tissue type. 50 force curves were obtained from 5 μm^2 area. Tissue elasticity was obtained by Hertz model by calculating the Young's Modulus. Only curves with a goodness of fit between 0.90 and 1 were considered for statistical analysis.

Due to sample surface's roughness and comparing the matrix produced by pellets and constructs with different chondrogenic medias paraffin embedded sections were utilized [314]. Slides were prepared as described in Section **2.10.3** Similarly to native tissue analysis sections were indented in fluid with identical scenarios as mentioned at ambient temperature. The indentation perpetually took place at <10% of total sample thickness, hence choosing a small triggering force to track the differences in-between sample conditions.

2.12.2 Macroscale (Tensile testing)

Uniaxial materials testing system (Instron Model 5900, UK) was employed to determine tensile properties with a 2 kN load cell. Briefly, samples were trimmed to the same size

(10 mm x 5 mm) and a thickness of 1-2 mm. Samples were placed to paper on tensile grips with sand paper to ensure stability during the measurement. Specimens were mounted with an initial grip-to- grip distance of 10 mm and were subjected to ramp displacements at a rate of 5 mm/s up to rupture. All samples broke within the gauge length. Applied displacements were normalized to initial grip- to-grip distance to yield values for tissue strain. Sample width and thickness were used to calculate cross-sectional area, which was used to convert measured loads to stresses. The tensile modulus was determined from the stress-strain data by calculating the slope of the linear region of the curve.

2.13 Immunohistochemistry

Paraffin wax embedded tissues/pellets/construct sections were dewaxed and rehydrated as describe in Section **2.10.3**. To reduce background stain samples were treated with 3% hydrogen peroxide (H_2O_2) in methanol. Following this step samples were washed in PBST (PBS plus 0.05% Tween-20) for 5 minutes. Samples were then treated for antigen retrieval and initially incubated at 65 °C in Tris EDTA at pH 9 overnight and washed with PBST before the next stage. Next, sections were subjected to enzymatic treatment using hyaluronidase (Sigma-Aldrich; 2U mL^{-1}) in PBST at 37 °C for 1 hour. Samples were then washed with PBST for 5 minutes and using a hydrophobic wax pen, circles were drawn around the samples before proceeding to the blocking step. 2.5% normal horse block serum (RTU Vectastain Kit, Vector Laboratories, USA) was added for 30 minutes to prevent non-specific biding of antibodies. Blocking serum was then tipped off and primary antibodies diluted in PBST was added to specimens and left at room temperature for 30 minutes. PBST was used instead of antibodies for negative control samples. Samples were then washed with PBST for 5 minutes and secondary antibodies were added for 10 minutes at room temperature (RTU Biotinylated pan specific antibody Universal Biotinylated Anti-Mouse/Rabbit /Goat IgG derived from horse). Samples were then washed with PBST for 5 minutes. Streptavidin/peroxidase complex reagent (RTU Vectastain Kit, Vector Laboratories, USA) was applied to samples at room temperature for 5 minutes, and then samples were rinsed in PBST for 5 minutes. After washing samples were developed for 5 minutes with NovaRED kit (Vector Laboratories,

USA) for detection of streptavidin/peroxidase enzymatic activity. Samples were then washed and in dH_2O and nuclei were counterstained with hematoxylin for one minute. The specimens were then dehydrated in graded alcohol and mounted. Samples were then analysed using light microscopy to examine extracellular matrix quality.

- List of antibodies used: Collagen type II (1:250, Devlopmental Studies Hybridoma Bank (DSHB) II-II6B3 raised in mouse); Aggrecan (1:10, DHSB 12/21/1-C-6 raised in mouse), Collagen type I (1:2000 Sigma C2456, UK).

2.14 Statistical analysis

All statistical approaches were performed using Minitab software for data analysis and Excel for plotting graphs. All data sets were first analysed for normality using the Anderson Darling test, as previously described [315]. For parametric data sets, statistical significance was calculated using student's *t* test for paired wise analysis and one-way or two-way ANOVA depending on the number of variance followed by Tukey's posthoc test. For non-parametric testing a whole sample analysis of variance was applied using the Kruksal-Wallace test, followed by differences in means assessment between pairs of data using the Mann Whitney U-test [316]. In this study, all statistical significance threshold values are $p < 0.05$, unless otherwise stated in the text. All statistical analysis for each data set described is listed in the figure legends.

Chapter 3: Identification and characterisation of tracheal C-ring derived stem cell populations

3.1 Introduction

Tissue engineering applications generally require high cell numbers and these are generated through long-term cell culture expansion *in vitro*, with the aim of maintaining phenotypic stability and potency of cells [89]. Culture expansion remains a challenge, with both cell source and culture conditions significantly affecting cell number yields [317]. Therefore, the ability to harvest stem/progenitor cells capable of extended expansion in culture is a prerequisite for stem cell-based therapies, enabling the regeneration or repair of damaged and diseased tissues [121]. Thus far the two major cell sources used to date in airway cartilage tissue engineering are chondrocytes from various locations and bone-marrow derived MSCs [297][298].

Despite considerable efforts to repair and regenerate damaged and missing tracheal tissues using native chondrocytes and MSCs, the engineered tissues lack organisation and functional properties at multiple levels [130]. At the genetic level, up-regulation of collagen types I and X are indicative of either inappropriate, incomplete or the failure of chondrocyte differentiation, or, epiphyseal-type chondrocytes and their terminal differentiation to form calcified cartilage, a precursor to bone formation, especially when bone-derived MSC derived progenitors are used [136]. The mechanical properties of repair tissues made using bone-derived MSCs have been shown to be compromised, with cartilage repair tissue unable to match native tissue properties [192][299]. Cell choice therefore is at the heart of the complex regenerative challenge; an optimal cell source would have stem/progenitor cell characteristics, with the capacity for extensive cell expansion and the maintenance of a latent ability to undergo chondrogenic differentiation when exposed to inducing stimuli [321].

Many cartilage tissue engineering strategies now employ stem or progenitor cell populations especially where, as is the case with tracheal repair, residual tissue as a source for cells is scarce or not available [301][302]. To isolate stem/progenitor cells of the mesenchymal lineage certain minimal selection criteria have been suggested based upon the inability to use cell-specific biomarkers [303][304]. Generally, isolation of MSCs relies primarily on their ability to bind to plastic culture dishes, their expression of a specific subset of cell surface markers which consist of panels of positive and

negative hematopoietic-related biomarkers, as well as having the potency to differentiate into multiple mesodermal-derived lineages [135]. The latter criteria can be further refined by incorporating techniques such as differential adhesion to fibronectin as in the case of chondroprogenitor isolation in articular cartilage [219] and also using biophysical markers such as cytoplasmic/nuclei ratios to enhance isolation strategies [326].

New strategies are exploiting the use of tissue specific stem cells as they may contain the prerequisite memory to differentiate towards the tissue of origin. Approaches to isolate pure stem/progenitor subpopulations in cartilage exploit the fact that they express higher levels of fibronectin receptor integrins α5 and β1 [327]. Limited exposure of an unsorted freshly isolated cell populations to fibronectin coated culture dishes results in the binding of subpopulations with highest fibronectin receptor levels, with the remaining unbound population removed by washing. This form of enrichment generates colonies at higher frequency allowing expansion of either polyclonal or monoclonal progenitor populations. As an example, Jones *et al.* utilised differential adhesion to fibronectin *in vitro* to identify and isolate epidermal stem cells [328]. It was found that the epidermis layer contains two types of proliferative cells; sub-population of cells with lower expansion capacity and higher differentiation capacities known as transient amplifying cells, and, stem cells with significantly higher expansion capacity, termed progenitor or stem cells. Keratinocytes with stem cell-like behavior could be isolated using FACS based on high surface expression of integrin β1 and high affinity for ECM proteins such as fibronectin. In their studies, keratinocyte colony forming efficiency directly correlates to the relative levels of integrin β1 and fibronectin expression. Their study also delineated strategies to enrich and purify homogenous sub-populations capable of extensive proliferative capacity, as opposed to transient amplifying cells that undergo terminal differentiation after only five population doublings [329]. Prior to this finding Barrandon *et al.* identified three distinct types of colonies formed by keratinocytes when cultured at clonal density. They found that large circular colonies exhibit a high self-renewal capacity and that were proliferative. Small irregular shaped colonies containing 32-128 cells were also observed which had characteristics similar to transient amplifying

cells and a third type of clone which had intermediate characteristic to the first and second clones [330].

As mentioned previously, differential adhesion to fibronectin was used by Dowthwaite *et al.* [219] to enrich colony forming cell sub-populations from articular cartilage of the metatarsophalangeal joint of 7-day old bovine articular cartilage [331]. Previous studies have shown that chondrocytes in the superficial surface of articular cartilage express relatively higher expression of α5 and β1 integrin subunits compared to chondrocytes in the mid and deep zones [331]. Using this information, Dowthwaite *et al.* used differential adhesion to fibronectin to measure the frequency of colony forming cells in chondrocytes specifically isolated from the superficial, middle and deep zones of articular cartilage. They reported that chondrocytes isolated from the superficial zone formed significantly larger colonies and at higher frequency than chondrocytes from the other zones. Their results also showed that integrin β1 by itself could not be used as a chondroprogenitor marker as chondrocytes from middle zone expressed more affinity for fibronectin as opposed to the superficial zone cells, but lacked colony forming ability. The latter cell population showed similar characteristics to transient amplifying cells. Clonal chondroprogenitors were shown by Khan *et al.* to maintain telomerase activity and SOX9 expression during extended monolayer culture and retain chondrogenic potential when compared with their chondrocyte counterparts [222]. Further confirmation of the stem/progenitor status of colony forming cells isolated from articular cartilage required verification using the minimal criteria set down by The International Society for Stem Cell Research (ISSCR). The ISSCR set down a minimal criteria for the classification of MSCs to include; adhesion to plastic, expression of surface markers CD73, CD90, CD105 and lack of expression for haematopoietic lineage markers including CD11b, CD14, and CD45 and tri-potential differentiation into chondrogenic, osteogenic and adipogenic lineages [135].

Friedenstein first reported plastic adherent, clonogenic fibroblastic-like cells derived from bone marrow extracts [332]. These marrow stromal cells (MSCs) were inherently more prone towards differentiation towards the osteogenic lineage. Accumulation of data from many studies has shown that MSCs can be identified and also isolated from

heterogeneous populations using positive and negative markers. MSCs commonly express CD29, CD44, CD49a-f, CD51, CD73, CD90, CD105, CD106, CD166, and Stro-1 [121], [333]–[335] and must be negative for haematopoietic lineage markers including CD11b, CD14, and CD45 [336]. Based on this isolation criteria many tissue-specific MSCs have been identified and characterised [189][204]. For example, Williams *et al.* were able to isolate tissue specific chondroprogenitors using the cell surface criteria from healthy human adult articular cartilage; these cells differentially bound fibronectin, had a high colony forming efficiency, were capable of extensive self-renewal and multipotent differentiation [220].

Although efforts have been made to isolate pure MSC populations, the lack of specific biomarkers for these cells makes this process challenging. Using cartilage as an example, Alsalameh *et al.* identified a sub-population of stem-like cells expressing cell surface markers CD105 and CD166 in human cartilage at a frequency of 1.5% from normal cartilage and 3% from diseased osteoarthritic cartilage [337]. The majority of chondrocytes were found to express CD105 and a minority CD166. Grogan *et al.* reported using the expression and distribution of stem cell markers Notch-1, Stro-1 and CD105 a large sub-population of cells in articular cartilage, 45% of cells were labeled for these cell surface markers, therefore, the specificity of this combination is thought to be insufficient to isolate a putative low ratio progenitor MSC sub-population. It is clearly challenging to define a unique set of criteria that enables robust identification and isolation of a pure multipotent MSC cells [317][318]. Therefore, new approaches to describe and isolate specific subpopulations of MSCs and chondroprogenitors will significantly contribute to basic biological understanding of tissue growth, development and dysfunction and in turn consequently improve cell-based therapies.

MSCs lose their differentiation capacity over a long period of 2D culture expansion [340]. This decreased differentiation potential has been correlated with environmental cues that directly affects genetic and metabolic features of MSCs (refer to **1.9.1**) [260][262]. The lack of specific biomarkers, and, non-optimal culture conditions that affect the expression of the minimal criteria cell surface markers following extensive expansion, has therefore prompted researchers to investigate alternative methods to

predict the potency and stem/progenitor status of MSCs. The biophysical properties of a cell, which are known to change during growth and development, could potentially be used as an indicator of a cell identity, function and potency. Physical changes that take place over time in cells include measurable parameters such as cell size, morphology and stiffness [320][321], and these can potentially be used as predictive markers of cellular fate. For instance, metastatic cancer cell lines show an average mechanical creep compliance [343], and malaria infected [344] or sickle red blood cells [345] mechanical membrane stiffness have been directly linked to disease stage and progression. Common biophysical traits can also be interpreted as measures for cellular change. For example, changes in cell size are linked with cell cycle events [346] and cellular proliferation rates [347], but also indicate the differentiation capacity of progenitor cells derived from corneal epithelium [348], adipose tissue [349], or adult bone marrow [350]. Therefore, it is evident that a more comprehensive physical profile of stem cells can supplement the minimal criteria to form more reliable indicators.

Lee *et al.* used multivariate biophysical analysis of culture-expanded; bone marrow-derived MSCs, correlating these quantitative measures such as cell diameter and stiffness with biomolecular markers and *in vitro* and *in vivo* functionality. They reported no single biophysical property robustly predicts stem cell multipotency, but a combination of three biophysical markers together have the potential to predict multipotent subpopulations *in vitro* and *in vivo*. Subpopulations of culture expanded MSCs from adult and fetal bone marrow were found to have small cell diameter, low cell stiffness, and higher nuclear membrane fluctuations, and in addition they were highly clonogenic and also exhibited gene, protein, and functional signatures of multipotency [326]. Darling *et al.* revealed that terminated differentiated cells consisting of chondrocytes, adipocytes, osteocytes and MSCs isolated from adipose and bone marrow tissues had distinct mechanical properties indicating that even undifferentiated MSCs from two unique tissue sources exclusively differ from one another [294].

This chapter hypothesises that there is a mesodermal derived stem cell residing in the tracheal C-ring cartilage that would be an ideal source for repair strategies. Furthermore, an efficient and informative biological selection criterion of suitable cells will lead to an

isolated cellular population with the required gene expression and matrix deposition programmes which may in turn lead to repair strategies that reflect the correct functional cell and tissue mechanical properties. To test this hypothesis, the aim was to use differential adhesion to fibronectin to isolate cellular populations from each tissue layer of the trachea (adventitia, cartilage and connective tissues) and subsequently characterise these cells in line with ISSCR minimal criteria as well as biophysical properties. Mechanical stability is of great importance in airway tissue engineering. Identifying a population of cells with stem cell characteristic and epigenetic 'memory' towards cartilage differentiation that is able to maintain its phenotypic stability over long term culture will help researchers towards the successful generation of constructs with genetic and mechanical functionality

3.2 Results

Porcine trachea possesses functional and gross morphological similarities with human trachea, and therefore it was chosen as a suitable model for translational research [311].

The aims of this experimental chapter can be broken down into two distinct objectives as shown in **Figure 3.1**; first, characterisation of the key structural components of the tracheal cartilage C-rings utilising histological staining, mechanical testing and mRNA comparison to articular cartilage. Secondly, isolation of tracheal C-ring derived progenitor-like subpopulations utilising, differential adhesion to fibronectin and characterisation of these progenitor subpopulations using minimal criteria as recommended by the ISSCR, as well as morphological analysis and mechanical properties of single cells.

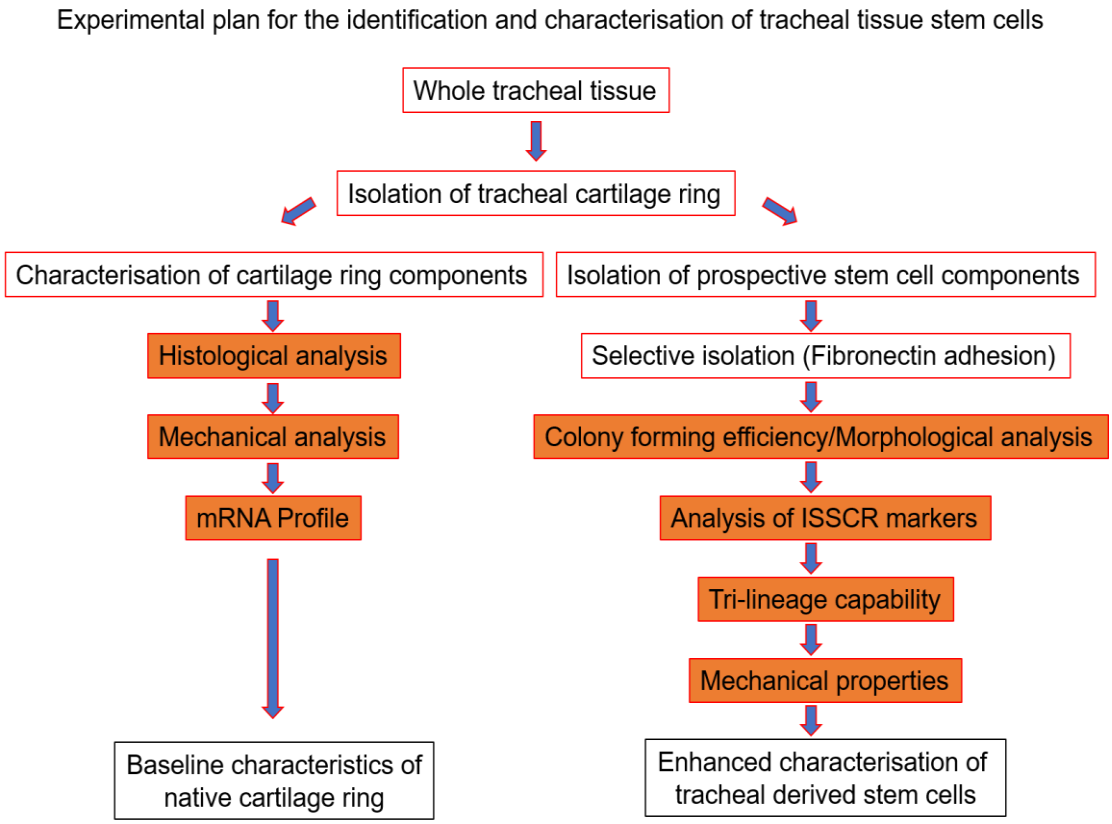

Figure 3.1. Pipeline of porcine trachea characterisation. Experimental plan for tracheal tissue and identification and characterisation of tracheal tissue and stem cells.

3.2.1 Tracheal tissue characterisation

Fresh juvenile (6-month-old) porcine tracheal tissue was obtained from the local abattoir and used in compliance with institutional guidelines as set out by the University Research Ethics Committee.

3.2.2 Histological analysis of native porcine trachea

To visualise tissue and cellular organisation as well as detecting and localising the hyaline type matrix of tracheal cartilage, histological and immunohistochemical analysis were performed [351]. Upon arrival from the abattoir fresh trachea from 6-month-old porcine animals **(Figure 3.2A)** was sterilised and rinsed with PBS, dissected free from

annular ligaments and muscles, and cut into representative explants prior to fixation **(Figure 3.2B)** with 10% NBFS. The tissue was processed into wax and sectioned at 7 µm prior to rehydration and histological staining (Materials and methods Chapter 2, section **2.10.1- 2.10.3**).

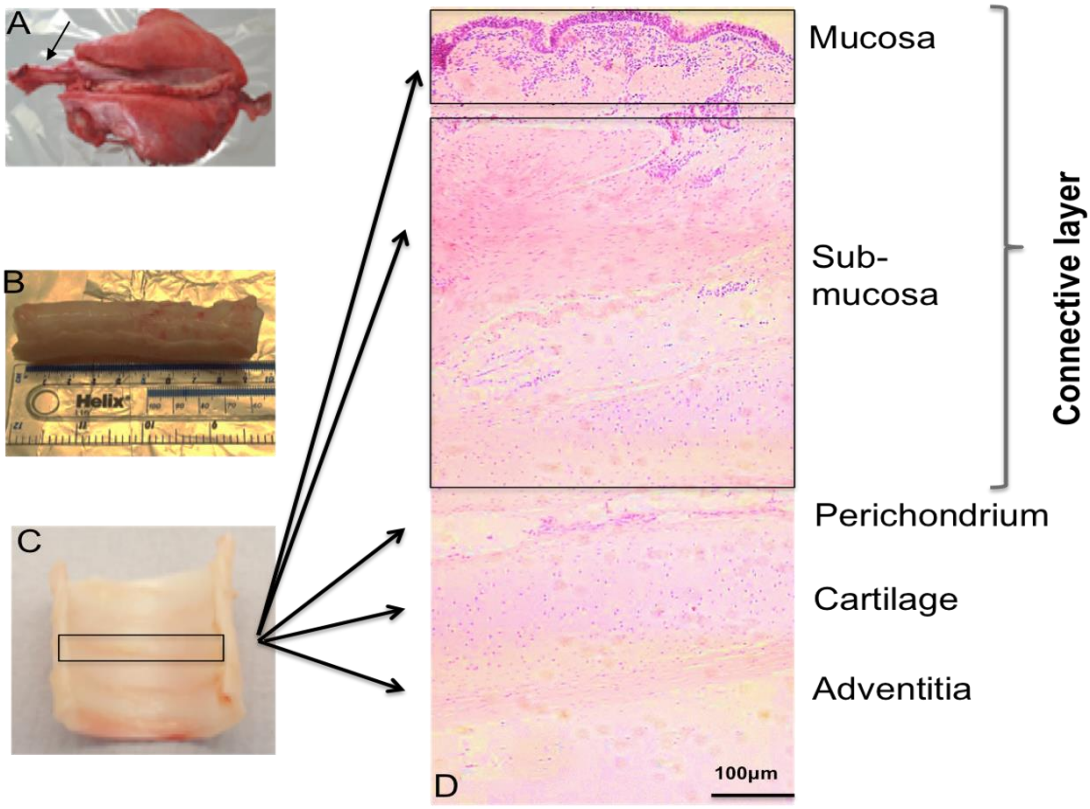

Figure 3.2. Porcine trachea haemotoxylin and eosin staining. (**A**) Location of trachea in the upper airway system (*arrowed*). (**B**) Trachea lumen dissected away from the lungs. (**C**) Shows a half-dissected portion of the tracheal ring structure and (**D**) a sagittal section displaying the morphology of tracheal tissue. Bar equals 100 microns.

Haematoxylin and eosin (H&E) stain was employed to display the cellular (with the cell nuclei stained blue) and tissue morphology (stained pink-purple). H&E staining was performed on tracheal C-rings excluding the muscle and annular ligament **(Figure 3.2C)**. Trachea is a multi-layered tissue, as shown in **Figure 3.2D**. The mucosal layer stained deep pink, as visualised in **Figure 2D**, at the top surface of the image identified clearly due to its pseudostratified ciliated columnar epithelium. The submucosal layer has a less organised architecture with submucosal glands present. There is also an

extensive underlying perichondrium or adventitia which is shown as a thin layer above tracheal cartilage, that itself, shows a typically large matrix to cell volume ratio.

To further analyse the ECM components of the native tissue toluidine blue histological staining was performed on the native trachea to localise the proteoglycan content of the C-ring. Toluidine blue labeling of proteoglycans was particularly evident in the cartilage layer, where it was stained intensely dark purple **(Figure 3.3B)**. Staining the native tracheal tissue with Verhoeff's stain revealed that elastin fibers are localised to the inner connective layer of the C-ring **(Figure 3.3C)** but not the cartilaginous component.

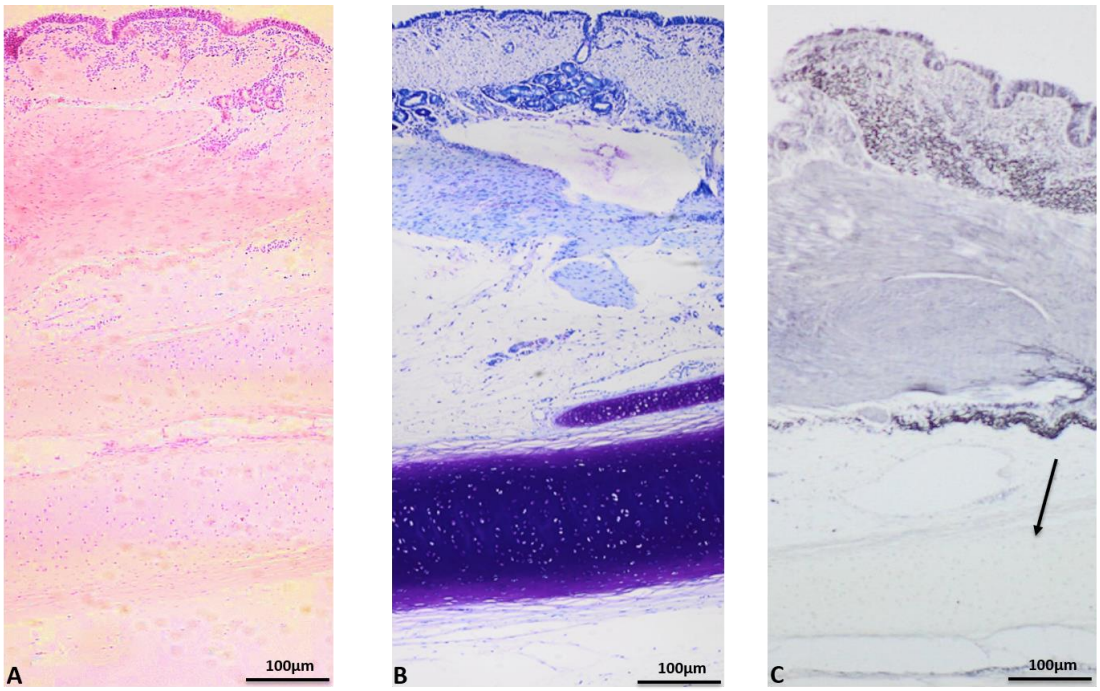

Figure 3.3. Histological analysis of native trachea tissue embedded for various stains in order to obtain the baseline control for the future production of C-ring cartilage *in vitro*. (**A**) Shows haeamotoxylin and eosin stain to represent the cellular structure and surrounding matrix. (**B**) Toluidine blue stain of tracheal tissue section to localise proteoglycan deposition. (**C**) Verhoeff's staining to identify elastin fibers in tracheal tissue where tracheal cartilage did not illustarte any stain uptake *(arrowed)*. Bar equals 100 microns. Images represent one porcine donor.

Immunohistochemical analysis of the 6-months-old porcine tracheal cartilage C-ring revealed strong collagen type II and aggrecan labelling throughout the cartilage layer **(Figure 3.4A-C)**. The connective and adventitia tissue layers were negative for antibody labeling for the two-main cartilage-specific ECM components.

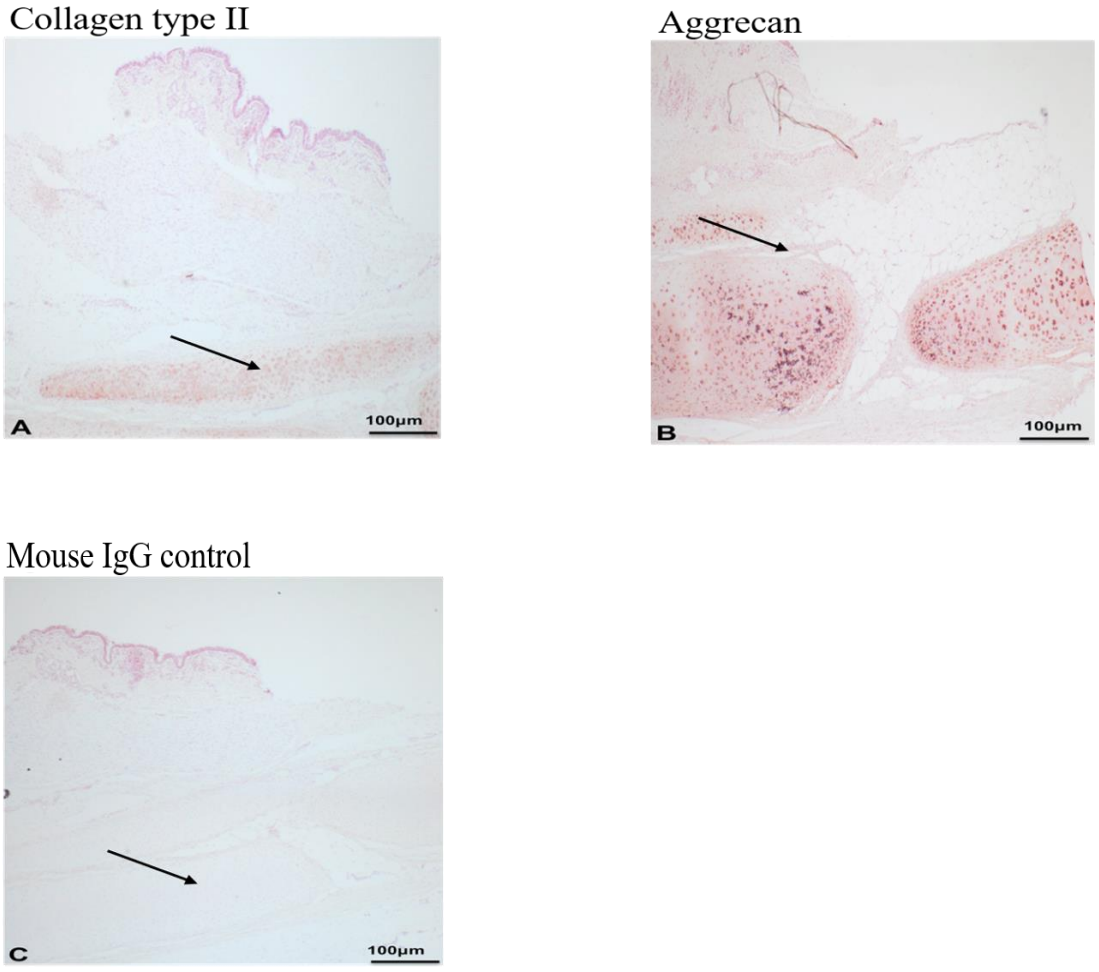

Figure 3.4. Immunohistochemical analysis of 6-month-old porcine trachea. Collagen type II (A), and aggrecan (B) immunostaining was performed and counterstained with haeamatoxylin to detect ECM specific proteins. (C) Mouse IgG was used at the same concentrations as the primary antibodies to identify any non-specific labelling in sections. Arrows indicate the tracheal cartilage. Bar equals 100 microns. Images represent one porcine donor.

Immunohistochemical collagen type I expression was absent in porcine tracheal cartilage and bovine auricular cartilage. However, the adventitia and the perichondrium

in trachea and auricular cartilage (used as a comparison of hyaline tissue) were both positive for labelling **(Figure 3.5)**.

The combined immunohistochemical and histological analysis enabled accurate identification of the mucosa, cartilage and adventitia components of the C-ring to enable uniaxial testing of the whole C-ring and different tissue layers of the tracheal C-ring (see below).

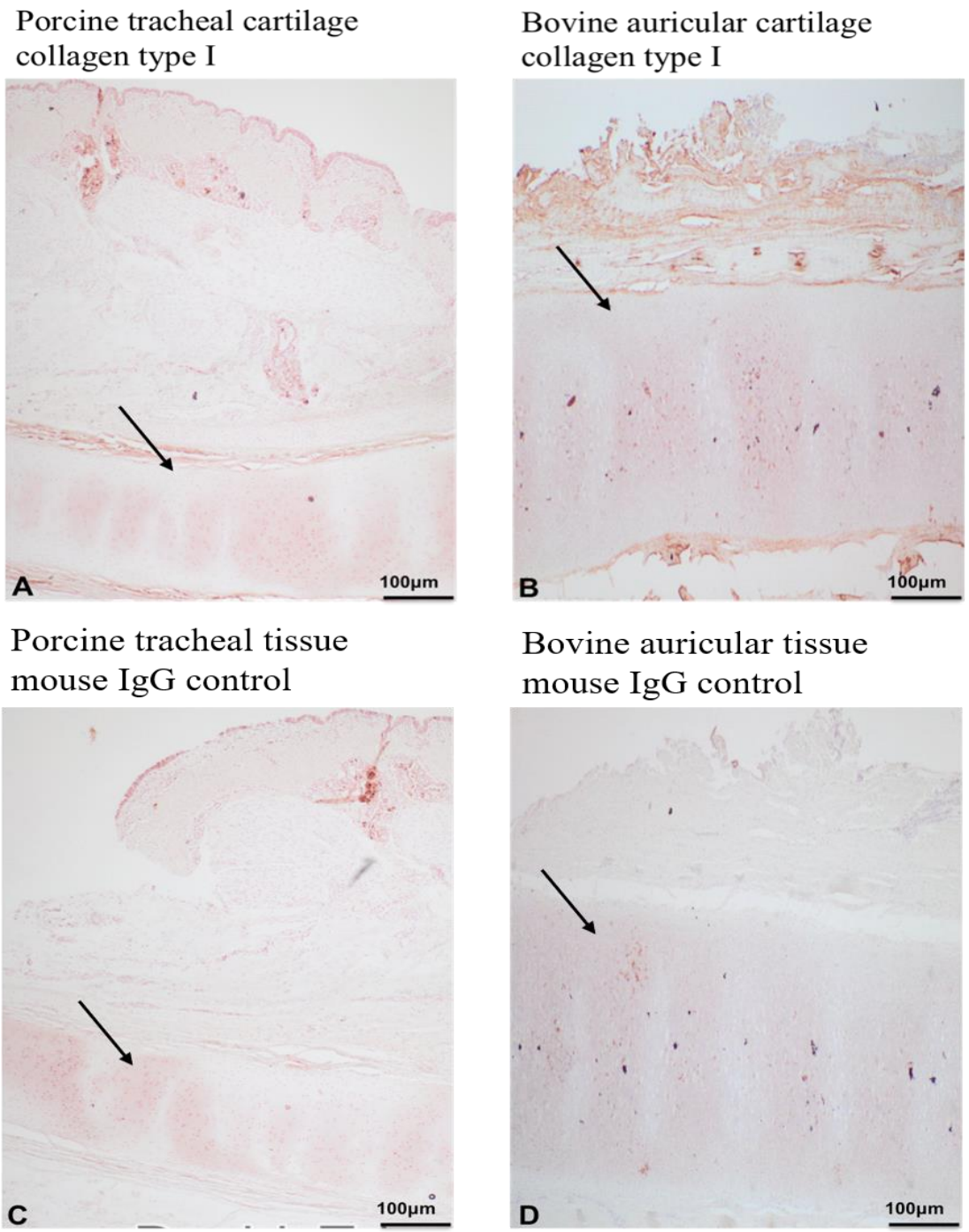

Figure 3.5. Immunohistochemical analysis of 6-months-old porcine tracheal cartilage and immature bovine auricular cartilage. Collagen type I immunohistochemical labelling of tracheal cartilage **(A,** *arrowed***)** and auricular cartilage **(B,** *arrowed***)** counterstained with haeamatoxylin. Control sections were examined using mouse IgG at the same concentrations as the primary antibodies and run in parallel to confirm specificity of labelling (**C**, **D;** *cartilage is arrowed*). Bar equals 100 microns. Images represent one porcine donor.

3.2.3 Uniaxial testing of native trachea tissue

Cartilage plays a crucial role in the mechanical function of the trachea and directly affects physiological respiratory function [4]. The cartilaginous parts are the stiffest tracheal constituents and they keep the lumen of the trachea open even during negative pressures, hence inhibiting tracheal collapse and maintaining airflow [306]. To understand how the mechanical properties of tracheal cartilage contribute to its function, the elastic and relaxation behaviors of cartilage samples were measured.

The mechanical strength of the trachea tissues was measured by ultimate tensile testing **(Chapter 2, Section 2.12.2)**. To differentiate the contribution of different tissue components to withstand the most amount of force applied, tracheal C-ring tissue layers were separated into connective tissue layer, cartilage layer, and cartilage with adventitia layer (due to difficulties in removing the adventitia layer intact in shape) and the composite tissue - comprised of all three tissue layers

The groups of tissue were trimmed to the same size (10 mm x 5 mm) and a thickness of 1-2 mm. Uniaxial testing was undertaken using fixed parameter of 5mm/s. The Young's modulus was obtained from the linear region of the stress-strain curves **(Figure 3.6A)**. Fixed cartilage had the highest value of 228.8 kPa and was higher when compared with fresh cartilage 122.7 kPa. All the groups were higher when compared with fresh connective 3.97 and fixed connective tissue 3.1 kPa. However, no major difference was found across cartilage, cartilage ADV 148 kPa and composite 197.6 kPa **(Figure 3.6B)**. From **Figure 3.6A** it is evident that cartilage is the stiffest tissue whereas the connective tissue is highly elastic giving trachea its remarkable deformability properties. This data correlates with the immunohistological and histology images where connective tissue has heavily stained for elastin making this tissue more elastic, cartilage which is mostly made up of aggrecan and collagen type II provide mechanical rigidity, and, adventitia that is made up of collagen type I re-enforce the mechanically stability of the tracheal C-ring.

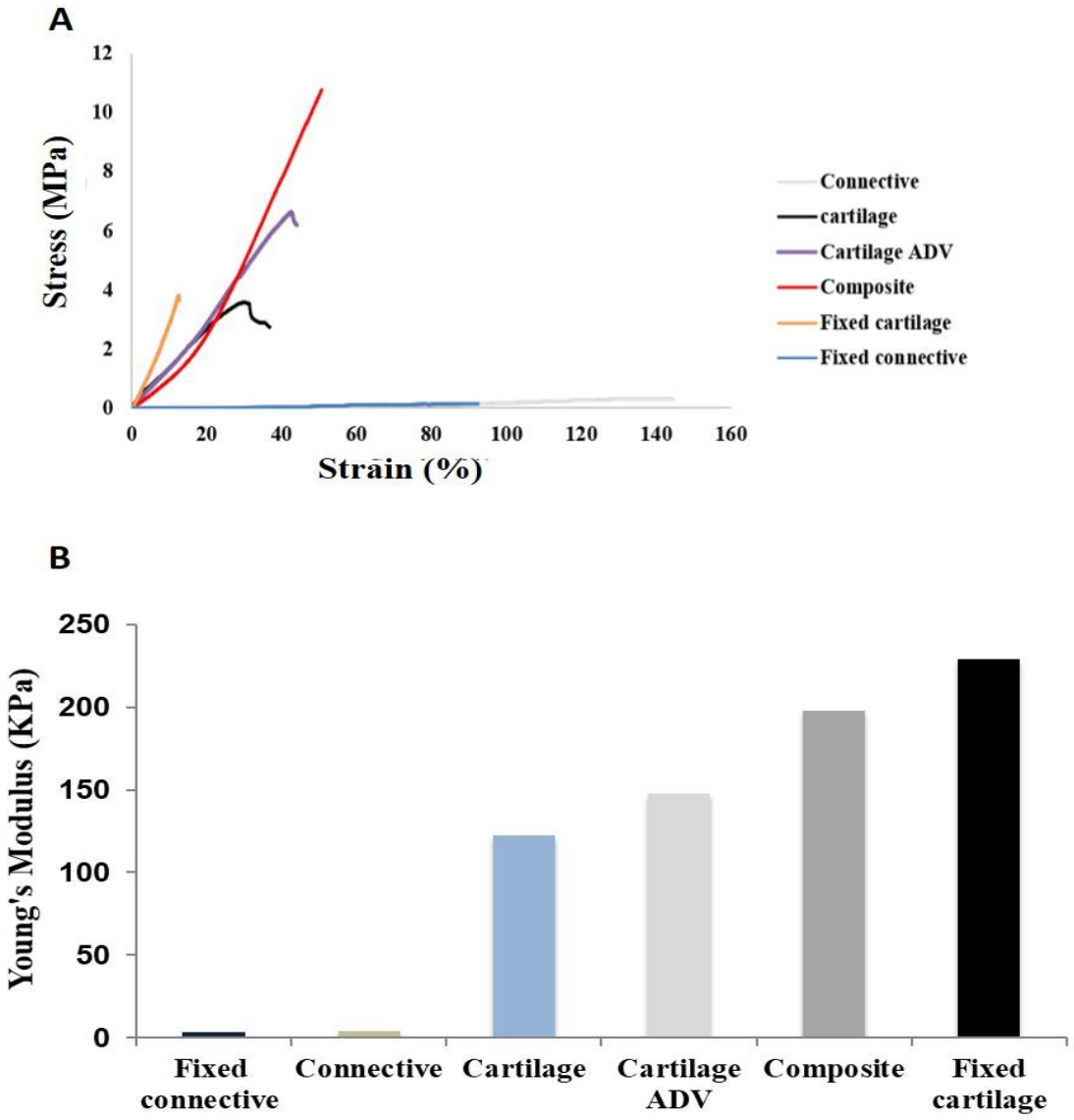

Figure 3.6. Comparison of stress–strain curves of different tracheal tissues from the same sample in uniaxial direction (elongation to break at 5 mm/min). Young's modulus of native tracheal tissue components calculated from the linear portions of stress-strain curves (A) and plotted as bar charts (B). All data are presented from two biological repeats each containing three technical replicates.

Having now identified the histological components of the tracheal C-ring and the mechanical properties of the components, the tracheal cartilage was then characterised at mRNA level to examine if tracheal cartilage exemplified the typical hyaline-type baseline cartilage gene profile based on the common markers used for the tissue engineered articular cartilage, using end-point RT-PCR.

3.2.4 mRNA expression of cartilage matrix markers between two sources of hyaline cartilage

Articular cartilage tissue was used as a baseline validator for hyaline cartilage properties. Articular cartilage showed weak band intensity of collagen type I (COL1) and elastin (ELN) genes and a stronger band intensity for collagen type II (COL2), collagen type X (COLX), SOX9, aggrecan (ACAN) and proteoglycan-4 (PRG4, also known as superficial zone protein or (lubricin) specific for hyaline cartilage found in articulating joints.

Tracheal cartilage tissue also showed weak banding for COL1 and ELN, whilst being strongly positive for COL2 and SOX9 and ACAN. The most notable differences amongst the two sources of hyaline cartilage was COLX (a hypertrophic chondrocyte marker) and PRG4 that are present in articular and absent in tracheal cartilage **(Figure 3.7)**.

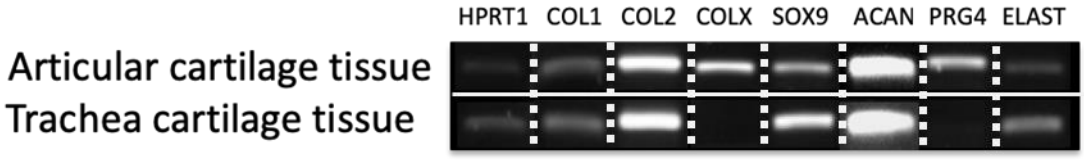

Figure 3.7. PCR gene expression characterisation of 6 months old articular and tracheal cartilage. The expression of several cartilage matrix biomarkers was analyzed by RT-PCR. Articular tissue was utilised as a comparison and to validate the expression of cartilage-specific genes, collagen type I (COLI), collagen type II (COL2), collagen type X (COLX), sry-box protein 9 (SOX9), aggrecan (ACAN), proteoglycan-4 (PRG4), elastin (ELN). Articular and trachea tissue showed very similar molecular signature, the main difference was in the presence and absence of collagen type X and PRG4 (Superficial zone protein, lubricin) in articular and trachea respectively. Hypoxanthine Phosphoribosyltransferase 1 (HPRT1) was used as a control for PCR amplification. Gels were constructed from various individual gels and separated with white banding.

Having made a preliminary analysis of the morphological and mechanical properties of 6-months-old porcine tracheal cartilage, these measurements may provide a useful comparison for tissue-engineered structures that are fabricated as part of this study. To

provide a cell source for tissue-engineered constructs an effort was made to isolate and characterise putative stem/progenitor sub-populations derived from the tracheal C-ring.

3.2.5 Isolation of colony forming cells from tracheal tissue using differential adhesion to fibronectin

Stem/progenitor cells *in vivo* have the ability to self-renew and facilitate growth and repair unlike differentiated cells. The ability of self-renewal is evident in 2D culture as assessed by colony forming ability. The colony forming efficiency (CFE) of cell populations can be quantified based on a known cell seeding density. In this study we used differential adhesion to fibronectin to isolate tracheal tissue-specific stem/progenitor cells and visualised colony forming cells using crystal violet staining **(Figure 3.8A-C)**. Colonies comprised of over 32 cells can arise from stem/progenitor populations whereas more committed transit-amplifying populations, whose proliferation rate is limited to five population doublings <=32 cells, will not generate large colonies.

In this study the CFE of connective tissue (CT), adventitia (ADV) and tracheal cartilage (TC) colony forming cells were calculated by initially seeding 1000 enzymatically isolated cells from carefully dissected tissue onto fibronectin-coated culture dishes for differential adhesion assays. Following 10 days of culture incubation the cells were fixed and stained with crystal violet and colonies larger than 32 cells counted and the CFE calculated. Distinct colony formations with different morphologies were observed across all three types of the stem/progenitor cells **(Figure 3.8A-C)**. TC-derived cells showed significant increases of 1.6-fold higher in CFE, 10.46±1.44% and 3.6-fold higher CFE when compared to ADV 6.5±1.5% ($p < 0.005$) and CT 2.9±0.5% ($p < 0.05$). Distinct morphological appearances were also observed between TC, ADV and CT colony forming cells, which was further investigated.

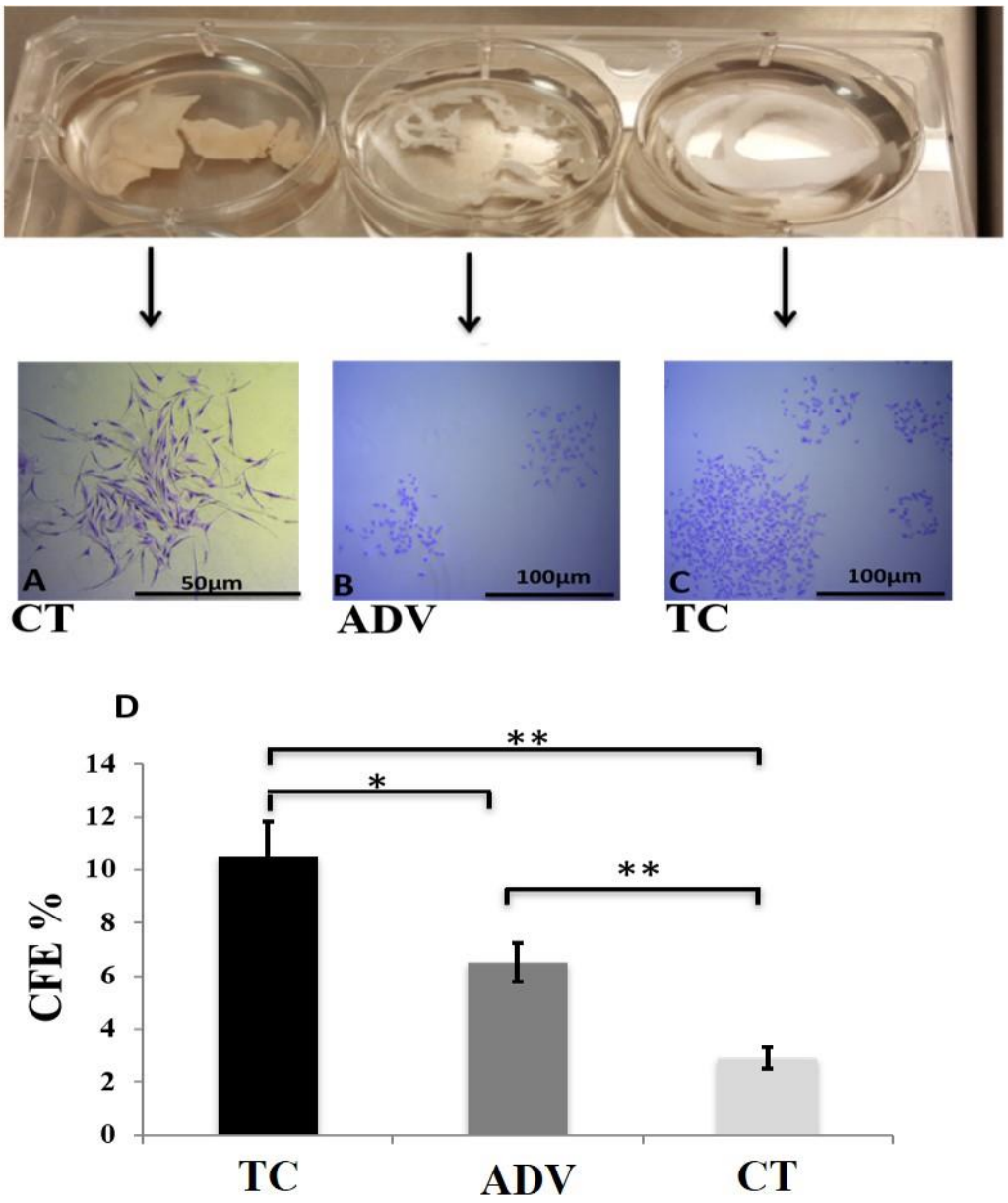

Figure 3.8. Colony forming efficiency (CFE) of cell sub-populations from distinct dissected tracheal tissue. Image showing colony formation by (A) connective tissue (CT) cell sub-populations, (B) adventitia tissue (ADV) cell sub-populations and (C) tracheal cartilage (TC) tissue cell sub-populations stained with crystal violet. Colonies containing at least 32 cells arose from an initially mixed cell population from each tissue. (D) Colony forming efficiency of specific progenitor populations. All data shown is average CFE (± standard deviation) from five biological repeats, tested for significance using one-way ANOVA analysis. * and ** are used to indicate $p < 0.05$ and $p < 0.005$ respectively. Images represent one porcine donor.

3.2.6 Cell shape analysis of trachea tissue specific stem/progenitor populations

Using InCell (GE Healthcare, UK) an immunofluorescence-imaging platform, a morphological study was undertaken to confirm whether distinct differences exist between colony forming cells isolated from the three distinct tracheal tissues; connective tissue, adventitia and cartilage.

20,000 cells at passage 2 (P2) were plated and fixed with 10% NBF to analyse their cytoskeleton by staining of F-actin with phalloidin and the cell nucleus by staining with DAPI **(Figures 3.9A, B and C)**. Of primary interest was the cell area and roundness of the stem/progenitor cells. A significant difference was observed between all cell types for cytoplasmic area **(Figure 3.9D)**. Fixed cell images of TC, CT and ADV colony derived cells following fibronectin adhesion are shown in **Figure 3.9A-C** respectively. Cells were stained with phalloidin (red) and DAPI (blue) and the images captured by InCell pseudo confocal microscopy. The images demonstrated clear differences in cell shape and morphology which were then subjected to software specific algorithm analysis which uses a segmentation analysis to evaluate cell and nuclear circularity or shape. These images were analysed at single cell level across whole populations, and these quantitative parameters were used to analyse any potential changes in cell morphology between the tracheal tissue compartment derived progenitor cells.

The CT cells had a more spindle-shaped morphology whereas; TC and ADV were more cuboidal. TC cells had a 2-fold increase in circularity versus ADV and CT and ADV showed a 0.4-fold increase compared to CT (TC: 0.42 interquartile range 0.31-0.54; CT: 0.2 interquartile range 0.16-0.29; ADV: 0.24 interquartile range 0.18-0.36), which was also significantly different ($p < 0.005$).

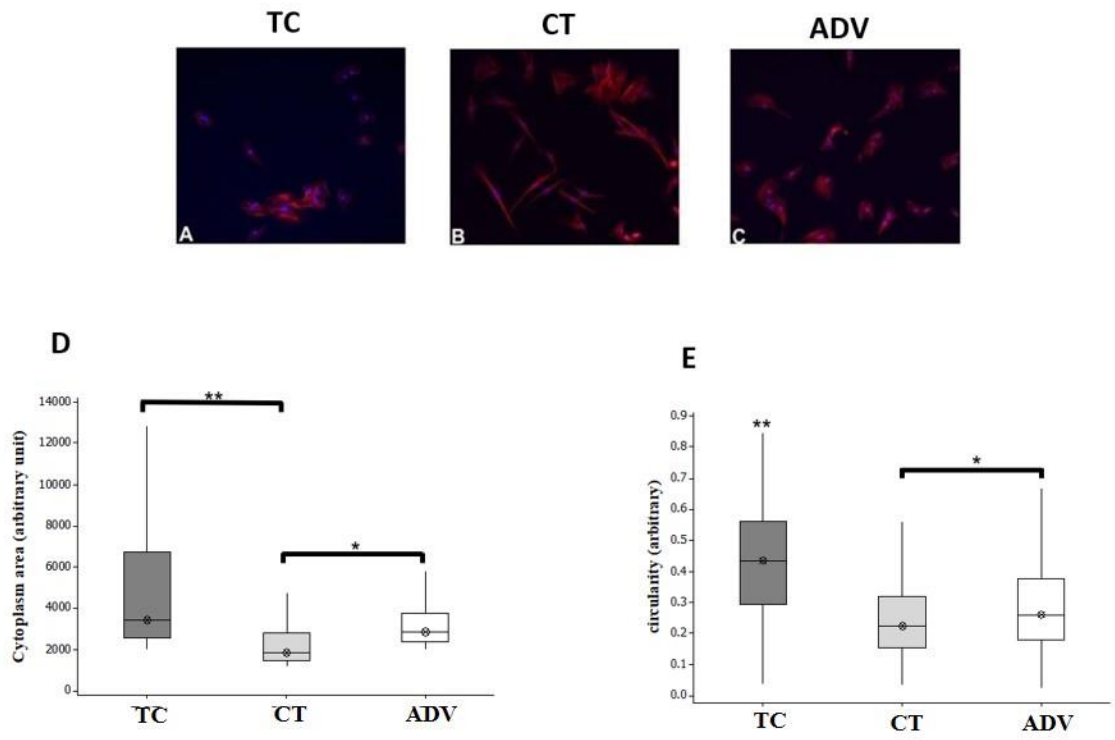

Figure 3.9. Fluorescent images of isolated colony forming cells stained for F-actin filament with phalloidin and cell nucleus with Dapi for morphological analysis. Tracheal cartilage (TC), connective tissue (CT) and aventitia tissue (ADV) single cells from the three different tissue components (**A**-**C**). (**D**) Quantitative morphological analysis of cytoplasm area shows that TC cells possess the largest cytoplasmic area followed by ADV and CT. (**E**) shows the circularity of three cell types and TC cells are more rounded and cuboidal compare to CT and ADV cells. These differences are visualised in the boxplot representation and were shown to be significant through Kruskal-Wallis statistical analysis. (300 cells per cell type were analysed three biological repeats; ** represents $p < 0.001$ and * represents $p < 0.05$). Images represent one porcine donor.

The cytoplasmic area of TC colony forming-derived cells showed a 1.7-fold and 1.3-fold increase versus CT ($p < 0.001$) and ADV colony forming-derived cells respectively, and ADV showed almost a 2-fold increase versus CT (TC: 3235.4 interquartile range 2435.7-6745.8; CT: 1867.7 interquartile range 1643.7-2863.2; ADV: 2435.2 interquartile range 2236.9-3756.5), which was significantly different ($p < 0.05$). This in fact followed the same trend for the circularity where values range from 0 to 1, where 1 represents a perfect circle. TC cells were most rounded following by ADV and CT **(Figure 3.9E)**.

Having now isolated three distinct morphological different cell populations the minimal criteria for the characterisation of adult mesenchymal stromal cells as set out by ISSCR was used. Due to the lack of well-characterised and validated commercially available antibodies to porcine MSC cell surface markers, the presence or absence of markers was characterised using RT-PCR.

3.2.7 Tracheal cartilage colony forming cells displayed progenitor-like qualities

Molecular analysis of specific gene expression profiles was undertaken, to further assess the presence of progenitor-like transcriptional profiles of colony forming populations in the distinct tissue layers of the porcine trachea. An accepted panel of stem cell surface markers was adopted according to the criteria outlined by ISSCR.

Gene expressions of several stem cell surface markers were analysed for isolated articular chondroprogenitors (ACP), TC, ADV and CT cells by RT-PCR **(Figure 3.10)**. ACPs were used as a control as these cells had previously been characterised as adult tissue specific progenitor cells by other groups [201][331]. Both articular chondroprogenitors and TC cells were negative for hematopoietic markers CD34 and the leukocyte marker CD45. ACPs and TC cells were positive for CD14, CD73, CD90, CD105, CD166 and nestin (NES). Conversely, ADV and CT cells were positive for both CD34 and CD45. ADV and CT cells were also positive for CD14, CD73, CD90, CD105, CD166 and NES. Thus, at the transcript level, ACPs and TC colony forming cells match the minimal requirements to be classified a potential source of adult stem/progenitor cells. However, to fully validate stem/progenitor cell characteristics tri-lineage differentiation was performed.

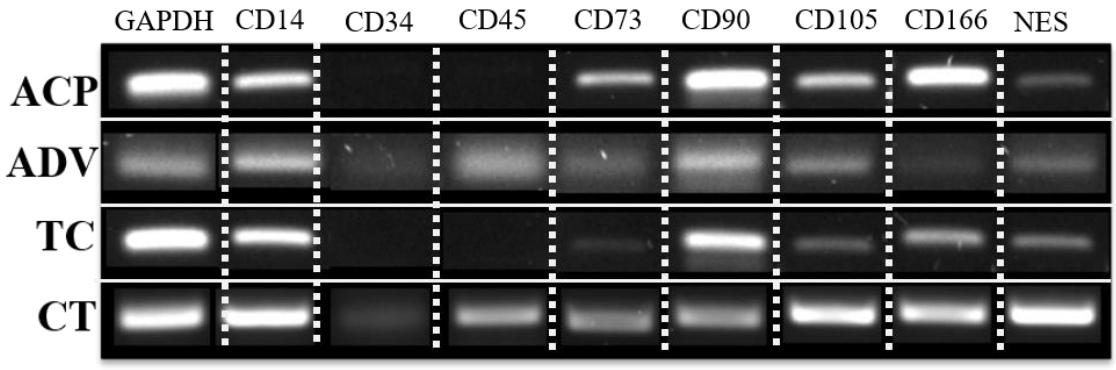

Figure 3.10. RT-PCR analysis of articular cartilage-derived chondroprogenitors (ACP), adventitia (ADV), connective tissue (CT) and tracheal cartilage (TC) derived colony forming cells. Articular progenitor cells were used as reference point as these cells have previously been characterized. Gels were constructed from various individual gels and separated with white banding.

Phenotypic plasticity of CT, ADV and TC colony forming cells was assessed through a tri-lineage differentiation assay. Previously it's been shown that ACP derived cells through differential adhesion to fibronectin are capable of tri-lineage differentiation into chondrogenic, osteogenic and adipogenic lineages [220].

All cells were seeded at P3 at 10,000 cells per well. CT cells did not exhibit any evidence of lineage specific differentiations (**Figure 3.11A, D & G**). However, ADV and TC colony forming cells both successfully committed to all three lineages. Chondrogenesis was indicated by alcian blue staining, which labels the GAG chains of proteoglycans in the extracellular matrix. Adipogenesis was confirmed by Oil-red-O staining of the intracellular fat containing vacuoles, and osteogenesis, in which intracellular and extracellular calcium deposits stain red with alizarin red, was present in cells derived from ADV and TC colony forming populations. The degree of differentiation varied between TC and ADV cells where TC cells showed a more potent differentiation capability **(Figure 3.11 C, F & I)**. CT cells were not capable of performing any of the mesoderm lineages.

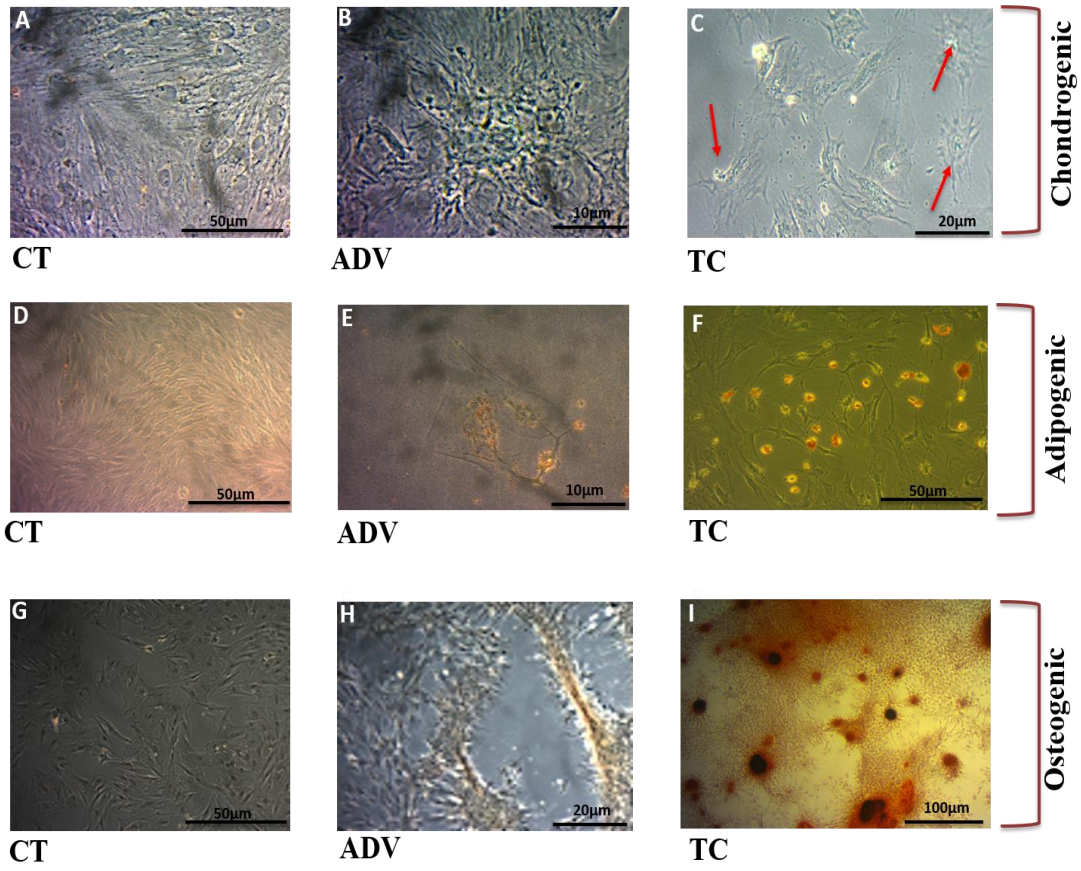

Figure 3.11. Tri-lineage potential of tracheal-derived colony forming cell populations. Tri-lineage was performed by 2D culture to analyze the multipotent differentiation potential of connective tissue (CT), adventitia (ADV) and tracheal cartilage (TC) derived colony forming cell populations. (**A**-**I**) Alcian blue staining labelled nodule formation of ADV and TC cells indicative of successful differentiation (**A**-**C**). Oil red O stains lipid vacuoles confirming adipogenic differentiation (**D**-**F**) and alizarin red staining demonstrating osteogenic differentiation (**G**-**I**) was also evident in ADV and TC cells. Connective stem/progenitor cells were not capable of tri-lineage differentiation (**A**, **D** and **G**). Bar equals 100 microns. Images represent one porcine donor.

Having now shown the minimal criteria for classification of adult stem cells and tri-lineage capability of CT, ADV & TC, we further explored the possibility of cellular mechanics as a further refinement in the characterisation of stem cells isolated from the tracheal tissue C-ring cartilage.

3.2.8 Nanomechanical characterisation of trachea tissue specific colony forming populations

Nanomechanical analysis has the capability of providing high-resolution analysis of cell characteristics and these measurements may be associated with cellular origin. Here, nanomechanical analysis was used to assess the presence of any association between porcine tracheal-derived cell population nanomechanical properties and progenitor-like features.

Tracheal cells were fixed with 10% NBFS for 10 minutes at room temperature and washed with PBS thrice prior to preforming the analysis to avoid inconsistency with ambient temperature and oxygen tension. An AFM cantilever with a pyramidal probe was used, in force volume, nanoindentation mode, to measure the mechanical properties of the single cells. The indentation depth was confined to be in the range of 100-500nm to avoid the effect of substrate, therefore the limit of deformation was assumed to be 10% of the total cell thickness [353]. All the measurements took place by placing the probe at the centre of the nuclear region due to in part the smaller cytoplasmic area of connective tissue cells, as shown in **Figure 3.9B**.

A series of increasing loads ranging from 1-3 nN indentations was used primarily on full depth chondrocytes as previous studies have shown chondrocytes to be the softest and most viscoelastic when compared with other types of MSCs [294]. Only curves with R^2 between 0.9 and 1 were chosen by proprietary manufacturers software were chosen for the analysis. To provide physiological relevant data freshly isolated full depth chondrocytes (FD) along with TC, ADV and CT colony forming cells were analysed (because they did not experience the 2D culture shock and were analysed directly after tissue enzymatic digest). The FD cells were plated immediately after the enzymatic digest and fixed whereas colony-forming cells had to remain in culture for a minimum of 10 days in order to derive the cells and to ensure that transit-amplifying committed populations were not included.

TC colony forming cells were the stiffest cell type ($p < 0.05$) when compared to ADV and CT-derived cells (TC: 4.57 pN/nm interquartile range 4.87-3.31; ADV 3.05 pN/nm interquartile range 4.45-2.76 and CT 3.50 pN/nm interquartile range 3.92-3.41).

However, the FD cells (1.51 pN/nm interquartile range 1.42-2), was shown to be the most elastic compare to all other cell types analysed ($p < 0.001$) **(Figure 3.12)**.

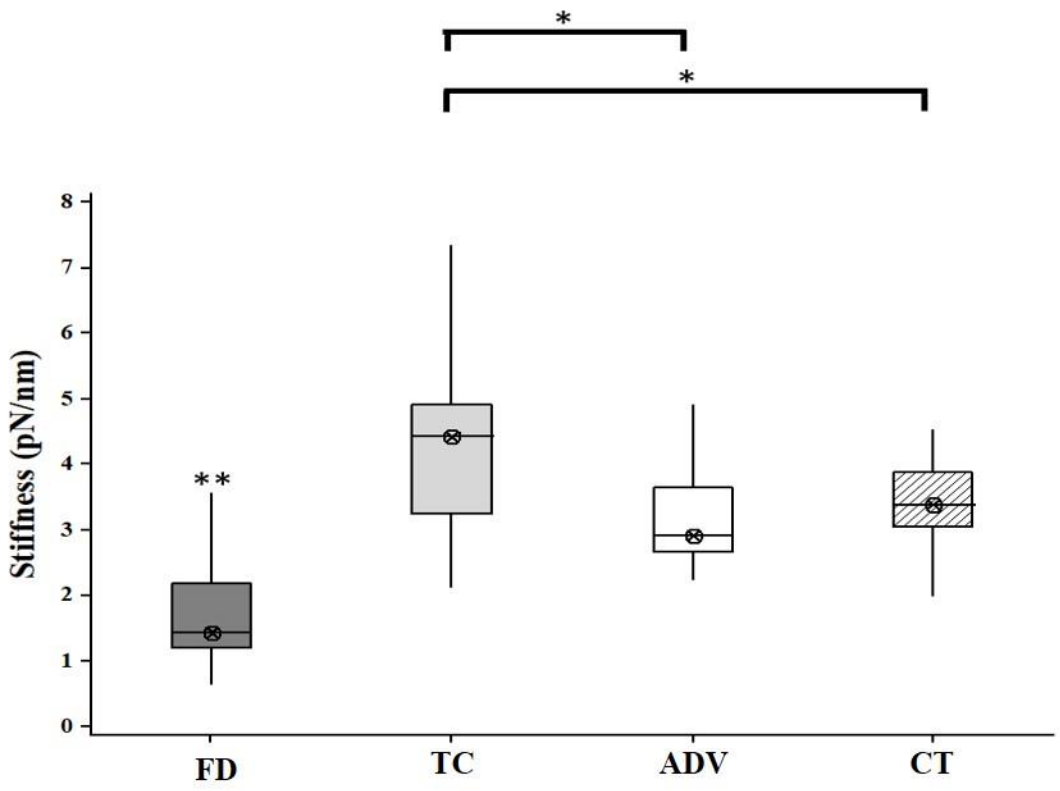

Figure 3.12. Nanomechanical profiling of nuclei using atomic force microscopy of freshly isolated tracheal cells. Tracheal cartilage (TC), adventitia and connective tissue colony forming cells and tracheal cartilage full depth (FD) populations were fixed with 10% NBFS for 10 minutes prior to obtaining the nanomechanical data. Full depth cells were used on day of isolation whereas colony forming cells required a minimum of 7 days of culture before performing the experiment. The FD population showed the softest mechanical profile compared to the colony forming populations and these differences are shown as boxplot representations. Results are shown to be significant through Kruskal-Wallis statistical analysis. (30 cells per cell type was analysed from five biological repeats; ** represents $p < 0.001$ and * represents $p < 0.05$).

3.2.1.1 Nanomechanical characterisation of tracheal tissue derived colony forming populations during long term passage

Cells have been shown to de-differentiate or change their phenotype during long-term culture. In order to analyse the culture stability, AFM nano-indentation was used to monitor changes in cellular mechanical phenotype over long periods of culture (P0-P6). The same experimental protocol for nanomechanical analysis was followed as described in Section **3.2.8** (above).

TC at P6 and P0 were significantly stiffer ($p < 0.001$) than P2 cells. TC P4 cells were also significant when compared with P2 cells ($p < 0.05$). No significance was observed between TC populations between P0 and P6.

No significant changes were observed between ADV progenitors between P0 and P2 but a sharp increase in stiffness was seen from P2 onwards. P6 and P4 progenitors were both significantly stiffer than P0 and P2 ($p < 0.05$).

CT cells showed a similar stiffness pattern to the ADV cells. Cells at P6 were significantly stiffer compared with P4, P2 and P0 ($p < 0.05$). No significance was observed between P4 and P2, but they were both stiffer than P0 cells.

The only tissue compartments isolated cell populations that maintained a constant mechanical phenotype between P0 and P6 were the TC colony forming cells. While significant variation was observed at P2 and P4, the data distribution recovered at P6. Otherwise, significant increases in stiffness were observed associated with increased passage across all cell types. Order of magnitude: (TC: $P6 \geq P0 > P4 > P2$; ADV: $P4 > P6 > P2 > P0$; CT: $P6 > P4 > P2 > P0$). All the measurements from the nanomechanical analysis are summarised in Table 3.1.

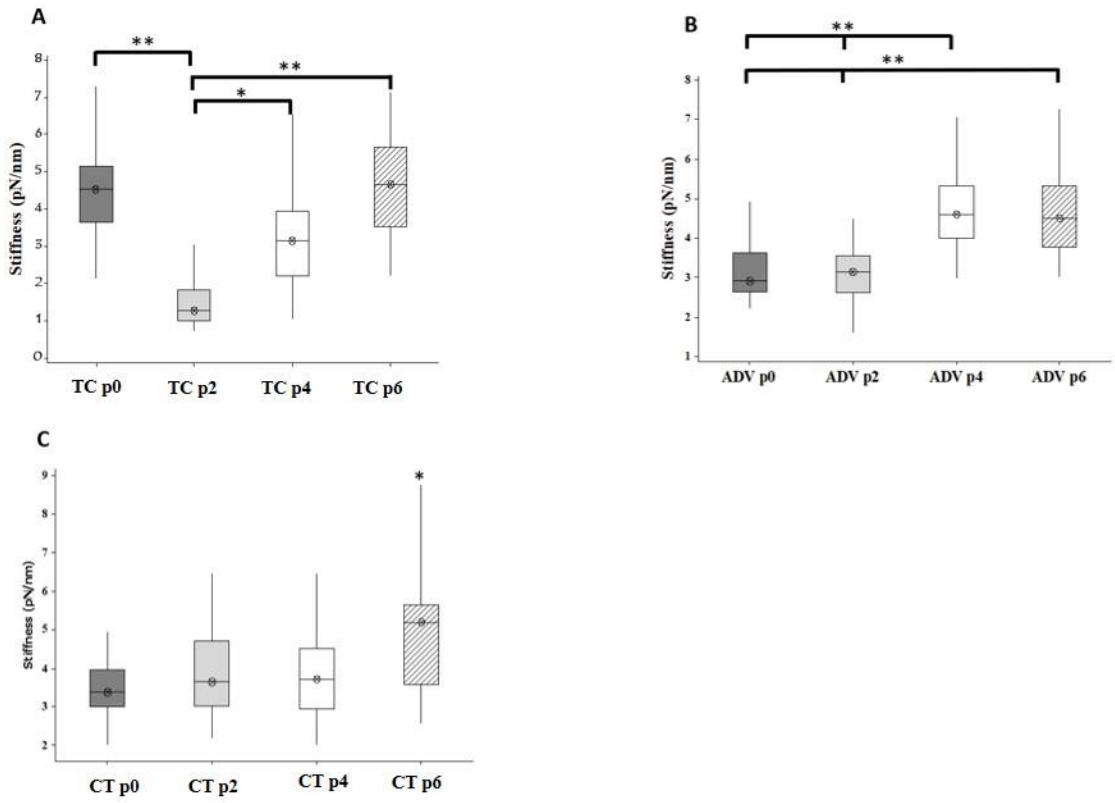

Figure 3.13. Nanomechanical profiling of long-term cultured tissue specific colony forming cells. Cells were fixed with 10% NBFS for 10 minutes prior to obtaining the nanomechanical data. At each passage 10 cells were analysed to monitor nanomechanical changes. Differences in nanomechanical profiling of colony forming cell populations weare visualised as boxplot representations and were analysed for significance by Kruskal-Wallis statistical analysis. (30 cells per cell type and passage was analysed from fivebiological repeats; ** represents $P < 0.001$ and * represents $p < 0.05$). Cells were re-plated at 1:4 ratio at each passage and underwent approximately three population doublings per passage.

	Higher	lower	median
TCP p0	5.13	3.65	4.54
TCP p2	1.83	1	1.28
TCP p4	3.95	2.21	3.16
TCP p6	5.68	3.51	4.65

	Higher	lower	median
ADV p0	3.62	2.64	2.92
ADV p2	3.56	2.63	3.14
ADV p4	5.3	4	4.6
ADV p6	5.32	3.78	4.5

	Higher	lower	median
CPC p0	3.96	3	3.39
CPC p2	4.70	3.02	3.66
CPC p4	4.53	2.95	3.72
CPC p6	5.6	3.6	5.2

Table 3.1. Stiffness (pN/nm) range of TC, ADV and CT cells over long-term passage culture.

COL1 and COLX are known markers for chondrocyte de-differentiation and hypertrophy respectively [159]. No significant expression of COL1 and COLX were observed in native tissue. In order to determine if TCP cells had maintained a mechanical and genetic phenotypic stability at P0 and P6, COL2, COL1 and COLX expression were analysed by qPCR and normalised against the housekeeping gene GAPDH. COLII expression was used here as a positive control and to analyse for potential differentiation.

Gene expression levels for COL2 showed significant 10000-fold reduced expression in TCP cells **($p < 0.001$; Figure 3.14A)**. Despite a reduction in COL1 and COLX being observed at P6, these differences were not significant ($p > 0.05$).

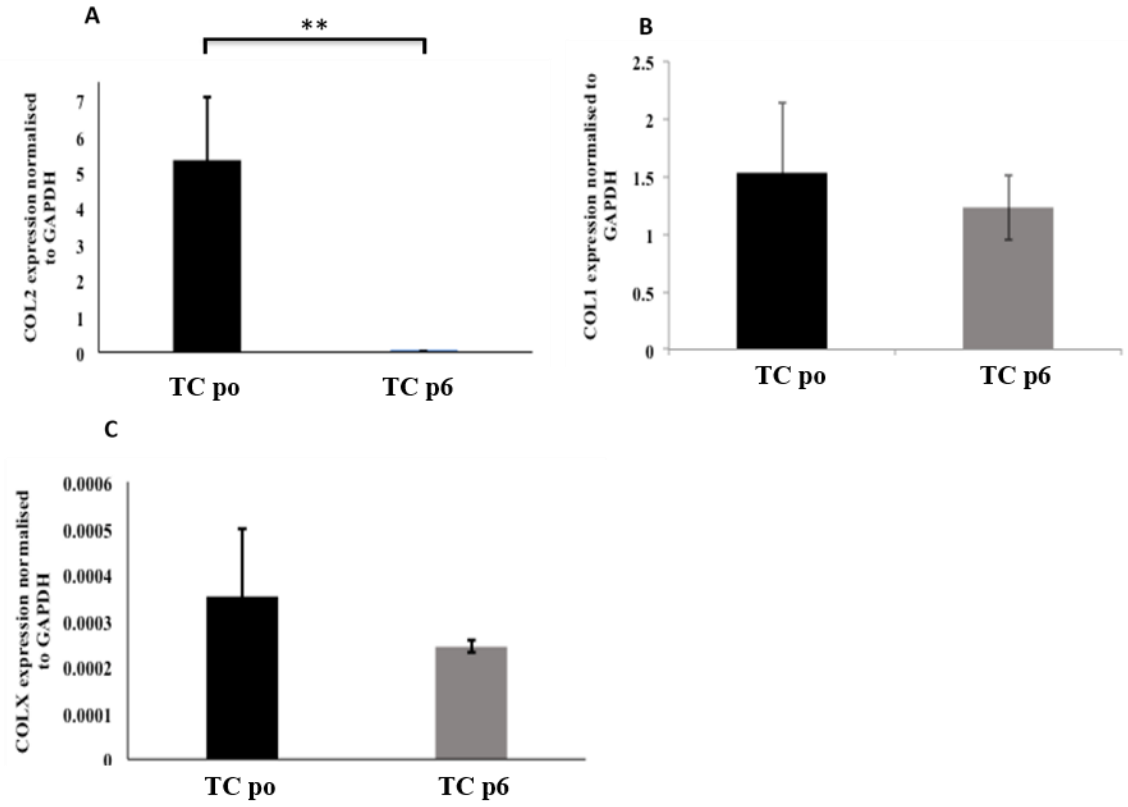

Figure 3.14. Chondrogenic gene expression with monolayer expansion of tracheal chondroprogenitor at an early and late stage of 2D culture using Δ*CT* method. Gene expression levels for collagen type II (COL2) fell approximately 10000-fold after 6 passages in culture. Gene expression levels for collagen type I (COL1), and collagen type X (COLX) showed no significant changes. All data shown (**A**, **B** and **C**) are

averages (± standard deviation) from three biological repeats, tested for significance using Student's t-test. (** represents $p < 0.001$).

3.3 Discussion

More advanced understanding of cellular phenotypes are needed if promising, novel stem cell-based regenerative therapy for the repair of airway cartilage defects [354], are to progress to successful clinical trials and translation to patient benefit. Recently, various cartilages have been shown to contain a stem/progenitor cell reservoir [200][201][302], and cartilage-derived stem/progenitor cells have been hypothesised to be suitable starting populations for tissue engineering repair tissue. Presented in this chapter is the ISSCR-compliant characterisation of tracheal tissue compartment isolated progenitor cells. Fibronectin-adherent cellular populations were detected in the adventitia, cartilage and connective layers, with single cell isolates from each layer capable of plastic adherence, formation of colony forming units and stable proliferation. Importantly, tracheal cartilage progenitor cell population demonstrated unstable culture expansion, correlating with COL1, COL2 and COLX expression profiles. This tissue-specific progenitor cell population will form the focus for the following experimental work; to analyse their phenotypic plasticity in the presence of growth factors and in early tests of tissue engineering of C-ring cartilage.

Studies have shown that non-tissue-specific stem/progenitor cell sources, such as bone marrow [355] and adipose tissue [356], are not the ideal cell sources for the treatment of cartilage injuries and the optimum cell source remains to be definitely identified.

Although efforts have been made to characterise the trachea tissue there is insufficient information for baseline characterisation of native trachea for the ECM composition to match functional mechanics as well as the potential presence of progenitor populations as a source for tissue specific regenerative medicine suitable cells. Trachea cartilage is believed to be a mostly hyaline type cartilage, due to the shiny appearance and protein expression of the specific hyaline cartilage biomarker collagen type II. Further analysis of the immunohistochemistry of 6-month-old porcine trachea was undertaken for collagen type I, collagen type II and aggrecan to identify the major cartilage proteins

within the tracheal C-ring cartilage. Collagen type I was absent within the dense cartilage component of the C-ring while collagen type II stained strongly throughout the cartilage C-ring in a banding architecture alongside a periodic banding architecture observed for aggrecan. Conversely, the periphery of the tracheal cartilage C-ring exhibited strong staining for collagen type I which is indicative of perichondrial and connective tissue layers and agrees with previous publications [351].

Onnertjord *et al.* compared the proteome of human cartilages from eight distinct tissue locations throughout the body. There were significant variations in the protein composition of the ECM from different anatomical sources, and it was reported tracheal cartilage has similarities with rib cartilage particularly in matrilin-1 and epiphycan expression [119]. Similarly, Wachsmuth *et al.* compared various types of human cartilage tissues and reported that tracheal cartilage has high cell to matrix ratio and is composed of collagen types II, III, V, VI, and X with some variation between the ring margins and centre [120]. However, collagen type X was not detectable at mRNA level in the porcine trachea, just as had been described in this study. Yet, Wacshmuth *et al.* presented no microscopic images validating the claim of the presence of collagen type X. Tracheal cartilage has no functional relevance or proximity to bone, in comparison to the deep zone articular cartilage and therefore no requirement for the hypertrophic chondrocyte marker collagen type X. The presence of collagen type X in human tracheal tissue may be indicative of tracheal calcification as observed in some congenital disorders [357], trauma post-surgery [358], chondrodysplasia and diastrophic dysplasia [359]. Elastin was noticeable in the connective layer of the C-ring trachea beneath mucosa and submucosa and its presence is in agreement with what has previously been reported in mouse lung epithelium where elastin is the most abundant ECM protein in the submucosa layer [360].

To date, no mesoderm derived stem/progenitor population has been identified within the tracheal tissue. This study is the first to report the presence of porcine stem/progenitor sub-populations in tracheal C-ring cartilage. Isolated cells from all three tissue compartments (adventitia, cartilage and connective) were able to attach to fibronectin-coated culture dishes after 20 minutes, a methodology previously used to enrich for

stem/progenitor cells [219]. Adhesion to fibronectin can be explained by high expression of α5β1 integrin subunits, the 'classical' fibronectin receptor [331] which has been reported in many stem cell lines such as bone marrow MSC [324], auricular derived chondroprogenitor cells [138] and articular cartilage derived chondroprogenitors [137]. Up to ten integrin αβ subunit combination of receptors have been shown to bind fibronectin, many of these are also expressed by mesenchymal cells, such as α3β1, α5β1 and α5β3 integrins, and the binding of these receptors to fibronectin cannot be excluded [361], [362]. Nevertheless, previously the isolation and characterisation of mesenchymal stem cells from adult mouse bone marrow using differential adhesion to human fibronectin has been reported where the isolation technique was not clear in terms of length of time for fibronectin adhesion and whether the analysed cells were past the transient amplifying stage [363].

The cell populations isolated from the tracheal tissue were capable of colony forming from an initially low seeding density. This is in accordance with other studies using differential adhesion to fibronectin to isolate stem/progenitor cells [200][202]. Colony forming TC cells had the highest CFE (10% of the initial cell density) and this could be due to partial adventitia tissue remaining on the top surface of tracheal cartilage or the presence of a high frequency of stem/progenitors, which may be linked to the young age of the porcine donor of 6 months. The CFE value observed here is greater than that of Dowthwaite *et al.* [219] who reported a mean CFE of 0.27% in cells digested from 7-day-old bovine articular cartilage. The increase in CFE in porcine tissue could be due to species variation or difference between an immature tissue and a juvenile 6-months-old porcine tissue. It is also worth noting, that results from previous papers isolating stem/progenitor cell within articular cartilage specifically targeted clonogenic cells residing in the surface zone of articular cartilage. This study has used full thickness biopsies and, therefore, may contain progenitors from other regions of tracheal cartilage [200][201]. We hypothesised that tracheal progenitor cells are derived from cartilage based on the amount of tissue in which cartilage outweighed adventitia. The CT cells that originally came from mucosa and submucosa layer were able to form colonies, and this follows what previously has been reported i.e. the human epidermal stem cells with the highest colony-forming efficiency adhered most rapidly to fibronectin and there was

a log linear relationship between the relative level of β1 integrins on the cell surface and proliferative capacity [328]. The CT cells may be basal derived stem cells from epithelium as previously identified in lungs. Further characterisation to confirm this requires utilising specific cell surface markers such as cytokeratin-5 (Krt5) and cytokeratin-14 (Krt14). Cells expressing cytokeratin markers have shown the capacity to be self-renewal and form secretory and ciliated cells [364]. During microscopic evaluation of the fibronectin selective adhesion expansion of the isolated colony forming cells it became apparent two morphologically different cell populations were present. One colony was observed to be fibroblastic in appearance whilst the second cellular morphology appeared more cuboidal. Therefore, we utilised colony isolation to sub-culture pure populations of the morphologically different cells for gene analysis based on ISSCR marker panel for mesenchymal stem cell classification used along with tri-lineage. To be categorised as mesenchymal stem cells, cells must express CD90, CD105 and CD166 and lack expression of haematopoietic markers CD34 and CD45 [135]. Previous studies have used cell surface markers, to isolate potential stem cell populations from bone marrow stromal cells and from articular cartilage [316][344]. The colony forming TC, ADV and CT cells agree with the major characteristics of stem cells in that they adhere to plastic, express surface markers and are able to undergo tri-lineage differentiation.

Due to lack of verified antibodies able to label for cell surface markers the isolated cells were only characterised at mRNA level. Rapid characterisation using gene expression analysis of cell surface markers has been used previously to provide evidence to confirm the identity of ovine articular and auricular cartilage [138][345]. Nevertheless, there are discrepancies in the criteria for the minimum cell surface markers when applied to certain tissues, articular cartilage for example. In articular cartilage, CD105 and CD166 have been proposed as possible surface biomarkers but studies have demonstrated that mature chondrocytes also widely express these two markers [316][346]. Nestin in the panel of markers seemed logical as nestin-expressing cells are restricted to defined niches, where they may function as a quiescent stem cell reserve capable of proliferation, differentiation and migration once activated [368]. Nestin is widely utilised as a marker of proliferating and migrating adult stem cells [368]. Both ACP and

colony forming TC showed identical gene expression whereas ADV and CT colony forming cells were also positive for CD34 and CD45. Multi-lineage analysis demonstrated that TC and ADV, mesodermal derived colony forming cells were capable of tri-lineage. This is in accordance with other studies where cartilage derived stem/progenitor cells showed the same potency [138][201]. CT cells from mucosa and submucosa layer, an endodermal derived population was unable to perform tri-lineage differentiation.

Biophysical analysis of cells was undertaken to further provide quality control of our isolation technique [305][348]. It is clearly demonstrated here, that the nano-mechanical properties of cells may serve as phenotypic biomarkers at early cell culture passages and follow the same trend of stiffness as their tissue of origin as was shown in **Figure 3.6**. The FD cells had the lowest stiffness values and were utilised here as controls, to examine the effect of 2D culture on colony forming cells. The FD cells are thought to be comprised of stem/progenitors and chondrocytes from the superficial and middle zones of cartilage. In this study FD cells that had a rounded morphology were measured to avoid obtaining data from possible chondroprogenitors or dedifferentiated cells. Previous studies have reported chondrocytes from different zones exhibit varying mechanical properties, showing middle/deep zone cells are less stiff than superficial zone cells [370].

Our findings are in general agreement with previous studies when comparing the cartilage component of tracheal tissue with other cartilage-derived cells [275][279], certain unsurprising differences exist. These differences arise from variations in cell source, testing apparatus, culture environment and mathematical modelling employed to generate the data. In this study cells were harvested from several different locations within a 6-months-old porcine trachea and treated with the same culture environment. Testing methodology could also play a role. For example, AFM indentation tests occurred on cells adhered to an underlying substrate, which could affect the measured properties [371]. Moreover, the type of probe tips used whether spherical or pyramidal can influence measurements. Indentation experiments using sharp-tipped probes typically result in higher measured moduli than those obtained with spherical-tipped

indenters [351][352]. The indentation depth in this study was confined to within 200-500 nm; for deeper indentations, the effect of the cell-culture substrates on the measurement becomes significant and makes the subsequent analysis complicated [374]. Therefore, the deformation limit is 10% of the thickness of the cells. It is also important to note that all measurements were performed at the centre of the nuclear region to allow reliable comparison of different cells [300]. However, the trend of stiffness correlates with that shown at tensile level where the relationship between stress and strain determines the stiffness of tissues. Previously it has been shown that osteocytes are the stiffest cell types when compared to chondrocytes and adipocytes [294]. This data follows the same outcome as the macro-mechanics data of the parent tissue layers where the order of stiffness from highest to lowest was bone, cartilage and fat tissue [294], [375]. This data coupled with mRNA and the histology data could be indicative of tissue specific stem cells residing in each tissue compartment.

The mechanical signals exerted on stem/progenitor cells by their surrounding environment are vital in determining their phenotype and activity. In recent years it is becoming more apparent that culture conditions may affect MSC properties [159]. Since preparing high-quality stem/progenitor cells are a necessity for cell therapy treatment, efforts have been made to evaluate the consequences of cultivation processes on stem cell behaviour. The elastic moduli of a substrate that cells reside on greatly influence the cellular behaviour. Whilst most of research utilises plastic culture flasks to propagate the desired cells, it is mainly effective for the cell growth. High growth ultimately leads to morphological and genetics changes that can affect the functionality of cells [376]. It has been reported that long-term culture of bone marrow MSCs is associated with several functional changes, including reduced proliferation, ultimately inducing replicative senescence [377] and associated molecular changes [378], together with reduced [379] or shifting multilineage differentiation potentials [380].

Prolonged culture of the tracheal derived colony forming cells on tissue culture plastic resulted in gene transcriptional change that clearly correlated to passage number. This observation may be due to matrix protein expression changes, which may subsequently convey architecture changes in the protein matrix composition that contribute to the

observed mechanical signature changes [200]. Future studies should include protein analysis of the matrix composition along with telomere analysis to confirm the observations in this study, as any compositional matrix protein change will have an effect on not only the quality of the tissue engineered tracheal C-ring but may also ultimately affect the mechanical properties of the engineered tissue. During long-term culture, across all colony forming cells, a general increase in cell stiffness was observed, possibly indicating that cellular mechanical properties may provide a proportional insight into the state of the cells for stem cell characteristics and differentiation [359][360].

TC derived cells showed a dramatic decrease in COL2 gene expression with increasing passage. Although morphological changes were minimal over long-term passage and plastic culture dish supported proliferation, COLX was detectable. This may be due to the fact that plastic substrate stiffness is very close to that found in bones and teeth [375]. Cell culture in 2D may have stimulated this upregulation, as COLX was not detectable at tissue level when comparing tracheal cartilage against articular cartilage. Interestingly the stiffest cell type, which was TC, adapted to the culture environment at a steadier rate, where-as ADV and CT showing stiffer behaviour at P2 and P4. Due to the nature of the cells and their parent tissue this adaptation to 2D culture may stem from the initial matrix where they reside prior to cultivation. Cells from the stiffer native matrix may adapt slower whereas cells from a more elastic or less stiff matrix may adapt to the culture substrate faster. These finding could be indicative as a marker to stem cell senescence and decrease in differentiation potential as previously published in regards to MSCs [381].

3.4 Conclusion

Using differential adhesion to fibronectin we have successfully isolated mesodermal derived tracheal stem/progenitor cells. These cells showed the ability to be plastic adherent, undergo self-renewal and demonstrate multipotent differentiation. Next, the chondrogenic ability of colony forming tracheal cartilage cells was assessed.

Chapter 4: Evaluation of chondrogenic capacity of tracheal cartilage derived stem cells using traditional pellet culture

4.1 Introduction

Identification and harvesting of an ideal cell source for the generation of functional, tracheal hyaline cartilage, remains an unmet challenge, which has been highlighted in the recent scandal concerning the work of Paolo Macchiarini [188][361]. While many regenerative medicine approaches have been applied in tracheal repair, significant deficiencies are attributed to current cellular, acellular and combined cell-scaffold approaches [89][130]. Autologous cell therapies are preferred mechanisms, representing an ideal model, preventing the need for immunosuppression drugs and tissue rejection [90]. The search for autologous, tracheal derived cell sources able to create hyaline like cartilage is a major theme of this study.

Many of an organism's tissues such as adipose tissue, muscle tissue, skin and tendon contain stem cells, that are capable of driving continual maintenance and reparative responses throughout its lifetime [217]. Therefore, identifying and targeting tissue-specific stem cells is the logical approach for better understanding endogenous repair and disease processes but also for tissue engineering applications. To date, airway tissue engineering has mainly focused on chondrocytes from other 'redundant' anatomical tissue sources other than trachea, such as nasal septum cartilage that has similar properties to tissue found in tracheal cartilage, and, MSCs from various tissues [130]. Nasal tissue is preferred for tracheal tissue engineering due to its ease of harvest and the presence of all required cell types such as chondrocytes, epithelial cells, and connective tissue that can all be obtained from a small biopsy of nasal septum [319].

Use of culture-expanded chondrocytes is proven to be disadvantageous and unfeasible due to donor site morbidity, low harvestable cell numbers, and, loss of cellular specialisation/functionality and inefficient recapitulation of cell function and specialisation following long-term culture [382]. Being plastic adherent, colony-forming, and multi-potential cell types [363][364], adult MSCs are a promising source of cells for such repair strategies. However, the final tissue derived from typical MSCs such as bone marrow-derived cells during chondrogenesis is fibrocartilage [385] and mineralization [386] characterised by the up-regulation of collagen type X that leads to calcification to produce epiphyseal-like tissue [387]. This latter biological process

resembles the earliest stages of endochondral ossification, which subsequently leads to bone formation [388]. Therefore, identification of a stem cell population that inherently differentiates towards a hyaline chondrogenic lineage should produce a more favorable outcome in terms of phenotype stability. In hyaline cartilage such stem cell populations have been isolated from various tissues using differential adhesion to fibronectin [137] and it has been shown that these cells are superior in culture than their chondrocyte counterparts and MSCs in their ability to differentiate into permanent hyaline cartilage [223].

Chondrogenesis is the initiation of cartilage formation when precursor stem/progenitor cells give rise to chondrocytes which in turn secrete tissue-specific extracellular matrix components such as collagen type II and aggrecan [136]. Many factors drive chondrogenesis, as previously mentioned in Chapter 1 Section 1.9, but in general this process is growth factor-dependent [389].

Many growth factors have been identified to regulate the stem/progenitor differentiation such as fibroblast growth factors (FGFs), transforming growth factor-beta (TGFβ), wingless-type integration site family (WNTs), bone morphogenetic proteins (BMPs) and insulin-like growth factors (IGFs) [390]. To date, many cell lineages have been differentiated from MSCs. MSCs have successfully been differentiated towards the bone lineage using BMP2, BMP6, BMP7 and BMP9 [391], chondrocyte lineage using individual growth factors such as TGFβ1, TGFβ2 or TGFβ3 or combinational exposure to BMP2 and TGFβ1 [175]. Therefore, this study will use TGFβ1, the most common growth factor used for chondrogenesis of MSCs, and also BMP9 which has been previously identified as a potent osteogenic and chondrogenic growth factor, to test the ability of tracheal-derived colony forming cells to undergo chondrogenic differentiation. The TGFβ ligands, which bind activin-like kinase receptors 1 and 5, signal via intracellular proteins SMADs 2/3 and are the most established drivers of *in vitro* chondrogenesis [176]. Activation of the latter two receptors is believed to modulate chondrocyte phenotype and differentiation by upregulating SOX9 and in turn synthesis of collagen type II and aggrecan [372][373]. The role of TGFβ ligands in chondrogenesis during limb development rationalises their use in *in vitro* models of stem

cell chondrogenesis [394]. Hence, the TGFβ family of growth factors have been used extensively for cartilage tissue engineering for both differentiated and non-differentiated cells [395]–[397].

It is currently unknown how tracheal cartilage stem/progenitor cells react to growth factors when induced to undergo chondrogenesis, therefore, the chondrogenic ability of newly identified tracheal chondroprogenitors was tested with a well-defined medium containing TGFβ1 or BMP9. The BMP signaling cascade to induce chondrogenesis is facilitated by distinct pathways to TGFβ signaling; BMP signaling is mediated by SMADs 1/5/8 **(Figure 4.1)** [398]. BMPs are involved in all stages of chondrogenesis and endochondral bone formation [158], and BMP2 the most well studied BMP growth factor is associated with chondrocyte proliferation and matrix synthesis through regulation of SOX9 [399]. Deletion of BMP2 and BMP4 has also been reported to result in the lack of mesenchymal chondrogenesis and in turn loss of proliferation and differentiation in chondrocytes which ultimately affect cartilage formation [380][381]. The role of BMP4 has been highlighted in trachea formation and ablation of BMP4 that reduces epithelial and mesenchymal proliferation results in loss of tracheal cell phenotypes [402]. BMP9 is the least investigated of the BMP growth factor family members in the field of cartilage tissue engineering and this is mainly due to their induction of chondrocyte hypertrophy generated from MSCs [145][383]. However, BMP9 was selected to induc tracheal chondroprogenitors as previous results in our laboratory resulted in significant matrix deposition consisting of high levels of collagen type II and aggrecan using bovine immature and mature articular chondroprogenitors when compared with TGFβ1[*data not shown*].

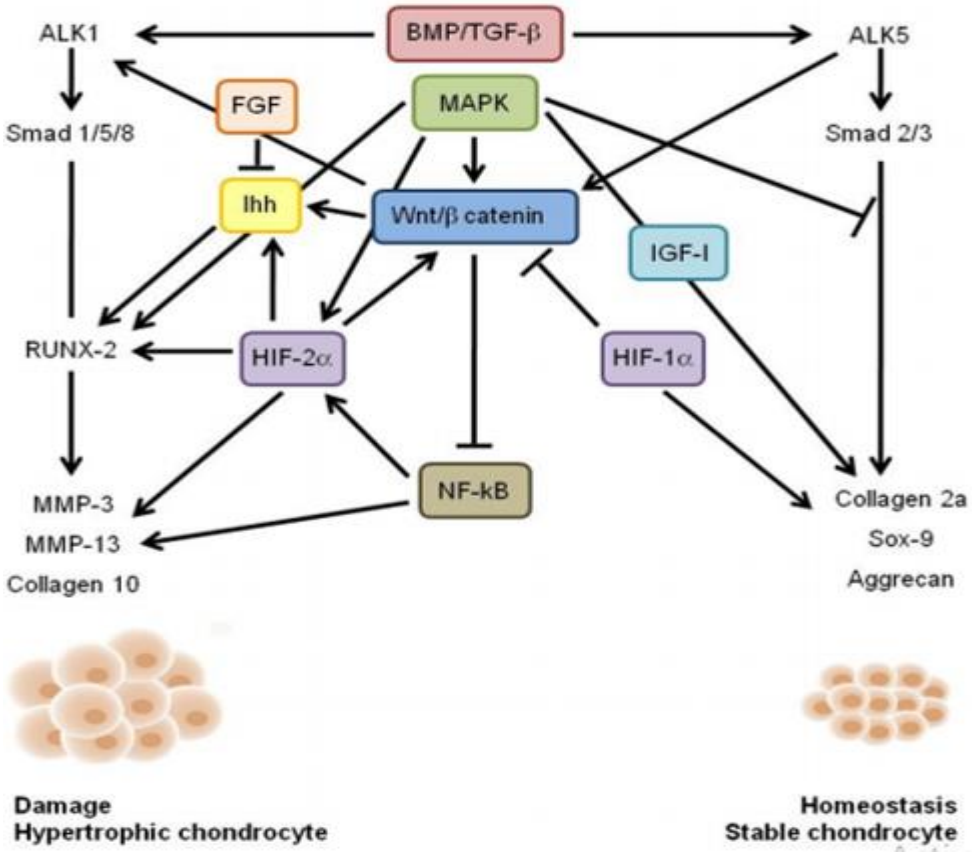

Figure 4.1. Summary of major signal transduction pathways of both TGFβ and BMP. The aim was to utilise two growth factors with two distinct pathways analyse the chondrogenic potential of tracheal chondroprogenitors [404].

To replicate condensation during the initial stages of *in vivo* cartilage formation, pellet culture is employed *in vitro* to mimic the microenvironment of developing cartilage and to facilitate chondrogenesis [405]. Pellet culture aims to promote 3D intercellular and cell-to-matrix interactions similar to those experienced by cells *in vivo* compared to those experienced by cells in 2D culture [406]. The supplementation of culture medium with TGFβ1 induces MSCs condensation during the differentiation phase, resulting in the stimulation of ECM production and deposition [407]. Based on these original findings, TGFβ1 is now routinely used during stem cell proliferation and chondrogenesis to induce cartilage formation [408], [409]. in general pellets are cultured with 10ng/ml of TGFβ1 for a period of 21-28 days, parameters that have been optimised through chondrogenic induction in bone marrow-derived MSCs [410]. TGFβ1 also is used in

conjunction with dexamethasone [411], l-proline [412] and ascorbic acid-2-phosphate [197] due to the synergistic role of these supplements in promoting cartilage ECM production and deposition *in vitro.*

4.2 Results

In this chapter we will compare the effect of two chondrogenic growth factors, TGFβ1 and BMP9, on the *in vitro* differentiation of tracheal chondroprogenitors. Histological, immunohistochemical, biochemical and qPCR analysis was performed to determine the extent of differentiation of cells under the stated culture conditions **(Figure 4.2)**.

To obtain a single cell suspension of tracheal chondrocytes, full-thickness tracheal cartilage was digested by sequential enzymatic incubation using first pronase and then collagenase. Full-depth chondrocytes were immediately pelleted down to act as a baseline control of native cell cartilage production. Tracheal cartilage-derived colony-forming cells were enriched from the full-depth population using differential adhesion to fibronectin. Colony forming cells (cells that had undergone more than 5 population doublings therefore ≥ 32 cells, were selectively trypsinised from dishes using 6 mm diameter cloning rings after 7-10 days in culture and the derived monoclonal cell-lines culture-expanded and treated with chondrogenic media as set out previously in materials and methods (**Chapter 2**, Section **2.3.5.1**) and then further supplemented with either TGFβ1 (10 ng/mL) or BMP9 (100 ng/mL).

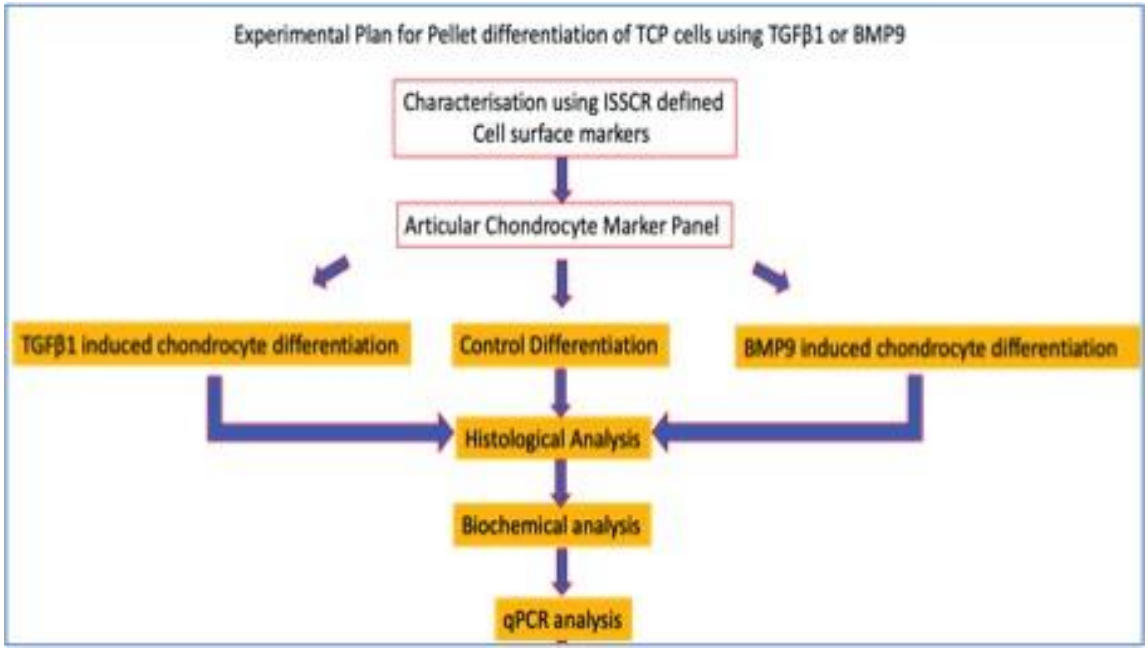

Figure 4.2. Pipeline of chondrogenic induction of porcine tracheal chondroprogenitors.

To ensure that culture expanded porcine tracheal chondroprogenitor (CP) monoclonal cell lines maintained the criteria for adult mesenchymal-like stem cells, PCR-based gene expression analysis was undertaken of relevant surface markers to monitor the expression of the positive biomarkers and negative haematopoietic-related markers prior to pellet culture. As shown in **Figure 4.3A**, the tested tracheal chondroprogenitor cell line was negative for both the hematopoietic marker CD34 and the leukocyte marker CD45, but weakly positive for monocyte cell surface marker CD14 (TLR4 co-receptor). Tracheal chondroprogenitors were weakly positive for CD166 (alcam) and CD105 (endoglin), and strongly positive for CD90 (thy-1) and CD73 (ecto-5'-nucleotidase). In addition, cells were also positive for gene transcription of nestin (NES) a well-characterised marker of stem/progenitor cells [368] Culture-expanded tracheal cartilage chondroprogenitors were pelleted down by low-speed centrifugation and incubated at 37 °C for a period of 21 days to analyse their chondrogenic ability in a three-dimensional (3D) pellet model of *in vitro* cartilage formation **(Figure 4.3B)**. **Figure 4.3B** clearly shows the smallest pellet as being the media that did not contain growth factors. The

pellet cultured in the presence of TGFβ1 was larger than the pellet cultured in the absence of growth factors and BMP9 supplemented media produced the largest pellet of all.

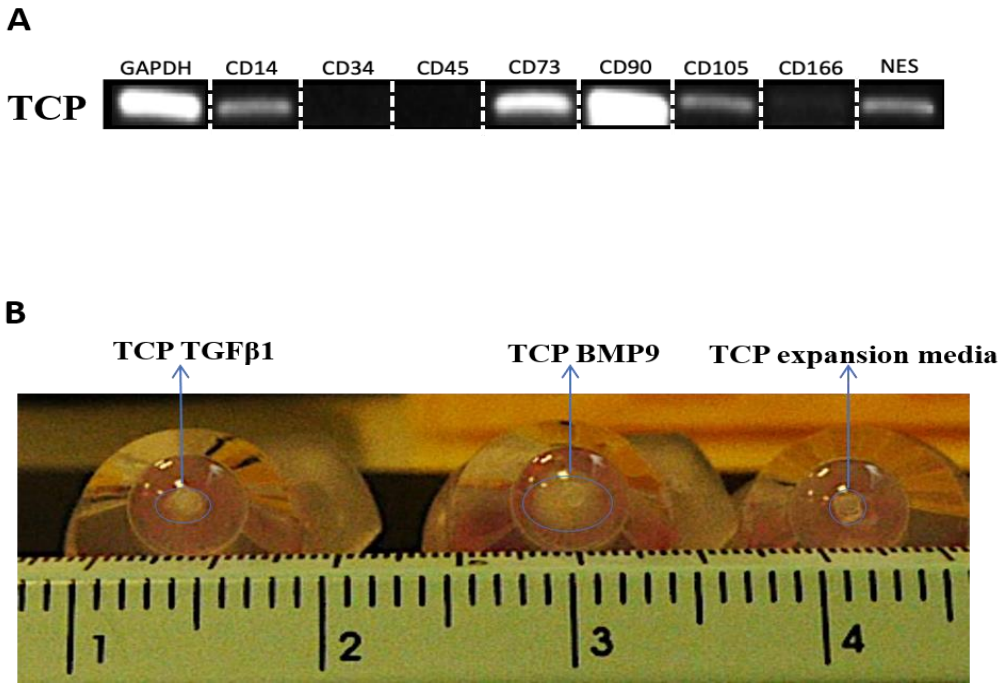

Figure 4.3. Characterisation of tracheal cartilage derived stem/progenitor cells before pellet culture. (A) Gene expression of stem cell surface markers defined by International Society for Stem Cell Research (ISSCR) for tracheal derived chondroprogenitors (TCP). Gels were constructed from various individual gels and separated with white banding. **(B)** Tracheal chondroprogenitors were pelleted down with chondrogenic medias supplemented with TGFβ1 and BMP9.

4.2.1 Histological analysis of 3D pellet culture

Tracheal chondroprogenitors and their full depth (FD) chondrocyte counterparts were cultured for 21 days with chondrogenic media, as described in **Chapter 2**, Section **2.3.5.1**, in the presence of 10 ng/mL TGFβ1 and 100 ng/mL BMP9. After 21 days, pellets were fixed, and paraffin wax embedded to assess the deposition and localisation of proteoglycans and collagens within the extracellular matrix. Full depth chondrocytes

were only treated with TGFβ1 whereas, chondroprogenitors were treated with both TGFβ1 and BMP9.

Haematoxylin and eosin staining were used to differentiate cell and extracellular matrix morphology. Using light microscopy, as shown in **Figure 4.4A**, the full-depth tracheal chondrocyte pellets displayed a more organised cellular and matrix orientation when compared to TGFβ1 **(Figure 4.4B)** and BMP9 **(Figure 4.4C)** treated chondroprogenitor pellets. Furthermore, both TGFβ1 and BMP9 cultured pellets presented with a dense cellular layer which formed the periphery of the pellet with a halo-like appearance. The full-depth tracheal chondrocyte pellet formed a small C-shape body while tracheal chondroprogenitor pellets formed rounder structures with column like banding. The most obvious differences were that in full-depth tracheal and BMP9 treated pellet cultures there was more extracellular matrix evident between cells, whereas the TGFβ1 treated pellet was more cellular with considerably less extracellular matrix between chondrocytes. All three pellet types exhibited a darker pink stain around their periphery indicating a more defined matrix deposition.

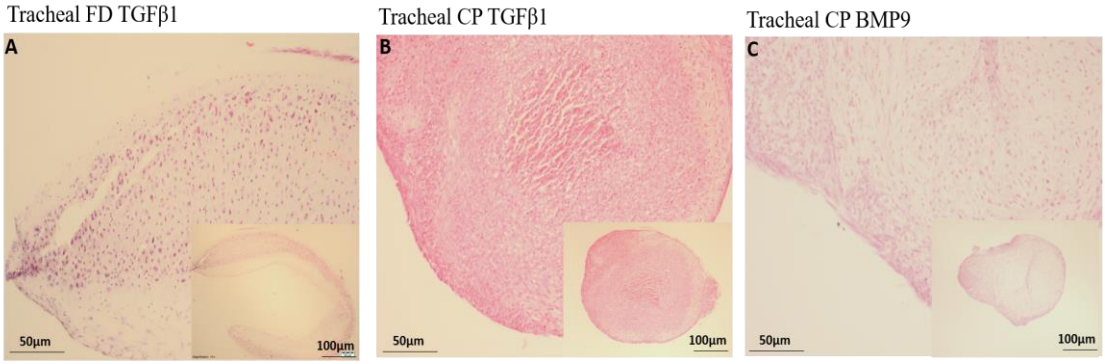

Figure 4.4. Haematoxylin and eosin stain of chondrogenic induced pellets after 21 days of chondrogenic culture. (A) Shows tracheal full depth chondrocytes (FD) in presence of TGFβ1, **(B)** tracheal chondroprogenitors (CP) in presence of TGFβ1 and **(C)** presence of BMP9. Images represent one porcine donor.

Toluidine blue is a basic thiazine metachromatic dye that selectively binds to acidic proteoglycans specifically glycosaminoglycans (GAGs) and is used as a histological stain to assess the quality of proteoglycan deposition in pellets. Light microscopy images of full depth tracheal pellet sections showed that the posterior convex part of the pellet stained very strongly for toluidine blue indicating abundant presence and deposition of proteoglycan. The anterior concave surface of the pellet stained less with toluidine blue and was more fibrous in appearance indicating the presence of more collagenous matrix in this location. Cell pellets formed with TGFβ1 **(Figure 4.5B)** also were positive for GAG content, however the GAG deposition was mostly observable around the periphery of the pellets. In the centre of the TGFβ1 pellets there were spaces, probably due to sections breaking apart during sectioning and this was probably due to the lack of extracellular matrix present. The latter distribution of extracellular matrix and cells is characteristic of the necrotic centres visible in articular cartilage pellets caused by either incomplete differentiation of cells by TGFβ1 growth factor, or, the lack of diffusion of nutrients and oxygen to cells at the core of the pellet [215]. In contrast, BMP9 treated pellets showed strong toluidine blue labelling throughout the whole depth of the pellet, with little evidence of a necrotic core, though there was relatively less staining at the pellet core. Chondroprogenitors grown in the presence of expansion medium but without growth factor did produce pellets but did not deposit substantial amounts of toluidine blue staining matrix **(Figure 4.5D)**.

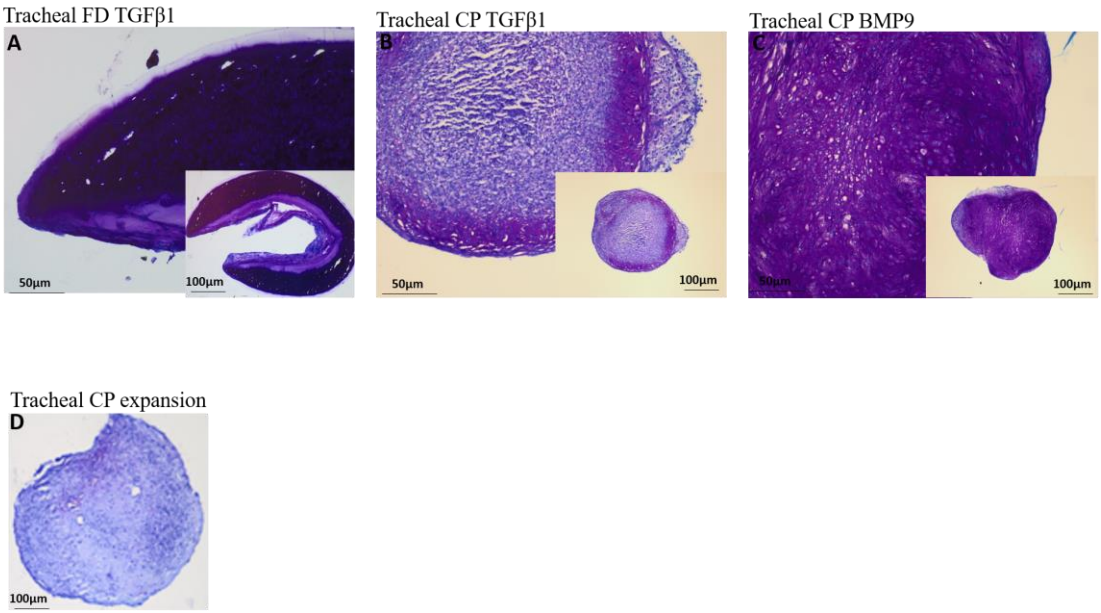

Figure 4.5. Toluidine blue stain of chondrogenic induced pellets after 21 days of chondrogenic culture to detect GAG deposition. (A) shows tracheal full depth chondrocytes (FD) in presence of TGFβ1, **(B)** tracheal chondroprogenitors (CP) in presence of TGFβ1 and **(C)** BMP9. **(D)** Shows tracheal chondroprogenitor cells (CP) in presence of growth media without any chondrogenic supplements. Images represent one porcine donor.

Alizarin red stain was performed to determine if any calcium deposition occurred as a consequence of cells undergoing terminal chondrocyte differentiation and possible osteogenic differentiation, as previously reported for bone marrow-derived mesenchymal stem cells [386]. No obvious staining for alizarin red was detected in the native tissue **(Figure 4.6A),** tracheal full depth differentiated **(Figure 4.6B)** or tracheal CP expansion medium pellets **(Figure 4.6C)**. Some intense staining was evident on the margins of pellets treated with the chondrogenic medias, but this may be non-specific **(Figure 4.6C& 6D)**.

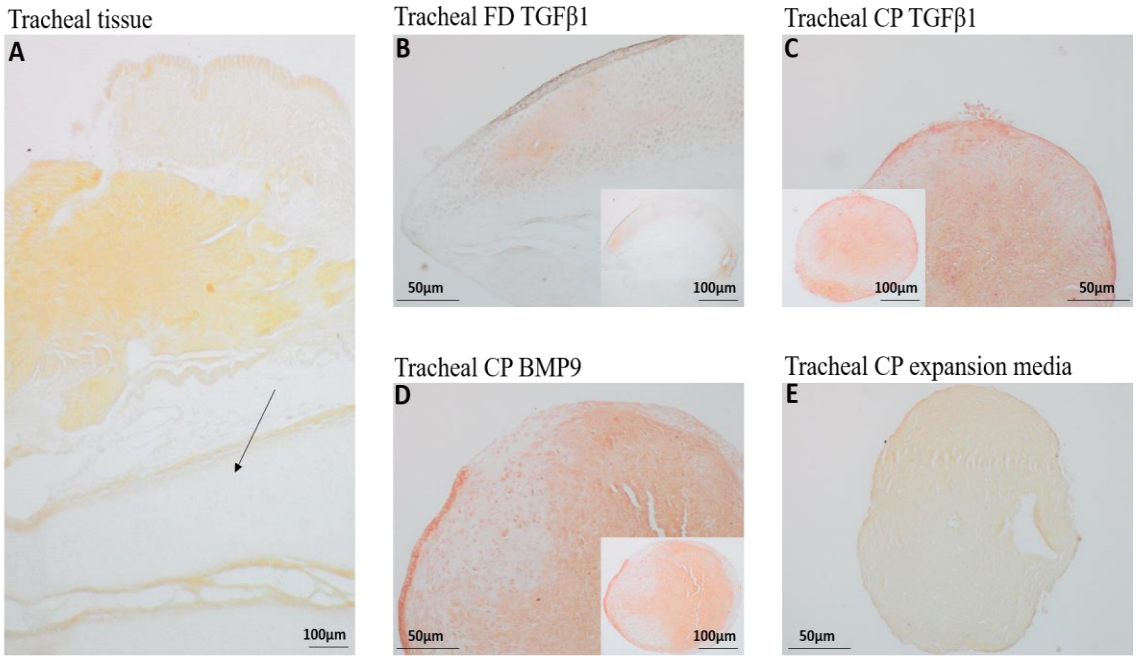

Figure 4.6. Alizarin red stain of chondrogenic induced pellets after 21 days of chondrogenic culture to detect calcium deposition. (A) shows the native tracheal tissue. Tracheal cartilage is indicated *(arrowed)*. **(B)** shows tracheal full depth chondrocytes (FD) in presence of TGFβ1, **(C)** tracheal chondroprogenitors (CP) in presence of TGFβ1 and **(D)** BMP9. **(E)** Tracheal chondroprogenitor cells (CP) in presence of growth media without any chondrogenic supplements. Images represent one porcine donor.

4.2.2 Immunohistochemical analysis of pellets

4.2.2.1 Aggrecan

Immunohistochemical analysis revealed that tracheal full-depth chondrocyte pellets **(Figure 4.7A)** differentially labelled for aggrecan antibodies with clear aggrecan column banding. Labelling was localised to the posterior convex part of the pellet with the highest levels of labelling at the periphery of this structure. The anterior convex surface did not label for aggrecan, indicating possibly that the surface is more collagenous. Tracheal chondroprogenitor pellets treated with TGFβ1 also labelled for aggrecan antibodies and with labelling at the periphery of the pellet **(Figure 4.7B)** in line with the observations seen with GAG deposition in toluidine blue stained sections and lacked the presence of aggrecan column. Tracheal chondroprogenitor pellets treated with BMP9

(Figure 4.7C) showed strong labelling for aggrecan throughout the full depth of the pellet (see inset, **Figure 7C**) with the exception of a non-labelling streak near the surface. Tracheal chondroprogenitors pelleted and cultured with non-growth factor supplemented medium **(Figure 7D)** labelled very weakly for aggrecan antibodies indicating that cell-cell contact induced by 3D culture also induces aggrecan expression, though weakly in comparison.

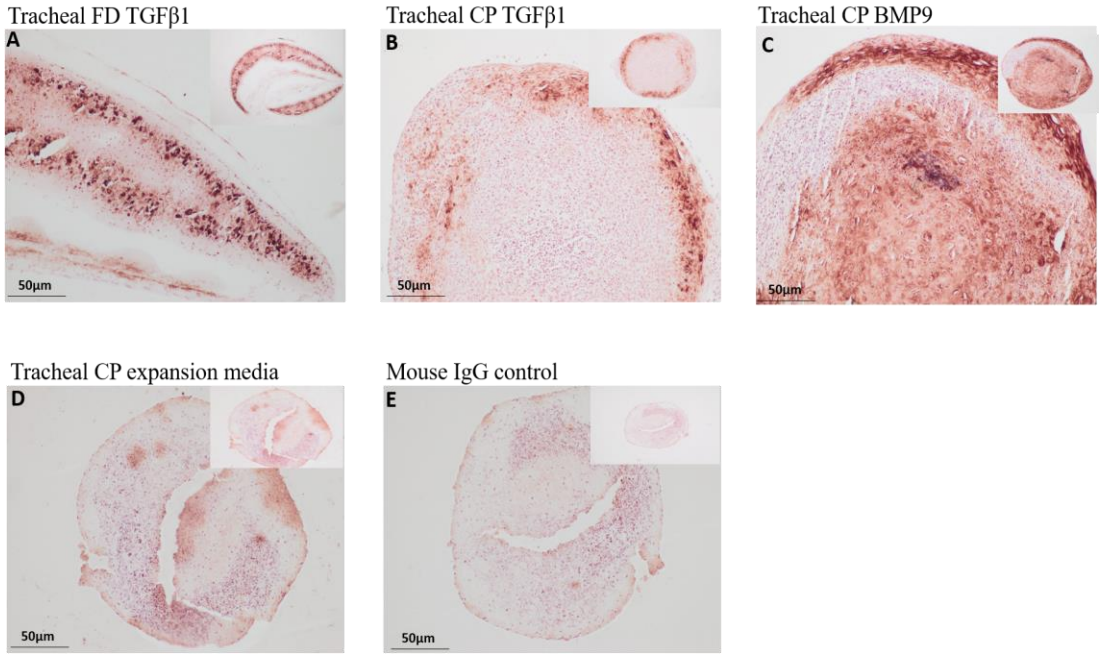

Figure 4.7. Immunohistochemical analysis chondrogenic induced pellets after 21 days of chondrogenic culture to detect aggrecan (A) shows tracheal full depth chondrocytes (FD) in presence of TGFβ1, **(B)** Tracheal chondroprogenitors (CP) in presence of TGFβ1, **(C)** tracheal chondroprogenitors (CP) in presence of BMP9, **(D)** tracheal chondroprogenitor cells (CP) in presence of growth media without any chondrogenic supplements and **(E)** Mouse Ig was used at the same concentrations as the primary antibodies to identify any non-specific labelling in sections. Images represent one porcine donor.

4.2.2.2 Collagen type II

Immunohistochemical analysis revealed that tracheal full-depth chondrocyte pellets **(Figure 4.8A)** labelled strongly for collagen type II antibodies, **(Figure 4.8A)**. Labelling

in full depth pellets was again predominantly in the posterior convex body, although some labelling was also evident on the anterior surface. The layer beneath the anterior end was not labelled by antibodies. Tracheal chondroprogenitor pellets treated with TGFβ1 labelled for collagen type II differentially, with weak labelling throughout the full depth of the pellets and more intense labelling at the periphery **(Figure 4.8B)**. BMP9-treated tracheal chondroprogenitor pellets displayed intense and even labelling throughout the whole pellet (see inset **Figure 4.8C**), especially in the extracellular regions surrounding the lacunae of differentiated progenitors. Tracheal chondroprogenitors grown in non-growth factor supplemented medium also labelled for collagen type II antibodies **(Figure 4.8D)** but this labelling was confined to the centre of the pellet and to a thin band on the surface of pellets. The mouse IgG control displayed little or no labelling **(Figure 4.8E)**.

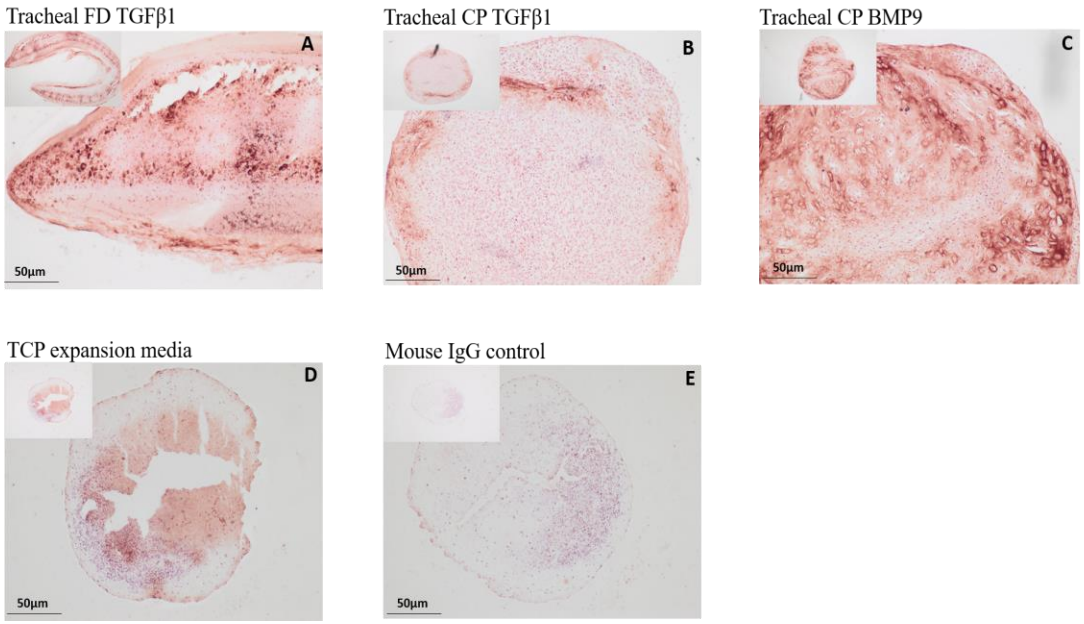

Figure 4.8. Immunohistochemical analysis chondrogenic induced pellets after 21 days of chondrogenic culture to detect collagen type II (A) shows tracheal full depth chondrocytes (FD) in presence of TGFβ1, **(B)** tracheal chondroprogenitors (CP) in presence of TGFβ1, **(C)** tracheal chondroprogenitors in presence of BMP9, **(D)** tracheal chondroprogenitor cells (CP) in presence of growth media without any chondrogenic supplements and **(E)** Mouse IgG was used at the same concentrations as the primary antibodies to identify any non-specific labelling in sections. Images represent one porcine donor.

4.2.2.3 Collagen type I

Collagen type I labelling was evident throughout the whole depth of the tracheal full depth chondrocyte pellets **(Figure 4.9A)** mainly located around chondrocytes and less intensely in the extracellular matrix. In tracheal chondroprogenitors induced to differentiate with TGFβ1 there was again differentiated labelling with weak labelling throughout the whole pellet with more intense labelling confined to the surface **(Figure 4.9B)**. Tracheal chondroprogenitors treated with BMP9 also exhibited strong labelling to collagen type I antibodies **(Figure 4.9B)** throughout the full-depth of the pellet. Labelling to collagen type I antibodies was less evident in tracheal chondroprogenitors cultured as pellets in non-chondrogenic medium **(Figure 4.9D)** and present as a weak signal on the surface of pellets. around the periphery of the pellet. No expression was observed on the control pellet labelled with mouse IgG **(Figure 4.9E)**.

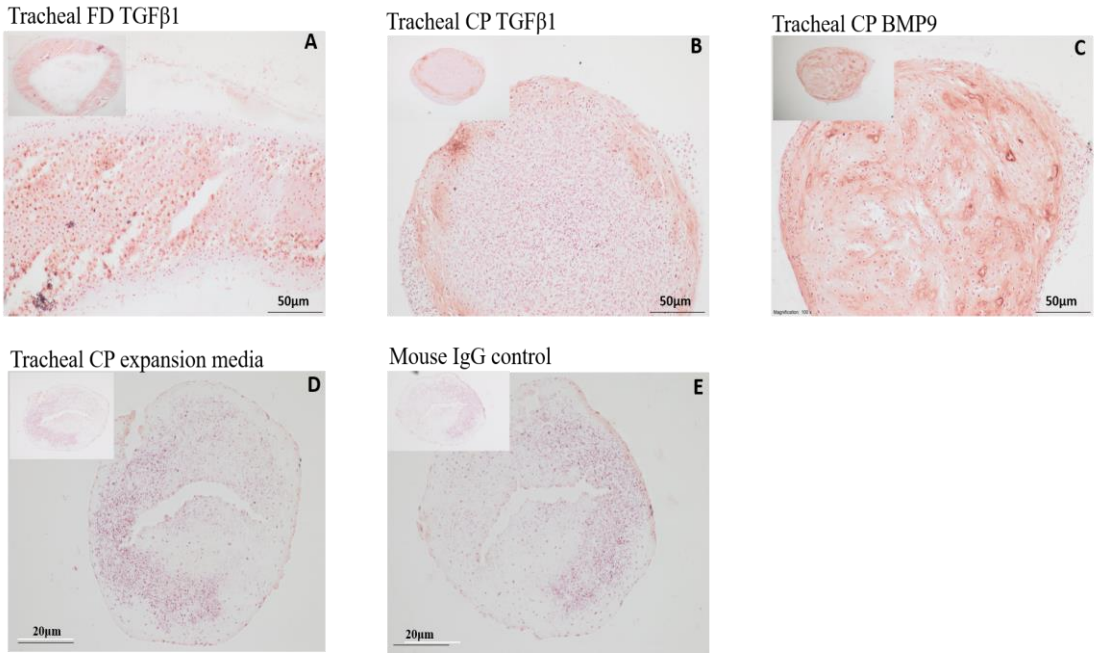

Figure 4.9. Immunohistochemical analysis chondrogenic induced pellets after 21 days of chondrogenic culture to detect collagen type I (A) shows tracheal full depth chondrocytes (FD) in presence of TGFβ1, **(B)** tracheal chondroprogenitors (CP) in presence of TGFβ1, **(C)** tracheal chondroprogenitors (CP) in presence of BMP9, **(D)** tracheal chondroprogenitor cells (CP) in presence of growth media without any chondrogenic supplements and **(E)** Mouse IgG was used at the same concentrations as

the primary antibodies to identify any non-specific labelling in sections. Images represent one porcine donor.

4.2.2.4 Collagen type X

Collagen type X immunostaining was performed to further validate alizarin red staining in pellets by detecting any specific chondrocytes hypertrophic markers such as collagen type X **(Figure 4.10)**. The antibody labelling however, was not specific and therefore both positive and negative controls stained false positive **(Figure 4.10A& 4.10B)**.

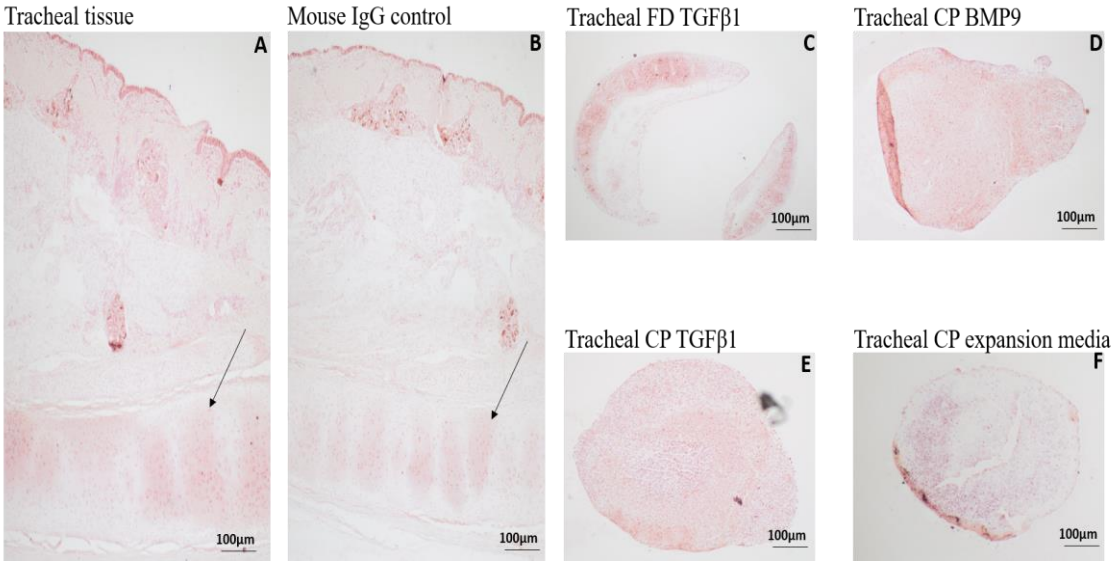

Figure 4.10. Immunohistochemical analysis chondrogenic induced pellets after 21 days of chondrogenic culture to detect collagen type X (A) shows the native tracheal tissue. Tracheal cartilage is indicated *(arrowed)*. **(B)** mouse IgG was used at the same concentrations as the primary antibodies to identify any non-specific labelling in sections. **(C)** tracheal full depth chondrocytes in presence of TGFβ1 and **(D)** and **(E)** shows tracheal chondroprogenitor cells in presence of BMP9 and TGFβ1 respectively. (F) shows tracheal chondroprogenitors in presence of growth media without any chondrogenic supplements. Images represent one porcine donor.

4.2.3 Biochemical quantification of pellet extracellular matrix content

To complement histological analysis, spectrophotometric quantification of GAG, collagen and DNA was performed using DMMB, hydroxyproline and DNA assays

respectively. The GAG content was quantified using DMMB dye, which is a cationic dye, that directly binds to negatively charged sulphated glycosaminoglycans (sGAG). The collagen content was measured indirectly by quantifying hydroxyproline content. 4-Hydroxyproline is an amino acid commonly found in hyaline cartilage collagen and functions to stabilise the helical structure. DNA was quantified using the picogreen dye assay to analyse whether the pellet culture induced proliferation as well as for normalisation of sGAG and hydroxyproline measurements in pellet cultures.

Full-depth tracheal chondrocyte pellets stimulated with TGFβ1 (120.3±7.6 μg/mL) produced significantly higher levels of proteoglycan, measured as raw sGAG, ($p < 0.0001$) than tracheal chondroprogenitors when stimulated with either TGFβ1 (1.6±0.8 μg/mL) or BMP9 (6.2±2.1 μg/mL) growth factors. Full depth tracheal chondrocyte pellets showed a 100-fold and 60-fold increase in total sGAG when compared to TGFβ1 and BMP9 pellets. There was also a 3.28-fold increase in BMP9 when compared to TGFβ1 pellets ($p < 0.05$) **(Figure 4.11A)**.

DNA quantifications revealed that full depth tracheal chondrocyte pellets (0.95±0.13 μg/mL) were significantly higher in DNA content than TGFβ1 (0.31±0.09 μg/mL; $p < 0.0001$) and not significantly different than BMP9 treated tracheal chondroprogenitors (0.88±0.35 μg/mL). Pellets formed with BMP9 had a 2.5-fold higher level of DNA than TGFβ1 treated pellets ($p < 0.05$; **Figure 4.11B**).

Raw hydroxyproline measurements **(Figure 4.11C)** showed that the total collagen amount was highest in full-depth tracheal chondrocyte pellets (0.098±0.0009 μg/mL) followed by BMP9 (0.097±0.0008 μg/mL) and TGFβ1 (0.096±0.0004 μg/mL) chondroprogeitor pellets. There was a significance difference when comparing FD with TGFβ1 and BMP9 treated pellets ($p < 0.001$; $p < 0.05$ respectively).

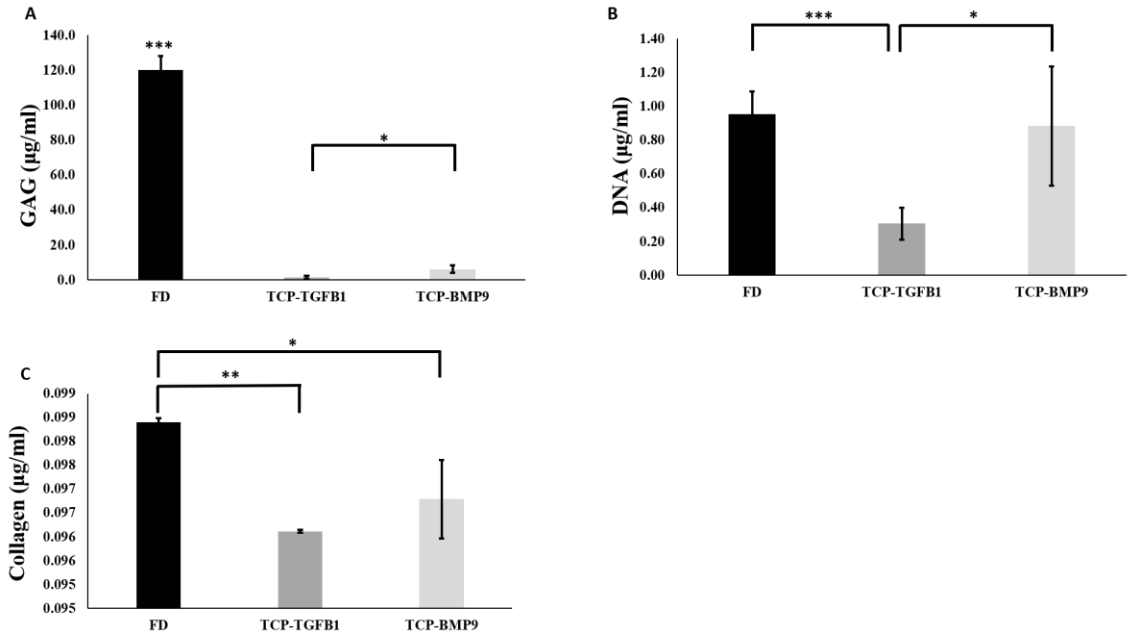

Figure 4.11. Quantification of tracheal full depth chondrocytes (FD) and chondroprogenitors (CP) for (A) sulphated GAG content, (B) DNA content and (C) total collagen content. All data shown is average (± standard deviation) from three biological repeats, tested for significance using two-way ANOVA analysis. * and ** and *** are used to indicate $p < 0.05$, $p < 0.001$ and $p < 0.0001$ respectively.

When total sGAG content was normalised to DNA for all pellet culture groups, full depth tracheal chondrocyte pellets (128.41±21.2 µg/µg) showed a 26-fold and 18-fold increase compared to TGFβ1 (5.17±2.21 µg/µg) and BMP9 (7.11±0.69 µg/µg) respectively **(Figure 4.12A)**. No significant difference was found between sGAG between TGFβ1 and BMP9 treated pellets. Similarly, when total collagen content was normalised to DNA **(Figure 4.12B)**, TGFβ1 pellet (0.33±0.097 µg/µg) was significantly higher than FD pellet (0.1±0.02 µg/µg; $p < 0.001$) and BMP9 pellet (0.122±0.05 µg/µg; $p < 0.05$). No significance difference in averages was observed between full depth tracheal chondrocyte pellets and BMP9-treated pellets.

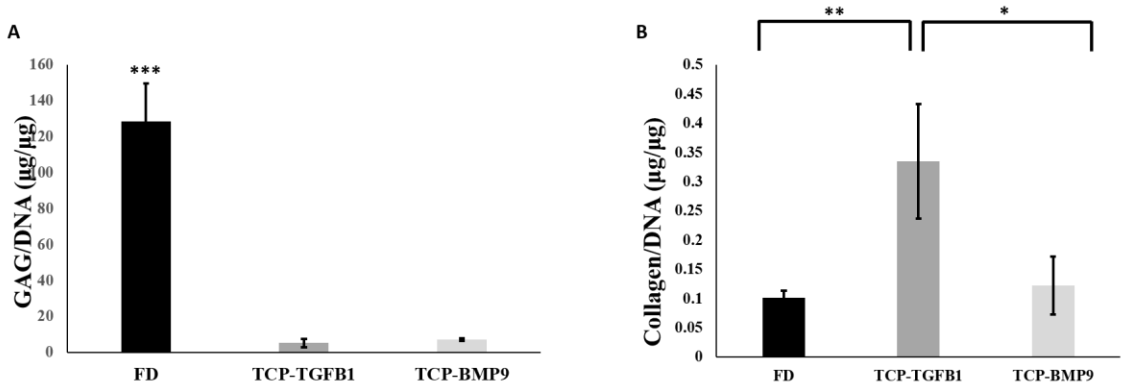

Figure 4.12. sGAG and collagen contents of pellets normalised to DNA. Tracheal full depth chondrocytes (FD) and tracheal chondroprogenitors (CP) pellets following 21 days chondrogenesis was analysed biochemically and normalized to DNA. All data shown is average (± standard deviation) from three biological repeats, tested for significance using two-way ANOVA analysis. * and ** and *** are used to indicate $p < 0.05$, $p < 0.001$ and $p < 0.0001$ respectively.

4.2.4 Gene expression analysis

To further quantify the extracellular matrix of pellets, steady-state gene expression levels of the most predominant cartilage matrix components were measured after 21-day culture period. Chondrogenesis *in vitro* is initiated by the expression of SOX9, the main chondrogenic transcriptional factor, which in turn, is required for the transcriptional activation of aggrecan and collagen type II promoters leading to the production of an organised extracellular matrix. Collagen types I and X were used to distinguish between the production of fibrocartilage (collagen type I) or calcified cartilage (collagen type X), as tracheal cartilage is principally classified as a hyaline-type cartilage. Glyceraldehyde 3-phosphate dehydrogenase (GAPDH) was used as a housekeeping gene.

Relative gene expression levels of SOX9 **(Figure 4.13C)** were significantly decreased for chondroprogenitor pellets when cultured in TGFβ1 (0.51±0.11; $p < 0.001$) and BMP9 (0.67±0.4; $p < 0.05$) when compared with full depth tracheal chondrocyte pellets (1.05±0.35). No significance difference in averages was observed between TGFβ1 and BMP9-treated tracheal chondroprogenitor pellets.

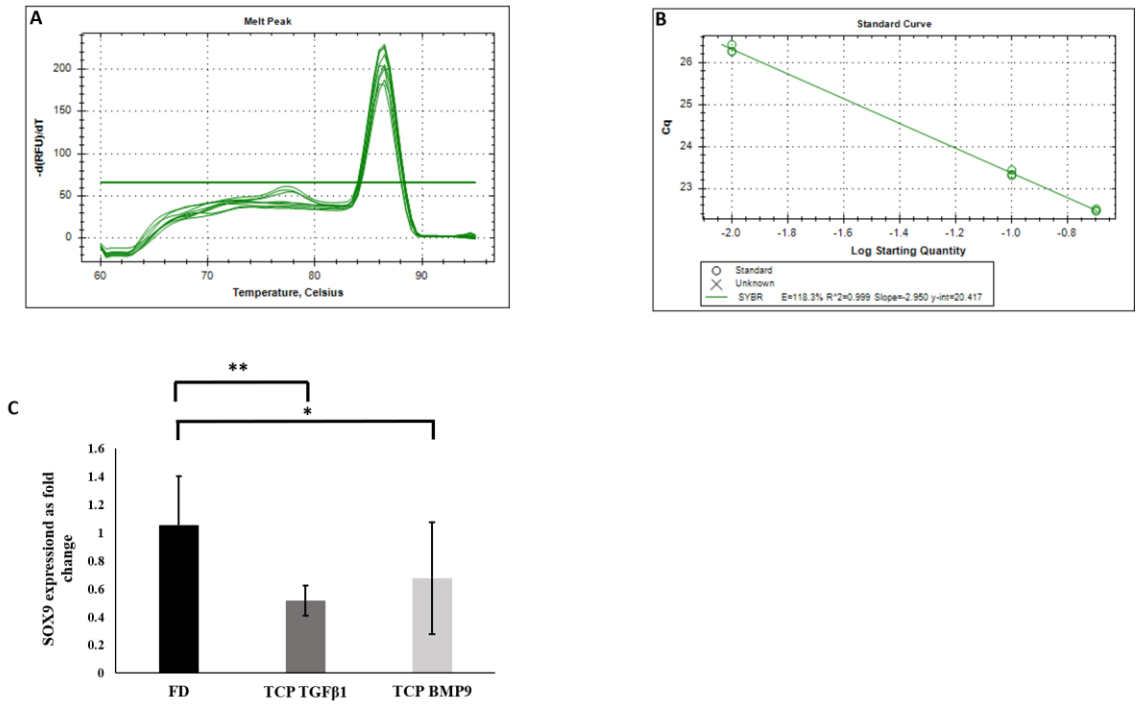

Figure 4.13. SOX9 gene expression shown as a fold change using ΔΔ*CT* method. (A) shows the melt-curve. **(B)** shows the efficiency of amplification which was 110%. **(C)** shows the fold change expression of tracheal full depth chondrocytes (FD) and tracheal chondroprogenitors (CP) after 21 days chondrogenic culture period. All data shown is average (± standard deviation) from three biological repeats, tested for significance using two-way ANOVA analysis. * and ** are used to indicate $p < 0.05$ and $p < 0.001$ respectively.

After 21 days culture the relative expression levels of collagen type II in full-depth tracheal chondrocyte pellets (1.01±0.16) were **(Figure 4.14C)** significantly higher ($p < 0.0001$) compared to TGFβ1 (0.03±0.01) and BMP9-treated tracheal chondroprogenitor pellets (0.09±0.01) showing a 33-fold and 11-fold increase respectively. BMP9-treated pellets had transcribed more collagen type II RNA when compared to TGFβ1 and showed a 3-fold increase ($p < 0.05$).

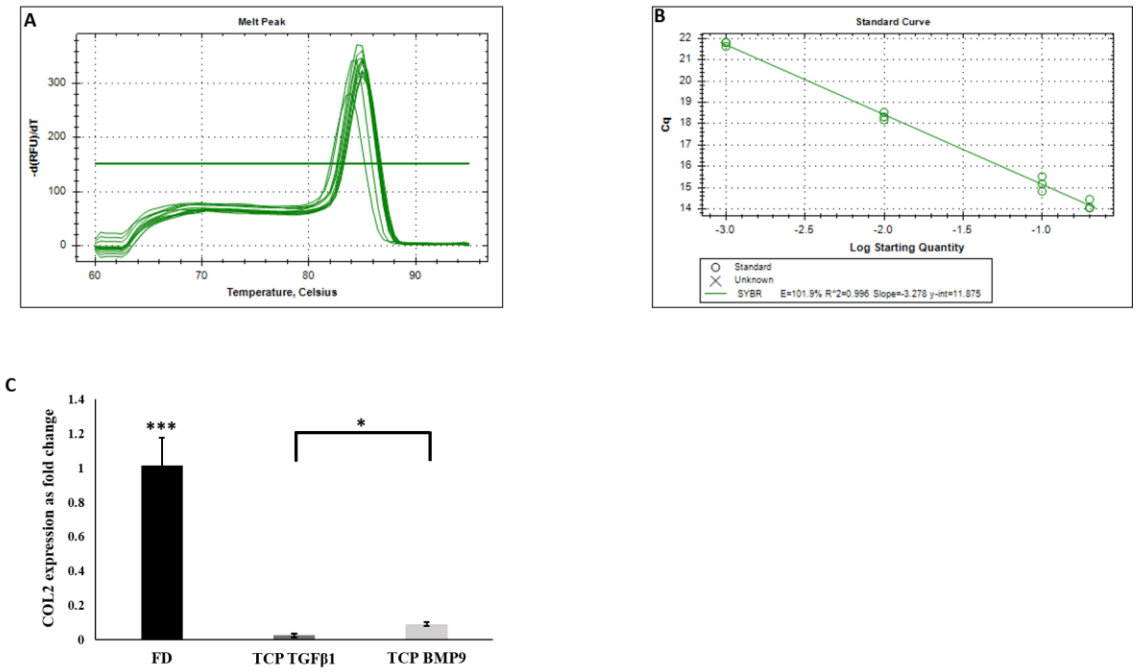

Figure 4.14. COL2 gene expression shown as a fold change using ΔΔ*CT* method. (A) shows the melt-curve. (B) shows the efficiency of amplification which was 101%. (C) shows the fold change expression of tracheal full depth chondrocytes (FD) and tracheal chondroprogenitors (CP) after 21 days chondrogenic culture period. All data shown is average (± standard deviation) from three biological repeats, tested for significance using ANOVA analysis. * and *** are used to indicate $p < 0.05$ and $p < 0.0001$ respectively.

The same trend as observed for collagen type II gene expression was seen for aggrecan (ACAN) expression. Aggrecan expression in full-depth tracheal chondrocyte pellets (1.1±0.44) was significantly higher when compared to chondroprogenitor pellets stimulated with either TGFβ1 (0.2±0.08) or BMP9 (0.45± 0.04) **(Figure 4.15C)**. BMP9-treated pellets had higher ACAN expression levels when compared to TGFβ1-treated tracheal chondroprogenitor pellets and showed a 2.25-fold increase overall in comparison ($p < 0.05$).

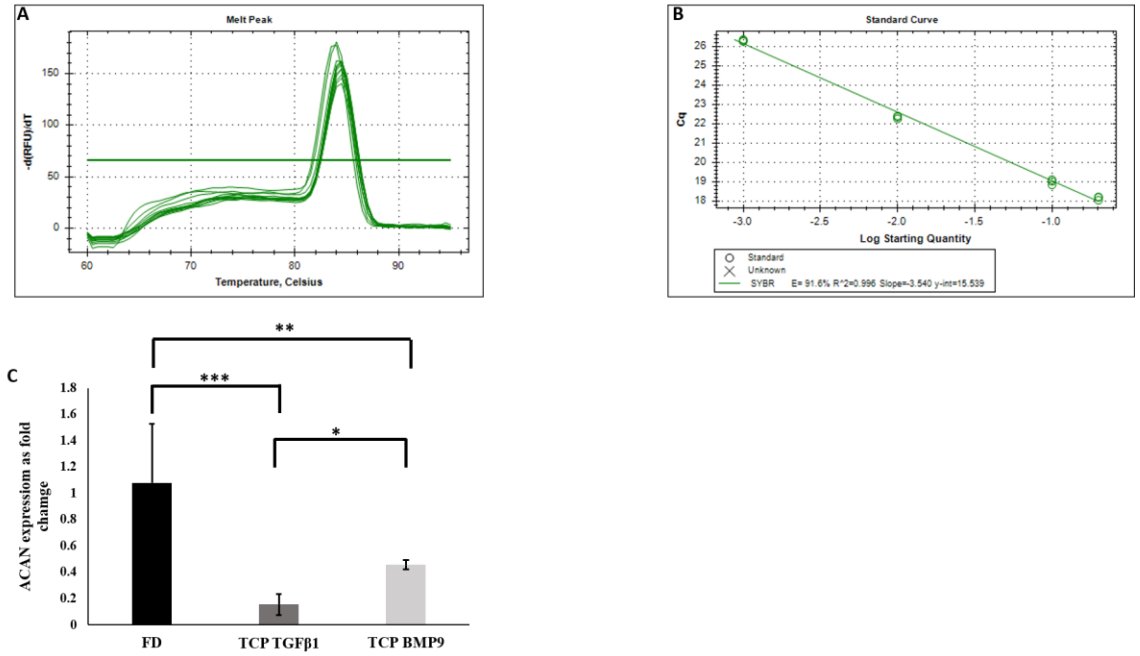

Figure 4.15. ACAN gene expression shown as a fold change using ΔΔ*CT* method. **(A)** shows the melt-curve. **(B)** shows the efficiency of amplification which was 91.9%. **(C)** shows the fold change expression of tracheal full depth chondrocytes (FD) and tracheal chondroprogenitors (CP) after 21 days chondrogenic culture period. All data shown is average (± standard deviation) from three biological repeats, tested for significance using two-way ANOVA analysis. * and ** and *** are used to indicate $p < 0.05$, $p < 0.001$ and $p < 0.0001$ respectively.

Tracheal chondroprogenitor pellets stimulated with TGFβ1 (3.9±1.18) showed the highest relative gene expression levels of collagen type I followed by BMP9 induced pellets (3.27±2.05) and full-depth tracheal chondrocyte pellets (1.01±0.2). There was a 3.86-fold increase in TGFβ1-treated progenitor pellets ($p < 0.0001$) and 3.23-fold increase by BMP9 progenitor pellets ($p < 0.05$) when compared to the relative levels of expression in full-depth tracheal chondrocyte pellets **(Figure 4.16C)**.

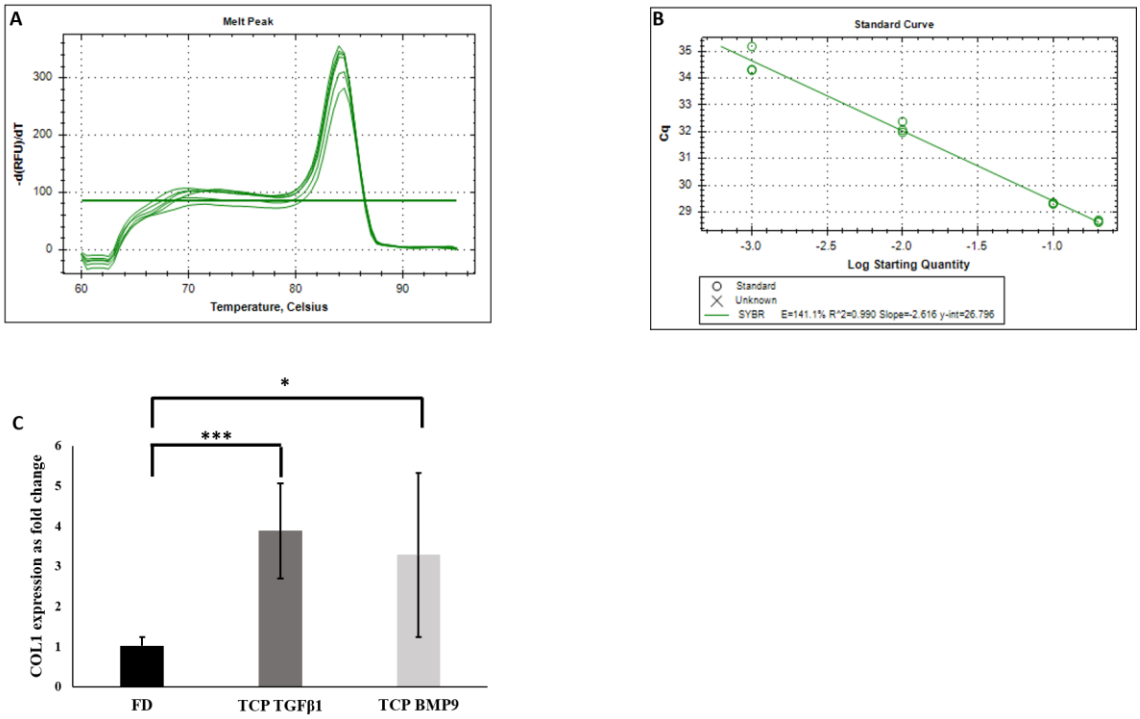

Figure 4.16. COL1 gene expression shown as a fold change using ΔΔ*CT* method. (A) shows the melt-curve. **(B)** shows the efficiency of amplification which was 140%. **(C)** shows the fold change expression of tracheal full depth chondrocytes (FD) and tracheal chondroprogenitors (CP) after 21 days chondrogenic culture period. All data shown is average (± standard deviation) from three biological repeats, tested for significance using two-way ANOVA analysis. * and *** are used to indicate $p < 0.05$ and $p < 0.0001$ respectively.

BMP9-induced chondroprogenitor pellets (98.1±40.06) showed the highest relative expression of collagen type X followed by TGFβ1-treated progenitor pellets (15.98±5.09) and full depth tracheal chondrocyte pellets (1.05±0.4). Both BMP9 and TGFβ1 displayed significantly higher transcriptional levels compared to full depth tracheal chondrocyte pellets with a 93-fold ($p < 0.001$) and 15-fold ($p < 0.05$) increase, respectively **(Figure 4.17C).**

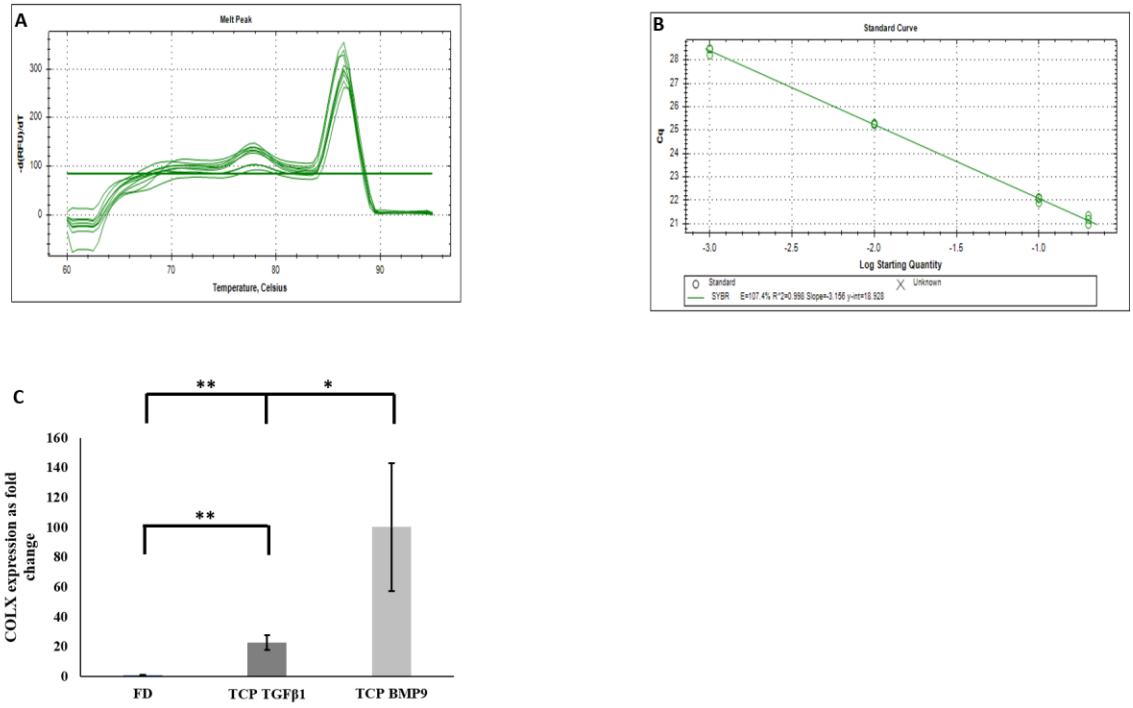

Figure 4.17. **COLX gene expression shown as a fold change using ΔΔ*CT* method. (A)** shows the melt-curve. **(B)** shows the efficiency of amplification which was 109%. **(C)** shows the fold change expression of tracheal full depth chondrocytes (FD) and tracheal chondroprogenitors (CP) after 21 days chondrogenic culture period. All data shown is average (± standard deviation) from three biological repeats, tested for significance using two-way ANOVA analysis. * and ** are used to indicate $p < 0.05$, $p < 0.001$ respectively.

4.3 Discussion

As previously stated the choice of cell and its origin tissue is a primary pivotal step towards reconstruction of aneural and avascular tracheal cartilage tissue [204]. In airway tissue engineering a particular focus has been placed on autologous approaches with chondrocytes and MSCs from other anatomical sources (nasal septum, auricular, adipose and bone marrow MSCs) being investigated [130]. To our knowledge no previous attempt has been taken to assess the chondrogenic ability of tracheal-derived chondroprogenitors, and therefore, the chondrogenic potential of tracheal chondroprogenitors was assessed by a standard chondrogenic pellet assay [23] [159]. This assay used a defined culture medium containing TGFβ1 [235] a widely used growth

factor in the field of cartilage tissue engineering and also another member of the TGFβ-superfamily, BMP9.

Tracheal full-depth chondrocytes were pelleted directly after tissue digest to provide a baseline control and were stimulated with TGFβ1 only, as the effect of this growth factor is well studied as opposed to BMP9. Tracheal chondroprogenitors cultured in the absence of growth factors were also included as a control group to examine the effect of cell-cell and cell-matrix interaction in matrix synthesis. Only histological images were shown for tracheal chondroprogenitors pellets grown in non-chondrogenic medium, and because of the lack of matrix deposition it was not feasible to perform other analysis. Therefore full-depth tracheal chondrocytes were considered as the main control group, a baseline for optimal induction of the chondrogenic phenotype.

Many studies have used chondrocytes or MSCs where these cells are expanded for many generations in 2D culture prior to chondrogenic induction [192][393]. In this study full-depth chondrocytes were not cultured in 2D plastic culture to avoid phenotypic changes caused by loss of cellular function and specialisation. It is well established that chondrocytes lose their phenotypic stability upon long-term 2D culture and therefore it is more logical to use fully chondrocyte committed cells directly after tissue enzymatic digest, as currently there are no published strategies to maintain the chondrogenic capacity of cells during long-term *in vitro* expansion [414]. For differentiation studies, pellet culture is employed as a standard model as this model recreates the initial stages of mesenchymal condensation observed during embryonic development of skeletal structures [415]. Although cell necrosis, principally due to a lack of diffusion of oxygen and nutrients, at the centre of pellet cultures can be problematic [196][396] and might interfere with some important aspects of chondrocyte function, such as ECM deposition, it is an acceptable model to understand if cells are capable of efficient chondrogenesis. Therefore, it is crucial to use fully differentiated cells alongside with stem/progenitor cells as a baseline of normal function to give a more physiologically relevant comparison to the degree of chondrogenesis produced by progenitor cell lines. It has been previously shown that stem/progenitor cells are more responsive when compared against their fully differentiated progeny and bone marrow MSCs during *in vitro*

chondrogenesis [138][204][345].

The standard concentration of TGFβ1 to induce chondrogenesis is 10 ng/mL for 21 days. This treatment was therefore adopted, as the standard quantity to induce chondrogenesis as shown in various cell sources [410]. BMP9 was used at a concentration of 100 ng/mL in this study as this concentration has been shown to optimally induce chondrogenesis in immature and mature bovine articular cartilage [*data not shown*]. This result agreed with a previous publication where 100ng/mL of BMP9 was able to potently induce chondrogenic induction of human bone marrow MSCs and resulted in the phosphorylation of SMAD1/5, which ultimately up-regulated SOX9 [191]. Chondrogenic induction of tracheal chondroprogenitors with BMP9 was more significant when compared with TGFβ1 treatment, using raw GAG and collagen content measurements. This data is in accordance with previous work done by Blunk *et al.* showing increased synthesis of sGAG and collagen from immature chondrocytes when cultured in polyglycolic acid in presence of 1-100 ng/mL of BMP9 against untreated samples [417]. Hills *et al.* also reported an increase in sGAG and collagen content in immature explants using 100 ng/mL BMP9 when compared with non-treated explants [418].

Collagen content normalized to DNA content however showed there is more potential for tracheal chondroprogenitor cells to secrete collagen per cell when stimulated with TGFβ1 as opposed to BMP9. When comparing full-depth tracheal cartilage pellets with tracheal chondroprogenitors treated with TGFβ1 and BMP9, the full-depth tracheal chondrocyte pellet outperformed both treatments for sGAG and collagen deposition. This result is not in line with what previously reported where chondrocytes were unable to synthesis sGAG and collagen as efficiently as articular and auricular chondroprogenitors incorporated in gelatin methacryloyl in the presence of TGFβ1. However, in both the latter referenced studies, equine culture expanded chondrocytes up to passage 1 were used and the period of chondrogenesis was 56 days [138][345]. Therefore, the latter studies used chondrocytes that might have partially undergone loss of function and specialisation and may have demonstrated an inability to efficiently recapitulate the chondrocyte functionality and specialisation. Hence, using full-depth

unexpanded cell populations provides a more physiologically relevant insight into the chondrogenic behavior of tracheal progenitors. However, to fully comprehend the main factor of chondrogenic potency it would be more desirable to utilize full depth chondrocytes and perform pellet cultures with the presence of BMP9 and also basal medium only.

Messenger RNA expression of cartilage specific markers confirmed tracheal chondroprogenitors differentiation towards the chondrogenic lineage. SOX9 expression was higher in BMP9 treated pellets when compared against TGFβ1 treated pellets after 21 days of chondrogenic induction. This ultimately resulted in elevated gene expression of ACAN and COL2A1 respectively in BMP9 compared to TGFβ1. A study done by Majumdar *et al.* demonstrated the chondrogenic differentiation of BMP2 and BMP9 combined on human MSCs in alginate beads. It showed that there was an increase in collagen type II and aggrecan gene expression showing similarities with our data when comparing the effects of BMP9 and TGFβ1 on chondrogenic differentiation of progenitors [403]. Although BMP9 seemed superior in producing the appropriate hyaline type matrix proteins, full-depth tracheal cartilage pellets treated with TGFβ1 outperformed both BMP9 and TGFβ1 progenitor treated cells at gene level and in turn protein matrix synthesis and secretion. This was also evident as shown by the histological and immunohistological images where the full-depth tracheal cartilage pellet produced a more homogenous and C-shape construct rich in aggrecan and collagen type II protein similar to their parental tissue by the presence of the columnar banding, as also shown in the previous chapter (Chapter 3). Tracheal chondroprogenitors pellets grown in the absence of growth factor supplemented and defined chondrogenic medium also exhibited positive staining for aggrecan and collagen type II indicating showing that close cell-cell contact also plays a role in stimulating chondrogenesis and therefore the synthesis of relevant matrix proteins. The fact that full depth tracheal pellets showed superior outcome could be indicative of chondroprogenitors being in the progressive differentiation phase and not that they are not fully committed, or that not all cells are committed. This was in accordance to previous data using chondroprogenitors from various cartilage sources upon chondrogenic induction [138][201][345].

The gene expression of COL1 and COLX was minimal in the full depth tracheal pellet, however an increase was observed with tracheal chondroprogenitor pellets treated with both TGFβ1 and BMP9. This effect was not observed in chondroprogenitors derived from articular and auricular cartilage embedded in gelatin methacryloyl in presence of TGFβ1 for a period of 56 days when compared with their counterparts' chondrocytes. The opposite effect was reported where chondrocytes exhibited an up-regulated expression of COL1 and COLX and chondroprogenitors displayed a negligible up-regulation of the aforementioned genes [138], [366]. This down-regulation could be due to incorporation of chondroprogenitors in a 3D scaffold and the longer period of chondrogenesis as at day 1 there was no significant difference in COL1 and COLX expression across the cell types. With regards to BMP9, previous publications have shown that up-regulation of COLX results in induced hypertrophic chondrocyte differentiation in bone marrow MSCs [217][373][399] which is in accordance with our data where tracheal chondroprogenitor pellets stimulated with BMP9 exhibited the highest expression of COLX a marker of chondrocyte hypertrophy which may lead to mineralization [386] . However, whether the levels of COLX produced are physiologically relevant, i.e. sufficient to induce calcification of tissues under the appropriate conditions has yet to be fully tested as the immunohistochemistry results for collagen type X was found to be non-specific. TGFβ receptors ALK-1 and ALK-5 activate Smad1/5/8 and Smad 2/3 respectively [372][400]. Activation of ALK-5 and subsequent signaling of Smad 2/3 have shown to provide inhibitory effects of chondrocyte hypertrophy [401][402]. Conversely the activation of Smad 1/5/8 that could stem from TGFβ and BMP correlates with RUNX-2, which directly results in hypertrophic differentiation with consequent production of collagen type X, osteocalcin and osteopontin [377][403]. Future studies should further investigate the ratio of ALK1/ALK5 signalling on stimulated chondroprogenitors and perform a time point analysis to constructively understand the effects of various chondrogenic growth factors.

The mRNA expression data matched the immunohistological images where BMP9 demonstrated the highest amount of collagen type I synthesis followed by TGFβ1 and full-depth pellets, but it was not visible for tracheal chondroprogenitors pellet within the

non-chondrogenic medium or native tracheal cartilage tissue, suggesting fibrocartilage formation. In a previous study using human articular chondroprogenitors and TGFβ2 treatment [220], the presence of collagen type I at protein level was associated with recapitulation of developmental processes in matrix synthesis, where primarily collagen type I is deposited and as well as collagen type II, then is progressively lost as cells mature [424]. The presence of collagen type I have also been shown immunohistochemically and by quantitative gene expression by Khan *et al.* in the superficial zone of juvenile (mature) and immature bovine explants [425]. We did not obtain similar observations with native tracheal tissue as shown in the previous chapter and the presence of collagen type I was absent as shown by immunohistochemical analysis yet present at mRNA level of the 6 months old native porcine tracheal tissue. This pattern was the same where COLX gene expression and alizarin red stain was performed. Although minimally visible for tracheal chondroprogenitors in absence of chondrogenic medium and full-depth pellets, a more intense staining was visible within the TGFβ1 and BMP9 pellets especially around the outer edges. However, it has been shown that alizarin red stain is not always specific for hypertrophic chondrocytes [426], but is routinely used for the detection and is specific to calcium deposition routinely used for detection of micro calcium crystals in synovial fluid when detecting osteoarthritis in relation to articular cartilage degeneration [427]. These results suggest a possible calcification where this trend is not seen within the tissue especially on the cartilage component of the native tracheal C-ring. Previous studies have outlined lack or minimal of collagen type X expression upon chondrogenic differentiation of chondroprogenitors at mRNA and protein level within human, bovine and equine animal models using the TGFβ family [138][201][204][345].

Therefore, these results suggest that the standard chondrogenic formulation adopted from articular cartilage chondroprogenitors needs further refining and given the right environment the likelihood formation of hyaline type cartilage derived from tracheal chondroprogenitors would improve. For example based on the developmental biology of the airway growth factors such as TGFβ2 and BMP4 have been shown to be heavily involved in up-regulating SOX9 resulting in cartilage patterning and formation [22]. Oxygen tension has been shown to play a pivotal role in cartilage tissue engineering.

Hypoxia, low-tension oxygen blocks hypertrophy and ossification of chondrocytes and bone marrow MSC [428]. From the formation of the limb bud, through to cartilage growth plate formation and during homeostasis of adult articular cartilage, there exists a hypoxic state in which mesenchymal progenitors and articular chondrocytes reside and function [429]. Hypoxia and hypoxia-inducible factor (HIF) play essential roles in the proliferation, differentiation and maintenance of the articular chondrocyte phenotype [430]. Unlike that of specific growth factors, which are expressed in specific temporal patterns, hypoxia is constitutively present and plays active role throughout articular cartilage development [411][412]. This suggests a potential role for hypoxia and cartilage tissue engineering. In terms of differentiation, the lineages of differentiation of BM-MSCs have been shown to be differentially altered in response to hypoxia, with adipogenesis and chondrogenesis being elevated by hypoxia and osteogenesis inhibited [413][414]. Currently, we are still at early stages of identifying the genetic mechanisms underlying trachea formation, growth and development, and thus far no studies have targeted the effect of hypoxia on trachea. Additionally, the role of hypoxia has been highlighted in developing lung where cellular hypoxia triggers diverse physiological responses in lung epithelial, endothelial, and smooth muscle cells that are mediated by transcriptional and posttranslational mechanisms [435].

4.4 Conclusion

This chapter focused on the chondrogenic capacity of the newly identified tracheal chondroprogenitor populations and demonstrated using traditional 3D pellet culture, these cells have the potential to undergo chondrogenesis. However, the presence of collagen type I and X could be indicative of fibrocartilage and possible hypertrophy using the current chondrogenic protocols. Overall the tracheal full-depth chondrocytes pellet produced the best outcome of chondrogenesis where the histological images, biochemical data (GAG and collagen) and gene expression analysis for the positive and negative matrix collagens proved to be the most ideal scenario. This is accepted as these cells were not expanded in 2D prior to chondrogenic induction and were terminally differentiated.

Chapter 5: Advanced expansion and differentiation of tracheal cartilage derived stem cells using microcarrier technology

5.1 Introduction

There is a global clinical need for effective therapies for patients suffering from tracheal stenosis. Of the many approaches proposed for airway tissue engineering (refer to **Chapter 1**, **Section 1.5**) decellularisation of donated cadaveric tracheal tissue has proved to be the most promising method but lack of donor availability and potential issues with immunogenicity are the major drawbacks [98]. Tissue engineering, the use of biosynthetic scaffolds, stem cells and growth factors, has the exciting potential to offer new approaches to overcome the current problems. For cellular based strategies preparing sufficient number of cells capable of either generating the correct tissue or driving a reparative response, for implantation is the crucial factor. It is becoming clear that the traditional 2D culture cannot economically generate enough cells, whether fully differentiated or dedifferentiated chondrocytes [416][417] or MSCs, with the required phenotypic properties in order to produce a physiologically relevant tissue resembling the characteristics found in the native tissue [262]. For example, in order to regenerate articular cartilage, approximately 15 to 45 million cells are needed for a small 1-2cm^3 defect, and, there are constraints on the amount of donor tissue that can be harvested to fill the defect and also economic constraints due to the time and materials required to expand a cell population that retains functionality for tissue engineering applications [418][419]. In recent years the use of biomaterials to create a 3D environment to guide cells to encourage proliferation and differentiation have thus become of greater interest.

The field of biomaterials is an ever-expanding discipline containing numerous classification and groups of materials (refer to **Chapter 1**, **Section 1.10.2**). An ideal biomaterial should promote proliferation, cellular viability, provide a temporary hosting environment and be biodegradable without releasing toxic by-products as well as being immunologically inert. The chemical and architectural properties of biomaterials are major contributors of triggering and promoting cellular responses [440]. A prerequisite characteristic for scaffold materials is the ability to facilitate cellular attachment. Not all scaffold materials permit direct cell-material interactions, principally due to extensive crosslinking shielding potential binding sites [441], and, coating either natural or synthetic biomaterials is often used to improve or enhance [442]. For cell culture and

growth of constructs, interconnected porous materials are usually preferred as they provide larger surface areas, enhance cell-cell interaction, enable homogenous cell distribution, and allow for the diffusion of oxygen, carbon dioxide, glucose and growth factors (media content), properties which together enhance cellular growth and differentiation [9,10]. A notable approach in the field of tissue engineering, cartilage in particular is the use of porous polymer scaffolds. As previously stated in Chapter 1 Section 1.6 both natural and synthetic polymers have been exploited in cartilage tissue engineering [445]. Natural polymers possess intrinsic abilities to support biological functions but one of the major drawbacks is the high variability between batches resulting in irreproducibility as well as a lack of mechanical stability [446]. Tuning the chemistry of synthetic biomaterial to optimise their architecture and consequently their biomechanical properties could potentially circumvent the latter disadvantages but modifications tend to remove binding sites for cells (for example by increased crosslinking to enhance material stiffness or stability) leading to a reduction in cell adhesion [447].

Microcarriers, a subtype of biomaterials with distinct set of characteristics such as high porosity, adaptable surface chemistry and surface topography have been developed for cell expansion and tissue engineering applications [257]. Although a wide variety of microcarriers manufactured from synthetic or natural materials with different properties are commercially available (refer to **Chapter 1, Section 1.10.3**), natural porous microcarriers are usually preferred for ease of homogenous distribution of cells, enhanced biological responses, nutrient diffusion and cell-cell contact as well as migration. This study focuses on gelatin-derived Cultisphers® microcarriers. Gelatin is a naturally derived polymer from collagen and has been widely used in food industry and medical applications due to its biodegradability, biocompatibility and cost-effectiveness [428][429]. Macroporous gelatin Cultispher® microcarriers have been previously shown in conjunction with different human and animal cell types to offer substantial surface areas for cell adhesion and proliferation [242][294][430][431].

Use of coating materials coupled with microcarriers is a common approach to promote functional attachment and support cellular growth. The surface of a microcarriers can be

chemically functionalised, for example with peptides or positively charged molecules to enhance cell adhesion (e.g. the RGD peptide). Positively charged microcarriers can then attract cells (which are overall negatively charged), by electrostatic forces [262]. Melero-Martin *et al.* showed that scaling up chondroprogenitor cell numbers using coated Cultispher® G with 10% and 40% FBS could be easily achieved by gradual addition of empty microcarriers in a spinner flask, where their work showed that cells were able to detach from confluent microcarriers and reattach to newly added microcarriers [313].

While many studies have used microcarrier technology to successfully expand both human and animal-derived chondrocytes [257], recently the use of microcarrier has also been highlighted as a potential aid towards maintaining the long term phenotypic stability of expanded human MSCs [452] and subsequently their ability to undergo cartilage differentiation. Experiments have shown that culturing human bone marrow MSCs on various types of microcarriers such as Cytodex1, Cytodex3, collagen and glass modulates the actin organisation of cells and allowed researchers to systematically guide MSCs to efficiently differentiate cells to all the mesoderm-lineages, most efficiently for adipogenesis [452]. Other studies by Tseng *et al.* and Chen *et al.* reported spontaneous osteogenesis of various types of MSCs on collagen-coated microcarriers [453] and aggregated cell-seeded Cultispher® S microcarriers [454], in order to fabricate large bone structures. This chapter focuses on using newly identified tracheal chondroprogenitors and gelatin-based Cultispher® microcarriers for culture expansion and on-scaffold differentiation of these cells towards chondrogenesis in the hope of developing robust methodologies for fabricating functional autologous tracheal C-rings.

5.2 Results

The first objective was to use tracheal chondroprogenitors and Cultisphers® microcarriers for large-scale cellular expansion of monolayer cultured chondroprogenitors. Initially, chondroprogenitors were grown on monolayer to Passage 4 (P4), to expand their numbers sufficiently to seed Cultisphers® G microcarriers. The overall aim was to improve chondroprogenitor expansion and then use microcarriers as intra- and inter-scaffolding material to support differentiation and fabrication of customisable cartilage C-rings. Three monoclonal chondroprogenitor cell lines (from colonies of more than 32 cells) were used and pooled together for Cultispher® microcarrier experiments to avoid excessive 2D expansion **(Figure 5.1)**.

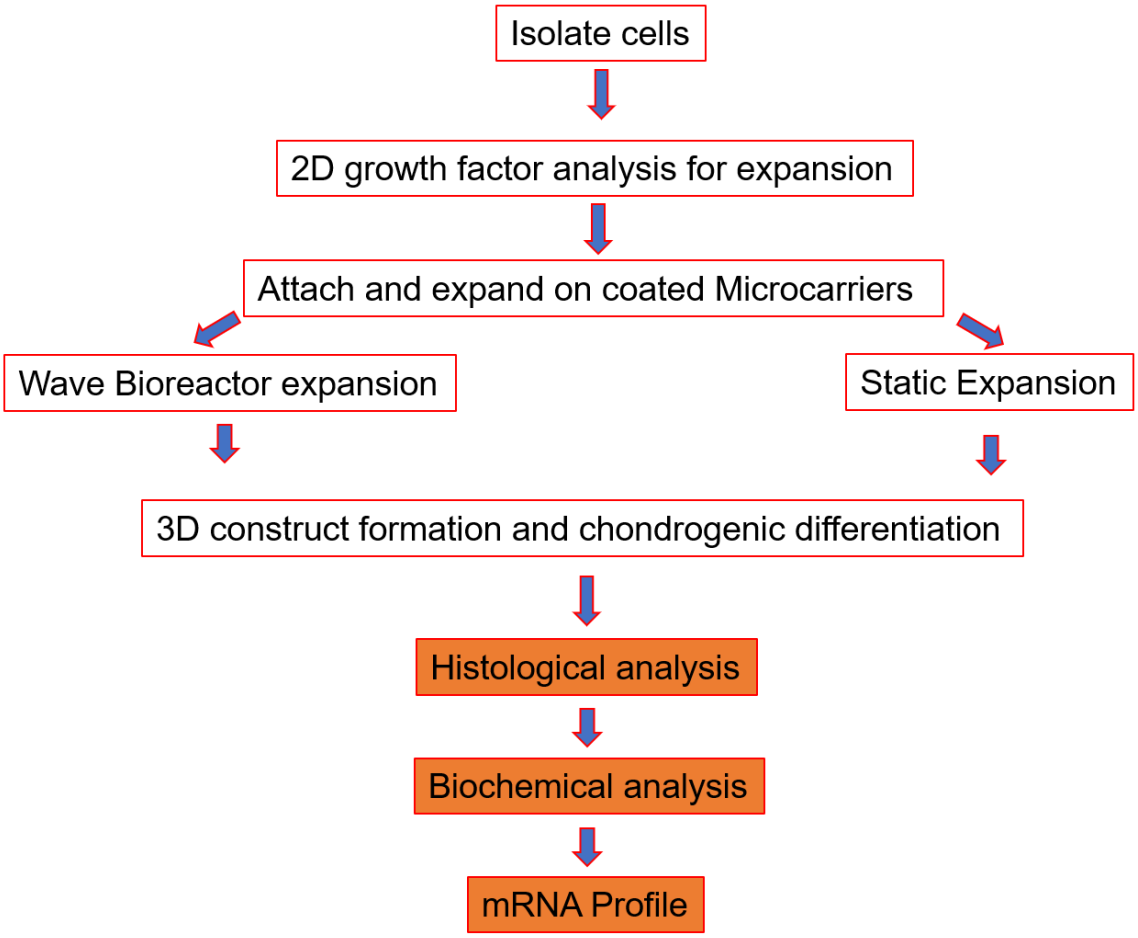

Figure 5.1. Pipeline of tracheal chondroprogeniotrs expansion and differentitaion on 3D microcarriers.

5.2.1 Growth analysis of monoclonal tracheal chondroprogenitors

First the growth kinetics of chondroprogenitors in the presence of various growth factors was tested in order to derive and optimise culture medium for cellular expansion. One thousand monoclonal chondroprogenitors at P4 were seeded per well in a 48-well plate. The control wells contained chondroprogenitor cells in expansion medium with no growth factor supplementation, as described in Material and Methods (**Chapter 2**, **Section 2.3.4**). The control medium was then also supplemented with various growth factors including fibroblast growth factor 2 (FGF2 at 10 ng/mL), transforming growth factor β1 (TGFβ1 at 1 ng/mL) and platelet-derived growth factor (PDGF at 10 ng/mL) plus combinations of these growth factors. The rate of cell growth was measured by the increase in absorbance of PrestoBlue™ dye incorporated into cells. At day 2 no significant changes from control medium values occurred across the treatments, whereas from day 5 onwards the growth rate using growth factor addition experienced a dramatic increase in relative cell number. At day 8 FT (FGF2+ TGFβ1), FTP (FGF2+ TGFβ1+PDGF) and PDGF were significantly ($p < 0.005$) higher in absorbance when compared to other groups **(Figure 5.2A)**. There were no significant differences in dye absorbance between FT, FTP and PDGF at day 8 and these 3 groups showed a 96-fold increase compared to day 0 where the initial cellular density was a 1000 cell – indicating cells had undergone at least 7 population doublings. The control group was also capable of rapid proliferation but when compared with growth factor groups there was a only a 3.84-fold decrease by day 8 **(Figure 5.2B)**. This experiment was performed to identify the appropriate growth factors to increase proliferation rate for chondroprogenitors when cultured on 3D Cultispher® microcarriers.

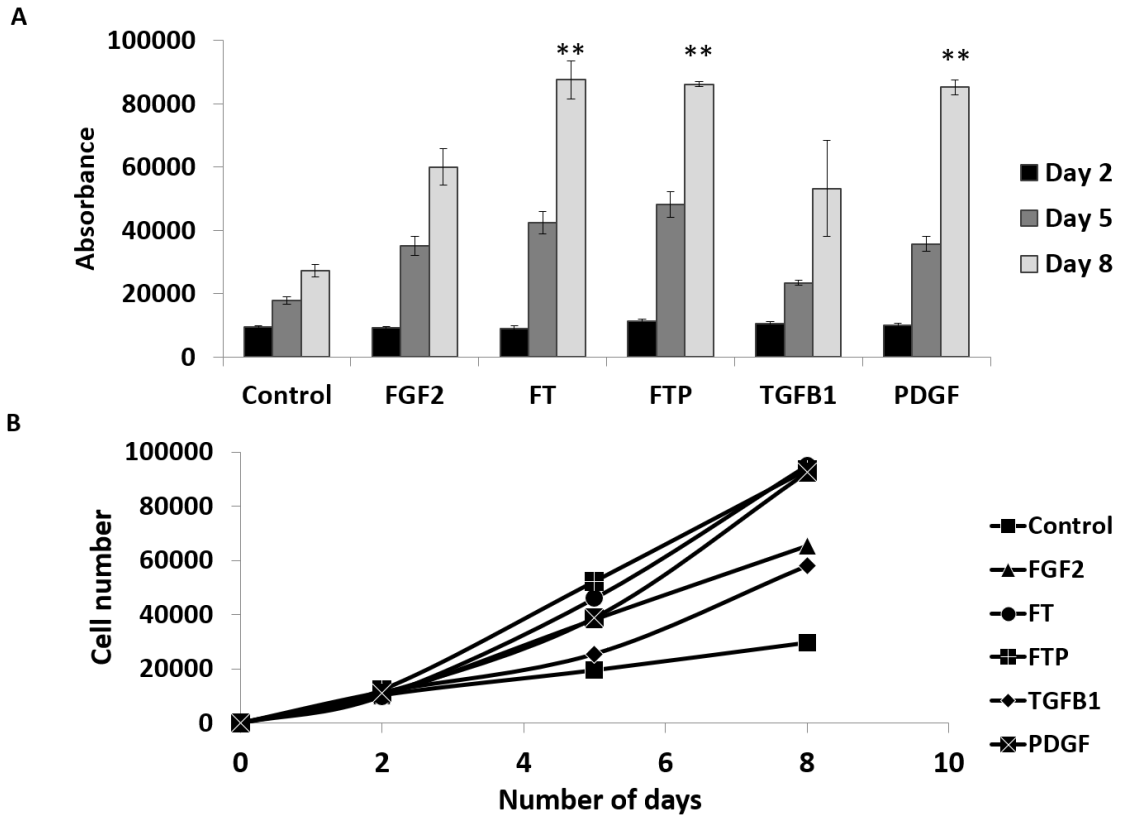

Figure 5.2. Growth curve analysis of chondroprogenitor cells on 2D cell culture in presence of growth factors using colorimetric PrestoBlue™ assay. Fibroblast growth factor (FGF2), transforming growth factor β (TGFβ1) and platelet-derived growth factor (PDGF) were used individually or combined to monitor the growth analysis of tracheal chondroprogenitors at 10ng/ml, 1ng/ml and 10ng/ml respectively to establish the optimum cell proliferative condition that would be used in 3D culture environment to expand cells on microcarriers. **(A)** Growth rate over a period of 8 days and **(B)** Cell number generated against untreated chondorprogenitors standard curve using Prestoblue™. All data in **(A)** is shown as average (± standard deviation) from a five biological monoclonal repeats, tested for significance using one-way ANOVA analysis. ** is used to indicate and $p < 0.001$ on day 8 only.

5.2.2 Expansion of tracheal chondroprogenitors on Cultispher® microcarriers

Cultispher® microcarriers were prepared as described in Material and Methods (Chapter 2, Section 2.5). The initial attempts at cell seeding with uncoated microcarriers proved inefficient for cellular attachment. Therefore, Cultispher® microcarriers were coated with 10% FBS or 3% gelatin to enhance attachment of porcine tracheal

chondroprogenitors. Chondroprogenitors were seeded onto the microcarriers as described in Materials and Methods (**Chapter 2**, **Section 2.5.3**) at a ratio of 20 cells per bead ($8x10^6$ cells in 0.4g as there are $1x10^6$ microcarriers per gram as stipulated by the manufacturer). The proliferative capacity of coated microcarriers plus seeded chondroprogenitors (±FT growth factors at 10 ng/mL FGF2 and 1 ng/mL TGFβ1) were assessed qualitatively using fluorescence microscopy detection of Dapi stained fixed cells bound to microcarriers over a period of 15 days. Both FBS and gelatin +FT treated groups showed higher expansion capacities when compared against their -FT counterparts and therefore all the future experiments utilised FT growth factor in conjunction with coated microcarriers to expand chondroprogenitors **(Figure 5.3)**. FBS exhibited a more supportive proliferative environment than gelatin in presence or absence of FT. However, gelatin was not excluded for the future studies, as we were interested in the potential effects of both coating solutions on chondrogenic differentiation.

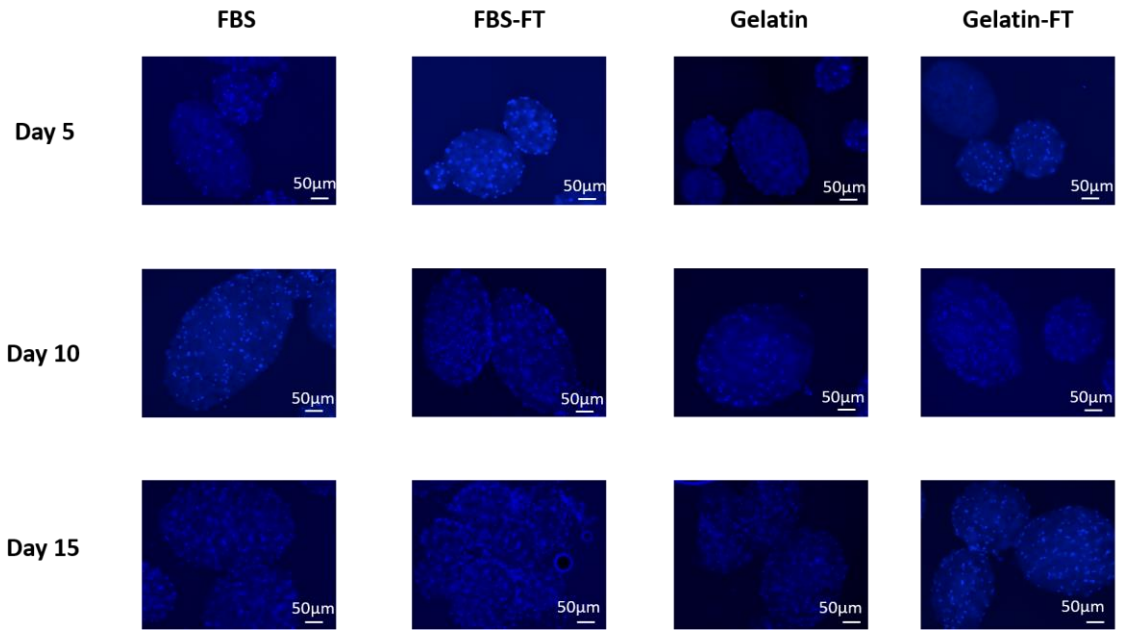

Figure 5.3. Visualising of tracheal chondroprogenitor distribution on macroporous Cultispher® microcarriers using fluorescent light microscopy. To further improve cell attachment and proliferation on 3D culture, microcarriers were coated with 10% FBS and 3% gelatin (± 1 ng/ml TGFβ1 and 10 ng/ml FGF2). 20 µl aliquots from each condition were collected on different days and fixed prior to staining with Dapi to visualise cell growth. Images represent one porcine donor.

5.2.3 Culture regime and its effect on proliferation

To further improve the growth rate and homogenous spreading of chondroprogenitors on microcarriers in the presence of growth factors FGF2 and TGFβ1 a comparison between static culture and wave culture at 37 °C and 5% CO2 was undertaken. Microcarriers cultured in either of the culture formats (wave or static) were at each time point stained with MTT then fixed as described in Materials and Methods (**Chapter 2**, **Section 2.5.4.2**). The stained microcarriers were visualised under light microscopy, and as shown in **Figure 5.4.** All four conditions supported proliferation where FBS-coated microcarriers were qualitatively superior in static and wave culture compared to gelatin-coated microcarriers. Gelatin-coated microcarriers in wave culture were the slowest proliferators as clearly indicated in **Figure 5.4D & H**.

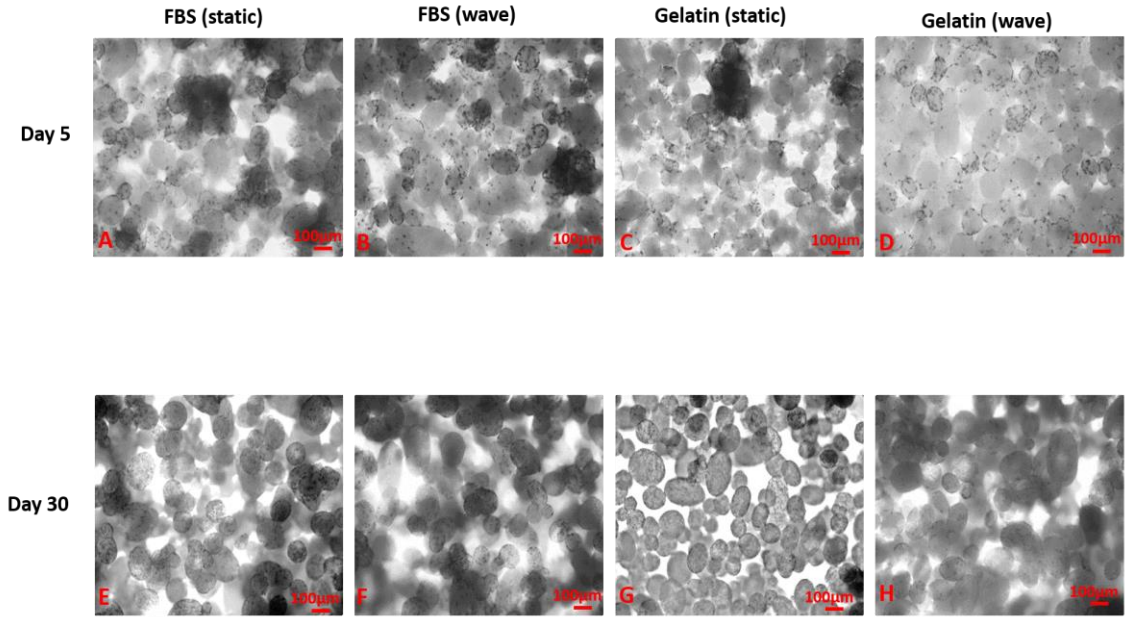

Figure 5.4. Combined effect of growth factors and culture regime on tracheal chondroprogenitors and Cultispher® microcarriers. To achieve a fast screening cultural effects on the cells and microporous beads 20 µl samples were selected and stained with MTT and imaged using a light microscopy at day 5 **(A-D)** and day 30 **(E-H).** Images represent one porcine donor.

To quantitatively assess the growth rate of chondroprogenitors grown in static or wave culture, cell numbers were quantified against a standard curve generated from pooled monoclonal tracheal chondroprogenitors grown on 2D using colorimetric PrestoBlue™ as described in Materials and Methods (**Chapter 2**, **Section 2.5.4.1**) **(Figure 5.5A)**. A general trend of increased cell number was observed in FBS-coated microcarriers in static (3.8-fold increase) and wave culture (3-fold), and gelatin-coated microcarriers in static culture (3.6-fold) for a period of 35 days. For the initial first 10 days, gelatin-coated microcarriers in static culture exhibited an accelerated growth and maintained this growth. Similarly, for the first 10 days FBS-coated microcarriers in static culture showed no dramatic growth kinetic and after, maintained a steady increasing growth rate to the end of the culture period. However, gelatin-coated microcarriers grown in wave culture showed fluctuation in growth over a period of 35 days **(Figure 5.5B & C)**. From this point onwards, it was concluded that the optimised culture conditions should be static culture, coated microcarriers with FBS and gelatin in presence of FGF2 and TGFβ1 growth factors, and these conditions were used for 3D fabrication of C-rings.

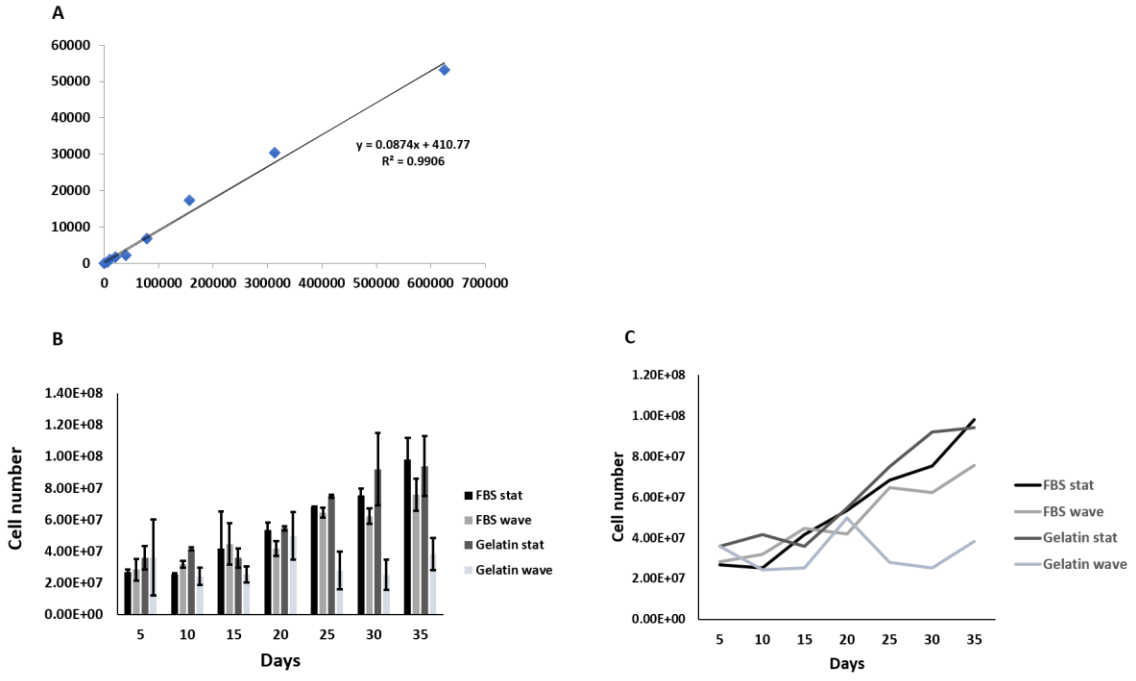

Figure 5.5. Growth curve analysis of chondroprogenitor cells on Cultispher® microcarriers on different regime of culture in presence of growth factors using colorimetric PrestoBlue™ assay. Cell numbers were quantified against the standard curve generated from tracheal chondroprogenitors grown on 2D **(A)** and plotted over the

period of 35 days of culture **(B and C)**. All data is shown as average (± standard deviation) from a five biological repeats

5.2.4 Characterisation of tracheal chondroprogenitors expanded on Cultispher® microcarriers

Three hundred microlitre aliquots of each culture condition (FBS or gelatin-coated, grown as static or wave cultures) were taken out to analyse the gene expression of minimal cell markers for the identification of mesenchymal stem cells. Cartilage gene biomarkers were also included in the panel. All four groups complied with the minimal criteria to be designated as MSC-like cells **(Figure 5.6)**. The most obvious differences were in chondroprogenitors expanded in FBS-coated microcarriers and gelatin-coated microcarriers in wave culture where PRG4 was transcribed upon the rocking movement. COL1 expression was evident when compared to COL2 and FBS wave showed the lowest band intensity of the latter gene.

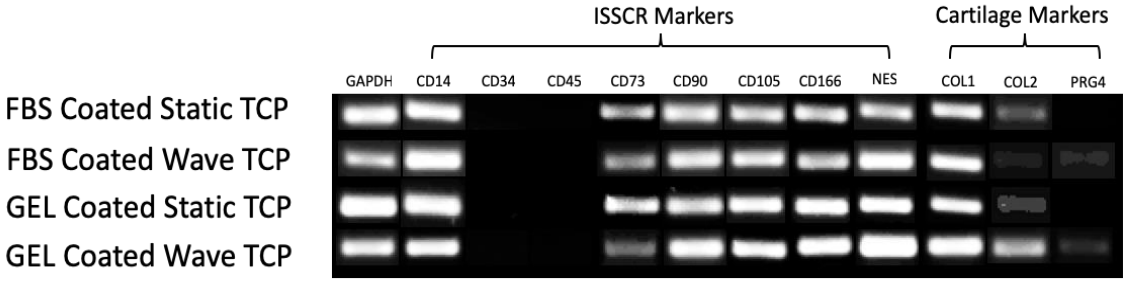

Figure 5.6. Characterisation of tracheal chondroprogenitors grown on Cultispher® microcarriers over 35 days of different regimes of culture. Gene expression of stem cell surface markers defined by International Society for Stem Cell Research (ISSCR) for tracheal derived chondroprogenitors and chondrogenic markers exhibits similarities for stem cell characteristics and district differences across the wave culture where presence of lubricin (PRG4) is evident.

5.2.5 Chondrogenesis of tracheal chondroprogenitors seeded upon Cultisphers® microcarriers

For early proof-of-concept experiments at tissue engineering airway cartilage, tracheal chondroprogenitors seeded and expanded upon Cultisphers® microcarriers were placed upon dry 12 mm diameter transwells with 0.4 μm pore size and cultured under chondrogenic conditions. **Figure 5.7A** represents the constructs in expansion medium in the presence of FT for 21 days where matrix formation was either not apparent or very poorly formed, resulting in the construct falling apart during routine sample handling. **Figure 5.7B** represents constructs cultured under chondrogenic conditions, with medium containing 10 ng/mL of TGFβ1, and all four groups were capable of self-assembly into malleable disks which were robust enough to be handled. By using a transwell support as a mould, the Cultisphers® microcarriers were able to form disk-like structures using gravity and weight of the medium to aggregate microcarriers. **Figure 7C** is an example of a light microscopy image of cell and matrix spanning multiple Cultisphers® microcarriers as *arrowed*.

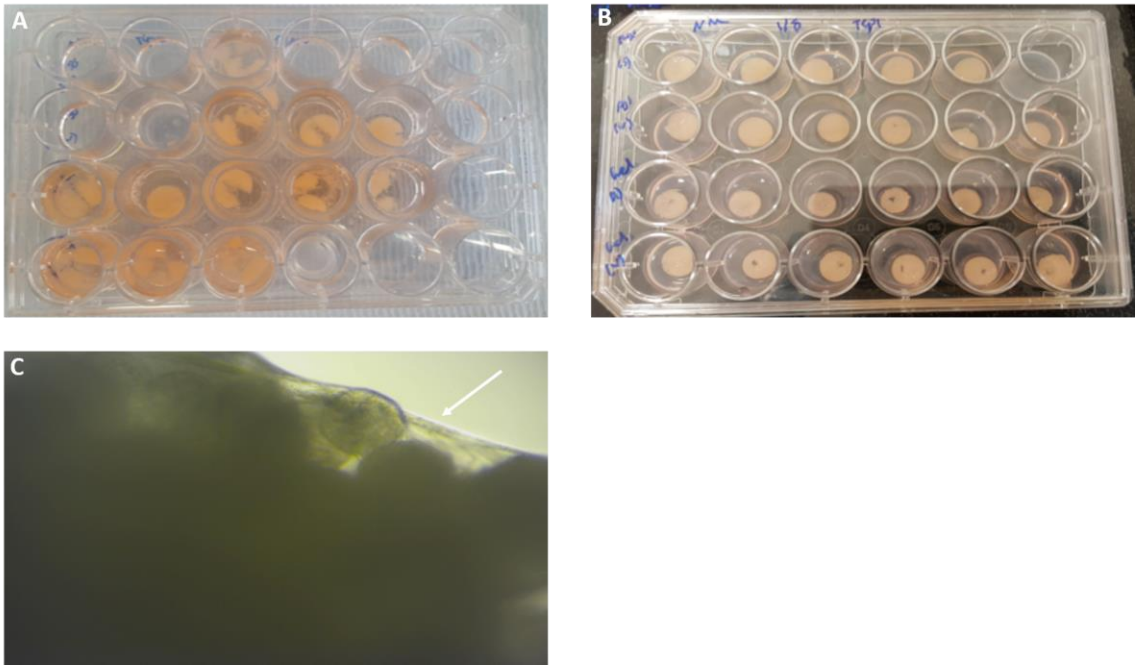

Figure 5.7. Tracheal chondroprogenitors and Cultispher® microcarriers placed on transwells. **(A)** represents tracheal chondroprogenitors and Cultispher® microcarriers in expansion medium containing 1 ng/ml TGFβ1 and 10 ng/ml FGF2. Lack of matrix formation is evident as the constructs have collapsed upon collection. **(B)** represents tracheal chondroprogenitors and Cultispher® microcarriers in presence of chondrogenic medium containing 10 ng/ml TGFβ1 for a period of 21 days. **(C)** Light microscopy image of matrix formation post chondrogenesis showed by *arrow*.

To examine whether different coatings and culture regimes influenced the disks physical appearance, gross morphological measurements were undertaken using a caliper. Gelatin-coated static samples exhibited the lowest average diameter (8.09±0.29 mm) and were significantly different when compared with larger FBS coated static-cultured disks (8.6±0.15 mm, $p < 0.001$) and gelatin-coated wave cultured disks (8.52±0.24 mm, $p < 0.05$). FBS-coated wave cultured disks (8.35± 0.3 mm) showed no significant differences compared with other groups **(Figure 5.8A)**. Same trend was observed for the height measurement **(Figure 5.8B**) where gelatin-coated static disks (2.73±0.5 mm) showed the lowest height and were significantly lower when compared against disks grown in FBS static (3.78±0.18 mm, $p < 0.001$) or FBS-wave cultured groups (3.3± 0.17 mm, $p < 0.05$). There were also significant differences ($p < 0.001$) in height between FBS-static and wave coated groups. Gelatin-wave cultured disks (3.55± 0.94 mm) exhibited no differences in height when compared against other groups.

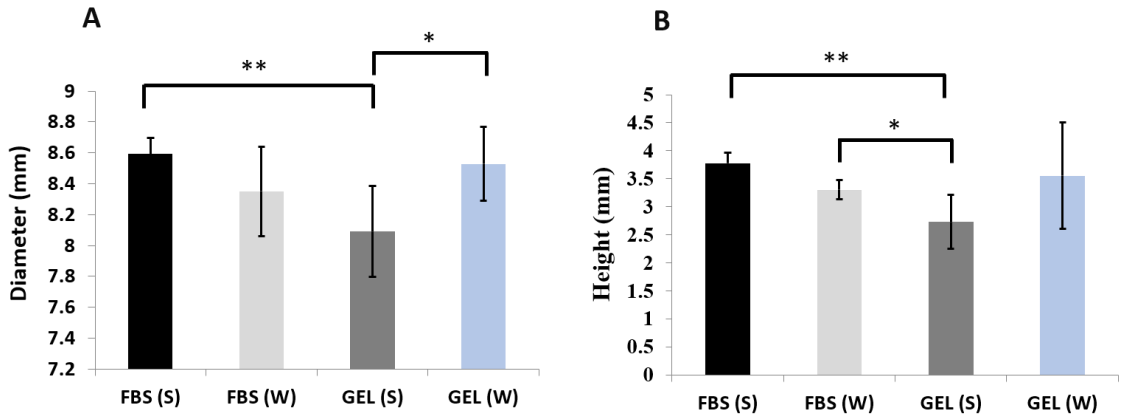

Figure 5.8. Gross morphological analysis of disks fabricated from tracheal chondroprogenitors and Cultispher® microcarriers placed on transwells after 21 days of chondrogenesis. Using a caliper the diameter (A) and height (B) was measured. All data shown is average (± standard deviation) from three biological repeats, tested for significance using one-way ANOVA analysis. * and ** are used to indicate $p < 0.05$ and $p < 0.001$ respectively.

5.2.6 Histological analysis of disks fabricated from tracheal chondroprogenitors and Cultisphers® microcarriers

After 21 days of culture in chondrogenic medium the disks were cut into quarters and prepared for analysis as described in Materials and Methods (Chapter 2, Section 2.6.4.2). Haematoxylin and eosin staining **(Figure 5.9)** showed the weak formation of matrix around the periphery of all four groups of disks. Cellular alignment is clearly visible around the periphery disks. Cultisphers® microcarriers displayed uneven distribution of cells, and cellular density decreases were associated with increased depth from the periphery of microcarriers. Furthermore, within the central region of the disk, large spaces were present which were void of cells and Cultisphers® microcarriers and this may have been caused by a lack of matrix holding the structure together which would have been exposed following sectioning and this may have been caused by chemotaxis for the cells to the periphery.

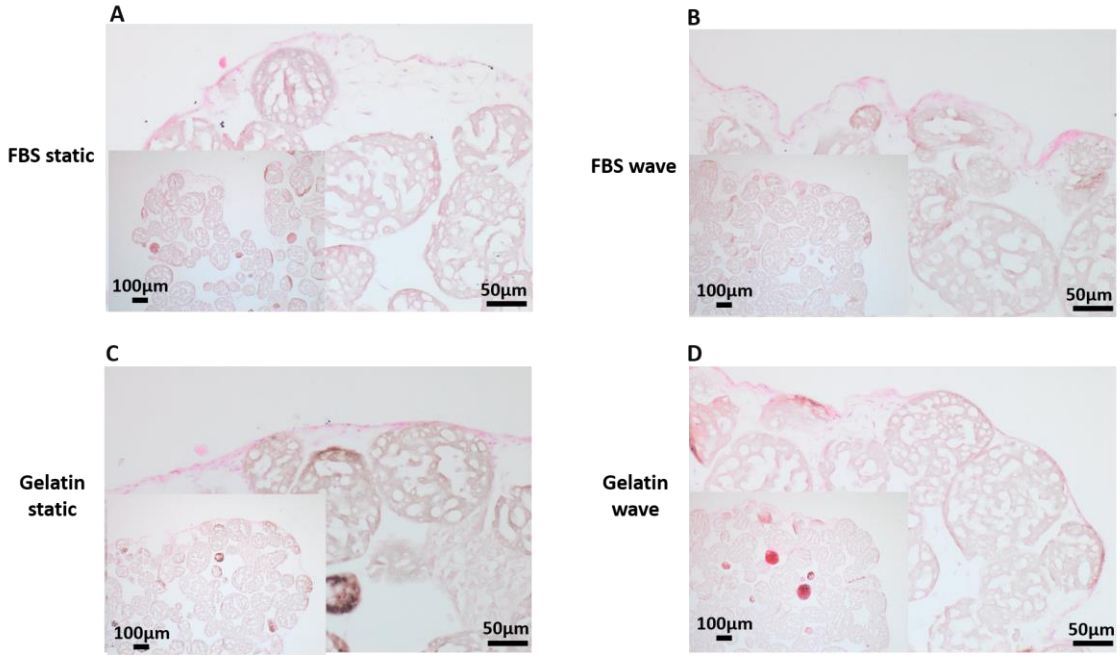

Figure 5.9. Haematoxylin and eosin stain of chondrogenic induced disks fabricated from tracheal chondroprogenitors and Cultispher® microcarriers after 21 days of chondrogenic culture in the presence of 10 ng/ml TGFβ1. (A) Shows FBS coated beads in static culture, **(B)** shows FBS coated beads in wave culture, **(C)** shows gelatin coated beads in static culture and **(D)** shows gelatin coated beads in wave culture. Images represent one porcine donor.

Figure 5.10 represents the cartilaginous matrix formation around the periphery of each group. Although all four groups supported differentiation there are no obvious

differences in degree of differentiation and majority of matrix formation has weakly formed around the edges with cellular density highest in this region.

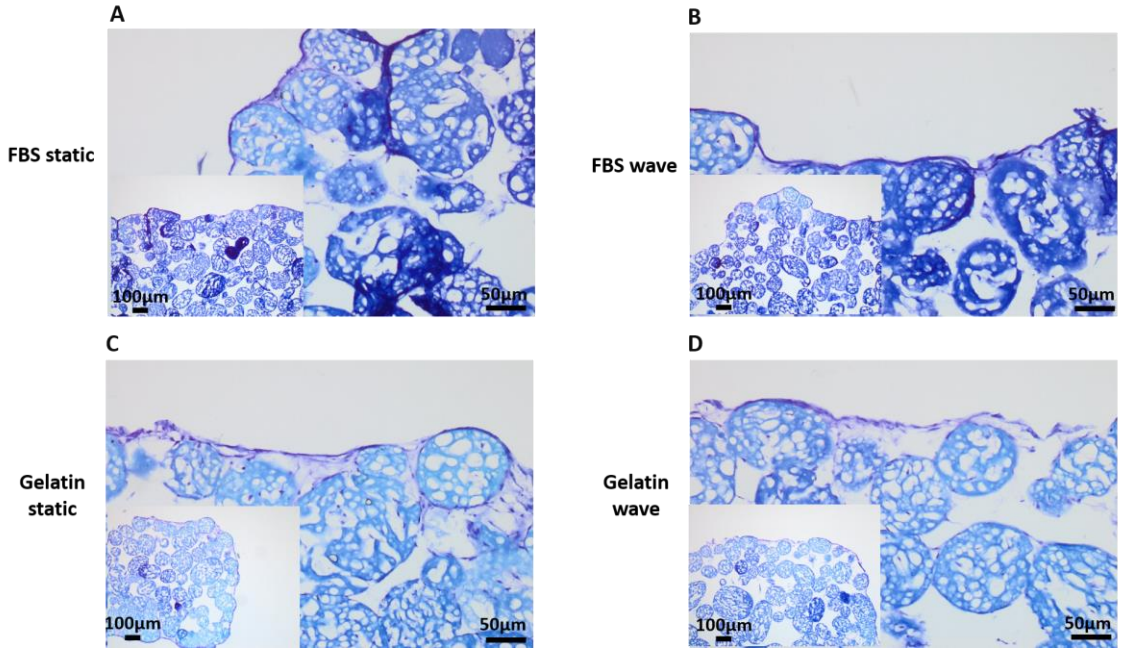

Figure 5.10. Toluidine blue stain of chondrogenic induced disks fabricated from tracheal chondroprogenitors and Cultispher® microcarriers after 21 days of chondrogenic culture in the presence of 10 ng/ml TGFβ1. (A) Shows FBS coated beads in static culture, **(B)** shows FBS coated beads in wave culture, **(C)** shows gelatin coated beads in static culture and **(D)** shows gelatin coated beads in wave culture. Images represent one porcine donor.

Figure 5.11 shows alizarin red staining of constructs and the same trend of matrix staining is visible round the periphery of the disks. The major difference was seen in the gelatin wave group where clusters of cells and Cultisphers® microcarriers stained red. This intensity was less around the edges the intensity is less, and the matrix formation was denser.

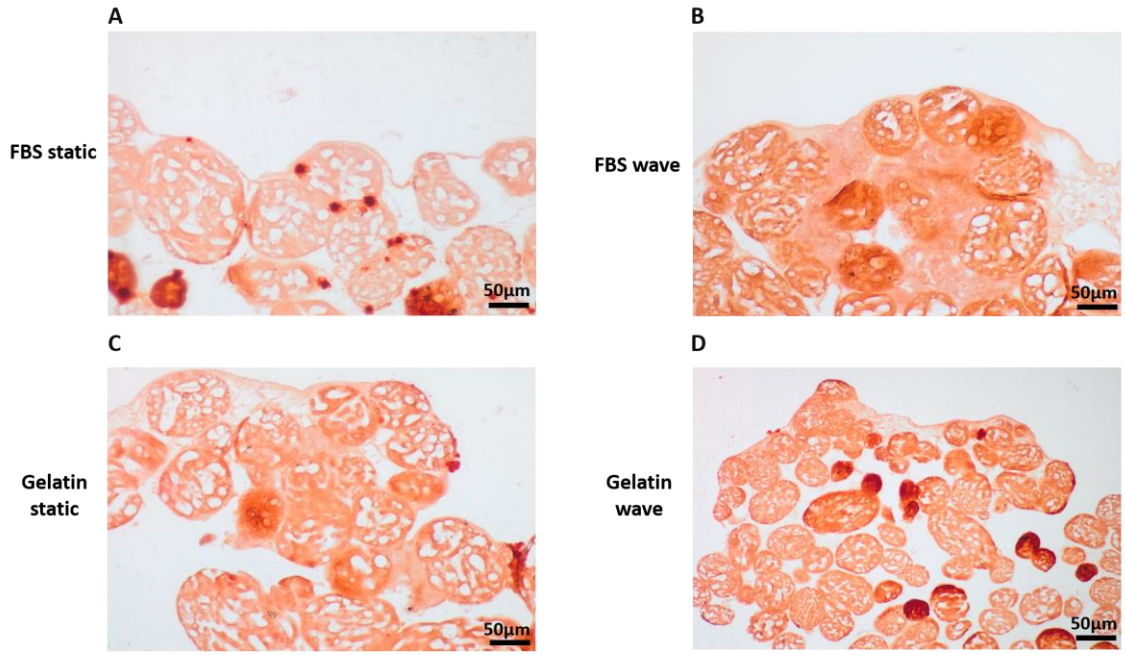

Figure 5.11. Alizarin red stain of chondrogenic induced disks fabricated from tracheal chondroprogenitors and Cultispher® microcarriers after 21 days of chondrogenic culture in the presence of 10 ng/ml TGFβ1. (A) Shows FBS coated beads in static culture, **(B)** shows FBS coated beads in wave culture, **(C)** shows gelatin coated beads in static culture and **(D)** shows gelatin coated beads in wave culture. Images represent one porcine donor.

5.2.7 Biochemical quantification of tracheal chondroprogenitors and Cultisphers® microcarriers

Chondroprogenitors seeded onto microcarriers and expanded in FBS-coated static disks exhibited the highest raw sGAG measurements (9.5±5 µg/mL) following 21 days of chondrogenic induction when compared to other groups. However, the only significant differences observed was between gelatin -coated static disks (9±1 µg/mL, $p < 0.05$) and gelatin-coated wave cultured disks (5.7±0.8 µg/mL), which produced the least sGAG synthesis **(Figure 5.12A)**. No significant difference was observed in FBS-coated microcarriers wave condition (6.3±4.8 µg/mL).

FBS-coated wave cultured disks (1.95±0.32 µg/mL) were significantly higher ($p < 0.05$) in DNA content compared to the other groups. Gelatin -coated static cultured disks (0.96±0.17 µg/mL contained the least DNA content and was significantly ($p < 0.05$)

different compared with FBS-coated static cultured disks (1.30±0.15 µg/mL). No significant difference was observed in gelatin-coated wave cultured disks (1.23±0.16 µg/mL) **(Figure 5.12B)**.

FBS-coated wave cultured disks (35.74±0.45 µg/mL) showed the lowest collagen synthesis (deposition) ability when compared with other groups but this data was not significantly different from the values in the other experimental groups. FBS-coated static cultured disks (36.4±0.18 µg/mL) produced the highest collagen content when compared with gelatin-coated wave cultured disks (35.9± 0.13 µg/mL) and gelatin-coated static cultured disks (0.96±0.17 µg/mL) and was more significant at $p < 0.05$ and $p < 0.001$ respectively **(Figure 5.12C)**.

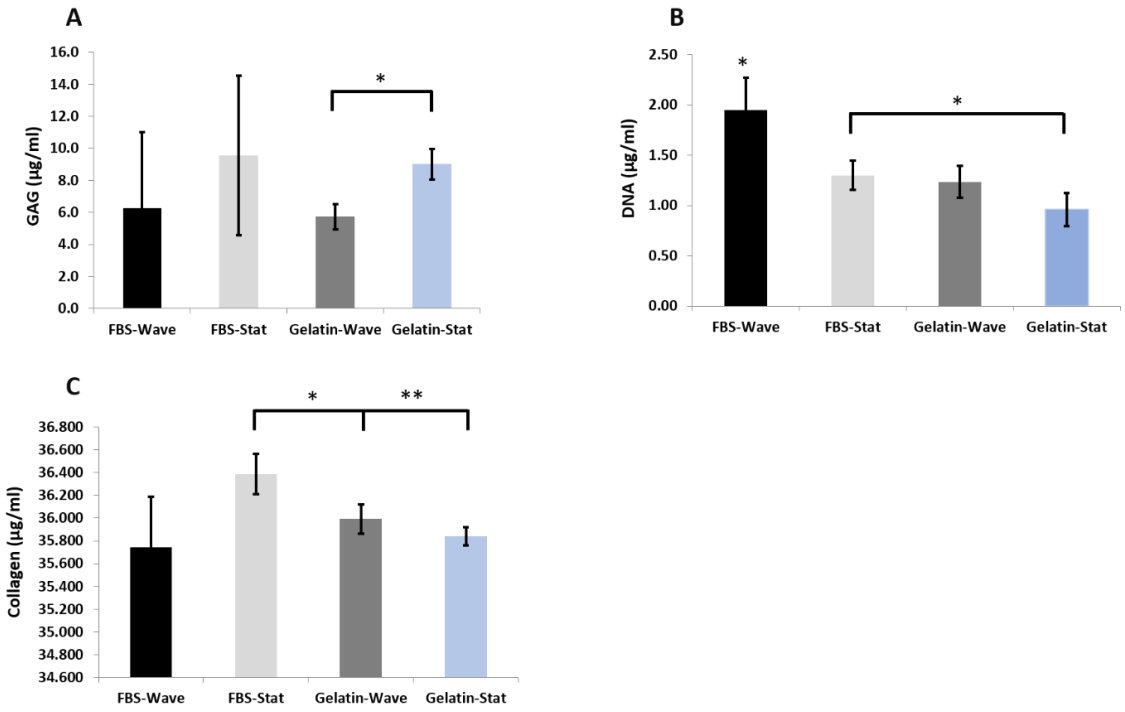

Figure 5.12. Quantification of disks fabricated from tracheal chondroprogenitors and Cultispher® microcarriers placed on transwells after 21 days of chondrogenesis for (A) sulphated GAG content, (B) DNA content and (C) total collagen content. All data shown is average (± standard deviation) from three biological repeats, tested for significance using ANOVA analysis. * and ** are used to indicate $p < 0.05$ and $p < 0.001$ respectively.

The normalised sGAG to DNA data of gelatin-coated static cultured disks (9.6±1.95 μg/μg) showed a 2-fold and 2.7-fold increase compared with gelatin-coated wave cultured disks (4.68±0.79 μg/μg, $p < 0.05$) and FBS-coated wave cultured disks (3.45±2.27 μg/μg, $p < 0.05$) respectively **(Figure 5.13A)**. The total collagen content normalised to DNA exhibited no significant differences across FBS-coated static cultured disks (28.22±3.13 μg/μg), gelatin-coated wave cultured disks (29.5±3.5 μg/μg) and gelatin-coated static cultured disks (38.07±5.91 μg/μg). However, FBS-coated wave cultured disks (18.7±3.5, $p < 0.05$) were significantly lower compared to other groups **(Figure 5.13B)**.

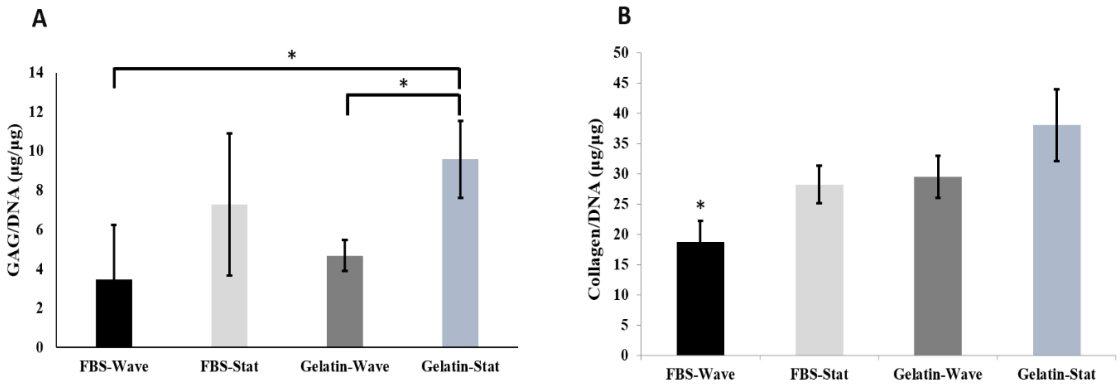

Figure 5.13. sGAG and collagen contents of disks fabricated from tracheal chondroprogenitors and Cultispher® microcarriers normalised to DNA. tracheal chondroprogenitors and Cultispher® microcarriers following 21 days chondrogenesis was analysed biochemically and normalized to DNA. All data shown is average (± standard deviation) from three biological repeats, tested for significance using ANOVA analysis. * is used to indicate $p < 0.05$.

5.2.8 Relative gene expression of disk constructs

Total RNA was isolated from the chondroprogenitor seeded microcarriers that had undergone chondrogenesis in transwell supports, and 10 ng of this RNA from each sample was converted into cDNA for gene expression analysis. Tracheal chondroprogenitor pellets induced with TGFβ1 from the previous chapter was used as calibrator sample to examine whether the disk constructs are a comparable to pellet culture. After 21 days of chondrogenesis the relative expression of SOX9 in pellets

(1±0.06) was significantly higher ($p < 0.001$) when compared with other groups. FBS-coated wave cultured disks (0.80± 0.14) showed the highest relative expression of SOX9 when compared with FBS-coated static cultured disks (0.39±0.09, $p < 0.05$), gelatin-coated wave cultured disks (0.42±0.016, $p < 0.005$) and gelatin-coated static cultured disks (0.43±0.057, $p < 0.05$) **(Figure 5.14A)**. **Figure 14B** shows the relative expression of COL2 and tracheal chondroprogenitor pellet (0.87±0.14) was significantly ($p < 0.001$) higher than the disk groups. Gelatin-coated static cultured disks (0.55±0.07) showed a 2.75-fold and a 2.2-fold increase against gelatin-coated wave cultured disks (0.20±0.09, $p < 0.05$) and FBS-coated static cultured disks (0.25±0.02, $p < 0.001$) respectively. FBS-coated wave cultured disks (0.38±0.09) exhibited a higher relative expression of COL2 than gelatin-coated wave cultured disks and FBS-coated static cultured disks, but no significant differences were observed. The same order of magnitude as COL2 expression was observed in relative expression of ACAN **(Figure 5.14C)**. Tracheal chondroprogenitor pellet (1±0.1, $p < 0.001$) once again showed the highest expression of ACAN when compared with the disk groups. Gelatin-coated static cultured disks (0.33±0.02) showed a 1.73-fold and a 1.5-fold increase against gelatin-coated wave cultured disks (0.19±0.02, $p < 0.001$) and FBS-coated static cultured disks (0.22±0.02, $p < 0.001$) respectively. FBS-coated wave cultured disks (0.33±0.05) was significantly higher than FBS-coated static cultured disks and gelatin-coated wave cultured disks ($p < 0.05$).

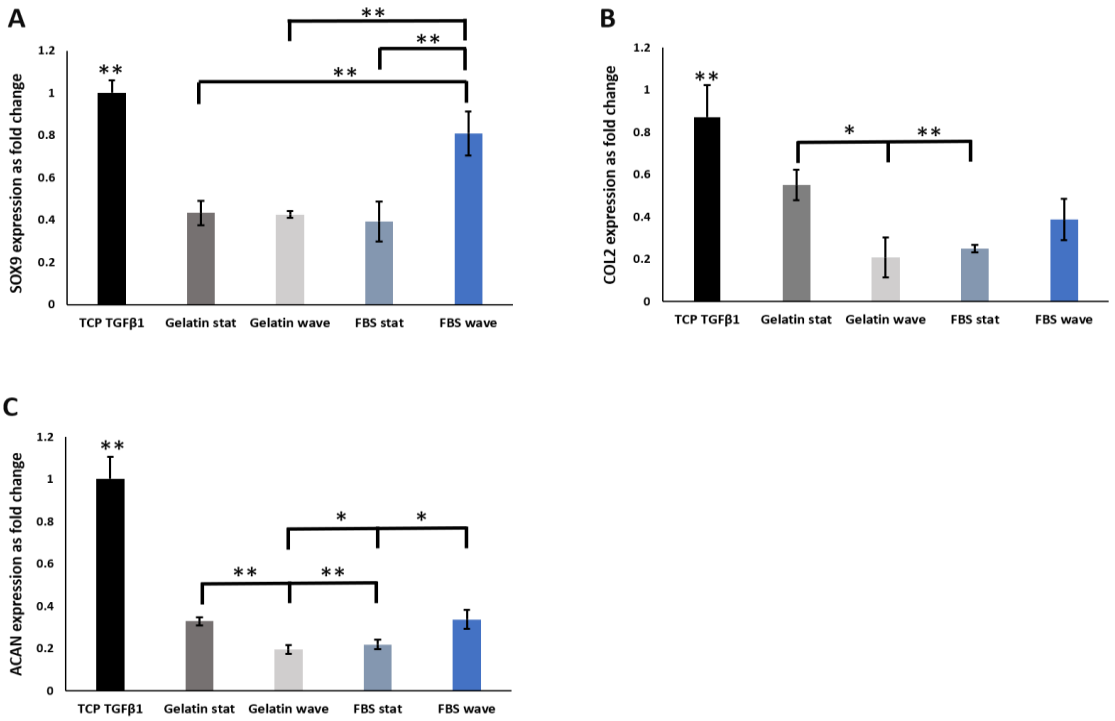

Figure 5.14. Relative gene expression shown as a fold change using ΔΔ*CT* method. **(A)** shows the SOX9 expression of disks fabricated from tracheal chondroprogenitors and Cultispher® microcarriers placed on transwells after 21 days of chondrogenesis. **(B)** shows the COL2 expression of disks fabricated from tracheal chondroprogenitors and Cultispher® microcarriers placed on transwells after 21 days of chondrogenesis and **(C)** shows the ACAN expression of disks fabricated from tracheal chondroprogenitors and Cultispher® microcarriers placed on transwells after 21 days of chondrogenesis. All data shown is average (± standard deviation) from three biological repeats, tested for significance using one-way ANOVA analysis. * and ** are used to indicate $p < 0.05$ and $p < 0.001$ respectively.

Figure 5.15A shows the relative expression of COL1 where tracheal chondroprogenitor pellets (1.03±0.3, $p < 0.001$) were significantly lower than disks. Gelatin-coated static cultured disks (3.26±0.06) exhibited a 1.56-fold and 1.41-fold increase versus FBS-coated static cultured disks (2.08±0.27, $p < 0.001$) and FBS-coated wave cultured disks (2.32±0.41, $p < 0.05$) respectively. Gelatin-coated wave cultured disks was also significantly higher ($p < 0.05$) in COL1 expression against FBS-coated static cultured disks. **Figure 5.15B** displays the relative expression of COLX where tracheal chondroprogenitor pellet (1.2±0.84) showed no significance difference compared with the disk groups. Gelatin-coated static cultured disks (1.5±0.47) exhibited the highest

COLX expression and was only significant ($p < 0.05$) when compared with FBS-coated static cultured disks (0.75±0.08). Gelatin-coated wave cultured disks (0.63±0.43) demonstrated the lowest expression but no significant differences were observed across the disk groups.

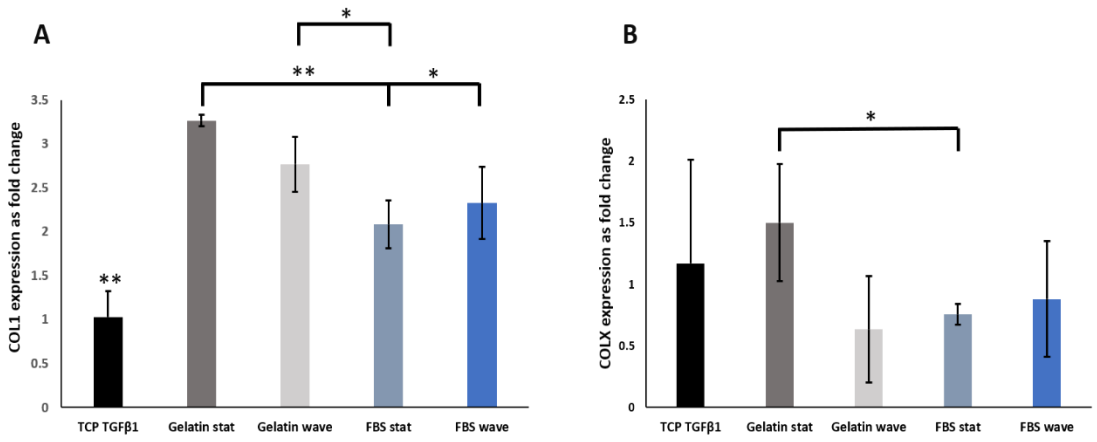

Figure 5.15. Relative gene expression shown as a fold change using ΔΔ*CT* method. (A) shows the COL1 expression of disks fabricated from tracheal chondroprogenitors and Cultispher® microcarriers placed on transwells after 21 days of chondrogenesis. **(B)** shows the COLX expression of disks fabricated from tracheal chondroprogenitors and Cultispher® microcarriers placed on transwells after 21 days of chondrogenesis. All data shown is average (± standard deviation) from three biological repeats, tested for significance using ANOVA analysis. * and ** are used to indicate $p < 0.05$ and $p < 0.001$ respectively.

5.2.9 Cartilage C-ring fabrication using tracheal chondroprogenitors and Cultisphers® microcarriers

The goal of this experiment was to use microcarriers as intra-scaffolding material and fabricate cartilage C-rings using 3D printed polylactic acid moulds using the same principles as the experiments conducted using transwell supports, as described in Section 2.5.6. FBS-coated tracheal chondroprogenitor seeded Cultisphers® microcarriers and gelatin-coated tracheal chondroprogenitor seeded Cultisphers® microcarriers, expanded under a static culture regime were, used for this experiment. Once individual C-rings were printed the ultimate aim was to suture individual C-rings

together to make a lumen-like cartilaginous structure. As shown in in **Figure 16** this method of C-ring fabrication was very highly reproducible in bulk structure, but the same problems occurred as with transwells where the internal structure lacked cartilage formation (shown by histological staining) throughout the whole depth of construct. Therefore, the decision was made not to further analyse the fabricated C-ring at other levels until refinement and improvements of 3D culture and differentiation medias was undertaken.

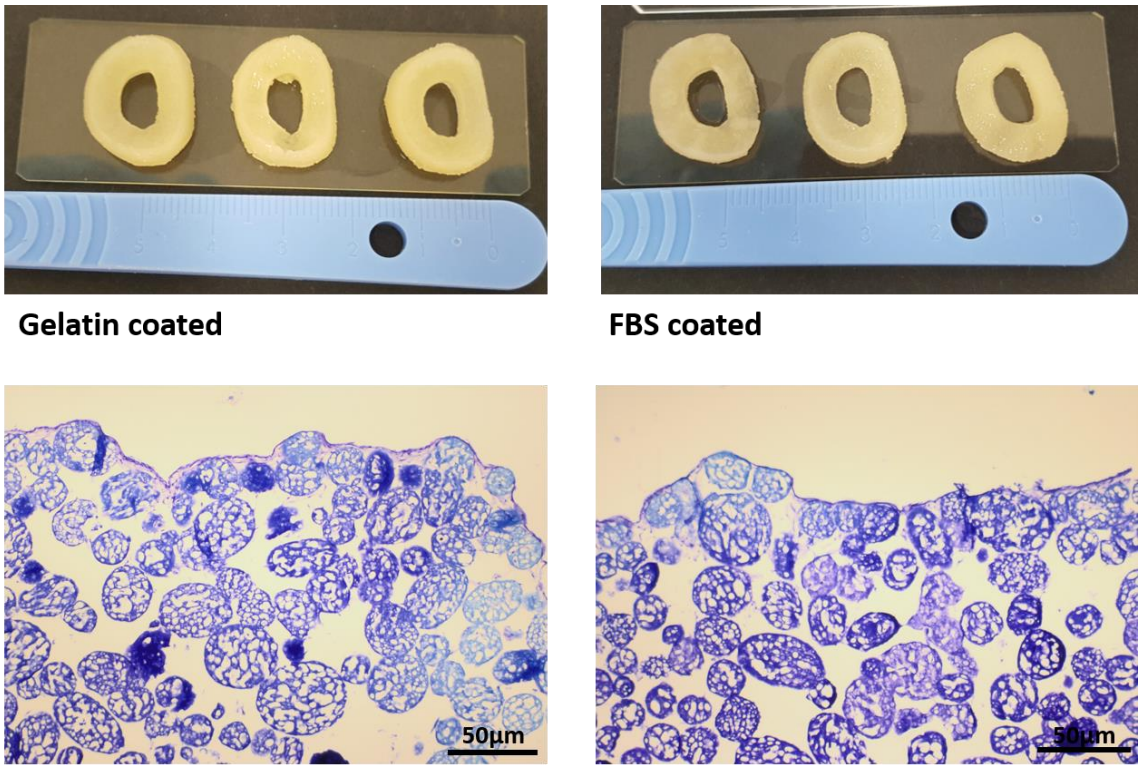

Figure 5.16. Proof of concept of 3D-printed PLA scaffolds seeded with tracheal chondroprogenitors and Cultispher® microcarriers coated with gelatin and FBS placed on to the mould for 21 days of chondrogenesis. Same principle as transwells were adopted in the C-ring scaffold. This mould was designed to be placed in a 6-well plate with porous structure for improved nutrient diffusion. As a proof of concept this method exhibited a reproducible C-ring fabrication where Cultispher® acted as intra scaffolding support.

5.2 Discussion

In order to regenerate or replace any damaged tissues large numbers of cells with stable phenotypes are needed from expansion to differentiation and maturation. The current techniques for cellular expansion are heavily reliant on 2D culture in order to generate enough cells to be seeded into scaffolding biomaterials in order to generate large enough constructs to be clinically useful. However, the use of 2D culture has reached its potential as shown by many groups expanding differentiated and undifferentiated cells [455]. Hence the aim of this chapter was to use naturally derived microcarriers to expand tracheal chondroprogenitors as it has been shown in Chapter 3, that long term passage of these cells will dramatically results in loss of genetic function, stiffening of cells which could be indicative of possible aging and upregulation of undesirable genes such as COL1 and COLX (refer to **Chapter 3**, **Figure 3.14**). The initial results of seeding uncoated Cultisphers® microcarriers with chondroprogenitors led to extremely low attachment of cells and slow proliferation rates which was far from optimal. Therefore, to enhance attachment and consequently the proliferation rate, FBS and gelatin coated microcarriers (± growth factors) were used. Initially the effect of growth factors on tracheal chondroprogenitors were examined on 2D by measuring the individual and combinatorial effect of fibroblast growth factor (FGF2 at 10 ng/mL), transforming growth factor β (TGFβ1 at 1 ng/mL) and platelet-derived growth factor (PDGF at 10 ng/mL) on cell kinetics. After 8 days of culture FT (FGF2+TGFβ1), FTP (FGF2+TGFβ1+PDGF) and PDGF showed the highest growth kinetics **(Figure 5.2)**. Based on our observations and previous publications FGF2 and TGFβ1 were chosen as the growth factor culture supplement during the growth phase of tracheal chondroprogenitors seeded upon macroporous Cultisphers® microcarriers. Previous studies have demonstrated that embryonic stem cells and MSCs cultured with FGF2 (5ng/mL) and TGFβ1 (10ng/mL*) in vitro* remain undifferentiated while also exhibiting increased rates of proliferation [456]. Solchaga *et al.* also reported that FGF2 exposure during monolayer expansion delays the loss of MSC chondrogenic potential [457], which is consistent with the upregulation of SOX9 by mouse chondrocytes when treated with FGF2 [458]. Thus, increased expression of SOX9 therefore maintains chondrogenic phenotype of stem cells *in vitro*. FGF2 may also promote proliferation of a specific sub-

population of chondroprogenitors that possess an increased chondrogenic potency [459] or alter the intrinsic molecular machinery of the entire or subset population to become more chondrogenically potent [460]. A very recent study done by Komura *et al.* also demonstrated that single injection of FGF2 in New Zealand white rabbit resulted in enlargement of mean tracheal luminal area [461].

In this study FBS or gelatin were used as microcarrier coating materials. FBS was employed as a control coating material, as it has been previously shown to successfully improve the expansion of chondroprogenitors on microcarriers [313]. However using animal derived serums for clinical applications are not ideal, therefore, gelatin was also included as a coating material as the use of this denatured collagen derived material is more suitable for clinical settings [462]. The combinatorial effect of FGF2 and TGFβ1 was also evident when applied to Cultisphers® microcarriers seeded with tracheal chondroprogenitors. After 15 days of culture FBS-FT (FGF2+TGFβ1) and gelatin-FT (FGF2+TGFβ1) were evidently supporting cellular proliferation more than their counterparts without growth factor supplementation **(Figure 5.3)**. This data agrees with what Melero-Martin *et al.* reported when immature bovine articular chondroprogenitors were expanded on Cultisphers® G microcarriers in conjunction with FGF2 and TGFβ1 growth factors in FBS-containing medium [313]. The FBS and gelatin appeared to increase cell attachment to microcarriers probably due to some serum proteins within FBS (for example, fibronectin) and gelatin itself acting as a cell adhesion substrate. To enhance homogenous cellular distribution, static and rocking culture regimes in the presence of FBS or gelatin-coated microcarriers (supplemented with FGF2 and TGFβ1) was tested to assess their effect on cellular proliferation **(Figure 5.4)**. The static culture condition exhibited a higher proliferation rate after 30 days when compared with the wave culture, and FBS-coated microcarriers appeared to be more advantageous for proliferation as observed from microscopic images of MTT stained Cultispher® microcarriers. The growth data showed that both FBS and gelatin static culture conditions are the most supportive for proliferation while the microscopic images of MTT stained microcarriers showed that gelatin coated beads on static culture were largely acellular. There are also cluster/aggregates of cells visible on microcarriers in every condition which is in line with that previously shown by Chen *et al.* [264] and

Eibes *et al.* [463], and in addition, dynamic culture also positively affects aggregate formation of microcarriers [464]. Aggregate formation has been associated with negative proliferative effects on human MSCs [243][445]. Another reason for lack of proliferation during wave culture could be due to cells detaching from the microcarriers caused by the shear stresses during the rocking motion of the platform, and therefore, further optimising the speed of the platform may reduce aggregation and improve this method of culture [160].

The preservation of stemness in microcarrier culture was important to demonstrate, as cell phenotype can be significantly influenced by differences in substrate material and geometry, as well as agitation induced stresses [466]. All four culture conditions (FBS-coated microcarrier static and wave, gelatin-coated microcarrier static and wave) agreed at gene level with the minimal requirements of ISSCR for the designation of cells maintaining mesenchymal stem cell characteristics [463]. Whilst all four groups showed a strong positive band intensity for COL1, the band visibility for COL2 expression was most obvious for gelatin-coated microcarriers in wave culture followed by gelatin-coated microcarriers in static culture, FBS-coated microcarriers grown in static culture and barely visible for FBS-coated microcarriers grown in wave culture. This could be an indicative of possible shift in change of cellular phenotype as the switch of collagen type II to collagen type I is associated with chondrocyte dedifferentiation and therefore the lack of chondrogenic potential of tracheal chondroprogenitors [261]. Another interesting observation was the presence of PRG4 in both microcarriers grown in wave conditions, which could be due to shear stress experienced by the chondroprogenitors during the rocking motion of the platform during wave culture. PRG4 was included in the panel as a distinct marker between articular and tracheal cartilage as previous studies had shown the correlation between shear stress and up-regulation of PRG4 both *in vivo* and *in vitro* both in chondrocytes and bone marrow MSCs at gene and protein level [467], [468].

Once characterised at the gene expression level, tracheal chondroprogenitors seeded and expanded on microcarriers were placed onto transwell culture supports and cultured either with expansion medium containing FGF2+TGFβ1 or chondrogenic medium containing 10 ng/mL of TGFβ1. As shown in **Figure 5.6A** samples in transwell inserts

containing expansion medium lack structural integrity and during sample handling the constructs had collapsed. The top row are the FBS-coated microcarriers expanded in static conditions constructs where the samples were too soft and ‘slushy’ and sample handling was not possible, and this followed by FBS-coated microcarriers expanded in wave culture (2nd row), gelatin-coated microcarriers expanded in static and gelatin-coated microcarriers expanded in wave culture. **Figure 5.6B** shows the formation of disks following 21 days of chondrogenesis. All four culture pre-conditions successfully formed solid structures with gelatin wave culture having hollow spaces mainly in the centre of disks, a possible indication of the lack of matrix formation. The gross morphological analysis of the disks was almost identical with gelatin-coated microcarriers expanded in static culture being significantly lower in diameter and height indicating a possible denser disk formation. Using microcarriers for macrotissue formation had previously been reported when culturing human fibroblasts on Cultisphers® S in a perfusion bioreactor resulted in cylindrical formations very similar to the disks fabricated in this study in terms of gross morphology and histology with edges clearly forming matrix [313], [463], [469].

The histological staining showed that most of the matrix formation occurred at the periphery of the disks and the middle section was free of matrix formation. There was a lack of evidence for cellular attachment post chondrogenesis in the middle/deep zone of the disks apart from the occasional cluster of tracheal chondroprogenitors and Cultisphers® microcarriers. The matrix in all four groups of pre-conditioned microcarriers induced to undergo chondrogenic differentiation stained positively for proteoglycan. The intensity of alizarin red staining was minimal on the periphery of disks where matrix deposition had occurred but stained stronger for individual microcarriers throughout the depth of construct. This could be due to the presence of high number of cells on individual Cultisphers® microcarriers and also indicative of a differentiation or possible nonspecific staining. The lack of matrix synthesis in the centre and middle part of disks could be explained by lack of cell-cell contact, which is a pre-requisite for cartilage condensation and formation [154]. Lack of cellular content in the centre of the disk may also be due to chemotaxis of cells [470] to the surface of the disk for the purpose of access to nutrients or cellular necrosis due to reduced oxygen and

nutrients in the centre of the disks. One possibility is that the periphery of constructs had formed matrix around the edges and possible lack of diffusion in nutrients to the inner depth of disks could have impacted cells to migrate towards the periphery [470]. Using blood derived biological glues have shown to improve disk formation when coupled with human articular chondrocytes and microcarriers, and this effect may have been due to the fibrin scaffold reducing cellular migration. The latter study extended the length of chondrogenesis to 12 weeks which ultimately resulted in mature disk formations [471].

The biochemical raw data revealed that FBS and gelatin-coated microcarriers expanded in static conditions produced higher sGAG content, whereas FBS-coated microcarriers expanded in wave culture had higher DNA content. FBS-coated microcarriers expanded in static culture were more successful in collagen synthesis followed by gelatin-coated microcarriers expanded in wave and gelatin static culture. The values for hydroxyproline content are highly magnified due to the collagenous nature of Cultisphers® microcarriers. However, the level of collagen synthesis still can be validated as the level of collagen microcarriers are constant across all the conditions hypothesising that same number of Cultisphers® microcarriers were present in each disk condition. When collagen was normalised to DNA both gelatin conditions were more reactive in synthesising collagen when compared with FBS conditions but not significantly different.

The relative gene expression of disks was compared with the tracheal chondroprogenitor pellets stimulated with TGFβ1 from the previous chapter as calibrator samples. The disks expressed much lower levels of positive chondrogenic markers (SOX9, COL2 and ACAN) and conversely higher levels of COL1. The lack of up-regulation SOX9 and consequently COL2 and ACAN could be again due to the lack of cell-cell contact and resulting in the lack of matrix formation. Conversely, COLX was upregulated which is less than traditional pellet culture and the presence of calcium deposition was still evident showing potential mineralisation of the disk constructs. Taken together, the presence of both COLX and PRG4 would be indicative of articular cartilage differentiation rather than tracheal cartilage and as a direct result of

mechanotransduction induced by shear stress within the wave expansion of the chondroprogenitors, showing a distinct mechano-responsiveness of the cells [471].

An attempt was made to fabricate customisable C-ring structures using a 3D printed mould and chondroprogenitor-seeded microcarriers. This method is advantageous for cases where the length of defect/disease is over half the diameter of the total tracheal length. Although gross morphology of the fabricated rings looked very similar and reproducible, identical problems like those mentioned in the transwell disks were observed such as lack of cell-to-cell contact and matrix formation. To date no other study has used microcarriers for tracheal macro-tissue engineering. Given time to optimise culture conditions, both expansion and differentiation, this method of engineering individual rings and assembling to form lumen like structures can be of great promise for clinically relevant specific dimensions. Recently one study showed using high-density human bone marrow MSCs coupled with TGFβ1 incorporated microspheres, it was possible to take a modular tissue assembly approach. The gross morphology and reproducibility was highly achievable in terms of similarity to native rabbit trachea and a tri-layer tissue consisting of cartilage, vascular and epithelium was achieved [471].

5.3 Conclusion

Tracheal chondroprogenitors were successfully expanded on macroporous gelatin derived microcarriers. Upon expansion chondroprogenitors retained their stemness and were able to undergo limited chondrogenesis. Using additive manufacturing, we were able to fabricate C-rings with customisable properties that could, if the future culture conditions are optimised, be more advantageous for clinical applications.

Chapter 6: General discussion

Tracheal tissue engineering in order to find a suitable solution for the regeneration and repair of diseased or damaged trachea still remains a challenging subject area and continues to be under researched. Currently, it is very difficult, at multiple levels, to produce a trachea substitute prosthetic resembling the native tissue. The trachea is a biological composite material consisting of adventitia, cartilage rings, interconnecting ligament-like tissue, mucosa and submucosa, muscle. In addition, the trachea is well perfused through an extensive vascular network [30]. The majority of tracheal tissue engineering approaches have in large concentrated on recreating the cartilage rings and the epithelium layer [89]. As the cartilage provides the main structural component of the respiratory tract and the epithelium provides the first line of defense in prevention of infection and disease during reparation, engineering these tissues into substitute biological prostheses are viewed as the prerequisite steps [139].

Tissue engineering aims to reverse engineer the functional tissue via embryonic developmental program, which contains sequential steps of events ultimately leading to the stepwise formation and maturation of multiple cellular and extracellular components and tissues of the functional respiratory system. So far, we are at the infancy of identifying these sequential steps that occur during airway development. What is clear is the presence of crosstalk between the endoderm and mesoderm during trachea development which needs to be further understood in order to systematically generate ordered structures *in vitro* [9]. In addition, we must be able to identify the critical stem/progenitor cells involved in airway development, and thus far, the only mesodermal stem cell identified resides in the perichondrium of cartilage, and has the ability to give rise to cartilage and other mesodermal-derived tissues of the trachea [134].

In this study it was fundamentally important to characterise the trachea at the cellular and tissue level in order to identify the minimal or ideal characteristics of tissue-engineered cartilage C-rings in order for them to mimic native tissue features, especially mechanical properties. Therefore, characterisation of native juvenile porcine tracheal cartilage was undertaken to create a comprehensive baseline measurement for this and future studies. It was concluded, that tracheal cartilage contains aggrecan, collagen type

II and lacked protein expression for collagen type I and elastin. However, collagen type I was present in the adventitia layer, and, elastin was localised to the mucosal and submucosal layers. Interestingly, these findings correlated with the macro mechanical data of the various tissue layers of the tracheal ring, where connective tissue had very elastic properties, this latter finding was associated with elastin staining being localised to the connective tissue of the tracheal ring [32][330]. The tracheal cartilage on the other hand, was extremely stiff as predicted from the matrix composition, agreeing with previous studies where the presence of both aggrecan and collagen type II are linked with the mechanical stability and stiffness of articular cartilage [105]. So far, many attempts to mathematically model the tracheal C-ring structure have been attempted [306]. However, a model that includes the finite and complex interactions of all the structural components has yet to be generated. In this study, a simple elongate-to-break (tensile stiffness) method was adopted to eliminate other variables, such as the asymmetrical and anisotropic morphological and histological properties of the trachea, as the main objective was to obtain a reproducible measurement of the cartilage unidirectional tensile strength for future comparisons [319].

Given tracheal cartilage is generally assumed to be hyaline in nature [472], a comparison was undertaken between articular and trachea cartilages to further examine the extent of similarities and differences between these two cartilage-based tissues. The main differences observed were the presence of COLX and PRG4 at gene level in articular cartilage. Collagen type X is present surrounding chondrocytes embedded in the calcified zone of cartilage, which connects cartilage with subchondral bone (osteochondral interface) [473]. The main function of articular cartilage is to provide frictionless movements between the joints and the presence of PRG4 in the superficial zone is in line with the functionality of this tissue [474]. Lubrication is not required in the tracheal cartilage and therefore the finding that PRG4 was expressed by tracheal chondroprogenitors undergoing gene regulation in a wave bioreactor which is capable of producing mechanical stimuli indicates that these cells harbor the ability to adapt to specific environmental cues by being mechano-responsive and reproduce a location-dependent phenotype as observed in articular cartilage superficial zone.

Recently it is becoming clearer that tissue-specific stem cells reside within many, if not the majority of adult tissues [217]. Isolation, expansion and the use of tissue-specific stem cells for tissue engineering applications is a logical approach as these stem cells/progenitors have an epigenetic pre-disposition towards differentiation to the tissue of origin. The extracellular matrix the latter cells produce has a prominent role in maintaining tissue homeostasis and cell function [475]. Based on this logic tracheal cartilage-derived chondroprogenitors/stem cells were isolated using differential adhesion to fibronectin as a source of colony forming, mesodermal-derived stem cells [219].

During the first stages of this project different types of colonies with distinct morphologies were identified which led to further analysis of tissue specific cells from different tissue compartments of the trachea such as cartilage, adventitia and the connective layer consisting of mucosa and submucosa. The morphological data clearly indicated distinct morphological differences allowing a reliable way to separate tissue layers by dissection and identify and distinguish between the adventitia, cartilage and connective derived colony forming cells. The AFM based nano-mechanics of single cells and the multipotential differentiation assays of the newly identified colony forming cells also varied significantly, with cells derived from cartilage and adventitia being mechanically stiffer and more potent in tri-lineage differentiation when compared to connective, sub-mucosa and mucosal derived cells, These observations showed cells with differing mechanical and morphological appearance were capable of tri-lineage differentiations, with the exception being cells derived from the connective tissue layer. Tracheal stem/chondroprogenitors had a higher colony forming efficiency compared with adventitia and connective tissue-derived stem/progenitor cells and a more rounded morphological appearance when compared to connective and adventitia-derived cells. Their expression of surface markers also agreed with the minimal criteria set by the ISSCR for classification for mesenchymal stem cells. These requirements rely on the expression of a specific set of surface biomarkers to identify potential mesodermal stem cell populations [135]. Although all three types of colony forming cells from different compartments of the trachea tissue were plastic adherent and showed the same gene expression to meet minimal criteria, tri-lineage assays showed colony forming cells from cartilage and adventitia were able to differentiate to osteocytes, adipocytes and

chondrocytes whereas connective tissue-derived colony-forming cells had a more limited differentiation capacity. This was expected as the literature had previously identified the cells from connective layer that has the ability to give rise to ciliated and basal epithelial cells [364]. Differential adhesion to fibronectin therefore has the ability to isolate colony-forming cells that can further be expanded *in vitro* regardless of them being mesodermal or endodermal derived. The colony forming cells can be isolated as monoclonal cell lines and be used for *in vitro* studies or maintained as a polyclonal culture, which may reduce the physiological stresses experienced by monoclonal cell lines for extensive expansion and losing phenotypic stability.

One of the main advantages of enrichment of colony forming cells using differential adhesion to fibronectin is it's ease of use and cost-effectiveness as opposed to cell surface marker isolation, as well as the ability to derive homogeneous (monoclonal) cell populations using cell cloning of colonies [159]. Dowthwaite *et al.* utilised differential adhesion to fibronectin to isolate articular cartilage-derived chondroprogenitors from the superficial zone of articular cartilage [219]. Others have utilised the same technique to isolate chondroprogenitors using cells from the full depth of various cartilage tissues [138][202][345]. Other studies have also previously shown that differences in cellular properties exist between chondrocytes from different depths of articular cartilage, from nano-mechanical, to protein expression and gene expression [279][349][457]. Based on these data, variations in the properties of clonal isolates might exist depending on where the progenitor isolated might be derived from (whether superficial, middle or deep zone) and thus, by analogy, further analysis may require understanding if any differences exist between monoclonal and polyclonal cell populations from various zones of the trachea tissue. However, this would be extremely challenging as isolation of specific populations from the various zones would be technically difficult to achieve.

The single cell nano-mechanics analysis of colony forming cells derived from three different tissue layers in trachea showed a general trend of increased stiffness from passage P0 to P6 when grown and analysed on plastic tissue culture substrate. This type of result has previously been associated with decreased proliferation, differentiation [477] and potential aging [348][359] and senescence [384]. Chondrocyte gene

expression of tracheal chondroprogenitors decreased from passages P0 to P6, and this may be due to potential ageing or senescence and therefore more extensive analysis of telomere length analysis and differentiation potential from each passage could be undertaken in the future to confirm the current findings. Previously it has been shown the effect of culture substrate mediates cells function and differentiation potential and therefore more in depth analysis needs to be undertaken for *in vitro* expansion [260] [459][460].

The presence and expression of COLX gene transcription in tracheal-derived colony forming cells as early as P0 was unexpected, as this was not observed at the tissue level mRNA. Previous findings had highlighted the use of hypoxia [480] and matrix stiffness in dampening the expression of COLX, as cells are mechanosensitive entities responsive to the microenvironment they reside in, and therefore, this directly affects the actin filament organisation and in turn gene expression and functionality of cultured cells [481]. These finding could be useful in the future studies as the media used in this study is a standard basal medium containing 10% FBS which is used for the expansion of many mesodermal derived stem/progenitor cells ruling media choice out as a major contributor for the upregulation of COLX. Furthermore, a normoxic rather than hypoxic cell culture conditions along with altered adhesion environment may have more contribution to COLX expression as previously shown for articular chondrocytes and bone marrow MSCs [413][463]. Furthermore, batch-to-batch variations of FBS have previously been shown to influence cell behavior, and so a move towards animal-free derived expansion medium may also be advantageous for future clinical applications [483]. Further immunocytochemical studies should confirm the protein expression of collagen type X to validate the latter observations. This finding was used as a threshold of passage number in future chapters, which was designated to be P4 for differentiation studies and 3D expansion and differentiation of tracheal derived cartilage stem/progenitor which agrees with threshold for differentiation studies using mesenchymal stem cells where the earlier the passage used the higher the differentiation potential [369].

Once tracheal chondroprogenitors were identified their chondrogenic potential was examined by testing their differential potential using two different growth factors, TGFβ1 and BMP9, both members of the TGFβ-super-family. The tracheal chondroprogenitors were able to effectively undergo chondrogenesis but when compared with their native counterparts, full-depth freshly isolated chondrocytes treated with TGFβ1, the performance wasn't as optimal and distinctive differences were observed. Firstly, as was previously observed during 2D culture expansion of progenitors the expression of COLX was upregulated and the ratio of COL2 to COL1 dropped significantly and these changes could ultimately affect the differentiation outcome. Secondly, the duration of chondrogenesis induction and dose of growth factor administered may require further optimisation by means of titration analysis so that the differentiation of progenitors could reach the level of native cells. Thirdly it's been shown that environmental cues such as hypoxia could regulate chondrogenesis as conventional differentiation is undertaken at normoxic O_2 concentrations, whereas, the native environment for cartilage is between 3%-7% O_2 [429], [480].

Recent studies have shown the use of hypoxic cell culture results in the down regulation of expression of COLX gene transcript [428]. Fourthly, the growth factor choice could be further optimised, since the effect of TGFβ1 was previously uncharacterised for tracheal progenitors, and in airway development BMP4 and FGF10 has been reported to be involved in tracheal cartilage formation and patterning [22]. Therefore, TGFβ1 may not play any part in native tracheal cartilage formation. Fifthly, the question is: do different cartilage subtypes develop from distinct chondroprogenitor subtypes, which are developmentally restricted, or are their molecular, morphological, and functional differences determined by site-specific environment (e.g., load bearing for articular cartilage, tensile and compression in trachea), or both? And finally does the current protocol result in terminally differentiated events and progression to an osteoblast like phenotype? Or, are chondroprogenitors still in an early developmental growth stage? For example, the expression of collagen type 1 is associated with the early developmental program of articular cartilage and is transcribed both at gene and protein levels, whereas in trachea it's expression is absent [424]. Regardless, a sequential order of events was obvious at gene and protein level. The chondrocytes that had not been cultured on 2D

had the most elastic single cell mechanical properties, and produced the highest amount of GAG and collagen, had a homogenously distributed matrix formation and lacked collagen type 1 and calcified zone gene expression.

For future studies perhaps, adventitia colony derived cells could be targeted as an ideal cell source for the regeneration of tracheal cartilage. This tissue can be harvested from a patient whilst keeping the lumen intact and therefore having more suitable clinical applications in terms of surgical procedure and as shown before adventitial derived cells had very similar traits as tracheal chondroprogenitors.

To fabricate a cartilage C-ring large numbers of cells were required. To achieve this tracheal chondroprogenitors were expanded on microporous gelatin-derived Cultispher® microcarriers coated in either 3% gelatin or 10% FBS. These cells seeded microcarriers were then cultured in medium containing 10 ng/ml FGF2 and 1 ng/ml TGFβ1 in both static and wave culture. Cultispher® microcarriers supported better expansion in static culture in both FBS and gelatin coated formats. Static and wave culture groups both retained the stem cell phenotypic criteria during long-term culture, but a major finding was the presence of PRG4 in wave condition whereas this was absent in static. This data showed that the tracheal chondroprogenitors/stem cells are responsive to their microenvironment and the shear stress occurring between the cells might have resulted in a cellular sensing of mechanical forces produced by wave culture and subsequent mechanotransduction from the cell surface resulting in the transcription of PRG4. Previous research has shown the upregulation of lubricin (PRG4) due to shear stress induction [467]. During differentiation studies all four groups of Cultispher® microcarriers formed disk structures as a preliminary step towards fabricating multiple C-rings, even though the gross morphology of disks seemed robust the histological data showed very weak matrix formation with lack of architectural organisation. Although Cultispher® microcarriers encouraged cells to undergo chondrogenesis the large spaces in between each individual microcarriers in all four conditions mean lack of cell-cell contact which is one of the main key factors in cartilage formation [154]. Moreover, the matrix deposition exclusively occurred on the periphery of the constructs in all four groups and the lack of nutrient supply to the center of constructs might have caused cell

death or chemotaxis of cells [470] to the periphery where a layer of viable cells was clearly visible. To improve mechanical strength and shape fidelity the use of bioprinting and other co-polymers may be further investigated. Malda *et al.* demonstrated mechanical improvement and better structural organisation and in turn better osteogenic differentiation when encapsulating bone marrow MSCs grown on microcarriers in gelatin methacrylamide [352]. In this way the cells were shielded by the hydrogel and protected during the printing and also act as reinforcement for the entire construct. On the other hand, the mixture of solid and porous microcarriers can be further investigated to check whether mechanical improvements can be achieved.

In general, the pellet system showed an enhanced chondrogenesis at gene and protein level mainly due to the close cell-cell contact but further refining of culture conditions for 3D microcarrier constructs could perhaps improve matrix synthesis and deposition. The presence of calcium deposition observed with alizarin staining and the presence of COLX should not be overlooked as COLX is not present in tracheal C-ring and calcium deposition is a significant indicator to tracheal cartilage disease [336][337]. Although pellet models are not mechanically feasible, they are useful models to evaluate and study the effect of cell-cell contact and cell-matrix interactions [215]. The potency of chondrogenic factors were examined on stem cells/chondroprogenitors with two distinct growth factors before moving onto 3D culture with microcarriers. Due to financial constraints chondrogenesis induction with BMP9 was not included and perhaps future studies should first examine the effect of BMP9 in a 3D culture during differentiation. However, full data sets are required to be reported as showing chondrogenic differentiation is one element of successful tissue engineering, it is also equally and if not more important to show further developmental as progression towards early bone formation has not been initiated and therefore reporting histological, protein and genes specific to bone formation should be incorporated

Further improvements could be made on seeding strategies where Cultispher® microcarriers and cells could be made as small microtissues/aggregates first and then assemble these in a form of C-ring for enhanced cell-cell contact and optimised differentiation [484]. This was not feasible to do in our case as a bioprinting system

would have been an ideal way to perform this type of scaffold generation. Also, the effect of cell-matrix could be further investigated with AFM but requires an exposure to collagenase or trypsinised to dissociate cells from the microcarriers and recover viable cells [262].

In this project, attempts were made to provide a more comprehensive overview of the native tissue and the journey of the cells from isolation to post-differentiation analysis. Unfortunately, this is not the case in most airway/tracheal cartilage tissue engineering research papers. The discrepancy lies mostly between the epithelial and cartilage tissues where comprehensive datasets are described at cell, genetic and protein level for only the epithelial layer [485]. This could be due to its biological function and the level of complexity of tissue function and cell types present in the native epithelial layer. The same principle must be applied when designing cellular based strategies for cartilage regeneration. Although, from a cellular point of view, cartilage is seen as a relatively simple tissue due to its sole cellular component, the chondrocyte, the possibility of cross-talk cannot be ruled out or ignored between adjacent tissues/compartments and perhaps future studies can further investigate the cross-talk between tracheal cartilage and adjacent tissues to elucidate this complex molecular interaction. The choice of cell selection for repair strategies may define the outcome of the fabricated tissues whether chondrocytes from different anatomical locations or cartilage-derived MSCs [100]. Due to the urgency to find a feasible solution for long segment tracheal replacements and the importance of the mechanical stability the focus therefore lies on the biochemistry, the positive gene regulation and protein expression of cartilage ECM and the mechanical properties which currently fails to report the whole image of the outcome. For example, assays such as hydroxyproline and sGAG report the total content of the matrix synthesized. Similarly stains such as toluidine blue and picrosirius red show the total GAG and collagen architectures respectively but lack specificity. It is well established that the use of chondrocytes or MSCs, which are the main cell focus in airway tissue engineering using the traditional culture methods have reached their potential limits, which do not fulfill the requirements for the clinical settings. Therefore, due to the common problems seen with current cell types and animal models selected, proliferation and differentiation media coupled with many different growth factors each having

unique signaling cascades it is necessary to report the full scale of results to narrow down feasible strategies and models to further enhance our understanding of tissue engineering these tissues [89], [90].

Realistically, we are far from re-creating the complexity of developmental biology to generate nascent tracheal tissues by reverse engineering, and therefore, a radical re-think is required. What is obvious is that the cellular and molecular mechanisms involved during development and post-natally produce highly dynamic environments and a synergy and sequence of specific events leads to formation of tracheal tissue. Traditional *in vitro* approaches using normoxia, 2D culture and various chemical based protocols which mainly focus on one type of growth factor, although effective to some degree cannot recapitulate or replicate the native environment, they result in cartilage-like formation but not true hyaline cartilage. If using chondrocytes that are already committed is troublesome, using undifferentiated cells and subsequently reprogramming these cells to become differentiated is a more complex challenge with many variables to consider and overcome. Therefore, new strategies in cartilage tissue engineering have started to take a different approach and include as many physiological relevant factors as possible such as hypoxia, mechanical induction and 3D cultures and therefore we enter a new dawn of tissue engineering where we implement native cellular environments in an attempt to replicate developmental biological processes.

Ideal experimental set up:

Isolate chondroprogenitors via flow cytometry, immediately seed onto coated Cultispher® microcarriers and expand cells by addition of empty microcarriers in the presence of FGF2 and TGFβ1, to avoid environment as 2D is not an optimised environment and mechanotransduction is a well-known fact, use a low oxygen tension system at all times for propagation and differentiation, bioprint microaggregates of cells and microcarriers encapsulated within a hydrogel and stimulate chondrogenesis by mechanical induction, growth factors or a combination of both.

Conclusion:

This study indicates that tracheal cartilage tissue specific chondroprogenitors were identified as plastic adherent, colony forming, proliferative and tri-potent. As a proof of concept, it was shown that customisable C-ring cartilages could be fabricated using ste/progenitor seeded gelatin microcarriers. However, further investigation is needed for optimisation of culture conditions and fabrication techniques. Therefore, tracheal chondroprogenitors have the potential as suitable cell sources for airway tissue engineering.

Chapter 7: Bibliography

[1] N. A. Campbell, *Biology*, 2nd ed. Redwood city, California: Benjamin/Cummings Pub. Co, 1990.
[2] T. Des Jardins, *Cardiopulmonary Anatomy & Physiology: Essentials for Respiratory Care*, 5th ed. New York, 2007.
[3] F. D. McCool, "Global Physiology and Pathophysiology of Cough," *Chest*, vol. 129, no. 1, p. 48S–53S, Jan. 2006.
[4] B. B. ROSS, R. GRAMIAK, and H. RAHN, "Physical dynamics of the cough mechanism.," *J. Appl. Physiol.*, vol. 8, no. 3, pp. 264–8, Nov. 1955.
[5] G. A. Lyubimov, "The physiological function of the posterior tracheal wall.," *Dokl. Biol. Sci. Proc. Acad. Sci. USSR, Biol. Sci. Sect.*, vol. 380, pp. 421–3.
[6] M. Boiani and H. R. Schöler, "Regulatory networks in embryo-derived pluripotent stem cells," *Nat. Rev. Mol. Cell Biol.*, vol. 6, no. 11, pp. 872–881, Nov. 2005.
[7] P. P. L. Tam and D. A. F. Loebel, "Gene function in mouse embryogenesis: get set for gastrulation," *Nat. Rev. Genet.*, vol. 8, no. 5, pp. 368–381, May 2007.
[8] M. Wegner, "From head to toes: the multiple facets of Sox proteins.," *Nucleic Acids Res.*, vol. 27, no. 6, pp. 1409–20, Mar. 1999.
[9] E. A. Hines and X. Sun, "Tissue Crosstalk in Lung Development," *J. Cell. Biochem.*, vol. 115, no. 9, pp. 1469–1477, Sep. 2014.
[10] W. V. Cardoso and J. Lü, "Regulation of early lung morphogenesis: questions, facts and controversies," *Development*, vol. 133, no. 9, pp. 1611–1624, May 2006.
[11] J. Que *et al.*, "Multiple dose-dependent roles for Sox2 in the patterning and differentiation of anterior foregut endoderm," *Development*, vol. 134, no. 13, p. 2521, 2007.
[12] M. Herriges and E. E. Morrisey, "Lung development: orchestrating the generation and regeneration of a complex organ," *Development*, vol. 141, no. 3, pp. 502–513, 2014.
[13] H. Kubba and T. Moores, "Developmental anatomy of the airway," *Anaesth. Intensive Care Med.*, vol. 7, no. 5, pp. 158–160, May 2006.
[14] S. R. Fausett and J. Klingensmith, "Compartmentalization of the foregut tube: developmental origins of the trachea and esophagus," *Wiley Interdiscip. Rev. Dev. Biol.*, vol. 1, no. 2, pp. 184–202, Mar. 2012.
[15] A. S. Ioannides *et al.*, "Foregut separation and tracheo-oesophageal malformations: The role of tracheal outgrowth, dorso-ventral patterning and programmed cell death," *Dev. Biol.*, vol. 337, no. 2, pp. 351–362, Jan. 2010.
[16] E. E. Morrisey and B. L. M. Hogan, "Preparing for the First Breath: Genetic and Cellular Mechanisms in Lung Development," *Dev. Cell*, vol. 18, no. 1, pp. 8–23, 2010.
[17] J. Que, "The initial establishment and epithelial morphogenesis of the esophagus: a new model of tracheal-esophageal separation and transition of simple columnar into stratified squamous epithelium in the developing esophagus," *Wiley Interdiscip. Rev. Dev. Biol.*, vol. 4, no. 4, pp. 419–430, Jul. 2015.
[18] J. A. McAteer, "Tracheal morphogenesis and fetal development of the

mucociliary epithelium of the rat.," *Scan. Electron Microsc.*, no. Pt 4, pp. 1995–2008, 1984.
[19] R. G. Elluru and J. A. Whitsett, "Potential role of Sox9 in patterning tracheal cartilage ring formation in an embryonic mouse model.," *Arch. Otolaryngol. Head. Neck Surg.*, vol. 130, no. 6, pp. 732–6, Jun. 2004.
[20] E. A. Hines, M.-K. N. Jones, J. M. Verheyden, J. F. Harvey, and X. Sun, "Establishment of smooth muscle and cartilage juxtaposition in the developing mouse upper airways," *Proc. Natl. Acad. Sci.*, vol. 110, no. 48, pp. 19444–19449, Nov. 2013.
[21] F. G. Sala *et al.*, "FGF10 controls the patterning of the tracheal cartilage rings via Shh," *Development*, vol. 138, no. 2, pp. 273–282, Jan. 2011.
[22] D. M. Ornitz, Y. Yin, J. Nichols, and A. Smith, "Signaling Networks Regulating Development of the Lower Respiratory Tract," pp. 1–20, 2014.
[23] Y. Mori-Akiyama, H. Akiyama, D. H. Rowitch, and B. de Crombrugghe, "Sox9 is required for determination of the chondrogenic cell lineage in the cranial neural crest," *Proc. Natl. Acad. Sci.*, vol. 100, no. 16, pp. 9360–9365, Aug. 2003.
[24] A.-K. T. Perl, R. Kist, Z. Shan, G. Scherer, and J. A. Whitsett, "Normal lung development and function afterSox9 inactivation in the respiratory epithelium," *genesis*, vol. 41, no. 1, pp. 23–32, Jan. 2005.
[25] R. Arora, R. J. Metzger, and V. E. Papaioannou, "Multiple Roles and Interactions of Tbx4 and Tbx5 in Development of the Respiratory System," *PLoS Genet.*, vol. 8, no. 8, p. e1002866, Aug. 2012.
[26] L.-A. D. Miller, S. E. Wert, J. C. Clark, Y. Xu, A.-K. T. Perl, and J. A. Whitsett, "Role ofSonic hedgehog in patterning of tracheal-bronchial cartilage and the peripheral lung," *Dev. Dyn.*, vol. 231, no. 1, pp. 57–71, Sep. 2004.
[27] J. Park, J. J. R. Zhang, A. Moro, M. Kushida, M. Wegner, and P. C. W. Kim, "Regulation of Sox9 by Sonic Hedgehog (Shh) is essential for patterning and formation of tracheal cartilage," *Dev. Dyn.*, vol. 239, no. 2, pp. 514–526, Feb. 2010.
[28] F. G. Sala *et al.*, "FGF10 controls the patterning of the tracheal cartilage rings via Shh," vol. 282, pp. 273–282, 2011.
[29] J. Snowball, M. Ambalavanan, J. Whitsett, and D. Sinner, "Endodermal Wnt signaling is required for tracheal cartilage formation," vol. 14, no. 1, pp. 1–14, 2015.
[30] J. P. Sasson, N. G. Abdelrahman, S. Aquino, and M. H. Lev, "Trachea: Anatomy and Pathology," pp. 1700–1726, 2003.
[31] G. Pocock and C. D. Richards, *Human physiology : the basis of medicine*, 3rd ed. Oxford: Oxford University Press, 2006.
[32] Z. Teng, O. Trabelsi, I. Ochoa, J. He, J. H. Gillard, and M. Doblare, "Anisotropic material behaviours of soft tissues in human trachea: An experimental study," *J. Biomech.*, vol. 45, no. 9, pp. 1717–1723, 2012.
[33] L. Stehlik, V. Hytych, J. Letackova, P. Kubena, and M. Vasakova, "Biodegradable polydioxanone stents in the treatment of adult patients with tracheal narrowing.," *BMC Pulm. Med.*, vol. 15, p. 164, 2015.
[34] M. W. Leigh, "The airway epithelium: Physiology, pathophysiology and

pharmacology.," *Pediatr. Pulmonol.*, vol. 21, no. 4, pp. 262–263, Apr. 1996.
[35] N. Hamilton, A. J. Bullock, S. Macneil, S. M. Janes, and M. Birchall, "Tissue engineering airway mucosa: A systematic review," *Laryngoscope*, vol. 124, no. 4, pp. 961–968, 2014.
[36] "Trachea + Lungs." [Online]. Available: https://www.slideshare.net/saktivinayaga/trachea-lungs. [Accessed: 04-Oct-2018].
[37] "British Lung Foundation | The UK's lung charity." [Online]. Available: https://www.blf.org.uk/. [Accessed: 10-Apr-2018].
[38] M. Den Hondt, "Reconstruction of defects of the trachea," *J. Mater. Sci. Mater. Med.*, pp. 0–1, 2017.
[39] M. Kalathur, S. Baiguera, and P. Macchiarini, "Translating tissue-engineered tracheal replacement from bench to bedside," *Cell. Mol. Life Sci.*, vol. 67, no. 24, pp. 4185–4196, 2010.
[40] T. Hirano, B. Franzén, H. Kato, Y. Ebihara, and G. Auer, "Genesis of squamous cell lung carcinoma. Sequential changes of proliferation, DNA ploidy, and p53 expression.," *Am. J. Pathol.*, vol. 144, no. 2, pp. 296–302, Feb. 1994.
[41] A. Bailhache, D. Dehesdin, A. François, J.-P. Marie, and O. Choussy, "Rhinoscleroma of the sinuses.," *Rhinology*, vol. 46, no. 4, pp. 338–41, Dec. 2008.
[42] S. Ergun, T. Tewfik, and S. Daniel, "Tracheal agenesis: A rare but fatal congenital anomaly.," *Mcgill J. Med.*, vol. 13, no. 1, p. 10, Jun. 2011.
[43] D. F. Smith, S. Rasmussen, A. Peng, C. Bagwell, and C. Johnson, "Complete traumatic laryngotracheal disruption—A case report and review," *Int. J. Pediatr. Otorhinolaryngol.*, vol. 73, no. 12, pp. 1817–1820, Dec. 2009.
[44] J. W. Brown, K. Bando, K. Sun, and M. W. Turrentine, "Surgical management of congenital tracheal stenosis.," *Chest Surg. Clin. N. Am.*, vol. 6, no. 4, pp. 837–52, Nov. 1996.
[45] K. Kusafuka, A. Yamaguchi, T. Kayano, and T. Takemura, "Ossification of tracheal cartilage in aged humans : a histological and immunohistochemical analysis," pp. 168–174, 2001.
[46] E. F. Maughan *et al.*, "A comparison of tracheal scaffold strategies for pediatric transplantation in a rabbit model," *Laryngoscope*, pp. 1–9, 2017.
[47] D. C. Barbancho, J. Antón-Pacheco, M. L. Diaz, R. T. Sánchez, J. C. García, and A. G. Fraile, "Acquired tracheal stenosis: diagnosis and treatment.," *Cir. Pediatr.*, vol. 20, no. 1, pp. 19–24, Jan. 2007.
[48] H. C. Grillo, "Tracheal replacement: a critical review," *Ann. Thorac. Surg.*, vol. 73, no. 6, pp. 1995–2004, 2002.
[49] T. V. McCaffrey, "Classification of Laryngotracheal Stenosis," *Laryngoscope*, vol. 102, no. 12, pp. 1335–1340, Dec. 1992.
[50] T. V. McCAffrey, "Management of Laryngotracheal Stenosis on the Basis of Site and Severity," *Otolaryngol. Neck Surg.*, vol. 109, no. 3, pp. 468–473, Sep. 1993.
[51] P. Monnier, C. Ikonomidis, Y. Jaquet, and M. George, "Proposal of a new classification for optimising outcome assessment following partial cricotracheal resections in severe pediatric subglottic stenosis," *Int. J. Pediatr.*

Otorhinolaryngol., vol. 73, no. 9, pp. 1217–1221, Sep. 2009.
[52] C. M. Myer, D. M. O'Connor, and R. T. Cotton, "Proposed Grading System for Subglottic Stenosis Based on Endotracheal Tube Sizes," *Ann. Otol. Rhinol. Laryngol.*, vol. 103, no. 4, pp. 319–323, Apr. 1994.
[53] V. Tsang, A. Murday, C. Gillbe, and P. Goldstraw, "Slide tracheoplasty for congenital funnel-shaped tracheal stenosis.," *Ann. Thorac. Surg.*, vol. 48, no. 5, pp. 632–5, Nov. 1989.
[54] H. C. Grillo, "Slide tracheoplasty for long-segment congenital tracheal stenosis.," *Ann. Thorac. Surg.*, vol. 58, no. 3, pp. 613-9 discussion 619-21, Sep. 1994.
[55] S. R. Chung *et al.*, "Clinical outcomes of slide tracheoplasty in congenital tracheal stenosis.," *Eur. J. Cardio-Thoracic Surg.*, vol. 47, no. 3, pp. 537–542, Mar. 2015.
[56] D. Fabre *et al.*, "Successful tracheal replacement in humans using autologous tissues: An 8-year experience.," *Ann. Thorac. Surg.*, vol. 96, no. 4, pp. 1146–1155, Oct. 2013.
[57] M. Ninkovic, H. Buerger, D. Ehrl, and U. Dornseifer, "One-stage reconstruction of tracheal defects with the medial femoral condyle corticoperiosteal-cutaneous free flap.," *Head Neck*, vol. 38, no. 12, pp. 1870–1873, Dec. 2016.
[58] S. Zhang and Z. Liu, "Airway Reconstruction with Autologous Pulmonary Tissue Flap and an Elastic Metallic Stent," *World J. Surg.*, vol. 39, no. 8, pp. 1981–1985, Aug. 2015.
[59] S. Al-Khudari, S. Sharma, W. Young, R. Stapp, and T. A. Ghanem, "Osteocutaneous radial forearm reconstruction of large partial cricotracheal defects," *Head Neck*, vol. 35, no. 8, pp. E254–E257, Aug. 2013.
[60] K. Y. Detwiller, J. S. Schindler, D. S. Schneider, R. Lindau, and M. K. Wax, "Complex adult laryngotracheal reconstruction with a prefabricated flap: A case series," *Head Neck*, vol. 35, no. 12, pp. E376–E380, Dec. 2013.
[61] C. L. Backer, C. Mavroudis, M. E. Dunham, and L. D. Holinger, "Reoperation after pericardial patch tracheoplasty.," *J. Pediatr. Surg.*, vol. 32, no. 7, pp. 1108-11; discussion 1111–2, Jul. 1997.
[62] A. Beigel, R. Steffens-Knutzen, B. Müller, U. Schumacher, and H. Stein, "Tracheal transplantation. III. Demonstration of transplantation antigens on the tracheal mucosa of inbred rat strains.," *Arch. Otorhinolaryngol.*, vol. 241, no. 1, pp. 1–8, 1984.
[63] P. Delaere, J. Vranckx, G. Verleden, P. De Leyn, and D. Van Raemdonck, "Tracheal Allotransplantation after Withdrawal of Immunosuppressive Therapy," *N. Engl. J. Med.*, vol. 362, no. 2, pp. 138–145, Jan. 2010.
[64] K. G. Rose, K. Sesterhenn, and F. Wustrow, "Tracheal allotransplantation in man.," *Lancet (London, England)*, vol. 1, no. 8113, p. 433, Feb. 1979.
[65] A. Wurtz *et al.*, "Surgical technique and results of tracheal and carinal replacement with aortic allografts for salivary gland–type carcinoma," *J. Thorac. Cardiovasc. Surg.*, vol. 140, no. 2, p. 387–393.e2, Aug. 2010.
[66] A. Wurtz *et al.*, "Tracheal Replacement with Aortic Allografts," *N. Engl. J. Med.*, vol. 355, no. 18, pp. 1938–1940, Nov. 2006.
[67] J. D. Cooper *et al.*, "Use of silicone stents in the management of airway

problems.," *Ann. Thorac. Surg.*, vol. 47, no. 3, pp. 371–8, Mar. 1989.
[68] L. Freitag, R. Eicker, B. Linz, and D. Greschuchna, "Theoretical and experimental basis for the development of a dynamic airway stent.," *Eur. Respir. J.*, vol. 7, no. 11, pp. 2038–45, Nov. 1994.
[69] Y. Saito and H. Imamura, "Airway Stenting," *Surg. Today*, vol. 35, no. 4, pp. 265–270, Apr. 2005.
[70] R. A. DANIEL, "The regeneration of defects of the trachea and bronchi; an experimental study.," *J. Thorac. Surg.*, vol. 17, no. 3, pp. 335–49, Jun. 1948.
[71] H. M. MORFIT, A. J. NEERKEN, A. PREVEDEL, E. B. LIDDLE, and L. KIRCHER, "Sleeve resections of the trachea; experimental studies on regenerative capacity and principles of reconstruction and repair.," *AMA. Arch. Surg.*, vol. 70, no. 5, pp. 654–61, May 1955.
[72] A. J. Spinazzola, J. L. Graziano, and W. E. Neville, "Experimental reconstruction of the tracheal carina.," *J. Thorac. Cardiovasc. Surg.*, vol. 58, no. 1, pp. 1–13, Jul. 1969.
[73] T. W. Wykoff, "A preliminary report on segmental tracheal prosthetic replacement in dogs.," *Laryngoscope*, vol. 83, no. 7, pp. 1072–1077, Jul. 1973.
[74] D. KRAMISH and H. M. MORFIT, "THE USE OF A TEFLON PROSTHESIS TO BRIDGE COMPLETE SLEEVE DEFECTS IN THE HUMAN TRACHEA.," *Am. J. Surg.*, vol. 106, pp. 704–8, Nov. 1963.
[75] B. H. COTTON, B. HILLS, and J. R. F. PENIDO, "Resection of the trachea for carcinoma; report of two cases.," *J. Thorac. Surg.*, vol. 24, no. 3, pp. 231–45, Sep. 1952.
[76] E. J. BEATTIE, B. BLADES, and J. M. KESHISHIAN, "Tracheal reconstruction.," *J. Thorac. Surg.*, vol. 32, no. 6, pp. 707–25; discussion, 725–7, Dec. 1956.
[77] H. Toomes, G. Mickisch, and I. Vogt-Moykopf, "Experiences with prosthetic reconstruction of the trachea and bifurcation.," *Thorax*, vol. 40, no. 1, pp. 32–7, Jan. 1985.
[78] O. T. CLAGETT, H. J. MOERSCH, and J. H. GRINDLAY, "Intrathoracic tracheal tumors: development of surgical technics for their removal.," *Ann. Surg.*, vol. 136, no. 3, pp. 520–32, Sep. 1952.
[79] S. EKESTROM and E. CARLENS, "Teflon prosthesis in tracheal defects in man.," *Acta Chir. Scand. Suppl.*, vol. Suppl 245, pp. 71–5, 1959.
[80] D. L. Wilhelm, "Regeneration of tracheal epithelium," *J. Pathol. Bacteriol.*, vol. 65, no. 2, pp. 543–550, Apr. 1953.
[81] B. J. Bailey and J. Kosoy, "Observations in the development of tracheal prostheses and tracheal transplantation.," *Laryngoscope*, vol. 80, no. 10, pp. 1553–1565, Oct. 1970.
[82] R. Guijarro Jorge, A. Sanchez-Palencia Ramos, A. Cueto Ladrón de Guevara, F. Marti Huedo, M. G. de Vega, and F. Paris Romeu, "Experimental study of a new porous tracheal prosthesis.," *Ann. Thorac. Surg.*, vol. 50, no. 2, pp. 281–7, Aug. 1990.
[83] C. Z. Wang *et al.*, "Morphologic changes in basal cells during repair of tracheal epithelium.," *Am. J. Pathol.*, vol. 141, no. 3, pp. 753–9, Sep. 1992.
[84] R. R. Shaw, A. Aslami, and W. R. Webb, "Circumferential Replacement of the Trachea in Experimental Animals," *Ann. Thorac. Surg.*, vol. 5, no. 1, pp. 30–35,

Jan. 1968.
[85] R. J. Nelson, L. Goldberg, R. A. White, E. Shors, and F. M. Hirose, “Neovascularity of a tracheal prosthesis/tissue complex.,” *J. Thorac. Cardiovasc. Surg.*, vol. 86, no. 6, pp. 800–8, Dec. 1983.
[86] J. Li, P. Xu, H. Chen, Z. Yang, and Q. Zhang, “Improvement of tracheal autograft survival with transplantation into the greater omentum.,” *Ann. Thorac. Surg.*, vol. 60, no. 6, pp. 1592–6, Dec. 1995.
[87] W. G. CAHAN, “Carcinoma of intrathoracic trachea: excision and repair by tantalum gauze-fascia lata graft; report of a case.,” *J. Thorac. Surg.*, vol. 23, no. 5, pp. 513–27, May 1952.
[88] M. Yamashita *et al.*, “Tracheal Regeneration After Partial Resection: A Tissue Engineering Approach,” *Laryngoscope*, vol. 117, no. 3, pp. 497–502, Mar. 2007.
[89] K. Kojima and C. A. Vacanti, “Tissue engineering in the trachea,” *Anat. Rec.*, vol. 297, no. 1, pp. 44–50, 2014.
[90] S. L. Bogan, G. Z. Teoh, and M. A. Birchall, “Tissue Engineered Airways: A Prospects Article,” *J. Cell. Biochem.*, vol. 117, no. 7, pp. 1497–1505, 2016.
[91] M. Zang, Q. Zhang, E. I. Chang, A. B. Mathur, and P. Yu, “Decellularized Tracheal Matrix Scaffold for Tracheal Tissue Engineering,” *Plast. Reconstr. Surg.*, vol. 132, no. 4, p. 549e–559e, Oct. 2013.
[92] A. A. Abouarab, H. H. Elsayed, H. Elkhayat, A. Mostafa, D. C. Cleveland, and A. El Nori, “Current Solutions for Long-Segment Tracheal Reconstruction,” *Ann. Thorac. Cardiovasc. Surg.*, vol. 23, no. 2, pp. 66–75, 2017.
[93] L. Zhao *et al.*, “Engineered Tissue-Stent Biocomposites as Tracheal Replacements.,” *Tissue Eng. Part A*, vol. 22, no. 17–18, pp. 1086–97, 2016.
[94] M. Komura *et al.*, “An animal model study for tissue-engineered trachea fabricated from a biodegradable scaffold using chondrocytes to augment repair of tracheal stenosis,” *J. Pediatr. Surg.*, vol. 43, pp. 2141–2146, 2008.
[95] Y. Nomoto, W. Okano, M. Imaizumi, A. Tani, M. Nomoto, and K. Omori, “Bioengineered prosthesis with allogenic heterotopic fibroblasts for cricoid regeneration,” *Laryngoscope*, vol. 122, no. 4, pp. 805–809, Apr. 2012.
[96] D. W. Wang, B. Fermor, J. M. Gimble, H. A. Awad, and F. Guilak, “Influence of oxygen on the proliferation and metabolism of adipose derived adult stem cells,” *J. Cell. Physiol.*, vol. 204, no. 1, pp. 184–191, Jul. 2005.
[97] T. H. Petersen *et al.*, “Tissue-Engineered Lungs for in Vivo Implantation,” *Science (80-.).*, vol. 329, no. 5991, pp. 538–541, Jul. 2010.
[98] L. Partington *et al.*, “Biochemical changes caused by decellularization may compromise mechanical integrity of tracheal scaffolds,” *Acta Biomater.*, vol. 9, no. 2, pp. 5251–5261, 2013.
[99] M. Benjamin and J. R. Ralphs, “Fibrocartilage in tendons and ligaments-an adaptation to compressive load.,” *J. Anat.*, vol. 193 (Pt 4, no. Pt 4, pp. 481–94, Nov. 1998.
[100] P. S. Wiggenhauser, J. T. Schantz, and N. Rotter, “Cartilage engineering in reconstructive surgery: auricular, nasal and tracheal engineering from a surgical perspective,” *Regen. Med.*, vol. 12, no. 3, pp. 303–314, 2017.
[101] J. G. Betts *et al.*, *Anatomy & physiology.*, 4rd ed. Houston, Texas, 2013.

[102] A. M. Bhosale and J. B. Richardson, “Articular cartilage: structure, injuries and review of management,” *Br. Med. Bull.*, vol. 87, no. 1, pp. 77–95, Aug. 2008.
[103] P. A. Brama, J. M. Tekoppele, R. A. Bank, D. Karssenberg, A. Barneveld, and P. R. van Weeren, “Topographical mapping of biochemical properties of articular cartilage in the equine fetlock joint.,” *Equine Vet. J.*, vol. 32, no. 1, pp. 19–26, Jan. 2000.
[104] C. Di Bella, A. Fosang, D. M. Donati, G. G. Wallace, and P. F. M. Choong, “3D Bioprinting of Cartilage for Orthopedic Surgeons: Reading between the Lines,” *Front. Surg.*, vol. 2, p. 39, Aug. 2015.
[105] T. J. Klein, J. Malda, R. L. Sah, and D. W. Hutmacher, “Tissue engineering of articular cartilage with biomimetic zones.,” *Tissue Eng. Part B. Rev.*, vol. 15, no. 2, pp. 143–57, 2009.
[106] H. Muir, P. Bullough, and A. Maroudas, “The distribution of collagen in human articular cartilage with some of its physiological implications.,” *J. Bone Joint Surg. Br.*, vol. 52, no. 3, pp. 554–63, Aug. 1970.
[107] V. C. Mow, A. Ratcliffe, and A. Robin Poole, “Cartilage and diarthrodial joints as paradigms for hierarchical materials and structures,” *Biomaterials*, vol. 13, no. 2, pp. 67–97, Jan. 1992.
[108] D. R. Eyre, M. A. Weis, and J.-J. Wu, “Articular cartilage collagen: an irreplaceable framework?,” *Eur. Cell. Mater.*, vol. 12, pp. 57–63, Nov. 2006.
[109] J. A. Buckwalter and H. J. Mankin, “Articular cartilage: tissue design and chondrocyte-matrix interactions.,” *Instr. Course Lect.*, vol. 47, pp. 477–86, 1998.
[110] A. K. Jeffery, G. W. Blunn, C. W. Archer, and G. Bentley, “Three dimensional collagen architecture in bovine articular cartilage.,” *J. Bone Joint Surg. Br.*, vol. 73, no. 5, pp. 795–801, Sep. 1991.
[111] D. R. Eyre, “The collagens of articular cartilage.,” *Semin. Arthritis Rheum.*, vol. 21, no. 3 Suppl 2, pp. 2–11, Dec. 1991.
[112] J. Heino, M. Huhtala, J. Käpylä, and M. S. Johnson, “Evolution of collagen-based adhesion systems,” *Int. J. Biochem. Cell Biol.*, vol. 41, no. 2, pp. 341–348, Feb. 2009.
[113] J. E. Wagenseil and R. P. Mecham, “Vascular extracellular matrix and arterial mechanics.,” *Physiol. Rev.*, vol. 89, no. 3, pp. 957–89, Jul. 2009.
[114] T. E. Takala and P. Virtanen, “Biochemical composition of muscle extracellular matrix: the effect of loading.,” *Scand. J. Med. Sci. Sports*, vol. 10, no. 6, pp. 321–5, Dec. 2000.
[115] H. Jarvelainen, A. Sainio, M. Koulu, T. N. Wight, and R. Penttinen, “Extracellular Matrix Molecules: Potential Targets in Pharmacotherapy,” *Pharmacol. Rev.*, vol. 61, no. 2, pp. 198–223, Jun. 2009.
[116] K. Gelse, E. Pöschl, and T. Aigner, “Collagens-structure, function, and biosynthesis.,” *Adv. Drug Deliv. Rev.*, vol. 55, no. 12, pp. 1531–46, Nov. 2003.
[117] M. T. Bayliss, M. Venn, A. Maroudas, and S. Y. Ali, “Structure of proteoglycans from different layers of human articular cartilage.,” *Biochem. J.*, vol. 209, no. 2, p. 387, 1983.
[118] J. Thyberg, S. Lohmander, and D. Heinegård, “Proteoglycans of hyaline cartilage: Electron-microscopic studies on isolated molecules.,” *Biochem. J.*,

vol. 151, no. 1, pp. 157–66, Oct. 1975.
[119] P. Önnerfjord, A. Khabut, F. P. Reinholt, O. Svensson, and D. Heinegård, "Quantitative Proteomic Analysis of Eight Cartilaginous Tissues Reveals Characteristic Differences as well as Similarities between Subgroups * □ S," *Publ. JBC Pap. Press*, 2012.
[120] L. Wachsmuth, S. Söder, Z. Fan, F. Finger, and T. Aigner, "Immunolocalization of matrix proteins in different human cartilage subtypes.," *Histol. Histopathol.*, vol. 21, no. 5, pp. 477–85, 2006.
[121] G. Chamberlain, J. Fox, B. Ashton, and J. Middleton, "Concise review: mesenchymal stem cells: their phenotype, differentiation capacity, immunological features, and potential for homing.," *Stem Cells*, vol. 25, no. 11, pp. 2739–49, 2007.
[122] R. R. Mercer, M. L. Russell, V. L. Roggli, and J. D. Crapo, "Cell number and distribution in human and rat airways.," *Am. J. Respir. Cell Mol. Biol.*, vol. 10, no. 6, pp. 613–624, Jun. 1994.
[123] D. N. Kotton and E. E. Morrisey, "Lung regeneration: mechanisms, applications and emerging stem cell populations," *Nat Med*, vol. 20, no. 8, pp. 822–832, 2014.
[124] A. L. Herard, J. M. Zahm, D. Pierrot, J. Hinnrasky, C. Fuchey, and E. Puchelle, "Epithelial barrier integrity during in vitro wound repair of the airway epithelium.," *Am. J. Respir. Cell Mol. Biol.*, vol. 15, no. 5, pp. 624–632, Nov. 1996.
[125] E. L. Rawlins and B. L. M. Hogan, "Epithelial stem cells of the lung: privileged few or opportunities for many?," *Development*, vol. 133, no. 13, pp. 2455–2465, Jul. 2006.
[126] J. R. Rock *et al.*, "Basal cells as stem cells of the mouse trachea and human airway epithelium," *Proc Natl Acad Sci U S A*, vol. 106, no. 31, pp. 12771–12775, 2009.
[127] M. Ghosh *et al.*, "Context-dependent differentiation of multipotential keratin 14-expressing tracheal basal cells.," *Am. J. Respir. Cell Mol. Biol.*, vol. 45, no. 2, pp. 403–10, Aug. 2011.
[128] E. L. Rawlins *et al.*, "The Role of Scgb1a1+ Clara Cells in the Long-Term Maintenance and Repair of Lung Airway, but Not Alveolar, Epithelium," *Cell Stem Cell*, vol. 4, no. 6, pp. 525–534, Jun. 2009.
[129] A. E. Hegab *et al.*, "Novel Stem/Progenitor Cell Population from Murine Tracheal Submucosal Gland Ducts with Multipotent Regenerative Potential," *Stem Cells*, vol. 29, no. 8, pp. 1283–1293, Aug. 2011.
[130] X. He, W. Fu, and J. Zheng, "Cell sources for trachea tissue engineering: past, present and future.," *Regen. Med.*, vol. 7, no. 6, pp. 851–63, 2012.
[131] G. M. Roomans, "Tissue engineering and the use of stem/progenitor cells for airway epithelium repair.," *Eur. Cell. Mater.*, vol. 19, pp. 284–99, Jun. 2010.
[132] S. K. Ramasamy *et al.*, "Fgf10 dosage is critical for the amplification of epithelial cell progenitors and for the formation of multiple mesenchymal lineages during lung development," *Dev. Biol.*, vol. 307, no. 2, pp. 237–247, Jul. 2007.
[133] D. Warburton, L. Perin, R. Defilippo, S. Bellusci, W. Shi, and B. Driscoll,

"Stem/progenitor cells in lung development, injury repair, and regeneration.," *Proc. Am. Thorac. Soc.*, vol. 5, no. 6, pp. 703–6, Aug. 2008.
[134] M. Derks, T. Sturm, A. Haverich, and A. Hilfiker, "Isolation and chondrogenic differentiation of porcine perichondrial progenitor cells for the purpose of cartilage tissue engineering," *Cells Tissues Organs*, vol. 198, no. 3, pp. 179–189, 2013.
[135] M. Dominici *et al.*, "Minimal criteria for defining multipotent mesenchymal stromal cells. The International Society for Cellular Therapy position statement," *Cytotherapy*, vol. 8, no. 4, pp. 315–317, 2006.
[136] C. T. Jayasuriya and Q. Chen, "Potential benefits and limitations of utilizing chondroprogenitors in cell-based cartilage therapy.," *Connect. Tissue Res.*, vol. 56, no. 4, pp. 265–71, 2015.
[137] G. P. Dowthwaite *et al.*, "The surface of articular cartilage contains a progenitor cell population," *J. Cell Sci.*, vol. 117, no. 6, 2004.
[138] I. A. Otto, R. Levato, W. R. Webb, I. M. Khan, C. C. Breugem, and J. Malda, "Progenitor cells in auricular cartilage demonstrate cartilage-forming capacity in 3D hydrogel culture," *Eur. Cell. Mater.*, vol. 35, pp. 132–150, Feb. 2018.
[139] J. M. Fishman *et al.*, "Airway tissue engineering: an update," *Expert Opin. Biol. Ther.*, vol. 14, no. 10, pp. 1477–1491, 2014.
[140] J. M. Fishman *et al.*, "Skeletal Muscle Tissue Engineering: Which Cell to Use?," *Tissue Eng. Part B Rev.*, vol. 19, no. 6, pp. 503–515, Dec. 2013.
[141] B. N. Brown, J. E. Valentin, A. M. Stewart-Akers, G. P. McCabe, and S. F. Badylak, "Macrophage phenotype and remodeling outcomes in response to biologic scaffolds with and without a cellular component," *Biomaterials*, vol. 30, no. 8, pp. 1482–1491, Mar. 2009.
[142] J. E. Valentin, N. J. Turner, T. W. Gilbert, and S. F. Badylak, "Functional skeletal muscle formation with a biologic scaffold," *Biomaterials*, vol. 31, no. 29, pp. 7475–7484, Oct. 2010.
[143] B. G. Galvez *et al.*, "Complete repair of dystrophic skeletal muscle by mesoangioblasts with enhanced migration ability," *J. Cell Biol.*, vol. 174, no. 2, pp. 231–243, Jul. 2006.
[144] M. Sampaolesi *et al.*, "Mesoangioblast stem cells ameliorate muscle function in dystrophic dogs," *Nature*, vol. 444, no. 7119, pp. 574–579, Nov. 2006.
[145] S. Kanemaru *et al.*, "Functional regeneration of laryngeal muscle using bone marrow-derived stromal cells," *Laryngoscope*, vol. 123, no. 11, pp. 2728–2734, Nov. 2013.
[146] F. S. Tedesco *et al.*, "Transplantation of Genetically Corrected Human iPSC-Derived Progenitors in Mice with Limb-Girdle Muscular Dystrophy," *Sci. Transl. Med.*, vol. 4, no. 140, p. 140ra89-140ra89, Jun. 2012.
[147] A. Zampetaki, J. P. Kirton, and Q. Xu, "Vascular repair by endothelial progenitor cells," *Cardiovasc. Res.*, vol. 78, no. 3, pp. 413–421, Jan. 2008.
[148] X. Luo *et al.*, "Long-term functional reconstruction of segmental tracheal defect by pedicled tissue-engineered trachea in rabbits," *Biomaterials*, vol. 34, no. 13, pp. 3336–3344, Apr. 2013.
[149] T. Walles *et al.*, "Experimental generation of a tissue-engineered functional

and vascularized trachea," *J. Thorac. Cardiovasc. Surg.*, vol. 128, no. 6, pp. 900–906, Dec. 2004.
[150] Q. Tan *et al.*, "Accelerated angiogenesis by continuous medium flow with vascular endothelial growth factor inside tissue-engineered trachea," *Eur. J. Cardio-Thoracic Surg.*, vol. 31, no. 5, pp. 806–811, May 2007.
[151] S. Baiguera *et al.*, "Tissue engineered human tracheas for in vivo implantation," *Biomaterials*, vol. 31, no. 34, pp. 8931–8938, 2010.
[152] D. M. Bell *et al.*, "SOX9 directly regulates the type-ll collagen gene," *Nat. Genet.*, vol. 16, no. 2, pp. 174–178, Jun. 1997.
[153] V. Lefebvre, P. Li, and B. de Crombrugghe, "A new long form of Sox5 (L-Sox5), Sox6 and Sox9 are coexpressed in chondrogenesis and cooperatively activate the type II collagen gene.," *EMBO J.*, vol. 17, no. 19, p. 5718, 1998.
[154] A. M. DeLise, L. Fischer, and R. S. Tuan, "Cellular interactions and signaling in cartilage development," *Osteoarthr. Cartil.*, vol. 8, no. 5, pp. 309–334, Sep. 2000.
[155] B. K. Hall and T. Miyake, "Divide, accumulate, differentiate: cell condensation in skeletal development revisited.," *Int. J. Dev. Biol.*, vol. 39, no. 6, pp. 881–93, Dec. 1995.
[156] M. Demoor *et al.*, "Cartilage tissue engineering: Molecular control of chondrocyte differentiation for proper cartilage matrix reconstruction," *Biochim. Biophys. Acta - Gen. Subj.*, vol. 1840, no. 8, pp. 2414–2440, Aug. 2014.
[157] C. Vinatier, D. Mrugala, C. Jorgensen, J. Guicheux, and D. Noël, "Cartilage engineering: a crucial combination of cells, biomaterials and biofactors," *Trends Biotechnol.*, vol. 27, no. 5, pp. 307–314, 2009.
[158] H. Kwon, N. K. Paschos, J. C. Hu, and K. Athanasiou, "Articular cartilage tissue engineering: The role of signaling molecules," *Cell. Mol. Life Sci.*, vol. 73, no. 6, pp. 1173–1194, 2016.
[159] R. A. Somoza, J. F. Welter, D. Correa, and A. I. Caplan, "Chondrogenic differentiation of Mesenchymal Stem Cells: challenges and unfulfilled expectations.," *Tissue Eng. Part B. Rev.*, vol. 20, no. 216, pp. 1–50, 2014.
[160] S. Sart, S. N. Agathos, and Y. Li, "Engineering stem cell fate with biochemical and biomechanical properties of microcarriers," *Biotechnol. Prog.*, vol. 29, no. 6, pp. 1354–1366, 2013.
[161] W.-H. Chen, M.-T. Lai, A. T. H. Wu, C.-C. Wu, J. G. Gelovani, and C.-T. Lin, "In Vitro Stage-Specific Chondrogenesis of Mesenchymal Stem Cells Committed to Chondrocytes," *ARTHRITIS Rheum.*, vol. 60, no. 2, pp. 450–459, 2009.
[162] E. J. Kubosch, E. Heidt, A. Bernstein, K. Böttiger, and H. Schmal, "The trans-well coculture of human synovial mesenchymal stem cells with chondrocytes leads to self-organization, chondrogenic differentiation, and secretion of TGFβ.," *Stem Cell Res. Ther.*, vol. 7, no. 1, p. 64, 2016.
[163] X. Liu *et al.*, "In vivo ectopic chondrogenesis of BMSCs directed by mature chondrocytes," *Biomaterials*, vol. 31, no. 36, pp. 9406–9414, Dec. 2010.
[164] J. Fischer, A. Dickhut, M. Rickert, and W. Richter, "Human articular chondrocytes secrete parathyroid hormone-related protein and inhibit hypertrophy of mesenchymal stem cells in coculture during chondrogenesis," *Arthritis Rheum.*, vol. 62, no. 9, pp. 2696–2706, Sep. 2010.

[165] J. A. Panadero, S. Lanceros-Mendez, and J. L. G. Ribelles, “Differentiation of mesenchymal stem cells for cartilage tissue engineering: Individual and synergetic effects of three-dimensional environment and mechanical loading,” *Acta Biomater.*, vol. 33, pp. 1–12, 2016.
[166] D. J. Kelly and C. R. Jacobs, “The role of mechanical signals in regulating chondrogenesis and osteogenesis of mesenchymal stem cells,” *Birth Defects Res. Part C - Embryo Today Rev.*, vol. 90, no. 1, pp. 75–85, Mar. 2010.
[167] G. Vunjak-Novakovic *et al.*, “Bioreactor cultivation conditions modulate the composition and mechanical properties of tissue-engineered cartilage,” *J. Orthop. Res.*, vol. 17, no. 1, pp. 130–138, Jan. 1999.
[168] A. Bader and P. Macchiarini, “Moving towards in situ tracheal regeneration: the bionic tissue engineered transplantation approach.,” *J. Cell. Mol. Med.*, vol. 14, no. 7, pp. 1877–89, Jul. 2010.
[169] Y. J. Li *et al.*, “Oscillatory fluid flow affects human marrow stromal cell proliferation and differentiation,” *J. Orthop. Res.*, vol. 22, no. 6, pp. 1283–1289, Nov. 2004.
[170] R. L. Mauck, B. A. Byers, X. Yuan, and R. S. Tuan, “Regulation of Cartilaginous ECM Gene Transcription by Chondrocytes and MSCs in 3D Culture in Response to Dynamic Loading,” *Biomech. Model. Mechanobiol.*, vol. 6, no. 1–2, pp. 113–125, Jan. 2007.
[171] C.-H. Lin, S. Hsu, C.-E. Huang, W.-T. Cheng, and J.-M. Su, “A scaffold-bioreactor system for a tissue-engineered trachea,” *Biomaterials*, vol. 30, no. 25, pp. 4117–4126, Sep. 2009.
[172] A.-M. Kajbafzadeh *et al.*, “In-vivo trachea regeneration: fabrication of a tissue-engineered trachea in nude mice using the body as a natural bioreactor,” *Surg. Today*, vol. 45, no. 8, pp. 1040–1048, Aug. 2015.
[173] H. Betre, S. R. Ong, F. Guilak, A. Chilkoti, B. Fermor, and L. A. Setton, “Chondrocytic differentiation of human adipose-derived adult stem cells in elastin-like polypeptide,” *Biomaterials*, vol. 27, no. 1, pp. 91–99, Jan. 2006.
[174] M. C. Ronzière, E. Perrier, F. Mallein-Gerin, and A.-M. Freyria, “Chondrogenic potential of bone marrow- and adipose tissue-derived adult human mesenchymal stem cells,” *Biomed. Mater. Eng.*, vol. 20, no. 3–4, pp. 145–158, 2010.
[175] M. de Caestecker, “The transforming growth factor-β superfamily of receptors,” *Cytokine Growth Factor Rev.*, vol. 15, no. 1, pp. 1–11, 2004.
[176] T. Furumatsu, M. Tsuda, N. Taniguchi, Y. Tajima, and H. Asahara, “Smad3 Induces Chondrogenesis through the Activation of SOX9 via CREB-binding Protein/p300 Recruitment,” *J. Biol. Chem.*, vol. 280, no. 9, pp. 8343–8350, Mar. 2005.
[177] T. Furumatsu, T. Ozaki, and H. Asahara, “Smad3 activates the Sox9-dependent transcription on chromatin,” *Int. J. Biochem. Cell Biol.*, vol. 41, no. 5, pp. 1198–1204, May 2009.
[178] H. Akiyama, M.-C. Chaboissier, J. F. Martin, A. Schedl, and B. de Crombrugghe, “The transcription factor Sox9 has essential roles in successive steps of the chondrocyte differentiation pathway and is required for expression of Sox5 and Sox6,” *Genes Dev.*, vol. 16, no. 21, pp. 2813–2828, Nov. 2002.

[179] V. Y. L. Leung *et al.*, "SOX9 Governs Differentiation Stage-Specific Gene Expression in Growth Plate Chondrocytes via Direct Concomitant Transactivation and Repression," *PLoS Genet.*, vol. 7, no. 11, p. e1002356, Nov. 2011.
[180] G. Zhou *et al.*, "Dominance of SOX9 function over RUNX2 during skeletogenesis.," *Proc. Natl. Acad. Sci. U. S. A.*, vol. 103, no. 50, pp. 19004–9, Dec. 2006.
[181] F. L. J. Cals, C. A. Hellingman, W. Koevoet, R. J. Baatenburg de Jong, and G. J. V. M. van Osch, "Effects of transforming growth factor-β subtypes on in vitro cartilage production and mineralization of human bone marrow stromal-derived mesenchymal stem cells," *J. Tissue Eng. Regen. Med.*, vol. 6, no. 1, pp. 68–76, Jan. 2012.
[182] M. B. Mueller *et al.*, "Hypertrophy in mesenchymal stem cell chondrogenesis: effect of TGF-beta isoforms and chondrogenic conditioning.," *Cells. Tissues. Organs*, vol. 192, no. 3, pp. 158–66, 2010.
[183] A. W. James, Y. Xu, J. K. Lee, R. Wang, and M. T. Longaker, "Differential Effects of TGF-β1 and TGF-β3 on Chondrogenesis in Posterofrontal Cranial Suture–Derived Mesenchymal Cells In Vitro," *Plast. Reconstr. Surg.*, vol. 123, no. 1, pp. 31–43, Jan. 2009.
[184] R. Pogue and K. Lyons, "BMP Signaling in the Cartilage Growth Plate," in *Current topics in developmental biology*, vol. 76, 2006, pp. 1–48.
[185] B. K. Zehentner, C. Dony, and H. Burtscher, "The Transcription Factor Sox9 Is Involved in BMP-2 Signaling," *J. Bone Miner. Res.*, vol. 14, no. 10, pp. 1734–1741, Oct. 1999.
[186] J. Liao *et al.*, "Sox9 Potentiates BMP2-Induced Chondrogenic Differentiation and Inhibits BMP2-Induced Osteogenic Differentiation," *PLoS One*, vol. 9, no. 2, p. e89025, Feb. 2014.
[187] R. Fernández-Lloris *et al.*, "Induction of the Sry-Related Factor SOX6 Contributes to Bone Morphogenetic Protein-2-Induced Chondroblastic Differentiation of C3H10T1/2 Cells," *Mol. Endocrinol.*, vol. 17, no. 7, pp. 1332–1343, Jul. 2003.
[188] N. D. Miljkovic, G. M. Cooper, and K. G. Marra, "Chondrogenesis, bone morphogenetic protein-4 and mesenchymal stem cells," *Osteoarthr. Cartil.*, vol. 16, no. 10, pp. 1121–1130, 2008.
[189] Ľ. Danišovič, I. Varga, and Š. Polák, "Growth factors and chondrogenic differentiation of mesenchymal stem cells," *Tissue Cell*, vol. 44, no. 2, pp. 69–73, 2012.
[190] N. Tsumaki *et al.*, "Role of CDMP-1 in skeletal morphogenesis: promotion of mesenchymal cell recruitment and chondrocyte differentiation.," *J. Cell Biol.*, vol. 144, no. 1, pp. 161–73, Jan. 1999.
[191] A. Cheng, A. R. Gustafson, C. E. Schaner Tooley, and M. Zhang, "BMP-9 dependent pathways required for the chondrogenic differentiation of pluripotent stem cells," *Differentiation*, vol. 92, no. 5, pp. 298–305, 2016.
[192] T. M. Temu, K.-Y. Wu, P. A. Gruppuso, and C. Phornphutkul, "The mechanism of ascorbic acid-induced differentiation of ATDC5 chondrogenic cells," *Am. J. Physiol. Metab.*, vol. 299, no. 2, pp. E325–E334, Aug. 2010.

[193] N. Shintani and E. B. Hunziker, “Differential effects of dexamethasone on the chondrogenesis of mesenchymal stromal cells: Influence of microenvironment, tissue origin and growth factor,” *Eur. Cells Mater.*, vol. 22, pp. 302–320, 2011.
[194] W. Van, B. Robertson, and B. Schwartz, “ASCORBIC ACID AND THE FORMATION OF COLLAGEN.”
[195] W. V ROBERTSON, “The biochemical role of ascorbic acid in connective tissue.,” *Ann. N. Y. Acad. Sci.*, vol. 92, pp. 159–67, Apr. 1961.
[196] S. R. Sharma, R. Poddar, P. Sen, and J. T. Andrews, “Effect of vitamin C on collagen biosynthesis and degree of birefringence in polarization sensitive optical coherence tomography (PS-OCT),” *African J. Biotechnol.*, vol. 7, no. 12, pp. 2049–2054, 2008.
[197] S. Murad, D. Grove, K. A. Lindberg, G. Reynolds, A. Sivarajah, and S. R. Pinnell, “Regulation of collagen synthesis by ascorbic acid.,” *Proc. Natl. Acad. Sci. U. S. A.*, vol. 78, no. 5, pp. 2879–82, May 1981.
[198] H. Mistry *et al.*, “Autologous chondrocyte implantation in the knee: systematic review and economic evaluation,” *Health Technol. Assess. (Rockv).*, vol. 21, no. 6, pp. 1–294, Feb. 2017.
[199] C. M. Revell and K. A. Athanasiou, “Success Rates and Immunologic Responses of Autogenic, Allogenic, and Xenogenic Treatments to Repair Articular Cartilage Defects,” *Tissue Eng. Part B Rev.*, vol. 15, no. 1, pp. 1–15, Mar. 2009.
[200] N. Mahmoudifar and P. M. Doran, “Chondrogenesis and cartilage tissue engineering: The longer road to technology development,” *Trends Biotechnol.*, vol. 30, no. 3, pp. 166–176, 2012.
[201] E. Basad, B. Ishaque, G. Bachmann, H. Stürz, and J. Steinmeyer, “Matrix-induced autologous chondrocyte implantation versus microfracture in the treatment of cartilage defects of the knee: a 2-year randomised study,” *Knee Surgery, Sport. Traumatol. Arthrosc.*, vol. 18, no. 4, pp. 519–527, Apr. 2010.
[202] W. Wu, X. Cheng, Y. Zhao, F. Chen, X. Feng, and T. Mao, “Tissue Engineering of Trachea-like Cartilage Grafts by Using Chondrocyte Macroaggregate: Experimental Study in Rabbits,” *Artif. Organs*, vol. 31, no. 11, pp. 826–834, Nov. 2007.
[203] G. Tani, N. Usui, M. Kamiyama, T. Oue, and M. Fukuzawa, “In vitro construction of scaffold-free cylindrical cartilage using cell sheet-based tissue engineering,” *Pediatr. Surg. Int.*, vol. 26, no. 2, pp. 179–185, Feb. 2010.
[204] N. Isogai *et al.*, “Comparison of different chondrocytes for use in tissue engineering of cartilage model structures.,” *Tissue Eng.*, vol. 12, no. 4, pp. 691–703, 2006.
[205] J. Kramer, C. Hegert, K. Guan, A. M. Wobus, P. K. Müller, and J. Rohwedel, “Embryonic stem cell-derived chondrogenic differentiation in vitro: activation by BMP-2 and BMP-4,” *Mech. Dev.*, vol. 92, no. 2, pp. 193–205, Apr. 2000.
[206] L. Wu *et al.*, “Human Developmental Chondrogenesis as a Basis for Engineering Chondrocytes from Pluripotent Stem Cells,” *Stem Cell Reports*, vol. 1, no. 6, pp. 575–589, Dec. 2013.
[207] P. Macchiarini *et al.*, “Clinical transplantation of a tissue-engineered airway,”

Lancet, vol. 372, no. 9655, pp. 2023–2030, 2008.
[208] I.-S. Yoon *et al.*, "Proliferation and chondrogenic differentiation of human adipose-derived mesenchymal stem cells in porous hyaluronic acid scaffold," *J. Biosci. Bioeng.*, vol. 112, no. 4, pp. 402–408, Oct. 2011.
[209] Y. S. Choi *et al.*, "Chondrogenic differentiation of human umbilical cord blood-derived multilineage progenitor cells in atelocollagen," *Cytotherapy*, vol. 10, no. 2, pp. 165–173, 2008.
[210] C. Cournil-Henrionnet *et al.*, "Phenotypic analysis of cell surface markers and gene expression of human mesenchymal stem cells and chondrocytes during monolayer expansion.," *Biorheology*, vol. 45, no. 3–4, pp. 513–26, 2008.
[211] M. Schnabel *et al.*, "Dedifferentiation-associated changes in morphology and gene expression in primary human articular chondrocytes in cell culture.," *Osteoarthr. Cartil.*, vol. 10, no. 1, pp. 62–70, Jan. 2002.
[212] C. Chung and J. A. Burdick, "Engineering cartilage tissue.," *Adv. Drug Deliv. Rev.*, vol. 60, no. 2, pp. 243–62, Jan. 2008.
[213] M. F. Pittenger *et al.*, "Multilineage Potential of Adult Human Mesenchymal Stem Cells," *Science (80-.).*, vol. 284, no. 5411, 1999.
[214] B. Johnstone *et al.*, "Tissue engineering for articular cartilage repair-the state of the art.," *Eur. Cell. Mater.*, vol. 25, pp. 248–67, May 2013.
[215] L. Zhang, P. Su, C. Xu, J. Yang, W. Yu, and D. Huang, "Chondrogenic differentiation of human mesenchymal stem cells: A comparison between micromass and pellet culture systems," *Biotechnol. Lett.*, vol. 32, no. 9, pp. 1339–1346, 2010.
[216] A. Nazempour and B. J. Van Wie, "Chondrocytes, Mesenchymal Stem Cells, and Their Combination in Articular Cartilage Regenerative Medicine," *Ann. Biomed. Eng.*, vol. 44, no. 5, pp. 1325–1354, 2016.
[217] M. Mimeault and S. K. Batra, "Recent progress on tissue-resident adult stem cell biology and their therapeutic implications," *Stem Cell Rev.*, vol. 4, no. 1, pp. 27–49, 2008.
[218] A. J. Hayes, S. MacPherson, H. Morrison, G. Dowthwaite, and C. W. Archer, "The development of articular cartilage: evidence for an appositional growth mechanism.," *Anat. Embryol. (Berl).*, vol. 203, no. 6, pp. 469–79, Jun. 2001.
[219] G. P. Dowthwaite *et al.*, "The surface of articular cartilage contains a progenitor cell population," vol. 2, no. 35 mm, 2004.
[220] R. Williams *et al.*, "Identification and clonal characterisation of a progenitor cell sub-population in normal human articular cartilage," *PLoS One*, vol. 5, no. 10, 2010.
[221] C. R. Fellows *et al.*, "Characterisation of a divergent progenitor cell sub-populations in human osteoarthritic cartilage: the role of telomere erosion and replicative senescence.," *Sci. Rep.*, vol. 7, p. 41421, Feb. 2017.
[222] I. M. K. P. D, J. C. B. P. D, S. G. P. D, and C. W. A. P. D, "Clonal chondroprogenitors maintain telomerase activity and Sox9 expression during extended monolayer culture and retain chondrogenic potential," *Osteoarthr. Cartil.*, vol. 17, no. 4, pp. 518–528, 2009.
[223] H. E. McCarthy, J. J. Bara, K. Brakspear, S. K. Singhrao, and C. W. Archer, "The comparison of equine articular cartilage progenitor cells and bone marrow-

derived stromal cells as potential cell sources for cartilage repair in the horse," *Vet. J.*, vol. 192, no. 3, pp. 345–351, Jun. 2012.
[224] S.-H. Kim, J. Turnbull, and S. Guimond, "Extracellular matrix and cell signalling: the dynamic cooperation of integrin, proteoglycan and growth factor receptor," *J. Endocrinol.*, vol. 209, no. 2, pp. 139–151, May 2011.
[225] Q. Chen, M. Jin, F. Yang, J. Zhu, Q. Xiao, and L. Zhang, "Matrix metalloproteinases: inflammatory regulators of cell behaviors in vascular formation and remodeling.," *Mediators Inflamm.*, vol. 2013, p. 928315, Jun. 2013.
[226] P. Lu, V. M. Weaver, and Z. Werb, "The extracellular matrix: a dynamic niche in cancer progression.," *J. Cell Biol.*, vol. 196, no. 4, pp. 395–406, Feb. 2012.
[227] F. Gattazzo, A. Urciuolo, and P. Bonaldo, "Extracellular matrix: A dynamic microenvironment for stem cell niche," *Biochim. Biophys. Acta - Gen. Subj.*, vol. 1840, no. 8, pp. 2506–2519, 2014.
[228] L. Li and H. Clevers, "Coexistence of Quiescent and Active Adult Stem Cells in Mammals," *Science (80-.).*, vol. 327, no. 5965, pp. 542–545, Jan. 2010.
[229] T. H. Cheung and T. A. Rando, "Molecular regulation of stem cell quiescence," *Nat. Rev. Mol. Cell Biol.*, vol. 14, no. 6, pp. 329–340, Jun. 2013.
[230] E. Fuchs, T. Tumbar, and G. Guasch, "Socializing with the neighbors: stem cells and their niche.," *Cell*, vol. 116, no. 6, pp. 769–78, Mar. 2004.
[231] S. J. Morrison and A. C. Spradling, "Stem Cells and Niches: Mechanisms That Promote Stem Cell Maintenance throughout Life," *Cell*, vol. 132, no. 4, pp. 598–611, Feb. 2008.
[232] A. D. Lander *et al.*, "What does the concept of the stem cell niche really mean today?," *BMC Biol.*, vol. 10, no. 1, p. 19, Mar. 2012.
[233] A. J. Wagers, "The Stem Cell Niche in Regenerative Medicine," *Cell Stem Cell*, vol. 10, no. 4, pp. 362–369, Apr. 2012.
[234] D. L. Jones and A. J. Wagers, "No place like home: anatomy and function of the stem cell niche," *Nat. Rev. Mol. Cell Biol.*, vol. 9, no. 1, pp. 11–21, Jan. 2008.
[235] B. Johnstone, T. M. Hering, A. I. Caplan, V. M. Goldberg, and J. U. Yoo, "In VitroChondrogenesis of Bone Marrow-Derived Mesenchymal Progenitor Cells," *Exp. Cell Res.*, vol. 238, no. 1, pp. 265–272, Jan. 1998.
[236] M. B. Mueller and R. S. Tuan, "Functional characterization of hypertrophy in chondrogenesis of human mesenchymal stem cells," *Arthritis Rheum.*, vol. 58, no. 5, pp. 1377–1388, May 2008.
[237] A. D. Murdoch, L. M. Grady, M. P. Ablett, T. Katopodi, R. S. Meadows, and T. E. Hardingham, "Chondrogenic differentiation of human bone marrow stem cells in transwell cultures: generation of scaffold-free cartilage.," *Stem Cells*, vol. 25, no. 11, pp. 2786–96, 2007.
[238] R. Stoop, "Smart biomaterials for tissue engineering of cartilage," *Injury*, vol. 39, no. 1 SUPPL., pp. 77–87, 2008.
[239] A. J. Putnam and D. J. Mooney, "Tissue engineering using synthetic extracellular matrices," *Nat. Med.*, vol. 2, no. 7, pp. 824–826, Jul. 1996.
[240] T. B. F. Woodfield, C. A. Van Blitterswijk, J. De Wijn, T. J. Sims, A. P. Hollander, and J. Riesle, "Polymer Scaffolds Fabricated with Pore-Size Gradients as a Model for Studying the Zonal Organization within Tissue-Engineered

Cartilage Constructs," *Tissue Eng.*, vol. 11, no. 9–10, pp. 1297–1311, Sep. 2005.
[241] F. T. Moutos, "Biomimetic Composite Scaffolds for the Functional Tissue Engineering of Articular Cartilage," 2009.
[242] M. M. C. G. Silva *et al.*, "The effect of anisotropic architecture on cell and tissue infiltration into tissue engineering scaffolds," *Biomaterials*, vol. 27, no. 35, pp. 5909–5917, Dec. 2006.
[243] R. El-Ayoubi, C. DeGrandpré, R. DiRaddo, A.-M. Yousefi, and P. Lavigne, "Design and dynamic culture of 3D-scaffolds for cartilage tissue engineering.," *J. Biomater. Appl.*, vol. 25, no. 5, pp. 429–444, 2011.
[244] S. Grad, L. Zhou, S. Gogolewski, and M. Alini, "Chondrocytes seeded onto poly (L/DL-lactide) 80%/20% porous scaffolds: A biochemical evaluation," *J. Biomed. Mater. Res.*, vol. 66A, no. 3, pp. 571–579, Sep. 2003.
[245] V. Lefebvre, C. Peeters-Joris, and G. Vaes, "Production of collagens, collagenase and collagenase inhibitor during the dedifferentiation of articular chondrocytes by serial subcultures.," *Biochim. Biophys. Acta*, vol. 1051, no. 3, pp. 266–75, Mar. 1990.
[246] S. M. Lien, L. Y. Ko, and T. J. Huang, "Effect of pore size on ECM secretion and cell growth in gelatin scaffold for articular cartilage tissue engineering," *Acta Biomater.*, vol. 5, no. 2, pp. 670–679, 2009.
[247] S. L. Edwards, W. Mitchell, J. B. Matthews, E. Ingham, and S. J. Russell, "DESIGN OF NONWOVEN SCAFFOLD STRUCTURES FOR TISSUE ENGINEERING OF THE ANTERIOR CRUCIATE LIGAMENT," 2004.
[248] D. W. Hutmacher, "Scaffolds in tissue engineering bone and cartilage.," *Biomaterials*, vol. 21, no. 24, pp. 2529–43, Dec. 2000.
[249] T. B. F. Woodfield, J. Malda, J. de Wijn, F. Péters, J. Riesle, and C. A. van Blitterswijk, "Design of porous scaffolds for cartilage tissue engineering using a three-dimensional fiber-deposition technique," *Biomaterials*, vol. 25, no. 18, pp. 4149–4161, Aug. 2004.
[250] W.-J. Li, C. T. Laurencin, E. J. Caterson, R. S. Tuan, and F. K. Ko, "Electrospun nanofibrous structure: a novel scaffold for tissue engineering.," *J. Biomed. Mater. Res.*, vol. 60, no. 4, pp. 613–21, Jun. 2002.
[251] N. L. Nerurkar, S. Sen, B. M. Baker, D. M. Elliott, and R. L. Mauck, "Dynamic culture enhances stem cell infiltration and modulates extracellular matrix production on aligned electrospun nanofibrous scaffolds," *Acta Biomater.*, vol. 7, no. 2, pp. 485–491, Feb. 2011.
[252] W.-J. Li, R. L. Mauck, J. A. Cooper, X. Yuan, and R. S. Tuan, "Engineering controllable anisotropy in electrospun biodegradable nanofibrous scaffolds for musculoskeletal tissue engineering," *J. Biomech.*, vol. 40, no. 8, pp. 1686–1693, Jan. 2007.
[253] R. Landers and R. Mülhaupt, "Desktop manufacturing of complex objects, prototypes and biomedical scaffolds by means of computer-assisted design combined with computer-guided 3D plotting of polymers and reactive oligomers," *Macromol. Mater. Eng.*, vol. 282, no. 1, pp. 17–21, Oct. 2000.
[254] R. Landers, A. Pfister, U. Hübner, H. John, R. Schmelzeisen, and R. Mülhaupt, "Fabrication of soft tissue engineering scaffolds by means of rapid

prototyping techniques," *J. Mater. Sci.*, vol. 37, no. 15, pp. 3107–3116, 2002.
[255] W. Schuurman, V. Khristov, M. W. Pot, P. R. van Weeren, W. J. a Dhert, and J. Malda, "Bioprinting of hybrid tissue constructs with tailorable mechanical properties.," *Biofabrication*, vol. 3, no. 2, p. 021001, 2011.
[256] A. Panwar and L. P. Tan, "Current status of bioinks for micro-extrusion-based 3D bioprinting," *Molecules*, vol. 21, no. 6, 2016.
[257] J. Malda and C. G. Frondoza, "Microcarriers in the engineering of cartilage and bone," *Trends Biotechnol.*, vol. 24, no. 7, pp. 299–304, 2006.
[258] L. E. Freed, G. Vunjak-Novakovic, and R. Langer, "Cultivation of cell-polymer cartilage implants in bioreactors," *J. Cell. Biochem.*, vol. 51, no. 3, pp. 257–264, Mar. 1993.
[259] C. Frondoza, A. Sohrabi, and D. Hungerford, "Human chondrocytes proliferate and produce matrix components in microcarrier suspension culture.," *Biomaterials*, vol. 17, no. 9, pp. 879–88, May 1996.
[260] B. Y. Bouchet, M. Colón, A. Polotsky, A. H. Shikani, D. S. Hungerford, and C. G. Frondoza, "Beta-1 integrin expression by human nasal chondrocytes in microcarrier spinner culture.," *J. Biomed. Mater. Res.*, vol. 52, no. 4, pp. 716–24, Dec. 2000.
[261] J. Malda, C. A. van Blitterswijk, M. Grojec, D. E. Martens, J. Tramper, and J. Riesle, "Expansion of Bovine Chondrocytes on Microcarriers Enhances Redifferentiation," *Tissue Eng.*, vol. 9, no. 5, pp. 939–948, Oct. 2003.
[262] A. K.-L. Chen, S. Reuveny, and S. K. W. Oh, "Application of human mesenchymal and pluripotent stem cell microcarrier cultures in cellular therapy: Achievements and future direction," *Biotechnol. Adv.*, vol. 31, no. 7, pp. 1032–1046, 2013.
[263] S. Sart, A. Errachid, Y.-J. Schneider, and S. N. Agathos, "Modulation of mesenchymal stem cell actin organization on conventional microcarriers for proliferation and differentiation in stirred bioreactors," *J. Tissue Eng. Regen. Med.*, vol. 7, no. 7, pp. 537–551, Jul. 2013.
[264] A. K. L. Chen, X. Chen, A. B. H. Choo, S. Reuveny, and S. K. W. Oh, "Critical microcarrier properties affecting the expansion of undifferentiated human embryonic stem cells," *Stem Cell Res.*, vol. 7, no. 2, pp. 97–111, 2011.
[265] R. J. Stenekes, S. C. De Smedt, J. Demeester, G. Sun, Z. Zhang, and W. E. Hennink, "Pore sizes in hydrated dextran microspheres.," *Biomacromolecules*, vol. 1, no. 4, pp. 696–703, 2000.
[266] A. Bigi, G. Cojazzi, S. Panzavolta, N. Roveri, and K. Rubini, "Stabilization of gelatin films by crosslinking with genipin.," *Biomaterials*, vol. 23, no. 24, pp. 4827–32, Dec. 2002.
[267] N. E. Timmins *et al.*, "Closed system isolation and scalable expansion of human placental mesenchymal stem cells," *Biotechnol. Bioeng.*, vol. 109, no. 7, pp. 1817–1826, Jul. 2012.
[268] Y. Yang, F. M. V. Rossi, and E. E. Putnins, "Ex vivo expansion of rat bone marrow mesenchymal stromal cells on microcarrier beads in spin culture," *Biomaterials*, vol. 28, no. 20, pp. 3110–3120, Jul. 2007.
[269] R. L. Sammons, J. Sharpe, and P. M. Marquis, "Use of enhanced chemiluminescence to quantify protein adsorption to calcium phosphate

materials and microcarrier beads.," *Biomaterials*, vol. 15, no. 10, pp. 842–7, Aug. 1994.
[270] C. González-García, S. R. Sousa, D. Moratal, P. Rico, and M. Salmerón-Sánchez, "Effect of nanoscale topography on fibronectin adsorption, focal adhesion size and matrix organisation," *Colloids Surfaces B Biointerfaces*, vol. 77, no. 2, pp. 181–190, Jun. 2010.
[271] N. Giamblanco, E. Martines, and G. Marletta, "Laminin Adsorption on Nanostructures: Switching the Molecular Orientation by Local Curvature Changes," *Langmuir*, vol. 29, no. 26, pp. 8335–8342, Jul. 2013.
[272] A. Mukhopadhyay, S. N. Mukhopadhyay, and G. P. Talwar, "Influence of serum proteins on the kinetics of attachment of vero cells to cytodex microcarriers," *J. Chem. Technol. Biotechnol.*, vol. 56, no. 4, pp. 369–374, Apr. 2007.
[273] S. A. Brew and K. C. Ingram, "Purification of human plasma fibronectin," *J. Tissue Cult. Methods*, vol. 16, no. 3–4, pp. 197–199, Sep. 1994.
[274] C. Weber *et al.*, "Expansion and Harvesting of hMSC-TERT," *Open Biomed. Eng. J.*, vol. 1, no. 1, pp. 38–46, Dec. 2007.
[275] T. K.-P. Goh *et al.*, "Microcarrier Culture for Efficient Expansion and Osteogenic Differentiation of Human Fetal Mesenchymal Stem Cells," *Biores. Open Access*, vol. 2, no. 2, pp. 84–97, Apr. 2013.
[276] R. O. Hynes, "Integrins: bidirectional, allosteric signaling machines.," *Cell*, vol. 110, no. 6, pp. 673–87, Sep. 2002.
[277] Y.-R. V Shih, K.-F. Tseng, H.-Y. Lai, C.-H. Lin, and O. K. Lee, "Matrix stiffness regulation of integrin-mediated mechanotransduction during osteogenic differentiation of human mesenchymal stem cells," *J. Bone Miner. Res.*, vol. 26, no. 4, pp. 730–738, Apr. 2011.
[278] Z. Li, S.-J. Yao, M. Alini, and M. J. Stoddart, "Chondrogenesis of human bone marrow mesenchymal stem cells in fibrin-polyurethane composites is modulated by frequency and amplitude of dynamic compression and shear stress.," *Tissue Eng. Part A*, vol. 16, no. 2, pp. 575–84, Feb. 2010.
[279] A. J. Engler, S. Sen, H. L. Sweeney, and D. E. Discher, "Matrix Elasticity Directs Stem Cell Lineage Specification," *Cell*, vol. 126, no. 4, pp. 677–689, Aug. 2006.
[280] J.-Y. Jang *et al.*, "Combined effects of surface morphology and mechanical straining magnitudes on the differentiation of mesenchymal stem cells without using biochemical reagents.," *J. Biomed. Biotechnol.*, vol. 2011, p. 860652, Feb. 2011.
[281] R. McBeath, D. M. Pirone, C. M. Nelson, K. Bhadriraju, and C. S. Chen, "Cell shape, cytoskeletal tension, and RhoA regulate stem cell lineage commitment.," *Dev. Cell*, vol. 6, no. 4, pp. 483–95, Apr. 2004.
[282] D. Choquet, D. P. Felsenfeld, and M. P. Sheetz, "Extracellular matrix rigidity causes strengthening of integrin-cytoskeleton linkages.," *Cell*, vol. 88, no. 1, pp. 39–48, Jan. 1997.
[283] J. Solon, I. Levental, K. Sengupta, P. C. Georges, and P. A. Janmey, "Fibroblast adaptation and stiffness matching to soft elastic substrates.," *Biophys. J.*, vol. 93, no. 12, pp. 4453–61, Dec. 2007.
[284] F. Chowdhury *et al.*, "Material properties of the cell dictate stress-induced spreading and differentiation in embryonic stem cells," *Nat. Mater.*, vol. 9, no.

1, pp. 82–88, Jan. 2010.
[285] W. M. Petroll, H. D. Cavanagh, and J. V Jester, “Dynamic three-dimensional visualization of collagen matrix remodeling and cytoskeletal organization in living corneal fibroblasts.,” *Scanning*, vol. 26, no. 1, pp. 1–10.
[286] T. Wakatsuki, M. S. Kolodney, G. I. Zahalak, and E. L. Elson, “Cell mechanics studied by a reconstituted model tissue.,” *Biophys. J.*, vol. 79, no. 5, pp. 2353–68, Nov. 2000.
[287] A. C. Shieh and K. A. Athanasiou, “Principles of cell mechanics for cartilage tissue engineering.,” *Ann. Biomed. Eng.*, vol. 31, no. 1, pp. 1–11, Jan. 2003.
[288] N. Caille, O. Thoumine, Y. Tardy, and J.-J. Meister, “Contribution of the nucleus to the mechanical properties of endothelial cells.,” *J. Biomech.*, vol. 35, no. 2, pp. 177–87, Feb. 2002.
[289] V. M. Laurent *et al.*, “Gradient of Rigidity in the Lamellipodia of Migrating Cells Revealed by Atomic Force Microscopy,” *Biophys. J.*, vol. 89, no. 1, pp. 667–675, Jul. 2005.
[290] D. A. Fletcher and R. D. Mullins, “Cell mechanics and the cytoskeleton,” *Nature*, vol. 463, no. 7280, pp. 485–492, Jan. 2010.
[291] V. Lulevich, T. Zink, H. Chen, F. Liu, and G. Liu, “Cell mechanics using atomic force microscopy-based single-cell compression,” *Langmuir*, vol. 22, no. 19, pp. 8151–8155, 2006.
[292] N. Gavara and R. S. Chadwick, “Determination of the elastic moduli of thin samples and adherent cells using conical atomic force microscope tips,” *Nat. Nanotechnol.*, vol. 7, no. 11, pp. 733–736, Nov. 2012.
[293] Q. Guo, Y. Xia, M. Sandig, and J. Yang, “Characterization of cell elasticity correlated with cell morphology by atomic force microscope,” *J. Biomech.*, vol. 45, no. 2, pp. 304–309, Jan. 2012.
[294] E. M. Darling, M. Topel, S. Zauscher, T. P. Vail, and F. Guilak, “Viscoelastic properties of human mesenchymally-derived stem cells and primary osteoblasts, chondrocytes, and adipocytes,” *J. Biomech.*, vol. 41, no. 2, pp. 454–464, 2008.
[295] E. M. Darling, P. E. Pritchett, B. A. Evans, R. Superfine, S. Zauscher, and F. Guilak, “Mechanical properties and gene expression of chondrocytes on micropatterned substrates following dedifferentiation in monolayer,” *Cell. Mol. Bioeng.*, vol. 2, no. 3, pp. 395–404, 2009.
[296] E. M. Darling, S. Zauscher, J. A. Block, and F. Guilak, “A thin-Layer model for viscoelastic, stress-relaxation testing of cells using Atomic Force Microscopy: Do cell properties reflect metastatic potential?,” *Biophys. J.*, vol. 92, no. 5, pp. 1784–1791, Mar. 2007.
[297] T. Ochalek, F. J. Nordt, K. Tullberg, and M. M. Burger, “Correlation between cell deformability and metastatic potential in B16-F1 melanoma cell variants.,” *Cancer Res.*, vol. 48, no. 18, pp. 5124–8, Sep. 1988.
[298] E. M. Darling, S. Zauscher, and F. Guilak, “Viscoelastic properties of zonal articular chondrocytes measured by atomic force microscopy,” *Osteoarthr. Cartil.*, vol. 14, no. 6, pp. 571–579, 2006.
[299] D. L. Bader and M. M. Knight, “4 – Measuring the biomechanical properties of cartilage cells,” in *Regenerative Medicine and Biomaterials for the Repair of*

Connective Tissues, 2010, pp. 106–136.
[300] T. G. Kuznetsova, M. N. Starodubtseva, N. I. Yegorenkov, S. A. Chizhik, and R. I. Zhdanov, "Atomic force microscopy probing of cell elasticity," *Micron*, vol. 38, no. 8, pp. 824–833, Dec. 2007.
[301] S. Nawaz, P. Sánchez, K. Bodensiek, S. Li, M. Simons, and I. A. T. Schaap, "Cell Visco-Elasticity Measured with AFM and Optical Trapping at Sub-Micrometer Deformations," *PLoS One*, vol. 7, no. 9, p. e45297, Sep. 2012.
[302] M. D. Buschmann, E. B. Hunziker, Y. J. Kim, and A. J. Grodzinsky, "Altered aggrecan synthesis correlates with cell and nucleus structure in statically compressed cartilage.," *J. Cell Sci.*, vol. 109 (Pt 2), pp. 499–508, Feb. 1996.
[303] F. L. Gray, C. G. Turner, A. Ahmed, C. E. Calvert, D. Zurakowski, and D. O. Fauza, "Prenatal tracheal reconstruction with a hybrid amniotic mesenchymal stem cells–engineered construct derived from decellularized airway," *J. Pediatr. Surg.*, vol. 47, no. 6, pp. 1072–1079, Jun. 2012.
[304] S. M. Kunisaki, D. A. Freedman, and D. O. Fauza, "Fetal tracheal reconstruction with cartilaginous grafts engineered from mesenchymal amniocytes," *J. Pediatr. Surg.*, vol. 41, no. 4, pp. 675–682, Apr. 2006.
[305] R. BELSEY, "Resection and reconstruction of the intrathoracic trachea.," *Br. J. Surg.*, vol. 38, no. 150, pp. 200–5, Oct. 1950.
[306] E. M. Boazak and D. T. Auguste, "Trachea Mechanics for Tissue Engineering Design," *ACS Biomater. Sci. Eng.*, vol. 4, no. 4, pp. 1272–1284, Apr. 2018.
[307] J. K. Rains, J. L. Bert, C. R. Roberts, and P. D. Pare, "Mechanical properties of human tracheal cartilage," *J. Appl. Physiol.*, vol. 72, no. 1, pp. 219–225, Jan. 1992.
[308] E. M. Baile, J. Bert, P. D. Pare, and B. C. V. T. W, "A method for estimating the Young's modulus of complete tracheal cartilage rings," no. c, 1991.
[309] C. R. Roberts, J. K. Rains, P. D. Pare, D. C. Walker, B. Wiggs, and J. L. Bert, "Ultrastructure and tensile properties of human tracheal cartilage1.pdf," vol. 31, pp. 81–86, 1998.
[310] F. Safshekan, M. Tafazzoli-Shadpour, M. Abdouss, and M. B. Shadmehr, "Mechanical characterization and constitutive modeling of human trachea: Age and gender dependency," *Materials (Basel).*, vol. 9, no. 6, 2016.
[311] E. J. O. ten Hallers *et al.*, "Animal models for tracheal research," *Biomaterials*, vol. 25, no. 9, pp. 1533–1543, Apr. 2004.
[312] C. R. Chu, M. Szczodry, and S. Bruno, "Animal models for cartilage regeneration and repair," *Tissue Eng Part B Rev*, vol. 16, no. 1, pp. 105–115, 2010.
[313] J. M. Melero-Martin, M. A. Dowling, M. Smith, and M. Al-Rubeai, "Expansion of chondroprogenitor cells on macroporous microcarriers as an alternative to conventional monolayer systems," *Biomaterials*, vol. 27, no. 15, pp. 2970–2979, 2006.
[314] A. Anura, D. Das, M. Pal, R. R. Paul, S. Das, and J. Chatterjee, "Nanomechanical signatures of oral submucous fibrosis in sub-epithelial connective tissue," *J. Mech. Behav. Biomed. Mater.*, vol. 65, no. July 2016, pp. 705–715, 2017.
[315] N. Mohd Razali and Y. Bee Wah, *Power comparisons of Shapiro-Wilk, Kolmogorov-Smirnov, Lilliefors and Anderson-Darling tests*, vol. 2, no. 1. 2011.

[316] N. Nachar, “The Mann-Whitney U: A Test for Assessing Whether Two Independent Samples Come from the Same Distribution,” 2008.
[317] C. J. Connon, *Bioprocessing for cell based therapies*. .
[318] D. G. Phinney and D. J. Prockop, “Concise Review: Mesenchymal Stem/Multipotent Stromal Cells: The State of Transdifferentiation and Modes of Tissue Repair-Current Views,” *Stem Cells*, vol. 25, no. 11, pp. 2896–2902, Nov. 2007.
[319] K. Kojima, L. J. Bonassar, R. A. Ignotz, K. Syed, J. Cortiella, and C. A. Vacanti, “Comparison of Tracheal and Nasal Chondrocytes for Tissue Engineering of the Trachea,” *Ann. Thorac. Surg.*, vol. 76, no. 6, pp. 1884–1888, 2003.
[320] J. T. Connelly, C. G. Wilson, and M. E. Levenston, “Characterization of proteoglycan production and processing by chondrocytes and BMSCs in tissue engineered constructs,” *Osteoarthr. Cartil.*, vol. 16, no. 9, pp. 1092–1100, Sep. 2008.
[321] S. BADYLAK, D. FREYTES, and T. GILBERT, “Extracellular matrix as a biological scaffold material: Structure and function,” *Acta Biomater.*, vol. 5, no. 1, pp. 1–13, Jan. 2009.
[322] N. Barker, S. Bartfeld, and H. Clevers, “Tissue-Resident Adult Stem Cell Populations of Rapidly Self-Renewing Organs,” *Cell Stem Cell*, vol. 7, no. 6, pp. 656–670, Dec. 2010.
[323] K. Xue *et al.*, “Isolation and identification of stem cells in different subtype of cartilage tissue,” *Expert Opin. Biol. Ther.*, vol. 15, no. 5, pp. 623–632, May 2015.
[324] D. P. Lennon, S. E. Haynesworth, S. P. Bruder, N. Jaiswal, and A. I. Caplan, “Human and animal mesenchymal progenitor cells from bone marrow: Identification of serum for optimal selection and proliferation,” *Vitr. Cell. Dev. Biol. - Anim.*, vol. 32, no. 10, pp. 602–611, Nov. 1996.
[325] J. J. Montesinos *et al.*, “Human mesenchymal stromal cells from adult and neonatal sources: comparative analysis of their morphology, immunophenotype, differentiation patterns and neural protein expression,” *Cytotherapy*, vol. 11, no. 2, pp. 163–176, Jan. 2009.
[326] W. C. Lee *et al.*, “Multivariate biophysical markers predictive of mesenchymal stromal cell multipotency,” *Proc. Natl. Acad. Sci.*, vol. 111, no. 42, pp. E4409–E4418, Oct. 2014.
[327] R. F. Loeser, “Integrins and chondrocyte–matrix interactions in articular cartilage,” *Matrix Biol.*, vol. 39, pp. 11–16, Oct. 2014.
[328] P. H. Jones and F. M. Watt, “Separation of human epidermal stem cells from transit amplifying cells on the basis of differences in integrin function and expression,” *Cell*, vol. 73, no. 4, pp. 713–724, May 1993.
[329] C. S. Potten, “The epidermal proliferative unit: the possible role of the central basal cell.,” *Cell Tissue Kinet.*, vol. 7, no. 1, pp. 77–88, Jan. 1974.
[330] Y. Barrandon, J. R. Morgan, R. C. Mulligan, and H. Green, “Restoration of growth potential in paraclones of human keratinocytes by a viral oncogene.,” *Proc. Natl. Acad. Sci. U. S. A.*, vol. 86, no. 11, pp. 4102–6, Jun. 1989.
[331] R. O. Hynes, “Integrins: versatility, modulation, and signaling in cell adhesion.,” *Cell*, vol. 69, no. 1, pp. 11–25, Apr. 1992.

[332] A. J. Friedenstein, J. F. Gorskaja, and N. N. Kulagina, “Fibroblast precursors in normal and irradiated mouse hematopoietic organs.,” *Exp. Hematol.*, vol. 4, no. 5, pp. 267–74, Sep. 1976.
[333] F. P. Barry, R. E. Boynton, S. Haynesworth, J. M. Murphy, and J. Zaia, “The Monoclonal Antibody SH-2, Raised against Human Mesenchymal Stem Cells, Recognizes an Epitope on Endoglin (CD105),” *Biochem. Biophys. Res. Commun.*, vol. 265, no. 1, pp. 134–139, Nov. 1999.
[334] S. P. Bruder, M. C. Horowitz, J. D. Mosca, and S. E. Haynesworth, “Monoclonal antibodies reactive with human osteogenic cell surface antigens.,” *Bone*, vol. 21, no. 3, pp. 225–35, Sep. 1997.
[335] S. P. Bruder *et al.*, “Mesenchymal Stem Cell Surface Antigen SB-10 Corresponds to Activated Leukocyte Cell Adhesion Molecule and Is Involved in Osteogenic Differentiation,” *J. Bone Miner. Res.*, vol. 13, no. 4, pp. 655–663, Apr. 1998.
[336] S. Halfon, N. Abramov, B. Grinblat, and I. Ginis, “Markers Distinguishing Mesenchymal Stem Cells from Fibroblasts Are Downregulated with Passaging,” *Stem Cells Dev.*, vol. 20, no. 1, pp. 53–66, Jan. 2011.
[337] S. Alsalameh, R. Amin, T. Gemba, and M. Lotz, “Identification of mesenchymal progenitor cells in normal and osteoarthritic human articular cartilage,” *Arthritis Rheum.*, vol. 50, no. 5, pp. 1522–1532, May 2004.
[338] D. C. Colter, I. Sekiya, and D. J. Prockop, “Identification of a subpopulation of rapidly self-renewing and multipotential adult stem cells in colonies of human marrow stromal cells,” *Proc. Natl. Acad. Sci.*, vol. 98, no. 14, pp. 7841–7845, Jul. 2001.
[339] M. J. Whitfield, W. C. J. Lee, and K. J. Van Vliet, “Onset of heterogeneity in culture-expanded bone marrow stromal cells,” *Stem Cell Res.*, vol. 11, no. 3, pp. 1365–1377, Nov. 2013.
[340] R. J. McMurray *et al.*, “Nanoscale surfaces for the long-term maintenance of mesenchymal stem cell phenotype and multipotency,” *Nat. Mater.*, vol. 10, no. 8, pp. 637–644, Aug. 2011.
[341] I. A. Titushkin, J. Shin, and M. Cho, “A new perspective for stem-cell mechanobiology: biomechanical control of stem-cell behavior and fate.,” *Crit. Rev. Biomed. Eng.*, vol. 38, no. 5, pp. 393–433, 2010.
[342] A. J. S. Ribeiro *et al.*, “Mechanical characterization of adult stem cells from bone marrow and perivascular niches,” *J. Biomech.*, vol. 45, no. 7, pp. 1280–1287, Apr. 2012.
[343] D. Di Carlo, “A Mechanical Biomarker of Cell State in Medicine,” *J. Lab. Autom.*, vol. 17, no. 1, pp. 32–42, Feb. 2012.
[344] T. Herricks, M. Antia, and P. K. Rathod, “Deformability limits of Plasmodium falciparum-infected red blood cells,” *Cell. Microbiol.*, vol. 11, no. 9, pp. 1340–1353, Sep. 2009.
[345] J. L. Maciaszek, B. Andemariam, and G. Lykotrafitis, “Microelasticity of red blood cells in sickle cell disease,” *J. Strain Anal. Eng. Des.*, vol. 46, no. 5, pp. 368–379, Jul. 2011.
[346] F. B. Gao and M. Raff, “Cell size control and a cell-intrinsic maturation program in proliferating oligodendrocyte precursor cells.,” *J. Cell Biol.*, vol.

138, no. 6, pp. 1367–77, Sep. 1997.
[347] J. C. Angello, W. R. Pendergrass, T. H. Norwood, and J. Prothero, “Proliferative potential of human fibroblasts: An inverse dependence on cell size,” *J. Cell. Physiol.*, vol. 132, no. 1, pp. 125–130, Jul. 1987.
[348] C. S. De Paiva, S. C. Pflugfelder, and D.-Q. Li, “Cell Size Correlates with Phenotype and Proliferative Capacity in Human Corneal Epithelial Cells,” *Stem Cells*, vol. 24, no. 2, pp. 368–375, Feb. 2006.
[349] R. D. González-Cruz, V. C. Fonseca, E. M. Darling, and D. A. Weitz, “Cellular mechanical properties reflect the differentiation potential of adipose-derived mesenchymal stem cells.”
[350] J. R. Smith, R. Pochampally, A. Perry, S.-C. Hsu, and D. J. Prockop, “Isolation of a Highly Clonogenic and Multipotential Subfraction of Adult Stem Cells from Bone Marrow Stroma,” *Stem Cells*, vol. 22, no. 5, pp. 823–831, Sep. 2004.
[351] R. D. Wemer, “Immunohistochemical characterization of the rabbit tracheal cartilages,” *J. Biomed. Sci. Eng.*, vol. 03, no. 10, pp. 1007–1013, 2010.
[352] R. Levato, J. Visser, J. a Planell, E. Engel, J. Malda, and M. a Mateos-Timoneda, “Biofabrication of tissue constructs by 3D bioprinting of cell-laden microcarriers.,” *Biofabrication*, vol. 6, no. 3, p. 035020, 2014.
[353] R. E. Mahaffy, S. Park, E. Gerde, J. Käs, and C. K. Shih, “Quantitative analysis of the viscoelastic properties of thin regions of fibroblasts using atomic force microscopy.,” *Biophys. J.*, vol. 86, no. 3, pp. 1777–93, Mar. 2004.
[354] F. Veronesi, G. Giavaresi, M. Tschon, V. Borsari, N. Nicoli Aldini, and M. Fini, “Clinical Use of Bone Marrow, Bone Marrow Concentrate, and Expanded Bone Marrow Mesenchymal Stem Cells in Cartilage Disease,” *Stem Cells Dev.*, vol. 22, no. 2, pp. 181–192, Jan. 2013.
[355] J. H. Cui, S. R. Park, K. Park, B. H. Choi, and B. Min, “Preconditioning of Mesenchymal Stem Cells with Low-Intensity Ultrasound for Cartilage Formation In Vivo,” *Tissue Eng.*, vol. 13, no. 2, pp. 351–360, Feb. 2007.
[356] T. Hennig *et al.*, “Reduced chondrogenic potential of adipose tissue derived stromal cells correlates with an altered TGFβ receptor and BMP profile and is overcome by BMP-6,” *J. Cell. Physiol.*, vol. 211, no. 3, pp. 682–691, Jun. 2007.
[357] F. G. Mlynarski, S. M. Parnes, and S. Polanski, “Congenital Calcification of the Larynx and Trachea,” *Otolaryngol. Neck Surg.*, vol. 93, no. 1, pp. 99–101, Feb. 1985.
[358] M. D. Rifkin and H. A. Pritzker, “Tracheobronchial cartilage calcification in children. Case reports and review of the literature,” *Br. J. Radiol.*, vol. 57, no. 676, pp. 293–296, Apr. 1984.
[359] H. Onitsuka *et al.*, “Computed tomography of tracheopathia osteoplastica,” *Am. J. Roentgenol.*, vol. 140, no. 2, pp. 268–270, Feb. 1983.
[360] D. P. Wendel, D. G. Taylor, K. H. Albertine, M. T. Keating, and D. Y. Li, “Impaired Distal Airway Development in Mice Lacking Elastin,” *Am. J. Respir. Cell Mol. Biol.*, vol. 23, no. 3, pp. 320–326, Sep. 2000.
[361] S. Johansson, G. Svineng, K. Wennerberg, A. Armulik, and L. Lohikangas, “Fibronectin-integrin interactions.,” *Front. Biosci.*, vol. 2, pp. d126-46, Mar. 1997.
[362] J. Veevers-Lowe, S. G. Ball, A. Shuttleworth, and C. M. Kielty, “Mesenchymal

stem cell migration is regulated by fibronectin through 5 1-integrin-mediated activation of PDGFR- and potentiation of growth factor signals," *J. Cell Sci.*, vol. 124, no. 8, pp. 1288–1300, Apr. 2011.
[363] P. Tropel, D. Noël, N. Platet, P. Legrand, A.-L. Benabid, and F. Berger, "Isolation and characterisation of mesenchymal stem cells from adult mouse bone marrow," *Exp. Cell Res.*, vol. 295, no. 2, pp. 395–406, May 2004.
[364] J. R. Rock and B. L. Hogan, "Epithelial progenitor cells in lung development, maintenance, repair, and disease," *Annu Rev Cell Dev Biol*, vol. 27, pp. 493–512, 2011.
[365] S. P. Grogan, S. Miyaki, H. Asahara, D. D. D'Lima, and M. K. Lotz, "Mesenchymal progenitor cell markers in human articular cartilage: normal distribution and changes in osteoarthritis.," *Arthritis Res. Ther.*, vol. 11, no. 3, p. R85, 2009.
[366] R. Levato *et al.*, "The bio in the ink: cartilage regeneration with bioprintable hydrogels and articular cartilage-derived progenitor cells," *Acta Biomater.*, vol. 61, pp. 41–53, Oct. 2017.
[367] J. Diaz-Romero, D. Nesic, S. P. Grogan, P. Heini, and P. Mainil-Varlet, "Immunophenotypic changes of human articular chondrocytes during monolayer culture reflect bona fide dedifferentiation rather than amplification of progenitor cells," *J. Cell. Physiol.*, vol. 214, no. 1, pp. 75–83, Jan. 2008.
[368] K. Michalczyk and M. Ziman, "Nestin structure and predicted function in cellular cytoskeletal organisation.," *Histol. Histopathol.*, vol. 20, no. 2, pp. 665–71, 2005.
[369] C. E. LeBlon, M. E. Casey, C. R. Fodor, T. Zhang, X. Zhang, and S. S. Jedlicka, "Correlation between in vitro expansion-related cell stiffening and differentiation potential of human mesenchymal stem cells," *Differentiation*, vol. 90, no. 1–3, pp. 1–15, Jul. 2015.
[370] E. M. Darling, J. C. Y. Hu, and K. A. Athanasiou, "Zonal and topographical differences in articular cartilage gene expression," *J. Orthop. Res.*, vol. 22, no. 6, pp. 1182–1187, Nov. 2004.
[371] E. Takai, K. D. Costa, A. Shaheen, C. T. Hung, and X. E. Guo, "Osteoblast elastic modulus measured by atomic force microscopy is substrate dependent.," *Ann. Biomed. Eng.*, vol. 33, no. 7, pp. 963–71, Jul. 2005.
[372] G. T. Charras and M. A. Horton, "Determination of Cellular Strains by Combined Atomic Force Microscopy and Finite Element Modeling," *Biophys. J.*, vol. 83, no. 2, pp. 858–879, Aug. 2002.
[373] G. T. Charras and M. A. Horton, "Single Cell Mechanotransduction and Its Modulation Analyzed by Atomic Force Microscope Indentation," *Biophys. J.*, vol. 82, no. 6, pp. 2970–2981, Jun. 2002.
[374] X. Liang, X. Shi, S. Ostrovidov, H. Wu, and K. Nakajima, "Probing stem cell differentiation using atomic force microscopy," *Appl. Surf. Sci.*, vol. 366, pp. 254–259, 2016.
[375] A. Skardal, D. Mack, A. Atala, and S. Soker, "Substrate elasticity controls cell proliferation, surface marker expression and motile phenotype in amniotic fluid-derived stem cells," *J. Mech. Behav. Biomed. Mater.*, vol. 17, pp. 307–316, Jan. 2013.

[376] P. M. Gilbert *et al.*, "Substrate Elasticity Regulates Skeletal Muscle Stem Cell Self-Renewal in Culture," *Science (80-.).*, vol. 329, no. 5995, pp. 1078–1081, Aug. 2010.
[377] A. Schellenberg *et al.*, "Population dynamics of mesenchymal stromal cells during culture expansion," *Cytotherapy*, vol. 14, no. 4, pp. 401–411, Apr. 2012.
[378] J. Ren *et al.*, "Intra-subject variability in human bone marrow stromal cell (BMSC) replicative senescence: Molecular changes associated with BMSC senescence," *Stem Cell Res.*, vol. 11, no. 3, pp. 1060–1073, Nov. 2013.
[379] J. Yu *et al.*, "Differentiation potential of STRO-1+ dental pulp stem cells changes during cell passaging," *BMC Cell Biol.*, vol. 11, no. 1, p. 32, May 2010.
[380] M. Kim, C. Kim, Y. S. Choi, M. Kim, C. Park, and Y. Suh, "Age-related alterations in mesenchymal stem cells related to shift in differentiation from osteogenic to adipogenic potential: Implication to age-associated bone diseases and defects," *Mech. Ageing Dev.*, vol. 133, no. 5, pp. 215–225, May 2012.
[381] M. R. Choi *et al.*, "Gene expression during long-term culture of mesenchymal stem cells obtained from patients with amyotrophic lateral sclerosis," *BioChip J.*, vol. 6, no. 4, pp. 342–353, Dec. 2012.
[382] A. Mobasheri, G. Kalamegam, G. Musumeci, and M. E. Batt, "Chondrocyte and mesenchymal stem cell-based therapies for cartilage repair in osteoarthritis and related orthopaedic conditions," *Maturitas*, vol. 78, no. 3, pp. 188–198, Jul. 2014.
[383] K. Stenderup, J. Justesen, C. Clausen, and M. Kassem, "Aging is associated with decreased maximal life span and accelerated senescence of bone marrow stromal cells.," *Bone*, vol. 33, no. 6, pp. 919–26, Dec. 2003.
[384] W. Wagner *et al.*, "Replicative senescence of mesenchymal stem cells: a continuous and organized process.," *PLoS One*, vol. 3, no. 5, p. e2213, May 2008.
[385] J. L. Carey, "Fibrocartilage Following Microfracture Is Not as Robust as Native Articular Cartilage," *J. Bone Jt. Surgery-American Vol.*, vol. 94, no. 11, pp. e80-1–2, Jun. 2012.
[386] C. K. Abrahamsson *et al.*, "Chondrogenesis and mineralization during in vitro culture of human mesenchymal stem cells on three-dimensional woven scaffolds.," *Tissue Eng. Part A*, vol. 16, no. 12, pp. 3709–18, Dec. 2010.
[387] F. Barry, R. E. Boynton, B. Liu, and J. M. Murphy, "Chondrogenic Differentiation of Mesenchymal Stem Cells from Bone Marrow: Differentiation-Dependent Gene Expression of Matrix Components," *Exp. Cell Res.*, vol. 268, no. 2, pp. 189–200, Aug. 2001.
[388] K. Pelttari *et al.*, "Premature induction of hypertrophy during in vitro chondrogenesis of human mesenchymal stem cells correlates with calcification and vascular invasion after ectopic transplantation in SCID mice," *Arthritis Rheum.*, vol. 54, no. 10, pp. 3254–3266, Oct. 2006.
[389] A. M. Handorf and W.-J. Li, "Induction of Mesenchymal Stem Cell Chondrogenesis Through Sequential Administration of Growth Factors Within Specific Temporal Windows," *J. Cell. Physiol.*, vol. 229, no. 2, pp. 162–171, Feb. 2014.

[390] X. Guo and X.-F. Wang, “Signaling cross-talk between TGF-β/BMP and other pathways,” *Cell Res.*, vol. 19, no. 1, pp. 71–88, Jan. 2009.
[391] M. Beederman *et al.*, “BMP signaling in mesenchymal stem cell differentiation and bone formation,” *J. Biomed. Sci. Eng.*, vol. 06, no. 08, pp. 32–52, Aug. 2013.
[392] E. N. Blaney Davidson *et al.*, “Increase in ALK1/ALK5 Ratio as a Cause for Elevated MMP-13 Expression in Osteoarthritis in Humans and Mice,” *J. Immunol.*, vol. 182, no. 12, pp. 7937–7945, Jun. 2009.
[393] L. M. G. de Kroon *et al.*, “Activin Receptor-Like Kinase Receptors ALK5 and ALK1 Are Both Required for TGFβ-Induced Chondrogenic Differentiation of Human Bone Marrow-Derived Mesenchymal Stem Cells,” *PLoS One*, vol. 10, no. 12, p. e0146124, 2015.
[394] W. Wang, D. Rigueur, and K. M. Lyons, “TGFβ signaling in cartilage development and maintenance,” *Birth Defects Res. Part C Embryo Today Rev.*, vol. 102, no. 1, pp. 37–51, Mar. 2014.
[395] R. Tuli *et al.*, “Transforming Growth Factor-β-mediated Chondrogenesis of Human Mesenchymal Progenitor Cells Involves N-cadherin and Mitogen-activated Protein Kinase and Wnt Signaling Cross-talk,” *J. Biol. Chem.*, vol. 278, no. 42, pp. 41227–41236, Oct. 2003.
[396] X. Zhang *et al.*, “Primary murine limb bud mesenchymal cells in long-term culture complete chondrocyte differentiation: TGF-β delays hypertrophy and PGE2 inhibits terminal differentiation,” *Bone*, vol. 34, no. 5, pp. 809–817, May 2004.
[397] C. A. Hellingman *et al.*, “Smad signaling determines chondrogenic differentiation of bone-marrow-derived mesenchymal stem cells: inhibition of Smad1/5/8P prevents terminal differentiation and calcification.,” *Tissue Eng. Part A*, vol. 17, no. 7–8, pp. 1157–67, Apr. 2011.
[398] P. M. van der Kraan, E. N. Blaney Davidson, and W. B. van den Berg, “Bone Morphogenetic Proteins and articular cartilage,” *Osteoarthr. Cartil.*, vol. 18, no. 6, pp. 735–741, Jun. 2010.
[399] B. Schmitt *et al.*, “BMP2 initiates chondrogenic lineage development of adult human mesenchymal stem cells in high-density culture,” *Differentiation*, vol. 71, no. 9–10, pp. 567–577, Dec. 2003.
[400] B. Shu *et al.*, “BMP2, but not BMP4, is crucial for chondrocyte proliferation and maturation during endochondral bone development,” *J. Cell Sci.*, vol. 124, no. 20, pp. 3428–3440, Oct. 2011.
[401] A. Bandyopadhyay, K. Tsuji, K. Cox, B. D. Harfe, V. Rosen, and C. J. Tabin, “Genetic Analysis of the Roles of BMP2, BMP4, and BMP7 in Limb Patterning and Skeletogenesis,” *PLoS Genet.*, vol. 2, no. 12, p. e216, Dec. 2006.
[402] Y. Li, J. Gordon, N. R. Manley, Y. Litingtung, and C. Chiang, “Bmp4 is required for tracheal formation: A novel mouse model for tracheal agenesis,” *Dev. Biol.*, vol. 322, no. 1, pp. 145–155, Oct. 2008.
[403] M. K. Majumdar, E. Wang, and E. A. Morris, “BMP-2 and BMP-9 promotes chondrogenic differentiation of human multipotential mesenchymal cells and overcomes the inhibitory effect of IL-1,” *J. Cell. Physiol.*, vol. 189, no. 3, pp. 275–284, Dec. 2001.
[404] E. Mariani, L. Pulsatelli, and A. Facchini, “Signaling Pathways in Cartilage

Repair," *Int. J. Mol. Sci.*, vol. 15, no. 5, pp. 8667–8698, May 2014.
[405] B. T. Estes and F. Guilak, "Three-Dimensional Culture Systems to Induce Chondrogenesis of Adipose-Derived Stem Cells," in *Methods in molecular biology (Clifton, N.J.)*, vol. 702, 2011, pp. 201–217.
[406] J. F. Welter, L. A. Solchaga, and K. J. Penick, "Simplification of aggregate culture of human mesenchymal stem cells as a chondrogenic screening assay.," *Biotechniques*, vol. 42, no. 6, pp. 732, 734–7, Jun. 2007.
[407] A. W. James, Y. Xu, J. K. Lee, R. Wang, and M. T. Longaker, "Differential Effects of TGF-β1 and TGF-β3 on Chondrogenesis in Posterofrontal Cranial Suture–Derived Mesenchymal Cells In Vitro," *Plast. Reconstr. Surg.*, vol. 123, no. 1, pp. 31–43, Jan. 2009.
[408] M. Centola, B. Tonnarelli, S. Schären, N. Glaser, A. Barbero, and I. Martin, "Priming 3D Cultures of Human Mesenchymal Stromal Cells Toward Cartilage Formation Via Developmental Pathways," *Stem Cells Dev.*, vol. 22, no. 21, pp. 2849–2858, Nov. 2013.
[409] R. Narcisi *et al.*, "Long-term expansion, enhanced chondrogenic potential, and suppression of endochondral ossification of adult human MSCs via WNT signaling modulation.," *Stem cell reports*, vol. 4, no. 3, pp. 459–72, Mar. 2015.
[410] W. M. Kulyk, J. L. Franklin, and L. M. Hoffman, "Sox9 Expression during Chondrogenesis in Micromass Cultures of Embryonic Limb Mesenchyme," *Exp. Cell Res.*, vol. 255, no. 2, pp. 327–332, Mar. 2000.
[411] A. E. Grigoriadis, J. N. Heersche, and J. E. Aubin, "Differentiation of muscle, fat, cartilage, and bone from progenitor cells present in a bone-derived clonal cell population: effect of dexamethasone.," *J. Cell Biol.*, vol. 106, no. 6, pp. 2139–51, Jun. 1988.
[412] A. Barbul, "Proline Precursors to Sustain Mammalian Collagen Synthesis," *J. Nutr.*, vol. 138, no. 10, p. 2021S–2024S, Oct. 2008.
[413] A. G. Tay, J. Farhadi, R. Suetterlin, G. Pierer, M. Heberer, and I. Martin, "Cell yield, proliferation, and postexpansion differentiation capacity of human ear, nasal, and rib chondrocytes.," *Tissue Eng.*, vol. 10, no. 5–6, pp. 762–770, 2004.
[414] M. R. Homicz, B. L. Schumacher, R. L. Sah, and D. Watson, "Effects of Serial Expansion of Septal Chondrocytes on Tissue-Engineered Neocartilage Composition," *Otolaryngol. Neck Surg.*, vol. 127, no. 5, pp. 398–408, Nov. 2002.
[415] K. Pelttari, E. Steck, and W. Richter, "The use of mesenchymal stem cells for chondrogenesis," *Injury*, vol. 39, no. 1, pp. 58–65, Apr. 2008.
[416] W. Kafienah, S. Mistry, S. C. Dickinson, T. J. Sims, I. Learmonth, and A. P. Hollander, "Three-dimensional cartilage tissue engineering using adult stem cells from osteoarthritis patients," *Arthritis Rheum.*, vol. 56, no. 1, pp. 177–187, Jan. 2007.
[417] T. Blunk *et al.*, "Bone morphogenetic protein 9: a potent modulator of cartilage development in vitro.," *Growth Factors*, vol. 21, no. 2, pp. 71–7, Jun. 2003.
[418] R. L. Hills, L. M. Belanger, and E. A. Morris, "Bone morphogenetic protein 9 is a potent anabolic factor for juvenile bovine cartilage, but not adult cartilage," *J. Orthop. Res.*, vol. 23, no. 3, pp. 611–617, May 2005.

[419] E. Minina *et al.*, "BMP and Ihh/PTHrP signaling interact to coordinate chondrocyte proliferation and differentiation.," *Development*, vol. 128, no. 22, pp. 4523–34, Nov. 2001.
[420] K. W. Finnson, W. L. Parker, P. ten Dijke, M. Thorikay, and A. Philip, "ALK1 Opposes ALK5/Smad3 Signaling and Expression of Extracellular Matrix Components in Human Chondrocytes," *J. Bone Miner. Res.*, vol. 23, no. 6, pp. 896–906, Feb. 2008.
[421] X. Yang, L. Chen, X. Xu, C. Li, C. Huang, and C. X. Deng, "TGF-beta/Smad3 signals repress chondrocyte hypertrophic differentiation and are required for maintaining articular cartilage.," *J. Cell Biol.*, vol. 153, no. 1, pp. 35–46, Apr. 2001.
[422] T.-F. Li *et al.*, "Smad3-Deficient Chondrocytes Have Enhanced BMP Signaling and Accelerated Differentiation," *J. Bone Miner. Res.*, vol. 21, no. 1, pp. 4–16, Sep. 2005.
[423] C. C. van Donkelaar and W. Wilson, "Mechanics of chondrocyte hypertrophy," *Biomech. Model. Mechanobiol.*, vol. 11, no. 5, pp. 655–664, May 2012.
[424] F. M. Craig, G. Bentley, and C. W. Archer, "The spatial and temporal pattern of collagens I and II and keratan sulphate in the developing chick metatarsophalangeal joint.," *Development*, vol. 99, no. 3, pp. 383–91, Mar. 1987.
[425] I. M. Khan *et al.*, "In vitro growth factor-induced bio engineering of mature articular cartilage," *Biomaterials*, vol. 34, no. 5, pp. 1478–1487, 2013.
[426] C. A. Gregory, W. Grady Gunn, A. Peister, and D. J. Prockop, "An Alizarin red-based assay of mineralization by adherent cells in culture: comparison with cetylpyridinium chloride extraction," *Anal. Biochem.*, vol. 329, no. 1, pp. 77–84, Jun. 2004.
[427] H. Paul, A. J. Reginato, and H. R. Schumacher, "Alizarin red S staining as a screening test to detect calcium compounds in synovial fluid.," *Arthritis Rheum.*, vol. 26, no. 2, pp. 191–200, Feb. 1983.
[428] C. H. Coyle, N. J. Izzo, and C. R. Chu, "Sustained hypoxia enhances chondrocyte matrix synthesis," *J. Orthop. Res.*, vol. 27, no. 6, pp. 793–799, Jun. 2009.
[429] R. Amarilio, S. V. Viukov, A. Sharir, I. Eshkar-Oren, R. S. Johnson, and E. Zelzer, "HIF1 regulation of Sox9 is necessary to maintain differentiation of hypoxic prechondrogenic cells during early skeletogenesis," *Development*, vol. 134, no. 21, pp. 3917–3928, Oct. 2007.
[430] N. Zhou *et al.*, "HIF-1α as a Regulator of BMP2-Induced Chondrogenic Differentiation, Osteogenic Differentiation, and Endochondral Ossification in Stem Cells," *Cell. Physiol. Biochem.*, vol. 36, no. 1, pp. 44–60, 2015.
[431] E. Schipani, H. E. Ryan, S. Didrickson, T. Kobayashi, M. Knight, and R. S. Johnson, "Hypoxia in cartilage: HIF-1alpha is essential for chondrocyte growth arrest and survival.," *Genes Dev.*, vol. 15, no. 21, pp. 2865–76, Nov. 2001.
[432] S. Provot *et al.*, "Hif-1α regulates differentiation of limb bud mesenchyme and joint development," *J. Cell Biol.*, vol. 177, no. 3, pp. 451–464, May 2007.
[433] E. Duval *et al.*, "Molecular mechanism of hypoxia-induced chondrogenesis and its application in in vivo cartilage tissue engineering," *Biomaterials*, vol.

33, no. 26, pp. 6042–6051, Sep. 2012.
[434] T. Fink *et al.*, "Induction of Adipocyte-Like Phenotype in Human Mesenchymal Stem Cells by Hypoxia," *Stem Cells*, vol. 22, no. 7, pp. 1346–1355, Dec. 2004.
[435] P. T. Schumacker, "Lung Cell Hypoxia: Role of Mitochondrial Reactive Oxygen Species Signaling in Triggering Responses," *Proc. Am. Thorac. Soc.*, vol. 8, no. 6, pp. 477–484, Nov. 2011.
[436] H. Holtzer, J. Abbott, J. Lash, and S. Holtzer, "THE LOSS OF PHENOTYPIC TRAITS BY DIFFERENTIATED CELLS IN VITRO, I. DEDIFFERENTIATION OF CARTILAGE CELLS.," *Proc. Natl. Acad. Sci. U. S. A.*, vol. 46, no. 12, pp. 1533–42, Dec. 1960.
[437] K. VON DER MARK, V. GAUSS, H. VON DER MARK, and P. MÜLLER, "Relationship between cell shape and type of collagen synthesised as chondrocytes lose their cartilage phenotype in culture," *Nature*, vol. 267, no. 5611, pp. 531–532, Jun. 1977.
[438] S. Wakitani, K. Imoto, T. Yamamoto, M. Saito, N. Murata, and M. Yoneda, "Human autologous culture expanded bone marrow mesenchymal cell transplantation for repair of cartilage defects in osteoarthritic knees," *Osteoarthr. Cartil.*, vol. 10, no. 3, pp. 199–206, Mar. 2002.
[439] D. Y. Wohn, "Korea okays stem cell therapies despite limited peer-reviewed data," *Nat. Med.*, vol. 18, no. 3, pp. 329–329, Mar. 2012.
[440] J. M. O. and R. L. R. Cristiana Gonçalves, Hajer Radhouani, "Advances in Biomaterials for the Treatment of Articular Cartilage Defects Cristiana," vol. 21, pp. 97–126, 2017.
[441] C. J. Wilson, R. E. Clegg, D. I. Leavesley, and M. J. Pearcy, "Mediation of Biomaterial–Cell Interactions by Adsorbed Proteins: A Review," *Tissue Eng.*, vol. 11, no. 1–2, pp. 1–18, Jan. 2005.
[442] R. CHEN, S. CURRAN, J. CURRAN, and J. HUNT, "The use of poly(l-lactide) and RGD modified microspheres as cell carriers in a flow intermittency bioreactor for tissue engineering cartilage," *Biomaterials*, vol. 27, no. 25, pp. 4453–4460, Sep. 2006.
[443] C. G. Spiteri, R. M. Pilliar, and R. A. Kandel, "Substrate porosity enhances chondrocyte attachment, spreading, and cartilage tissue formationin vitro," *J. Biomed. Mater. Res. Part A*, vol. 78A, no. 4, pp. 676–683, Sep. 2006.
[444] H. J. Chung, I. K. Kim, T. G. Kim, and T. G. Park, "Highly Open Porous Biodegradable Microcarriers: In Vitro Cultivation of Chondrocytes for Injectable Delivery," *Tissue Eng. Part A*, vol. 14, no. 5, pp. 607–615, May 2008.
[445] D. Chimene, K. K. Lennox, R. R. Kaunas, and A. K. Gaharwar, "Advanced Bioinks for 3D Printing: A Materials Science Perspective," *Ann. Biomed. Eng.*, vol. 44, no. 6, pp. 2090–2102, 2016.
[446] J. Malda *et al.*, "25th anniversary article: Engineering hydrogels for biofabrication," *Adv. Mater.*, vol. 25, no. 36, pp. 5011–5028, 2013.
[447] N. Eslahi, M. Abdorahim, and A. Simchi, "Smart Polymeric Hydrogels for Cartilage Tissue Engineering: A Review on the Chemistry and Biological Functions," *Biomacromolecules*, vol. 17, pp. 3441–3463, 2019.
[448] S. Pettersson, J. Wetterö, P. Tengvall, and G. Kratz, "Human articular

chondrocytes onmacroporous gelatinmicrocarriers form structurally stable constructs with blood-derived biological glues in vitro," *Tissue Eng. Regen. Med.*, vol. 6, no. 6, pp. 450–460, 2009.
[449] R. M. and N. R. Elena Schuh, Sandra Hofmann, Kathryn S. Stok, Holger Notbohm, "The influence of matrix elasticity on chondrocyte behavior in 3D," *J. Tissue Eng. Regen. Med.*, vol. 4, no. 7, pp. 524–531, 2010.
[450] S. Ohlson, J. Branscomb, and K. Nilsson, "Bead-to-bead transfer of Chinese hamster ovary cells using macroporous microcarriers.," *Cytotechnology*, vol. 14, no. 1, pp. 67–80, 1994.
[451] A. Werner *et al.*, "Cultivation of immortalized human hepatocytes HepZ on macroporous CultiSpher G microcarriers.," *Biotechnol. Bioeng.*, vol. 68, no. 1, pp. 59–70, Apr. 2000.
[452] D. Schop *et al.*, "Expansion of human mesenchymal stromal cells on microcarriers: growth and metabolism," *J. Tissue Eng. Regen. Med.*, vol. 4, no. 2, pp. 131–140, Feb. 2010.
[453] P.-C. Tseng, T.-H. Young, T.-M. Wang, H.-W. Peng, S.-M. Hou, and M.-L. Yen, "Spontaneous osteogenesis of MSCs cultured on 3D microcarriers through alteration of cytoskeletal tension," *Biomaterials*, vol. 33, no. 2, pp. 556–564, Jan. 2012.
[454] M. Chen, X. Wang, Z. Ye, Y. Zhang, Y. Zhou, and W.-S. Tan, "A modular approach to the engineering of a centimeter-sized bone tissue construct with human amniotic mesenchymal stem cells-laden microcarriers," *Biomaterials*, vol. 32, no. 30, pp. 7532–7542, Oct. 2011.
[455] M. M. Nadzir *et al.*, "Comprehension of terminal differentiation and dedifferentiation of chondrocytes during passage cultures," *J. Biosci. Bioeng.*, vol. 112, no. 4, pp. 395–401, Oct. 2011.
[456] X. Zhou *et al.*, "Roles of FGF-2 and TGF-beta/FGF-2 on differentiation of human mesenchymal stem cells towards nucleus pulposus-like phenotype," *Growth Factors*, vol. 33, no. 1, pp. 23–30, Jan. 2015.
[457] L. A. Solchaga, K. Penick, V. M. Goldberg, A. I. Caplan, and J. F. Welter, "Fibroblast growth factor-2 enhances proliferation and delays loss of chondrogenic potential in human adult bone-marrow-derived mesenchymal stem cells.," *Tissue Eng. Part A*, vol. 16, no. 3, pp. 1009–19, Mar. 2010.
[458] S. Murakami, M. Kan, W. L. McKeehan, and B. de Crombrugghe, "Up-regulation of the chondrogenic Sox9 gene by fibroblast growth factors is mediated by the mitogen-activated protein kinase pathway.," *Proc. Natl. Acad. Sci. U. S. A.*, vol. 97, no. 3, pp. 1113–8, Feb. 2000.
[459] A. M. Handorf and W.-J. Li, "Fibroblast Growth Factor-2 Primes Human Mesenchymal Stem Cells for Enhanced Chondrogenesis," *PLoS One*, vol. 6, no. 7, p. e22887, Jul. 2011.
[460] B. Delorme *et al.*, "Specific Lineage-Priming of Bone Marrow Mesenchymal Stem Cells Provides the Molecular Framework for Their Plasticity," *Stem Cells*, vol. 27, no. 5, pp. 1142–1151, May 2009.
[461] M. Komura *et al.*, "Long-term follow-up of tracheal cartilage growth promotion by intratracheal injection of basic fibroblast growth factor," *J. Pediatr. Surg.*, vol. 53, no. 12, pp. 2394–2398, Dec. 2018.

[462] D. J. Jeanmonod, Rebecca, and K. et al. Suzuki, “Collagen- vs. Gelatine-Based Biomaterials and Their Biocompatibility: Review and Perspectives,” *Intech open*, vol. 2, p. 64, 2018.
[463] G. Eibes *et al.*, “Maximizing the ex vivo expansion of human mesenchymal stem cells using a microcarrier-based stirred culture system,” *J. Biotechnol.*, vol. 146, no. 4, pp. 194–197, Apr. 2010.
[464] S. Verbruggen, D. Luining, A. van Essen, and M. J. Post, “Bovine myoblast cell production in a microcarriers-based system,” *Cytotechnology*, vol. 70, no. 2, pp. 503–512, Apr. 2018.
[465] S. R. Caruso *et al.*, “Growth and functional harvesting of human mesenchymal stromal cells cultured on a microcarrier-based system,” *Biotechnol. Prog.*, vol. 30, no. 4, pp. 889–895, Jul. 2014.
[466] A.-C. Tsai and T. Ma, “Expansion of Human Mesenchymal Stem Cells in a Microcarrier Bioreactor.,” *Methods Mol. Biol.*, vol. 1502, pp. 77–86, 2016.
[467] Y. Lee, J. Choi, and N. S. Hwang, “Regulation of lubricin for functional cartilage tissue regeneration: a review,” *Biomater. Res.*, vol. 22, no. 1, p. 9, Dec. 2018.
[468] P. Niemeyer and A. Bernstein, “Mesenchymal stem cell chondrogenesis: Composite growth factor-bioreactor synergism for human stem cell chondrogenesis Association of clinical parameters and synovial cytokine expression after focal cartilage lesions in the knee View project Rapidos View project,” 2014.
[469] Y. Mei, H. Luo, Q. Tang, Z. Ye, Y. Zhou, and W.-S. Tan, “Modulating and modeling aggregation of cell-seeded microcarriers in stirred culture system for macrotissue engineering,” *J. Biotechnol.*, vol. 150, no. 3, pp. 438–446, Nov. 2010.
[470] D. A. Stout, J. Toyjanova, and C. Franck, “Planar Gradient Diffusion System to Investigate Chemotaxis in a 3D Collagen Matrix,” *J. Vis. Exp.*, no. 100, pp. 1–12, 2015.
[471] S. Pettersson, J. Wetterö, P. Tengvall, and G. Kratz, “Human articular chondrocytes on macroporous gelatin microcarriers form structurally stable constructs with blood-derived biological glues *in vitro*,” *J. Tissue Eng. Regen. Med.*, vol. 3, no. 6, pp. 450–460, Aug. 2009.
[472] C. M. Pauken, R. Heyes, and D. G. Lott, “Mechanical, Cellular, and Proteomic Properties of Laryngotracheal Cartilage,” *Cartilage*, p. 194760351774992, Jan. 2018.
[473] E. J. Mackie, Y. A. Ahmed, L. Tatarczuch, K.-S. Chen, and M. Mirams, “Endochondral ossification: How cartilage is converted into bone in the developing skeleton,” *Int. J. Biochem. Cell Biol.*, vol. 40, no. 1, pp. 46–62, 2008.
[474] D. P. Chang, F. Guilak, G. D. Jay, and S. Zauscher, “Interaction of lubricin with type II collagen surfaces: Adsorption, friction, and normal forces,” *J. Biomech.*, vol. 47, no. 3, pp. 659–666, Feb. 2014.
[475] R. O. Hynes, “The extracellular matrix: not just pretty fibrils.,” *Science*, vol. 326, no. 5957, pp. 1216–9, Nov. 2009.
[476] C. Chen, D. T. Tambe, L. Deng, and L. Yang, “Biomechanical properties and mechanobiology of the articular chondrocyte.,” *Am. J. Physiol. Cell Physiol.*, vol. 305, no. 12, pp. C1202-8, 2013.

[477] M. A. Baxter, R. F. Wynn, S. N. Jowitt, J. E. Wraith, L. J. Fairbairn, and I. Bellantuono, "Study of Telomere Length Reveals Rapid Aging of Human Marrow Stromal Cells following In Vitro Expansion," *Stem Cells*, vol. 22, no. 5, pp. 675–682, Sep. 2004.
[478] M. J. Dalby *et al.*, "The control of human mesenchymal cell differentiation using nanoscale symmetry and disorder," *Nat. Mater.*, vol. 6, no. 12, pp. 997–1003, Dec. 2007.
[479] S.-Y. Tee, J. Fu, C. S. Chen, and P. A. Janmey, "Cell Shape and Substrate Rigidity Both Regulate Cell Stiffness," *Biophys. J.*, vol. 100, no. 5, pp. L25–L27, Mar. 2011.
[480] J.-S. Lee, S. K. Kim, B.-J. Jung, S.-B. Choi, E.-Y. Choi, and C.-S. Kim, "Enhancing proliferation and optimizing the culture condition for human bone marrow stromal cells using hypoxia and fibroblast growth factor-2," *Stem Cell Res.*, vol. 28, pp. 87–95, Apr. 2018.
[481] S. Chen, P. Fu, R. Cong, H. Wu, and M. Pei, "Strategies to minimize hypertrophy in cartilage engineering and regeneration," *Genes Dis.*, vol. 2, no. 1, pp. 76–95, Mar. 2015.
[482] S. R. Herlofsen, A. M. Küchler, J. E. Melvik, and J. E. Brinchmann, "Chondrogenic differentiation of human bone marrow-derived mesenchymal stem cells in self-gelling alginate discs reveals novel chondrogenic signature gene clusters.," *Tissue Eng. Part A*, vol. 17, no. 7–8, pp. 1003–13, Apr. 2011.
[483] F. dos Santos *et al.*, "Toward a Clinical-Grade Expansion of Mesenchymal Stem Cells from Human Sources: A Microcarrier-Based Culture System Under Xeno-Free Conditions," *Tissue Eng. Part C Methods*, vol. 17, no. 12, pp. 1201–1210, Dec. 2011.
[484] A. D. Dikina *et al.*, "A Modular Strategy to Engineer Complex Tissues and Organs," *Adv. Sci.*, vol. 5, no. 5, p. 1700402, May 2018.
[485] S. Siddiqi, "Tissue Engineering of the Trachea: What is the Hold-up?," *MOJ Cell Sci. Rep.*, vol. 4, no. 1, pp. 1–5, 2017.

Chapter 8: Appendices

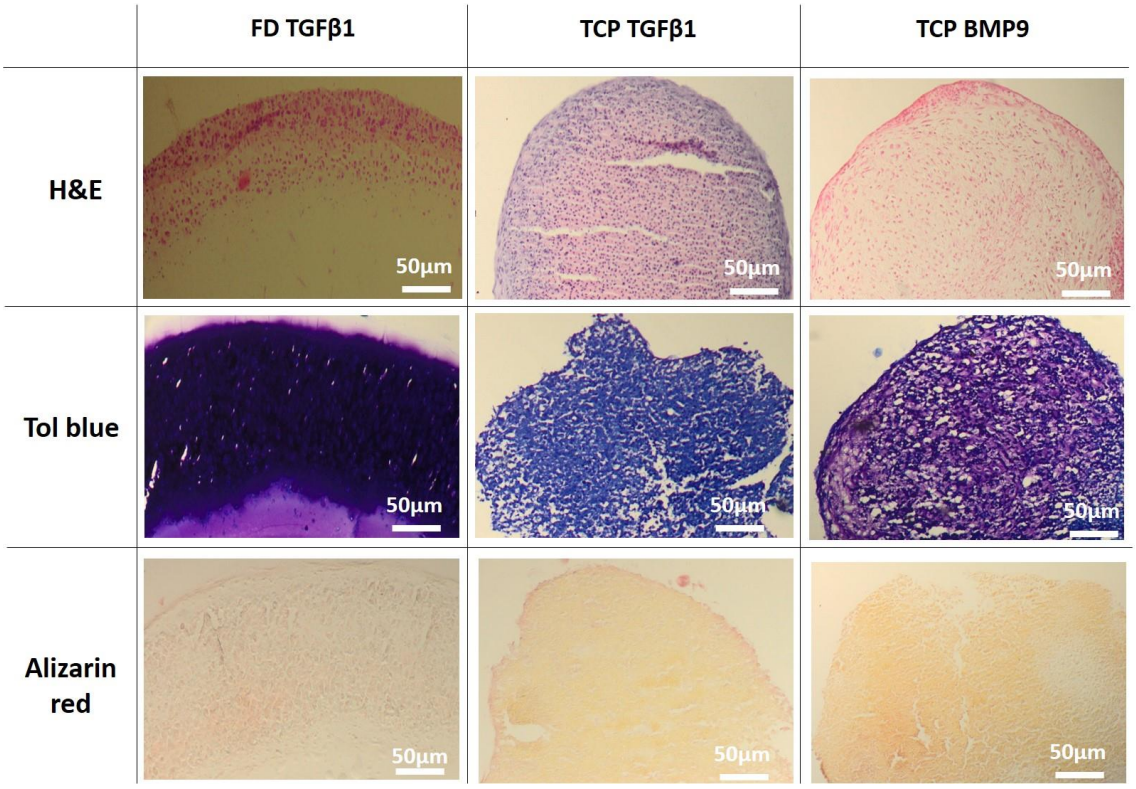
FD TGFβ1
TCP TGFβ1
TCP BMP9
H&E
Tol blue
Alizarin red
50µm

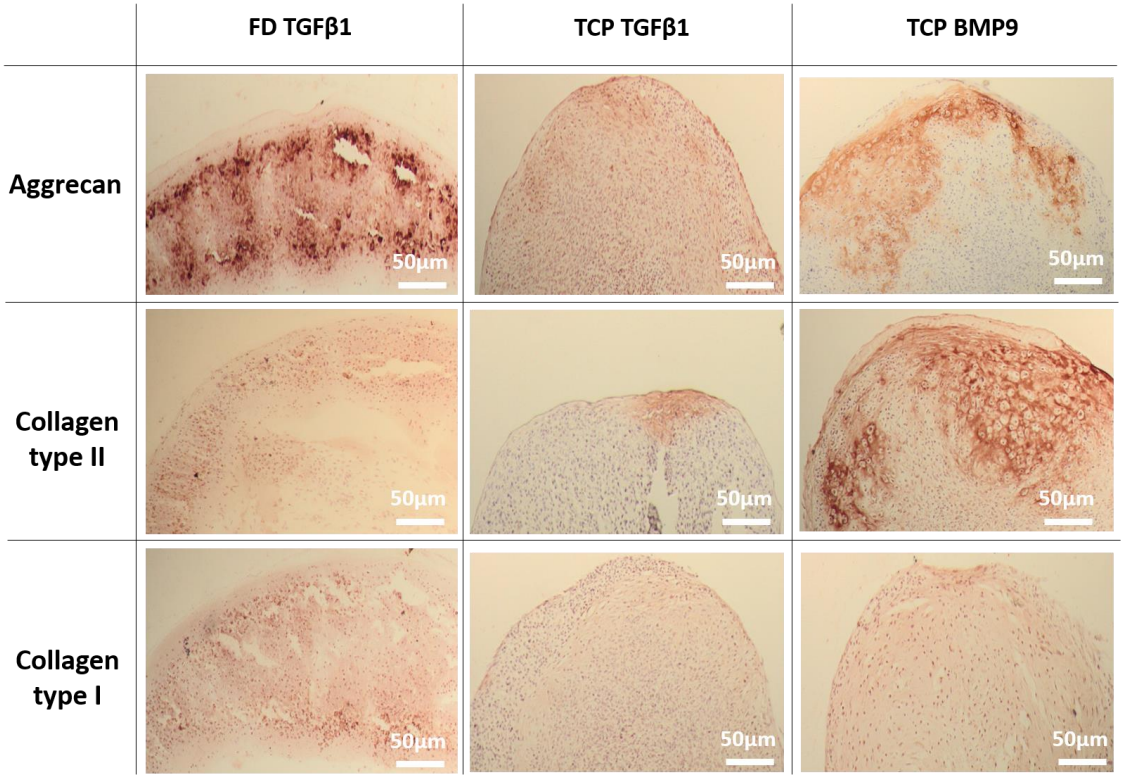
FD TGFβ1
TCP TGFβ1
TCP BMP9
Aggrecan
Collagen type II
Collagen type I
50µm